Y-Box Binding Protein-1 as a Potential Target to Improve Radiotherapy Outcomes

Dissertation

der Mathematisch-Naturwissenschaftlichen Fakultät

der Eberhard Karls Universität Tübingen

zur Erlangung des Grades eines

Doktors der Naturwissenschaften

(Dr. rer. nat.)

vorgelegt von

Shayan Khozooei

aus Teheran, Iran

Tübingen

2024

Gedruckt mit Genehmigung der Mathematisch-Naturwissenschaftlichen Fakultät der Eberhard Karls Universität Tübingen.

Tag der mündlichen Qualifikation:	19.11.2024
Dekan:	Prof. Dr. Thilo Stehle
1. Berichterstatter/-in:	Prof. Dr. Mahmoud Toulany
2. Berichterstatter/-in:	Prof. Dr. Ulrich Rothbauer

Contents

List of Figures

Abbreviations

7-HI	7-Hydroxyindirubin
aa	Amino acid
ABL	Abelson
AE	Aloe-emodin
ALK	Anaplastic lymphoma kinase
Alt-NHEJ	Alternative non-homologous end joining
BLM	Bloom syndrome helicase
BLM helicase	Bloom helicase
CDC42	Cell division cycle 42
cGAS	Cyclic GMP-AMP synthase
C-NHEJ	Classical non-homologous end joining
CRC	Colorectal cancer
CRS	Cytoplasmic retention signal
CRT	Chemoradiotherapy
CSD	Cold shock domain
CTD	C-terminal domain
CtIP	CtBP-interacting protein
DBPA	DNA binding protein A
DBPB	DNA binding protein B
DBPC	DNA binding protein C
DDR	DNA damage response
DFS	Disease-free survival
DNA2	DNA replication ATP-dependent helicase/nuclease 2
DNA-PKcs	DNA-PK catalytic subunit
Dox	Doxycycline

DSB	Double-strand break
EGF	Epidermal growth factor
EGFR	Epidermal growth factor receptor
EMT	Epithelial-mesenchymal transition
ER	Estrogen receptor
EXO1	Exonuclease 1
GAP	GTPase-activating protein
GDP	Guanosine diphosphate
GEF	Guanine nucleotide exchange factors
GFP	Green fluorescent protein
Grb2	Growth factor receptor-bound protein 2
GSH	Glutathione
GTP	Guanosine triphosphate
GTPases	Guanosine triphosphatases
HMGB1	High-mobility group box 1 protein
HR	Homologous recombination
HVR	Hyper Variable Region
IGF-IR	Insulin-like growth factor-I receptor
IR	Ionizing radiation
IRES	Internal ribosomal entry site
KRAS	Kirsten Rat Sarcoma Viral oncogene homologue
LET	Linear Transfer of Energy
LIG3	DNA Ligase 3
LIG4	DNA Ligase 4
MAPK	Mitogen-activated protein kinase
MEK	MAPK kinase
NCL	Nucleolin
NLS	Nuclear localization signal
NSCLC	Non-small cell lung cancer
OS	Overall survival
PAK	p21-activated kinase
PARP1	Poly (ADP-ribose) polymerase 1
PCNA	Proliferating cell nuclear antigen

PDGFR	Platelet-derived growth factor receptor
PFS	Progression-free survival
PI3K	Phosphatidylinositol 3-kinase
PIP2	Phosphatidylinositol (3,4)-bisphosphate
PIP3	Phosphatidylinositol (3,4,5)-tris
PLK	Polo-like kinase
P-loop	Phosphate-binding loop
PNKP	Polynucleotide kinase 3-phosphatase (3,4,5)-tris
POL	Polymerase
PR	Progesterone receptor
PTM	Post-translational modifications
RAC1	Ras-related C3 botulinum substrate 1
RAF	Rapidly Accelerated Fibrosarcoma
RFS	Recurrence-free survival
RNP	Ribonucleoprotein
ROS	Reactive oxygen species
RPA	Replication protein A
RSK	P90 ribosomal S6 kinase
RPA	Replication protein A
RTK	Receptor tyrosine kinase
rtTA	Reverse tetracycline transactivator
SCF	SKP1-CUL1-F-box protein
SH2	Src homology 2
SH3	Src homology 3
SOS	Son of Sevenless
SSB	Single-strand break
TDP1	Tyrosyl-DNA phosphodiesterase 1
TF	Transcription factor
TNBC	Triple-negative breast cancer
tTS	Tetracycline repressible transcriptional silencer
UPR	Unfolded protein response
UV	Ultraviolet
VEGFR	Vascular endothelial growth factor receptor

WT	Wild-type
XLF	XRCC4-like factor
XRCC4	X-ray cross complementing protein 4
YB-1	Y-box binding protein-1

Declaration

I hereby declare that the cumulative dissertation titled:

"Y-Box Binding Protein-1 as a Potential Target to Improve Radiotherapy Outcomes"

submitted for the award of Doctor rerum naturalium (Dr. rer. nat.) to the Mathematisch-Naturwissenschaftliche Fakultät of the Eberhard Karls Universität Tübingen is my own work. I further declare that::

- I have complied with the rules of good scientific practice as laid down by the Eberhard Karls Universität Tübingen.
- All contributions from other persons or organizations have been clearly acknowledged and cited.
- No part of this dissertation has been submitted for the award of any other degree at any other institution.
- The cumulative thesis includes the following published works and my individual contributions to these works are clearly outlined:
    1. Fisetin induces DNA double-strand break and interferes with the repair of radiation-induced damage to radiosensitize triple negative breast cancer cells, published in *J Exp Clin Cancer Res. 2022*
    2. Fisetin overcomes non-targetability of mutated KRAS induced YB-1 signaling in colorectal cancer cells and improves radiosensitivity by blocking repair of radiation-induced DNA double-strand breaks, published in *Radiother Oncol. 2023*
    3. YB-1 activating cascades as potential targets in KRAS-mutated tumors, published in *Strahlenther Onkol. 2023*
- I have not used any assistance from unauthorized sources in preparing this thesis.

Signed:

Date:

Summary

KRAS is frequently mutated in almost 30% of all cancers and these mutations are known to be strongly associated with chemoradiotherapy resistance (CRT). Y-box binding protein-1 (YB-1) is an oncoprotein that is overexpressed across different cancer entities and plays a significant role in cancer progression by being involved in almost all cancer hallmarks, in particular in resistance to radiotherapy-induced cell death. Phosphorylation of YB-1 at S102 is associated with poor prognosis and this phosphorylation and activation is mainly regulated by the MAPK/ p90 ribosomal S6 kinase (RSK) signaling pathway in *KRAS* mutated cells.

YB-1 has been shown to facilitate the repair of IR-induced double-strand breaks (DSBs) in breast cancer cells. However, due to the lack of kinase activity in YB-1 itself, designing a direct inhibitor is challenging. Therefore, one possible approach is to target YB-1 via upstream kinases that regulate YB-1. Data from our laboratory has shown that while inhibition of RSK leads to activation of the PI3K/AKT pathway, potentially diminishing the benefits of RSK targeting, dual targeting both RSK and AKT has proven to be the most effective strategy in breast cancer cells.

Fisetin, a natural flavonoid, has been known to interfere with the RSK-mediated YB-1 phosphorylation at S102 in melanoma. In our research, we demonstrated that fisetin, regardless of *KRAS* mutation status, blocks YB-1 phosphorylation at S102 in triple-negative breast cancer (TNBC) and colorectal cancer (CRC) cells, as well as in CRC tissue samples, *ex vivo*. Given to the role of YB-1 in stimulating the repair of ionizing irradiation (IR)-induced DSBs, fisetin was found to inhibit DSB repair partially through its inhibitory effect on YB-1. Phosphoproteomics analysis also revealed that fisetin targets multiple DNA damage response (DDR)-related phosphosites in irradiated cells, particularly those involved in DNA repair, replication, and chromatin binding, leading to inhibition of DSB repair predominantly via homologous recombination (HR) and classical non-homologous end joining pathways (C-NHEJ). These effects were associated with the radiosensitization effect of fisetin in TNBC and CRC cells, while having no effect on human skin fibroblast, suggesting the potential benefit in combination with radiotherapy.

Since RSK-mediated YB-1 phosphorylation and activity play a key role in stimulating the repair of IR-induced DSB in TNBC and CRC cells, the combination of fisetin with radiation therapy could significantly enhance radiation response, regardless of *KRAS* mutation status.

Zusammenfassung

Bei nahezu 30% aller Krebserkrankungen liegt eine Mutation des *KRAS*-Gens vor, wobei ein Zusammenhang mit einer Resistenz gegen Radiochemotherapie (RCT) evident ist. Das Y-Box-bindende Protein 1 (YB-1) ist ein Onkoprotein, dessen Expression bei verschiedenen Krebsarten erhöht ist. Es spielt eine wesentliche Rolle bei der Krebsentwicklung, da es an nahezu allen Krebsmerkmalen beteiligt ist, insbesondere an der Resistenz gegen den durch Strahlentherapie induzierten Zelltod. Die Phosphorylierung und Aktivierung von YB-1 erfolgt in *KRAS*-mutierten Zellen primär über den MAPK/p90 ribosomale S6-Kinase (RSK)-Signalweg. Die Phosphorylierung von YB-1 an S102 korreliert mit einer ungünstigen Prognose.

In diesem Kontext konnte nachgewiesen werden, dass YB-1 die Reparatur von durch ionisierende Strahlung induzierten Doppelstrangbrüchen (DSBs) in Brustkrebszellen fördert. Aufgrund der fehlenden Kinaseaktivität von YB-1 ist die Entwicklung eines direkten Inhibitors jedoch herausfordernd. Ein möglicher Ansatz besteht folglich darin, YB-1 über vorgeschaltete Kinasen, welche YB-1 regulieren, zu beeinflussen. Unsere Ergebnisse konnten zeigen, dass eine Hemmung von RSK zu einer Aktivierung des PI3K/AKT-Signalweges führt, wodurch die Vorteile der RSK-Targeting-Strategie möglicherweise beeinträchtigt werden. Ein effektiver Ansatz ist demnach die duale Targeting Strategie von RSK und AKT.

Fisetin, ein natürliches Flavonoid, ist dafür bekannt, die RSK-vermittelte YB-1-Phosphorylierung an S102 in Melanomen zu beeinträchtigen. Unsere Forschungsergebnisse belegen, dass Fisetin unabhängig vom *KRAS*-Mutationsstatus die YB-1-Phosphorylierung an S102 in dreifach negativen Brustkrebs- (TNBC) und Darmkrebszellen (CRC) sowie in CRC-Gewebeproben ex vivo hemmt. In Anbetracht der Funktion von YB-1 bei der Stimulierung der Reparatur von durch ionisierende Strahlung (IR) induzierten Doppelstrangbrüchen (DSBs) wurde festgestellt, dass die Hemmung der DSB-Reparatur durch Fisetin durch dessen hemmende Wirkung auf YB-1 begründet ist. Die Ergebnisse der Phosphoproteomics-Analysen legen zudem nahe, dass Fisetin auf mehrere mit der DNA-Schadensreaktion (DDR) assoziierte Phosphosites in bestrahlten Zellen abzielt, insbesondere auf solche, die an der DNA-Reparatur, Replikation und Chromatinbindung beteiligt sind. Dies führt zu einer Hemmung der DSB-Reparatur, die vorwiegend über homologe Rekombination und klassische nicht-homologe Endverbindungswege erfolgt. Dieser Effekt korrelierte mit der radiosensibilisierenden Wirkung von Fisetin in TNBC- und CRC-Zellen, während es keine Wirkung auf menschliche Hautfibroblasten hatte. Dies lässt einen potenziellen Nutzen in Kombination mit einer Strahlentherapie vermuten.

Aufgrund der essenziellen Bedeutung der RSK-vermittelten YB-1-Phosphorylierung und -Aktivität für die Stimulierung der Reparatur von IR-induzierten DSB in TNBC- und CRC-Zellen könnte eine Kombination von Fisetin mit einer Strahlentherapie die Strahlenreaktion unabhängig vom *KRAS*-Mutationsstatus signifikant verbessern.

List of Publications

Publication I:

Khozooei S, Lettau K, Barletta F, Jost T, Rebholz S, Veerappan S, Franz-Wachtel M, Macek B, Iliakis G, Distel LV, Zips D, Toulany M. Fisetin induces DNA double-strand break and interferes with the repair of radiation-induced damage to radiosensitize triple negative breast cancer cells. J Exp Clin Cancer Res. 2022 Aug 22;41(1):256. (IF: 11.3)

Publication II:

Khozooei S*, Veerappan S*, Bonzheim I, Singer S, Gani C, Toulany M. Fisetin overcomes non-targetability of mutated KRAS induced YB-1 signaling in colorectal cancer cells and improves radiosensitivity by blocking repair of radiation-induced DNA double-strand breaks. Radiother Oncol. 2023 Nov;188:109867. (IF: 4.9)

Publication III:

Khozooei S*, Veerappan S*, Toulany M. YB-1 activating cascades as potential targets in KRAS-mutated tumors. Strahlenther Onkol. 2023 Dec;199(12):1110-1127. (IF: 2.7)

Publication IV:

Lettau K, **Khozooei S**, Kosnopfel C, Zips D, Schittek B, Toulany M. Targeting the Y-box Binding Protein-1 Axis to Overcome Radiochemotherapy Resistance in Solid Tumors. Int J Radiat Oncol Biol Phys. 2021 Nov 15;111(4):1072-1087. (IF: 6.4)

Publication V:

Toulany M, Iida M, Lettau K, Coan JP, Rebholz S, **Khozooei S**, Harari PM, Wheeler DL. Targeting HER3-dependent activation of nuclear AKT improves radiotherapy of non-small cell lung cancer. Radiother Oncol. 2022 Sep;174:92-100. (IF: 4.9)

Contribution to the publications

Publication I:

Fisetin induces DNA double-strand break and interferes with the repair of radiation-induced damage to radiosensitize triple negative breast cancer cells (Khozooei et al. J Exp Clin Cancer Res. 2022)

General contribution

I maintained and treated all cells for further experiments. I detected all Western blots. I wrote the original draft of the manuscript, which was further developed by M. Toulany. I did the revision as well.

Contribution to every figure

Fig. 1: I prepared the samples and performed Western blotting with the assistance of S. Rebholz. I detected the blots, designed and generated these figures.

Fig. 2: I prepared the samples and performed Western blotting with the assistance of S. Rebholz. Blots were detected by me and the figure was designed and generated by me.

Fig. 3: The cells were treated by me and the clonogenic assays were performed and counted by S. Veerappan. Figures were generated by me and S. Veerappan.

Fig. 4: The experiments for Fig. 4A-C, were performed completely by myself, from cell maintenance until data analysis and figure generation. For the *in situ* hybridization analyses (for Fig. 4D), the cells were sent to LV. Distel and T. Jost, who conducted the chromosomal aberration analysis and generated the corresponding figure.

Fig. 5: I carried out all the experiments, data analysis for Fig. 5, and figure generation.

Fig. 6: I assisted in sample preparation and performed the FACS acquisition for Fig. 6A with the assistance of K. Lettau. I analyzed the FACS data and generated the figures. I independently performed all experiments, analyzed the data, and generated the figure for Figure 6B.

Fig. 7: I conducted all the experiments, analyzed the data, and prepared the figures.

Fig. 8: I have maintained the cells under the SILAC medium for phosphoproteomics analysis. I isolated the protein samples and sent them to M. Franz-Wachtel for mass spectrometry. F. Barletta generated the volcano plot in Fig. 8A, and the gene ontology in Fig. 8B. I prepared the pie chart in Fig. 8A, added gene annotations to the volcano

plot in Fig. 8A, and compiled the table for Fig. 8A. Detailed analysis of phosphoproteins to find out their role in DNA damage and repair pathways by literature review was performed by myself. The schematic in Fig. 8C was prepared by K. Lettau.

Fig. S1: I prepared the samples and performed Western blotting. I detected the blots, and designed the figure.

Fig. S2: The cells were treated by me and the clonogenic assays were performed and counted by S. Rebholz. The survival analysis was performed by M. Toulany.

Fig. S3: I performed the experiments and generated the figures.

Fig. S4: I have kept the cells under the SILAC medium for phosphoproteomics analysis. I extracted the proteins and sent them to M. Franz-Wachtel for mass spectrometry analysis. F. Barletta generated the heatmap for Fig. S4.

Fig. S5: Similar to the Fig. S4, I cultured the cells in SILAC medium and isolated the samples. M. Franz-Wachtel performed mass spectrometry analysis and based on the data from differentially regulated phosphoproteins, I analyzed gene ontology for Fig. S5 and generated the corresponding graph.

Publication II:

Fisetin overcomes non-targetability of mutated KRAS induced YB-1 signaling in colorectal cancer cells and improves radiosensitivity by blocking repair of radiation-induced DNA double-strand breaks. (Khozooei et al. Radiother Oncol. 2023)

General contribution

For this project, I assisted S. Veerappan in maintaining the CRC cells in culture, while I independently maintained the U2OS cells with various genetic constructs. I also contributed to writing the first draft of the manuscript. S. Veerappan and I were involved in the revision process

Contribution to every figure

Fig. 1: Together with S. Veerappan, we performed the Ras activity assay (Fig. 1A). The experiments for Fig. 1B and Fig. 1D were performed and detected by S. Veerappan. I generated the bar graph and analyzed the data shown in Fig. 1C.

Fig. 2: S. Veerappan performed the experiment for Fig. 2A. S. Veerappan and I jointly collected the tissue samples, processed them, treated, isolated proteins, ran Western blotting, and detected the blots for Figs. 2B,D,E, and F. Western blot images in Figs.

2A-F were prepared by S. Veerappan. Gene mutational analysis of patient tissue sample in Fig. 2C was performed by I. Bonzheim and S. Singer.

Fig. 3: I performed all the experiments, analyzed the data, and generated the figures for Figures 3A–D. I prepared the samples and assisted with Western blotting and blot detection, while Fig. 3E was prepared by S. Veerappan.

Fig. 4: I treated and irradiated the cells for Figs. 4A-B,D. I conducted the immunofluorescence staining, microscopy, data analysis, and figure preparations. Fig. 4C was generated by S. Veerappan. The clonogenic assay in Fig. 4E has been performed, counted, and graphed by me.

Fig. 5: The schematic was generated by S. Veerappan.

Fig. S1, S2, S3, and S4: These Western blotting were done by S. Veerappan and figures were generated by her.

Fig. S5 and S6: S. Veerappan treated and irradiated the cells. I performed the immunofluorescence staining, microscopy, data analysis, and figure preparations.

Fig. S7: The clonogenic assay was performed and analyzed by S. Veerappan.

Fig. S8: The cells were treated and irradiated by S. Veerappan. I did the staining, microscopy, and data analysis. I generated the figure. The clonogenic assay in Fig. S8B was performed and analyzed by S. Veerappan.

Fig. S9 and S10: I treated and irradiated the cells, isolated, and fixed the cells. I performed PI staining, FACS acquisition, data analysis, and generation of the figures.

Table S1: This table was generated by S. Veerappan.

Publication III:

YB-1 activating cascades as potential targets in KRAS-mutated tumors (Khozooei et al. Strahlenther Onkol. 2023)

Together with S. Veerappan, we wrote the review paper. The information regarding the biology of YB-1, its role in chemoradiotherapy resistance, and strategies to target KRAS/YB-1 axis in *KRAS* mutated tumors was reviewed in the literature and written by myself. The information about the biology of KRAS and its targeting was extracted and written by S. Veerappan. Fig. 1 was designed and generated by me. Together with S. Veerappan we designed and created Fig. 2 and Fig. 3.

Acknowledgements

First and foremost, I would like to express my deepest gratitude to my supervisor, Prof. Dr. Mahmoud Toulany, for accepting me as his PhD student and giving me the incredible opportunity to work on this exciting project. I am immensely thankful for your trust, which allowed me the independence to explore my own ideas and to work with a great degree of autonomy. Your expertise and insights have been invaluable, and your mentorship has profoundly shaped both my academic growth and my ability to think critically and independently.

I would also like to extend my heartfelt thanks to Prof. Dr. Ulrich Rothbauer for his constructive feedback, and invaluable advice, and for serving as my second PhD supervisor. Your guidance has been crucial in refining my research and approach.

I am also deeply grateful to all the co-authors of our publications for their collaboration and contributions, which enriched the outcomes of this research. Without all of you, these publications would not have been possible.

A special thanks to Soundaram Veerappan for all the stimulating and critical discussions we shared. Your constant motivation and encouragement have been a driving force in my scientific endeavors, and I have always been inspired by your passion for science.

I would also like to acknowledge my wonderful colleagues and lab mates for the engaging discussions and for fostering a supportive and collaborative research environment. Your friendship and encouragement have been a source of both motivation and joy throughout this journey.

Finally, I would like to express my deepest appreciation to those who mean the most to me: my family. Your unwavering support and encouragement have been invaluable throughout this journey. Thank you for constantly reminding me that there is more to life beyond the lab, and for being a source of comfort and distraction when I needed it most. A special thanks to my parents for their unconditional love, and sacrifices, and for preparing me for the future with such dedication. I am also incredibly grateful to my brothers, Shahin and Shadmehr, for their enthusiastic support and belief in me.

Above all, I would like to thank my life partner, Nazanin, for her unfailing support and continuous encouragement throughout my PhD journey. Your help with formatting this thesis in LaTeX and your constant presence have made all the difference, and I am deeply grateful.

In addition, I would like to extend my heartfelt thanks to my dear friends, especially Alauddin and Shabab, for their continuous support during all phases of my PhD.

Chapter 1

Introduction

1.1 Cancer

Cancer is often defined as abnormal cell growth and proliferation which is capable of invasion to the blood vessels and spread throughout the body (King et al. 2000; Schwartz 2024) and is the world's second most frequent cause of death. There were estimated around 20 million new cases and about 10 million deaths in 2022 worldwide. It is predicted that the number of new cancer cases will exceed over 35 million by 2050 (Bray et al. 2024).

1.1.1 Triple negative breast cancer

Triple-negative breast cancer (TNBC) represents the most aggressive subtype of breast cancer. TNBC is defined by the lack of the estrogen receptor (ER) and progesterone receptor (PR). Additionally, it is defined by the absence of HER2 amplification. TNBC represents about 20% of all diagnosed breast cancer cases and is observed more frequently in younger patients. Moreover, TNBC occurs more commonly in patients with BRCA1/2 mutations (Patel et al. 2024). In TNBC, metastasis to the liver, brain, and lung has been observed. The lack of receptors limits the range of potential treatment options for TNBCs and therefore makes it more challenging for effective treatment. At present, chemotherapy, and surgery are the primary treatment strategies for TNBCs (Patel et al. 2024). Furthermore, TNBCs have a high presence of tumor-infiltrating lymphocytes, rendering them a promising candidate for immunotherapy (Liu et al. 2023). In addition to the approaches mentioned, radiotherapy has been demonstrated to be an effective therapy for improving locoregional control in patients who have undergone breast-conserving surgery or mastectomy, and for increasing the patients' survival in

the long term (He et al. 2018b). However, TNBCs are frequently radioresistant, and therefore, targeting the mechanisms involved in radioresistance in TNBCs along with radiotherapy may enhance the treatment response.

1.1.2 Colorectal cancer

Colorectal cancer (CRC) ranks as the third most frequent cancer globally. The incidence of CRC in individuals above 50 years old has decreased, whereas it has increased in younger age groups (Li et al. 2021). Early-stage tumors can be resected by surgery, whereas late-stage tumors are treated with adjuvant and/or neoadjuvant chemoradiotherapy (CRT). The response rate to chemotherapy and CRT is between 10 and 60% and approximately 20%, respectively (Li et al. 2021; Hoendervangers et al. 2020). Furthermore, immunotherapy using immune checkpoint inhibitors (anti-PD-1 and anti-CTLA4) has shown promising results and is currently under investigation in clinical trials. Nevertheless, the efficacy of immune checkpoint inhibitors is enhanced in tumors with high microsatellite instability. In this context, high tumor burden mutations result in more neoantigens, which in turn, facilitates T-cell infiltration into the tumors (Parikh et al. 2021). In addition, molecular target therapies have been developed. These drugs target proteins that are involved in tumor development pathways. The most common form of molecular target therapy is the use of monoclonal antibodies and small molecule inhibitors. However, the efficacy of this treatment approach depends on the genetic background of the cancer cells which results in only a subset of populations benefiting from these treatments. For instance, anti-epidermal growth factor receptor (EGFR) targeting is only beneficial in *KRAS* wild-type ($KRAS^{wt}$) tumors and not in *KRAS* mutated ($KRAS^{mut}$) tumors (Ridouane et al. 2017). Another drawback is that in patients undergoing these treatments, often the tumor reoccurs and patients might suffer from therapy resistance (Ohishi et al. 2023). Therefore, monotherapy with single agents is limited and only few patients with specific genetic backgrounds may benefit. However, these limitations can be overcome by using combination treatments.

The combination of chemotherapy and surgery has been shown to be effective in improving treatment outcomes (Fan et al. 2015). In addition, the combination of chemotherapy and radiotherapy has also been investigated and it shows promising responses (Elbanna et al. 2021; Manzi et al. 2023; Rodriguez et al. 2007). Furthermore, molecular targeted therapy also showed an enhanced response rate when combined with chemotherapy or CRT. However, the treatment efficacy also depends on the genetic background of the cancer cells.

1.2 Repair of ionizing radiation-induced DNA damages

Maintaining genome integrity is vital for cell survival. Thousands of DNA damage occur in cells every day, potentially leading to gene mutations if these defects are not repaired. Cells have evolved mechanisms to sense the DNA damage, activate the DNA damage response (DDR) pathway, and induce cell cycle arrest to ultimately repair the broken DNA. Ionizing radiation (IR) generates ions by releasing electrons from DNA or water to break the covalent bonds. IR can directly induce double-strand breaks (DSBs). However, IR has an indirect effect through the formation of reactive oxygen species (ROS), which can further cause single-strand breaks (SSBs) (Borrego-Soto et al. 2015). There are different types of IR, including X-rays, gamma rays which are called low Linear Transfer of Energy (LET), and high LETs, including alpha and beta particles, each of which with different characteristics. Low LETs cause damage to the cells mainly through indirect effects, whereas, high LETs damage cells directly (Roy et al. 2022). IR is used to shrink the tumor cells before surgery or kill any remaining cells after surgery. Interestingly, the biological response to IR and the fate of the cells exposed to IR depend on a variety of factors, including the complexity of the DNA DBSs, the type of DNA damage, the dose rate, the dose of IR, and the genetic background of the cells (Mavragani et al. 2019). When the DNA is damaged, the DDR pathway is activated which involves several mechanisms including DNA repair pathways, pro-survival pathways, alteration of cell cycle progression, cell death pathways, changes in metabolic pathways, and the induction of senescence and autophagy (Roy et al. 2022). The interaction of these pathways plays a critical role in determining radiosensitivity and ultimately shaping the therapeutic response to radiation therapy. Following radiotherapy and DNA damage, if the cells are able to repair the DNA, the cells will continue to proliferate, but if the cells are unable to fix the defects, the cells will undergo apoptosis. In eukaryotic cells, DSBs are mainly repaired by three main mechanisms: homologous recombination (HR), classical non-homologous end joining (C-NHEJ), and alternative non-homologous end joining (Alt-NHEJ) (Fig. 1). There are differences in the fidelity and kinetics of these pathways. In addition, they are active in certain cell cycle phases. In this context, HR is a slow mechanism of repair, with error-free characteristics that is active during the S and G2 phases of the cell cycle. In contrast, C-NEHJ and Alt-NHEJ pathways are faster and error-prone and are active throughout the cell cycle (Dueva et al. 2013a).

1.2.1 Homologous recombination

The ability of the HR pathway to start the repair process depends on the presence of sister chromatids, which are available in the S and G2 phases of the cell cycle. Therefore,

the sister chromatids are used as templates to restore the broken sequence. Mechanistically, HR has three steps; pre-synaptic (Fig. 1), synaptic, and post-synaptic. Initially, after DSB occurs, the MRN complex, including Mre11, NBS1, and Rad50, detects the DSB, which further recruits CtBP-interacting protein (CtIP) (Mozaffari et al. 2021; Sartori et al. 2007). CtIP then enhances Mre11 nuclease activity at $3'$ to $5'$, to generate short $3'$ overhangs (Sakuno et al. 2015). Afterward, the long overhangs are further processed by the recruitment of other nucleases, such as the Bloom syndrome helicase/DNA replication ATP-dependent helicase/nuclease 2 (BLM/DNA2) complex, and exonuclease 1 (EXO1). Furthermore, the single strand $3'$ overhangs are covered by the heterotrimeric replication protein A (RPA) complex to protect them from nuclease activity. Thereafter, BRCA2, along with PALB2 and the BRCA1/BARD1 complex, displaces RPA from the single-stranded DNA and enhances the loading of Rad51 recombinase on the single-stranded DNA to form the Rad51 nucleoprotein filament (Mladenov et al. 2023). This step has been recognized as a pre-synaptic step in HR. In the synaptic step, Rad51 then searches for homology sequences in the sister chromatids to invade them to make holiday junctions. Rad54 then aids in DNA synthesis and removes Rad51 from the complex. In the post-synaptic step, the holiday junction is resolved and the newly synthesized DNA anneals to the DNA strand and finally ligates to restore the genome integrity (Mladenov et al. 2023).

1.2.2 Classical non-homologous end joining

C-NHEJ is active in all phases of the cell cycle, including proliferating and quiescent cells. When a DSB occurs, the Ku70/Ku80 heterodimer binds to the broken DNA and recruits the DNA-PK catalytic subunit (DNA-PKcs), a member of the Phosphatidylinositol 3-kinase-related kinase PIKK family of protein kinases, to form a DNA-PK holoenzyme (Ghosh et al. 2021; Shimazaki et al. 2008). The DNA-PK holoenzyme acts as a docking site and recruits other repair proteins to the damage site (Mladenov et al. 2023) (Fig. 1). Prior to the ligation step, DNA-PK is autophosphorylated to be removed from the damage site. To make the DNA end compatible for the ligation, there are several enzymes that are specific for end processing, including Artemis nucleases, polymerases of the POL X family, POL μ and POL λ, the tyrosyl-DNA phosphodiesterase 1 (TDP1), and the polynucleotide kinase $3'$-phosphatase (PNKP), depending on the type of DNA ends. Mechanistically, these enzymes can add, remove, or modify nucleotides at DNA ends (Mladenov et al. 2023), suggesting that the C-NHEJ is error-prone. DNA end processing is a crucial step in the repair of IR-induced DNA DSBs (Chang et al. 2016). DNA ends are then ligated with the DNA Ligase 4 (LIG4) and X-ray cross complementing protein 4 (XRCC4), which together form a complex. Ligation is facilitated by

XRCC4-like factor (XLF) and/or by a paralog of XRCC4 and XLF (PAXX) (Zhao et al. 2020).

1.2.3 Alternative non-homologous end joining

Alt-NHEJ is a backup pathway, also abbreviated as B-NHEJ, that is suppressed by C-NHEJ and HR and is therefore activated when these pathways are defective (Dueva et al. 2013b). This pathway is facilitated by microhomology sequences (between 2-20 nucleotides) found at the DNA ends, but they are not required for its function. Alt-NHEJ is active in all phases of the cell cycle, however, its activity peaks in the S and G2 phases. It is also slower than C-NHEJ, but more error-prone. It is known that Alt-NHEJ can rejoin unrelated sequences together without restoring the DNA sequences. Therefore, the frequency of gene translocations and large deletions is significantly high. As a result, this pathway is one of the major sources of genomic instability (Dueva et al. 2013b). The mechanism of Alt-NHEJ is independent of DNA-PKcs and KU70/KU80. However, the presence of these factors together with the major factors in Alt-NHEJ, shows that it begins when the other two pathways are initiated but failed to continue the repair processes. Another model of activation of this pathway is that PARP1 poly (ADP-ribose) polymerase 1 (PARP1) senses the DNA breaks and activates this pathway. Alt-NHEJ can also be active even when C-NHEJ is functional. However, the balance between these two pathways affects the pathway selection (Zhang et al. 2024). Recently, it has been shown that cGAS (cyclic GMP-AMP synthase), the main cytosolic DNA sensor, translocates to the nucleus in the presence of DNA damage, and forms a complex with KU80, which enhances its interactions with DNA-PKcs and thus promotes C-NHEJ (Zhang et al. 2024). Interestingly, this complex formation leads to the suppression of Alt-NHEJ. Therefore, the cGAS-KU80 complex modulates the balance between Alt-NHEJ and C-NHEJ.

In Alt-NHEJ, mechanistically, PARP1 promotes CtIP and MRN complex for a short-range DNA end resection (Fig. 1). The DNA ends can be rejoined using the homology sequences, and the DNA is then synthetized by DNA polymerase θ (POLθ). Ligation is further mediated by the DNA Ligase 3 (LIG3)/XRCC1 complex (Mladenov et al. 2023).

1.3 KRAS

Kirsten Rat Sarcoma Viral Oncogene Homologue (KRAS) is a commonly mutated oncoprotein in the RAS family of small guanosine triphosphatases (GTPases), which are linked to the plasma membrane. Three genes encode RAS GTPases, including *HRAS*,

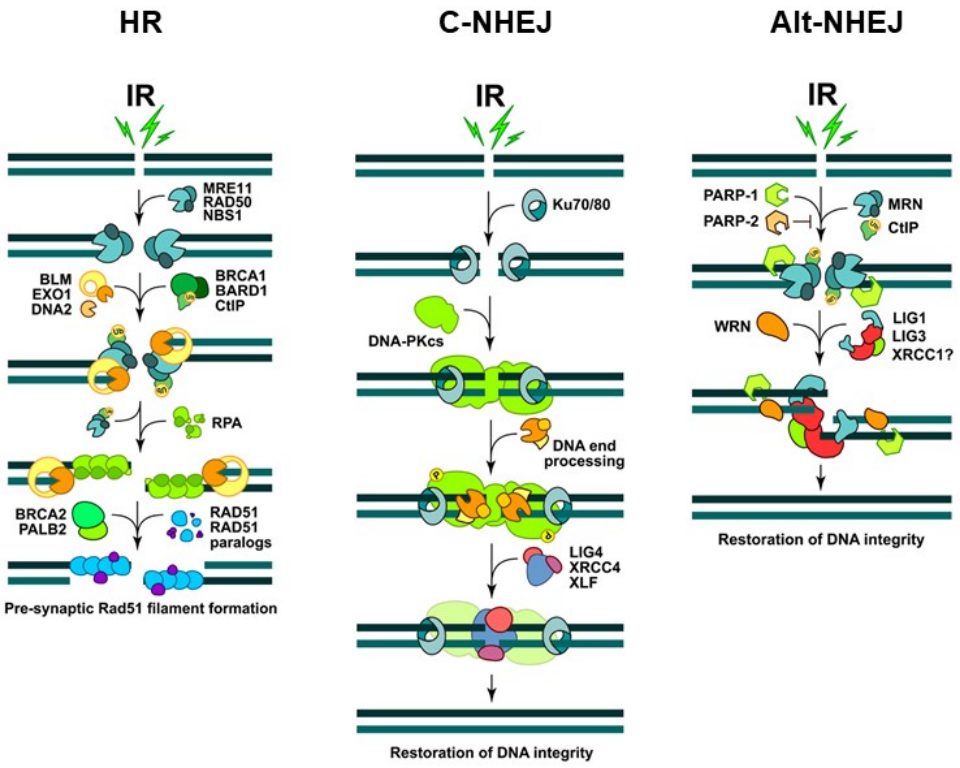

Figure 1: DNA DSB repair pathways after exposure to IR. DSBs are repaired mainly by HR, C-NHEJ, and Alt-NHEJ. Modified after (Mladenov et al. 2013). Please see the text for the details.

NRAS, and *KRAS*. Mutations in these GTPases are present in about 30% of all human cancers, with *KRAS* mutations responsible for 75% of these cases (Prior et al. 2020). Structurally, KRAS consists of two main domains; the N-terminal G-domain and the C-terminal Hyper Variable Region (HVR). The G-domain is the catalytic domain that regulates GDP/GTP binding. The catalytic domain contains switch I, switch II, and phosphate-binding loop (P-loop) regions (Fig. 2). $KRAS^{wt}$ switches between two states under normal physiological conditions, i. e. a guanosine diphosphate (GDP)-bound inactive state and a guanosine triphosphate (GTP)-bound active state. This transition is triggered by stimulation via receptor tyrosine kinases (RTKs). GTP binding to RAS causes conformational changes, particularly in the switch I and switch II regions of RAS, which then enables RAS to interact with other effector proteins. In this context, GTPase-activating proteins (GAPs) enhance the hydrolysis of GTP and therefore inactivate RAS. On the other hand, guanine nucleotide exchange factors (GEFs) cause the release of GDP, which helps the binding of GTP to RAS, thereby activating RAS (Kolch et al. 2023). KRAS transmits signals majorly through the RAF/MEK/ERK,

PI3K/AKT, and RalGDS signaling pathways. These pathways are significantly upregulated in *KRAS* mutated cells (Moodie et al. 1993; Rodriguez-Viciana et al. 1997; Zhang et al. 1993). Interestingly, these signaling pathways cross-talk at multiple points, enabling them to interact with each other. The interaction of the indicated pathways results in the activation of alternative pathways when one pathway is impaired (Eser et al. 2014).

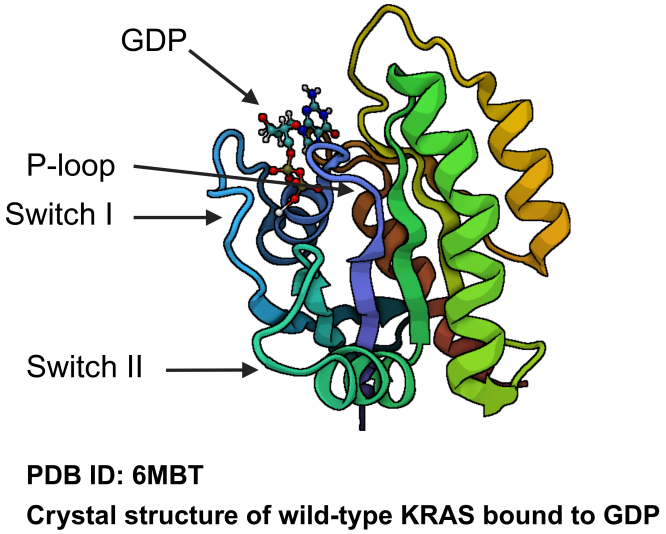

Figure 2: Crystal Structure of KRAS^{wt} bound to GDP. Created with BioRender.com

There are oncogenic mutations in the *KRAS* that generally affect GTP hydrolysis and keep RAS in a constitutively active state. Among them, mutations in G12, G13, and Q61 codons have been observed (Chen et al. 2013; Hunter et al. 2015; Smith et al. 2013). Interestingly, there are multiple substitutions that have also been found within these specific codons, including G12D, G12V, and G12C (Buhrman et al. 2007; Hunter et al. 2015; Haigis 2017; Muñoz-Maldonado et al. 2019), that the frequency of these mutations varies between tumors, which in turn causes the activation of different signaling pathways. For instance, it has been reported that in non-small cell lung cancer (NSCLC), the G12D mutation is linked to enhanced PI3K/AKT and MER/ERK pathways, whereas G12V and G12C mutations are more associated with the RalGDS signaling pathway (Ihle et al. 2012). In the clinical setting, these allelic variants may also cause diverse clinical outcomes. For example, it has been reported that in NSCLC, G12V, and G12C mutations are linked to poor progression-free survival (PFS) and disease-free survival (DFS), respectively (Jia et al. 2017; Nadal et al. 2014). In addition, the G12D mutation plays a critical role in decreasing the overall survival (OS) of pancreatic cancer patients compared to G12V and G12R (Dai et al. 2022). There are a number of studies that have also suggested that mutations in G12D, G12V, and G12C reduce recurrence-free survival

(RFS) and PFS in colorectal cancer patients (Chida et al. 2021; Park et al. 2021) further highlighting the importance of specific *KRAS* mutations in clinical outcomes.

1.4 Y-box binding protein-1

Y-box binding proteins are DNA/RNA binding proteins that bind to the CCAAT inverted sequence (Dolfini et al. 2013). This family of proteins is part of cold shock domain (CSD) proteins that play a significant role in the control of cell growth and development (Lindquist et al. 2018). Currently, three members of this family of proteins have been identified, including Y-box binding protein-1 (YB-1)/DNA binding protein B (DBP2), YB-2/ DNA binding protein C (DBPC), and YB-3/ DNA binding protein A (DBPA), which share a similar structure. Compared to YB-2 and YB-3, YB-1 is the most well-studied member that has been found to be highly expressed in solid tumors (Dahl et al. 2009; Fushimi et al. 2013; Nishio et al. 2014; Sinnberg et al. 2012; Zhan et al. 2022). Interestingly, YB-1 has been suggested to be involved in all cancer hallmarks, e.g., it stimulates resistance mechanisms by enhancing DDR, leading to CRT resistance (Chatterjee et al. 2008; Kim et al. 2013; Mylona et al. 2014; Shibahara et al. 2001; Zhang et al. 2012).

Structurally, YB-1 at the N-terminal site has Alanine/Proline-rich domain (A/P) with amino acid (aa) residues from 1 to 50. In addition, a highly conserved CSD from aa 51 till aa 129, and a C-terminal domain (CTD) from aa 129 to aa 324 (Yang et al. 2019) as illustrated in Fig. 3. The CDS comprises a five stranded β-barrel that contains two RNA-binding motifs known as ribonucleoprotein (RNP) particle domain-1 (RNP1) and RNP2 (Matsumoto et al. 1998), which play an important role in binding to DNA/RNA. YB-1 has function in both gene transcription (Lyabin et al. 2014) and protein translation (Evdokimova et al. 1998; Evdokimova et al. 1995; Minich et al. 1993) by binding to DNA and RNA, respectively. The CTD region of YB-1 has both positive and negative charges, but overall CTD domain is positively charged. Furthermore, the CTD contains one cytoplasmic retention signal (CRS) and three nuclear localization signals (NLS); NLS1 from aa 149 till aa 156, NLS2 from aa 185 to aa 194, and NLS3 from aa 176 to aa 292 (Roeyen et al. 2013). Additionally, there is a specific site for cleavage by the 20S proteasome located between glutamic acid 219 (Glu219) and glycine 220 (Gly220) (Roeyen et al. 2013).

The basic charge of the CTD is responsible for improving the binding capacity of YB-1 to the mRNA, thus playing a role in translation regulation (Hamon et al. 2022). In this context, YB-1 as a cytoplasmic protein is known to enhance the translation of certain mRNAs, such as HIF1α (El-Naggar et al. 2015), Snail1, Twist, and others genes that

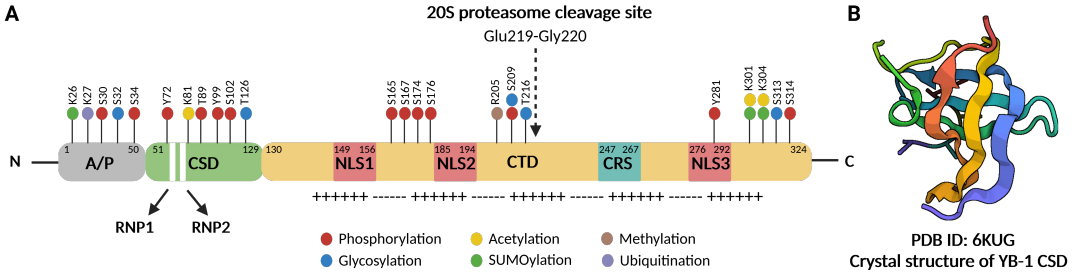

Figure 3: Diagram and crystal structure of YB-1. A YB-1 comprises three domains: N-terminal A/P, CSD, and CTD in total having 324 aa. The CSD possesses two RNP1 and RNP2 while the CTD has three NLS and one CRS. In addition, YB-1 has a 20S proteasome cleavage site that occurs between aa Glu219-Gly220. The CTD also displays clusters of positive and negative charges represented as indicated. Numerous post-translational modification sites are indicated. B The CSD, spanning aa 51 to aa 129, participates in DNA/RNA binding and features a five-stranded -barrel with RNP1 and RNP2. aa amino acid, A/P domain alanine/proline-rich domain, CRS cytoplasmic retention signal, CSD cold shock domain, CTD C-terminal domain, Glu219 Glutamic acid 219, Gly220 Glycin 220, NLS nuclear localization signals, PTM Post-translational modification, RNP1 ribonucleoprotein particle domain-1, RNP2 ribonucleoprotein particle domain-2, YB-1 Y-box binding protein 1. Adopted from (Khozooei et al. 2023). Please see the text for the details.

control epithelial-mesenchymal transition (EMT) in breast cancer cells (Evdokimova et al. 2009). Interestingly, YB-1 also boosts the translation and thus expression of the insulin-like growth factor-I receptor (IGF-IR) (Chu et al. 2018). Furthermore, YB-1 can be also translocated to the nucleus in response to different conditions such as ultraviolet (UV) irradiation (Koike et al. 1997), hypoxia (Rauen et al. 2016), and cisplatin treatment (Woolley et al. 2011). Once translocated, nuclear YB-1 either acts as a transcription factor to promote the expression of certain genes or physically interacts with certain proteins (Kim et al. 2013).

Various post-translational modifications (PTMs) take place on YB-1 under different conditions, which impact its function and subcellular localization. Among these modifications, phosphorylation has been well studied, particularly phosphorylation of serine 102 (S102). This phosphorylation site is located on the CSD and is known to affect the binding of YB-1 to the DNA. In this context, it has been suggested that phosphorylation at S102 enhances the binding of YB-1 to ErbB2 promoter thereby increasing the transcription of the *ErbB2* gene (Stratford et al. 2008; Wu et al. 2006). Moreover, this modification can facilitate the shuttling of YB-1 to the nucleus (Gieseler-Halbach et al. 2017; Sutherland et al. 2005). However, a previous study was able to show that once YB-1 is phosphorylated at S102, whether induced by IR, epidermal growth factor (EGF) treatment, or the conditional expression of $KRAS^{G12V}$, it does not translocate to the nucleus (Tiwari et al. 2018). This discrepancy in findings may be due to differences in the stimuli used and the specific patterns of PTMs required for YB-1 nuclear translocation.

Apart from S102 phosphorylation, other phosphorylation sites may also influence both the function and localization of YB-1. For example, a study reported that when YB-1 is phosphorylated at S209, YB-1 does not enter the nucleus even when S102 is phosphorylated (Sogorina et al. 2022). Given that S209 phosphorylation is located on the NLS, it may affect the accessibility of the NLS for translocation to the nucleus. Similar to this report, two other phosphorylation sites *i.e.*, at S165 and S176 have been discovered to decrease NLS exposure and subsequently impair YB-1 shuttling to the nucleus (Mehta et al. 2020). In addition, it has been reported that YB-1 translocates to the nucleus in *JAK2* mutated cells to regulate *MKNK1* gene splicing. Interestingly, in this study, subcellular localization of YB-1 has been identified to be controlled by S30 and S34 phosphorylation (Jayavelu et al. 2020). Furthermore, a new study has proposed that threonine 89 (T89) phosphorylation on YB-1 following IR and cisplatin, which is mediated by DNA-PKcs, results in nuclear transfer of YB-1 (Nöthen et al. 2023).

As a multifunctional oncoprotein, YB-1 has a broad role in tumor progression. An efficient and controlled cell cycle is required for the cells. It has been reported that YB-1 controls the cell cycle by regulating the expression of certain genes involved in the cell cycle such as cyclin A, cyclin B1, cyclin D, and E2F transcription factor (Fujiwara-Okada et al. 2013; Jurchott et al. 2003; Lasham et al. 2012). In line with this finding, knocking out *YBX1* in mouse models of TNBC and lung cancer significantly decreased tumor growth (Lasham et al. 2012; Tiwari et al. 2020).

Early evidence for the involvement of YB-1 in DNA repair comes from a study by Hasegawa et. al. (Hasegawa et al. 1991), which showed that YB-1 is capable of binding to DNA and preferentially to the depurinated DNA. Notably, this binding was not sequence-specific (Hasegawa et al. 1991). This was further supported by the other study showing that YB-1 recognizes and binds to cisplatin-modified DNA (Ise et al. 1999). Furthermore, Izumi et al. (Izumi et al. 2001) has reported that YB-1 has $3' \rightarrow 5'$ exonuclease activity through CSD region (Izumi et al. 2001). Interestingly, YB-1 has been shown to have strand separation activity on the DNA that is dependent on its CTD region (Guay et al. 2008). Another study reported that YB-1 physically interacts with some DNA damage and repair proteins, namely Ku80, MSH2, DNA polymerase δ, and WRN (Gaudreault et al. 2004). In addition, the interaction of YB-1 with proliferating cell nuclear antigen (PCNA) was observed by Ise et al. (Ise et al. 1999). YB-1 also causes resistance to CRT by impairing DNA repair mechanisms after CRT. In line with this, an in vitro study showed that knockdown of YB-1 impaired the repair of DSBs and sensitized breast cancer cells to IR (Toulany et al. 2011). Another study demonstrated that after DNA damage, YB-1 is cleaved by proteolysis and the C-terminal truncated YB-1 accumulates in the nucleus and binds to Mre11 and Rad50 (Kim et al. 2013).

These observations collectively strengthen the concept that YB-1 plays a role in DNA repair.

In *KRAS*-mutated tumors, YB-1 is constitutively phosphorylated at S102. Therefore, YB-1 can be considered an oncoprotein with potential prognostic value. In this context, it has been shown that YB-1 expression and nuclear localization are higher in pancreatic cancer compared to the normal tissues (Lu et al. 2017b), and this was associated with lymphatic/venous invasion (Shinkai et al. 2016). Additionally, a study by Shiraiwa et al. (Shiraiwa et al. 2016) has shown the association of nuclear YB-1 expression with reduced RFS in CRC. Interestingly, cytoplasmic YB-1 expression was found to be elevated in rectal cancer tissues (Zhang et al. 2015). In lung cancer, YB-1 expression was found to correlate with poor prognosis in nearly 50% of tumors (Gessner et al. 2004; Jiang et al. 2017; Shibahara et al. 2001). In addition, there are a number of studies that have also demonstrated the prognostic value of YB-1 in other tumor entities (Chao et al. 2016; Fushimi et al. 2013; Sheridan et al. 2015; Shibahara et al. 2001; Sinnberg et al. 2012; Song et al. 2014; Yan et al. 2014). Taken together, these studies have highlighted the prognostic value of YB-1 in various tumor entities that may play a role in the response to therapy.

As mentioned above, YB-1 phosphorylation at S102 is the most well-studied PTM in YB-1. This phosphorylation plays a critical role in the function of YB-1 and is mainly regulated by AKT and p90 ribosomal S6 kinase (RSK) (Sutherland et al. 2005). Consequently, YB-1 serves as a pivotal point where the phosphoinositide-3-kinase (PI3K) and mitogen-activated protein kinase (MAPK) pathways, downstream of KRAS, intersect (Evdokimova et al. 2006; Stratford et al. 2008).

1.5 Signaling pathways regulating YB-1 phosphorylation at S102

As mentioned earlier, phosphorylation of YB-1 at S102 plays a significant role in its functionality. This phosphorylation is majorly regulated by the two key serine/threonine protein kinases RSK and AKT (Sutherland et al. 2005; Evdokimova et al. 2006; Stratford et al. 2008) in the MAPK and PI3K pathways respectively.

1.5.1 MAPK/ERK pathway

This signaling pathway is triggered by RTKs, including EGFR, platelet-derived growth factor receptor (PDGFR), fibroblast growth factor receptor (FGFR), insulin receptor,

and vascular endothelial growth factor receptor (VEGFR) (Hubbard et al. 2007). These receptors are activated by ligand binding and IR, which causes receptor oligomerization. Afterward, the oligomerization facilitates the autophosphorylation of tyrosine residues in the cytosolic domain of these RTKs (Hubbard et al. 2007) (Fig. 4). Upon RTK phosphorylation, growth factor receptor-bound protein 2 (Grb2) binds via its Src homology 2 (SH2) domain to the phosphorylated tyrosine and via its Src homology 3 (SH3) domain binds to Son of Sevenless (SOS), a GEF that regulates RAS activity. Thereafter, the activated RAS binds and phosphorylates the serine/threonine protein kinase Rapidly Accelerated Fibrosarcoma (RAF). A series of serine/threonine protein kinases are then phosphorylated and activated. Following RAF activation, RAF phosphorylates and activates MAPK kinase (MEK), which further leads to phosphorylation and activation of extracellular signal-regulated kinase (ERK). ERK can act as a transcription factor (TF) to further regulate the expression of target genes that are involved in cell growth and proliferation, differentiation, and survival (Korzeniecki et al. 2021; Wagle et al. 2018). In addition, ERK phosphorylates downstream targets including RSK which has 4 isoforms; RSK1, RSK2, RSK3 and RSK4. Interestingly, activated RSK phosphorylates YB-1 at S102 (Stratford et al. 2008).

In *KRAS* mutated tumors, this pathway is constitutively active which causes the cells to become more dependent on the MAPK pathway (Lee et al. 2019). This was also supported by the data showing that in *KRAS* mutated cells when YB-1 is highly phosphorylated, the cells rely on the MAPK/RSK pathway (Tiwari et al. 2020).

1.5.2 PI3K/AKT signaling pathway

The phosphatidylinositol 3-kinase (PI3K)/protein kinase B/AKT signaling pathway regulates multiple cellular processes such as cell cycle, cell growth, and proliferation (Fig. 5). PI3K has three classes, including class I, class II, and class III. In total there are eight isoforms of PI3K and among them, type I is the most well-studied isoform that has been shown to be involved in tumor development (Vanhaesebroeck et al. 2010). Class I has 2 subunits; the catalytic subunit p110 and the regulatory subunit p85. Mechanistically, similar to the MAPK/ERK pathway, the PI3K/AKT pathway is also induced by the binding of growth factors to the RTKs, resulting in the binding of the PI3K to the phosphorylated tyrosine residues on the cytosolic domain of the RTKs. In addition, activated RAS can also activate PI3K (Shi et al. 2019). Once activated, PI3K changes phosphatidylinositol (3,4)-bisphosphate (PIP2) lipids to phosphatidylinositol (3,4,5)-trisphosphate (PIP3). PIP3 acts as a docking site to which AKT binds, allowing Phosphoinositide-dependent kinase-1 (PDK1) to phosphorylate AKT at T308. This phosphorylation leads to partial activation of AKT, which further activates mTORC1,

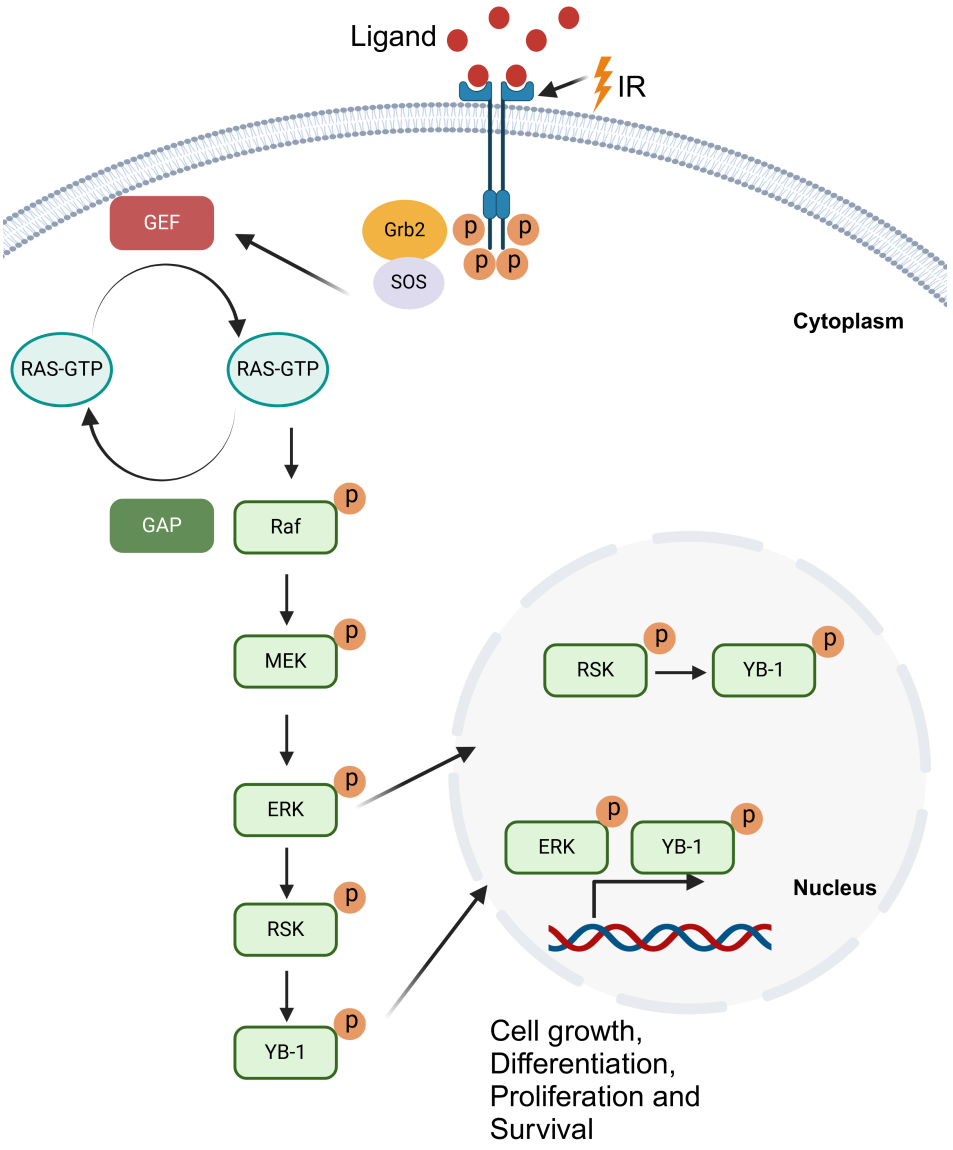

Figure 4: MAPK/ERK/RSK pathway. Ligand binding to the receptors and exposure to IR induce dimerization and activation of the RTKs resulting in autophosphorylation of tyrosine residues in the cytoplasmic domain of RTKs. Once phosphorylated, Grb2 binds to the phosphorylated tyrosine to make a docking site for SOS binding. This results in RAS activation which further induces a cascade of phosphorylation and activation of the kinases resulting in the regulation of the genes involved in cell growth, differentiation, proliferation, and survival. ERK extracellular signal-regulated kinase, GAD GTPase-Activating Proteins, GEF Guanine nucleotide exchange factors, Grb2 Growth factor receptor-bound protein 2, IR ionizing irradiation, MEK MAPK kinase, RAF Rapidly Accelerated Fibrosarcoma, P Phosphate, RSK P90 Ribosomal S6 kinase, SOS Son of sevenless, YB-1 Y-box binding protein 1. Created with BioRender.com.

which is involved in protein translation. In addition, mTORC2 phosphorylates AKT at S473, leading to full activation of AKT. Fully active AKT mediates various cellular activities such as the induction of angiogenesis, growth, proliferation, and survival (Hemmings et al. 2012). It has been reported that activated AKT, can also phosphorylate YB-1 at S102 as well (Bader et al. 2008; Evdokimova et al. 2006).

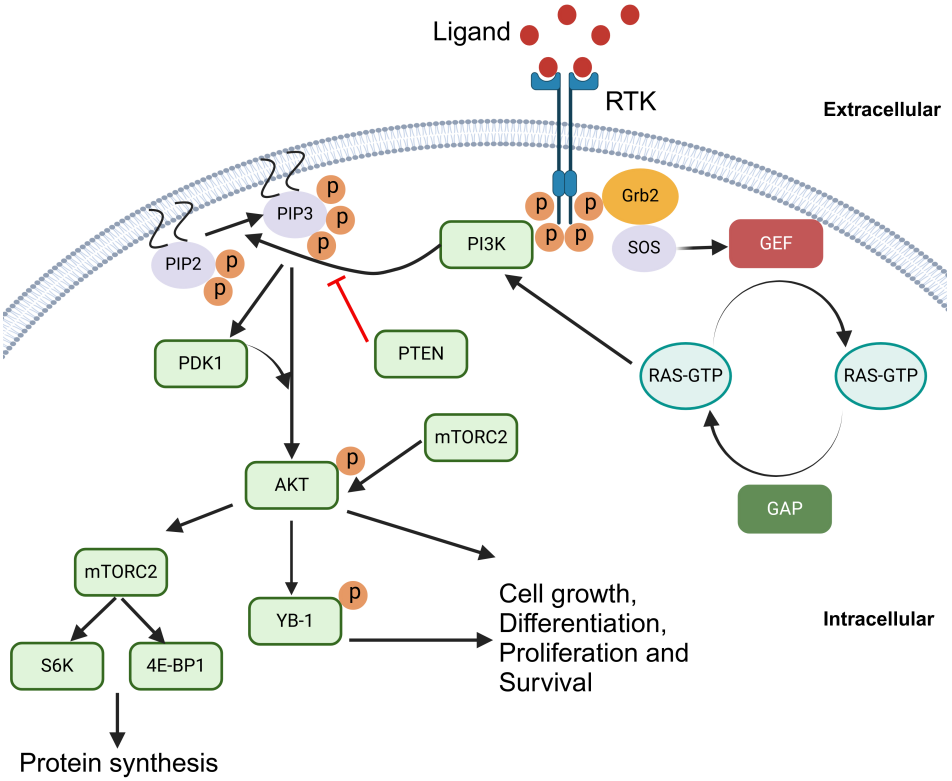

Figure 5: PI3K/AKT pathway.PI3K is activated by ligands such as growth factors or by RAS. Upon binding and dimerization and thus activation, PI3K binds to the phosphorylated tyrosine residue of the cytoplasmic part of the RTKs. This binding activates PI3K, which further converts PIP2 to PIP3. AKT binds to the PIP3 docking site at the plasma membrane where PDK1 phosphorylates it at T308. For full activation, AKT is further phosphorylated S473 by mTORC2. Activated AKT has a role in regulating physiological processes in a YB-1-dependent or independent manner. Furthermore, AKT activates mTORC1 which plays a crucial role in protein synthesis. AKT Protein kinase B, 4E-BP1 Eukaryotic translation initiation factor 4E-binding protein 1 GAD GTPase-Activating Proteins, GEF Guanine nucleotide exchange factors, Grb2 Growth factor receptor-bound protein 2, mTORC2 mammalian target of rapamycin complex 1, P Phosphate, PDK1 Phosphoinositide-dependent kinase-1, PI3K Phosphoinositide 3-kinase, PIP2 Phosphatidylinositol 4,5-bisphosphate, PIP3 Phosphatidylinositol (3,4,5)-trisphosphate, S6K S6 kinase, SOS Son of sevenless, YB-1 Y-box binding protein 1. Created with BioRender.com.

1.5.3 The p21-activated kinase family of proteins

The p21-activated kinases (PAK) are a family of conserved serine/threonine kinases that play a role in regulating various signaling pathways. PAKs are involved in the regulation of the cytoskeleton and actin polymerization (Fig. 6). PAKs are upregulated in different cancer entities and apart from their role in cytoskeleton remodeling, it has been reported that PAKs are involved in cell survival by upregulating anti-apoptotic proteins (Kumar et al. 2006). In addition, PAKs mediate growth factor signaling, cell migration, and tumor progression (Kumar et al. 2006). Based on their structural similarities, this family of proteins has been categorized into two groups; group I includes PAK1, PAK2,

and PAK3, and group II includes PAK3, PAK4, and PAK6 (Rudolph et al. 2015). PAK1 is the most well-studied isoform which is regulated by small GTPases cell division cycle 42 (CDC42) and Ras-related C3 botulinum substrate 1 (RAC1) (Manser et al. 1994). In line with this, studies have shown that RAS is involved in cytoskeleton remodeling through the TIAM1/RAC/PAK axis (Takács et al. 2020a). In addition, PAK1 can be regulated by PI3K, PDK1, and AKT (King et al. 2000; Tang et al. 2000; Tsakiridis et al. 1996). PAK1 itself is reported to be involved in regulating both PI3K and MAPK signaling pathways (Beeser et al. 2005; Lu et al. 2017a). In line with this, PAK has been shown to be involved in the controlling of RAF, MEK, and ERK kinases (Eblen et al. 2002; Higuchi et al. 2008; Park et al. 2007). Consequently, PAK proteins may also be a potential regulatory point in the signaling pathways that govern the phosphorylation of YB-1 at S102.

1.6 Targeting KRAS/YB-1 cascade

As mentioned earlier, *KRAS* mutations are the key factors in resistance to CRT, highlighting the importance of targeting KRAS. Comprehensive reviews outline various approaches to KRAS targeting (Khozooei et al. 2023; Singhal et al. 2024). Due to some intrinsic features, targeting KRAS is challenging. These features include conformational dynamics between active and inactive states which highlights the need for selective modulation of this balance. In addition, the high concentration of intracellular GTP, and thus the strong affinity of KRAS for GTP, impedes the use of GTP-competitive inhibitors. Furthermore, the lack of binding pockets on the KRAS also makes drug development complicated (Singhal et al. 2024). However, a number of different approaches that have been developed to inhibit KRAS, including targeting of KRAS PTMs with farnesyltransferase inhibitors (FTIs) in combination with geranylgeranyl transferase 1 inhibitors (GGTIs) (Hahn et al. 2002; Martin et al. 2004), inhibiting nucleotide exchange factors such as SOS1 inhibitors (Gort et al. 2020), blocking downstream pathways such as the MAPK and PI3K pathways (Toulany et al. 2016; Toulany et al. 2014; Wee et al. 2009), and using mutant-specific KRAS inhibitors such as sotorasib (Lanman et al. 2020) and adagrasib (McCormick 2020), which are specific against $KRAS^{G12C}$. In addition, other allele-specific inhibitors such as MRTX1133 against $KRAS^{G12D}$ have been developed and this drug is in phase I clinical trials (Wang et al. 2022). Overall, these strategies are being developed to overcome KRAS-mediated resistance and therefore to have better outcomes.

However, since YB-1 phosphorylation at S102 is mediated by KRAS, and YB-1 plays a pivotal role in tumor progression, another strategy to overcome *KRAS* mutated tumors

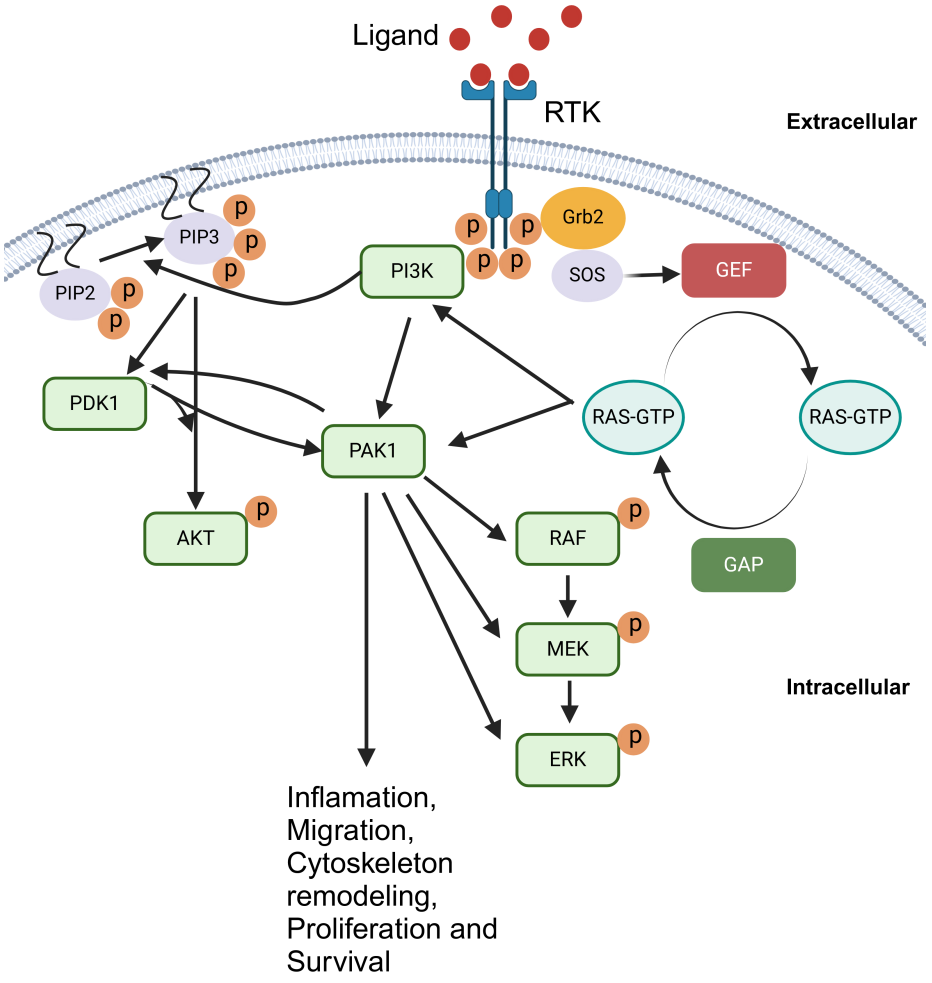

Figure 6: PAK1 as a cross point in the PI3K and MAPK pathways.PAK1 can be regulated by RAS, PI3K, PDK1 and AKT. It has ability to activate MEK and ERK independent of RAF induction. Furthermore, PAK1 stimulates PDK1, creating a positive loop where PDK1 may further activate PAK1. The activation of PAK1 influences many physiological processes such as inflammation, Migration, Cytoskeleton remodeling, proliferation, and cell survival. AKT Protein kinase B, ERK extracellular signal-regulated kinase, GAD GTPase-Activating Proteins, GEF Guanine nucleotide exchange factors, Grb2 Growth factor receptor-bound protein 2, MEK MAPK kinase, mTORC2 mammalian target of rapamycin complex 1, RAF Rapidly Accelerated Fibrosarcoma, P Phosphate, PDK1 Phosphoinositide-dependent kinase-1, PI3K Phosphoinositide 3-kinase, PIP2 Phosphatidylinositol 4,5-bisphosphate, PIP3 Phosphatidylinositol (3,4,5)-trisphosphate, S6K S6 kinase, SOS Son of sevenless. Created with BioRender.com

is to target YB-1. Table 1, summarizes the strategies that can target YB-1 directly or indirectly through upstream signaling pathways. Most of the approaches are in the preclinical stages, but there are a number of strategies that are in the clinical phases. In addition, a summarized schematic (Fig. 7) describes the targeting strategies of YB-1.

Table 1: Targeting YB-1 directly and indirectly by different inhibitors and their outcomes.

Targeting strategy	**Tumor**	**Inhibitor**	**Study outcome**	**Ref.**
Dual targeting of PI3K/AKT and MAPK/RSK pathways	Breast Cancer, Colorectal Cancer	Dual targeting of AKT and RSK inhibitors	Decreases YB-1 S102 phosphorylation, Chemosensitizes to 5-Fu and Radiosensitizes *in vitro*.	(Lettau et al. 2021; Maier et al. 2019)
	Prostate Cancer	RSK inhibitor PMD-026	Decreases YB-1 S102 phosphorylation, decreases AR-V7 mRNA, inhibits cell proliferation, enhances apoptosis *in vitro*, blocks tumor progression *in vivo*.	(Ushijima et al. 2022)
	Advanced or metastatic breast cancer	Multikinase inhibitor TAS0612 against AKT, p70S6K and RSK	Decreases S102 YB-1, inhibits cell cycle, enhances sensitivity to tamoxifen and fulvestrant, impairs tumor progression *in vivo*. Currently in phase I clinical trial (NCT04586270).	(Shibata et al. 2020)
Targeting the switch points between PI3K/AKT and MAPK/RSK pathways	*KRAS*-mutated NSCLC	FAK inhibitor as a switch point between PI3K/AKT and MAPK/RSK pathway	Enhances radiosensitivity.	(Tang et al. 2016)

	AR-positive TNBC	Ceritinib as an ALK inhibitor + enzalutamide	Decreases cell proliferation *in vitro* and *in vivo* through reducing S102 YB-1 in FAK/YB-1 signaling.	(Dong et al. 2022)
Impairing mRNA binding of YB-1	Breast Cancer Brain Metastasis	Abelson (ABL) inhibitors	Blocks YB-1 phosphorylation at Y72 and Y99, reducing binding of YB-1 to ErbB2 mRNA, thus blocking ErbB2 expression and inhibiting metastatic outgrowth.	(Khatri et al. 2019)
Natural compounds that target YB-1	TNBC	Luteolin as a RSK1/RSK2 inhibitor	Blocks YB-1 S102 phosphorylation, increases apoptosis when combined with paclitaxel.	(Lin et al. 2008; Reipas et al. 2013)
	Liver Cancer	7-Hydroxyindirubin (7-HI)	Increases anticancer properties of actinomycin D.	(Tanaka et al. 2021)
	Breast Cancer	Aloe-emodin (AE)	Inhibits YB-1 expression, cell migration and invasion. Blocks cancer stem cell proliferation *in vitro* and inhibits tumor progression *in vivo*.	(Ma et al. 2016)

Targeting YB-1 directly	Ovarian Cancer	Niraparib	Binds to YB-1 and impairs YB-1-RNA interactions. Currently in clinical trial phase II (NCT02657889).	(El Hage et al. 2023)
	Ovarian Cancer	SU056	Inhibits cell proliferation. When combined with paclitaxel, has a synergistic effect *in vitro* and *in vivo*.	(Tailor et al. 2021)
	Breast Cancer	2,4-Dihydroxy-5-pyrimidinyl imidothiocarbamate (DPI)	Directly inhibits YB-1 and induces apoptosis. Sensitizes cancer cells to Doxorubicin.	(Gunasekaran et al. 2018)
	Renal Damage and Fibrosis	HSc025	Binds to the CTD of YB-1, induces YB-1 nuclear translocation, and impairs YB-1 function in stabilizing Col1a1 mRNA in the cytoplasm, reducing renal damage and fibrosis.	(Higashi et al. 2011; Wang et al. 2016)
	Breast and Prostate Cancer	YB-1 blocking peptide	Interferes with S102 phosphorylation of YB-1, sensitizing cells to trastuzumab and IR *in vitro*.	(Law et al. 2010; Lettau et al. 2021)

Fisetin (3,7,3',4'-tetrahydroxyflavone) (Fig. 8), is a plant-based polyphenol that has been shown to have anti-cancer effects in several cancer entities. Different sources contain fisetin, including grapes, onions, strawberries and apples (Lall et al. 2016). The effects of fisetin on various cancer entities have been investigated (Adan et al. 2015; Kuntz et al. 1999; Li et al. 2011; Sechi et al. 2018; Suh et al. 2010; Yang et al. 2012; Ying et al. 2012; Zhuo et al. 2015) and reviewed (Lall et al. 2016; Rahmani et al. 2022) as shown in Fig. 9.

Interestingly, fisetin was found to bind to the CSD of YB-1 (Fig. 10), where phosphorylation occurs at S102. Mechanistically, fisetin binds to the $\beta_1 - \beta_4$ strand in the CSD. Molecular docking of fisetin with YB-1 shows that fisetin has a strong affinity for the residues valine 63 (Val63), lysine 64 (Lys64), tryptophan 65 (Trp65), phenylalanine (Phe66), isoleucine (Ile91), Gly104, aspartic acid 105 (Asp105), Gly106, and Glu107 residues. In particular, amino acid residue Trp65 is considered to be the binding packet (Khan et al. 2014). Interestingly, fisetin forms a trinary complex with S102 and Glu107, which could potentially disrupt S102 phosphorylation. In addition, the binding of fisetin to the CSD prevents the interaction of AKT with YB-1 (Khan et al. 2014).

Interestingly, in melanoma cells, fisetin exhibits a stronger affinity to bind to RSK2 compared to other RSK isoforms, thus decreasing RSK kinase activity. Furthermore, fisetin facilitates the binding of RSK2 to YB-1 to form a trinary complex. However, this complex is postulated to stabilize the RSK2-YB-1 interaction, which in turn interferes with YB-1 phosphorylation at S102 (Sechi et al. 2018).

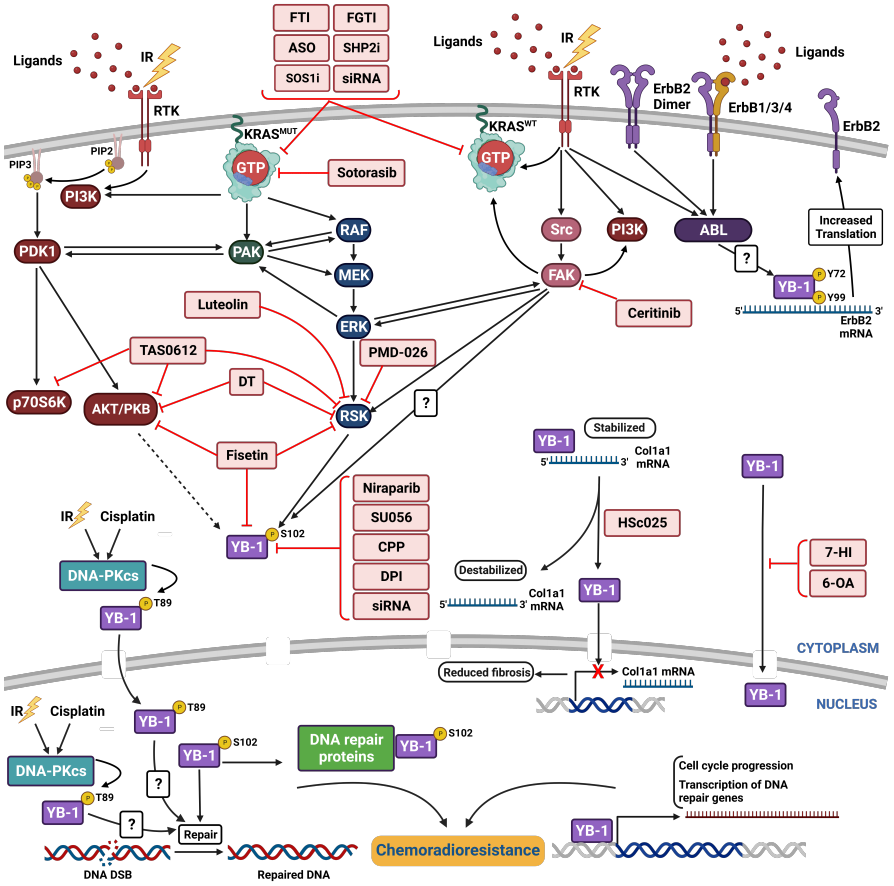

Figure 7: Targeting approaches in KRAS/YB-1 axis. S102 phosphorylation of YB-1 is predominantly controlled by MAPK/RSK and PI3K/AKT pathways. In *KRAS* mutated cells, the MAPK/RSK pathway mainly regulates YB-1 phosphorylation at S102. Phosphorylation of YB-1 at S102 has been shown to be involved in DNA repair and thus CRT resistance. In addition to the S102 phosphorylation, other phosphorylations are also induced which may involve in resistance to CRT. For example, DNA-PKcs activation following DNA damage may phosphorylate YB-1 at T89 in, which can be shuttled to the nucleus. In addition, another mechanism of YB-1-mediated CRT resistance may be through its function as a transcription factor that may regulate the expression of different DNA repair and cell cycle genes. Furthermore, YB-1 phosphorylation at Y72 and Y99 is induced by ABL kinase which causes increased binding of YB-1 as a translation activator to the ErbB2 mRNA. Different strategies to interfere with KRAS/YB-1 signaling are shown in red boxes. The question mark (?) indicates unknown mechanisms. 6-OA 6-O-Angeloylplenolin, 7-HI 7-hydroxyindirubin, ABL Abelson family of tyrosine kinases, AKT/PKB Protein kinase B, ASO Antisense oligonucleotide, Col1A1 collagen 1(I), CPP 9-mer cell permeable peptide, DPI 2,4-Dihydroxy-5-pyrimidinyl imidothiocarbamate, DNA-PKcs DNA-dependent protein kinase catalytic subunit, DSB Double strand break, DT Dual targeting, ERK Extracellular signal-regulated kinase, FAK Focal adhesion kinase, FTI Farnesyltransferase inhibitor, GGTI Geranylgeranyltransferase 1 inhibitor, GTP Guanosine triphosphate, IR Ionizing radiation, KRAS Kirsten Rat Sarcoma Viral Oncogene Homologue, MEK MAPK kinase, mRNA Messenger RNA, MUT Mutant, P Phosphate group, p70S6K p70 ribosomal S6 kinase, PAK p21-activated family of protein kinases, PDK1 Phosphoinositide-dependent kinase-1, PI3K Phosphoinositide 3-kinase, PIP2 Phosphatidylinositol 4,5-bisphosphate, PIP3 Phosphatidylinositol (3,4,5)-trisphosphate, RAF Rapidly activated fibrosarcoma kinase, RSK p90 ribosomal S6 kinase, RTK Receptor tyrosine kinase, S102 Serine 102, SHP2i Src homology-2 domain-containing protein tyrosine phosphatase-2 inhibitor, Src SRC Proto-Oncogene, siRNA small interfering RNA, SOS1i Son of sevenless 1 inhibitor, WT Wild-type, Y72 Tyrosine 72, Y99 Tyrosine 99, YB-1 Y-box binding protein 1, ? Unknown effector. Black arrows indicate the direction of the signaling cascade, and the red arrows are the inhibitory signals. (Adopted from Khozooei et al. 2023).

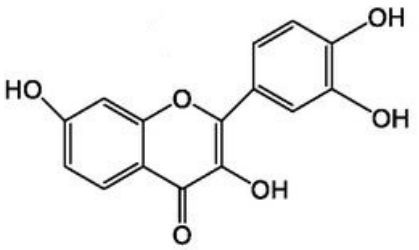

Figure 8: Chemical structure of fisetin. Modified after (Grynkiewicz et al. 2019).

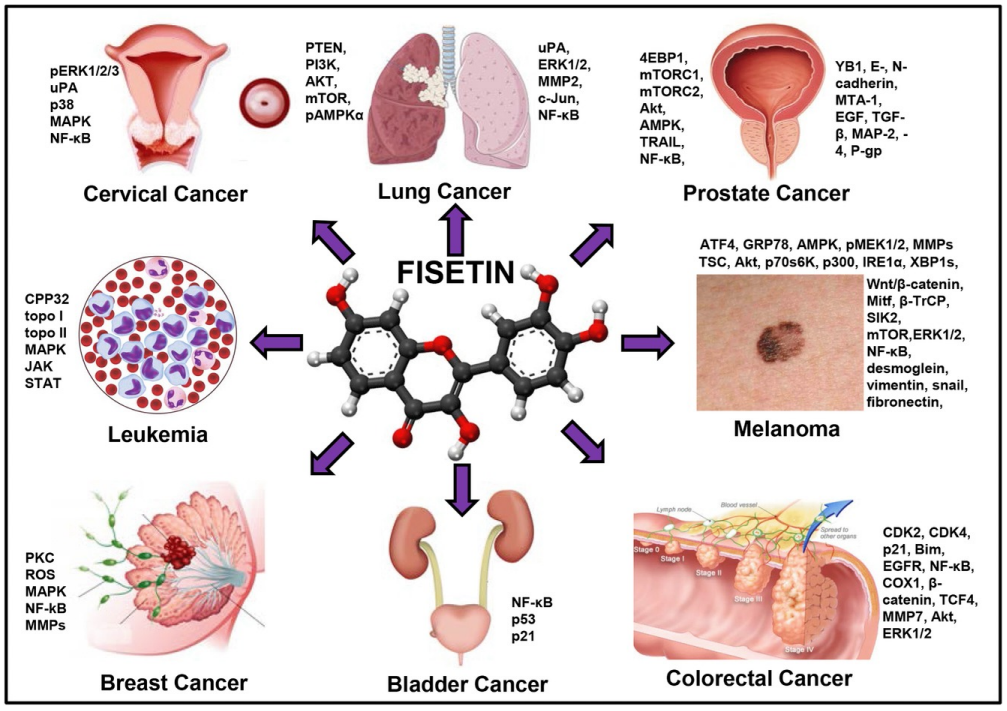

Figure 9: Anti-cancer effects of fisetin. Adopted from (Lall et al. 2016).

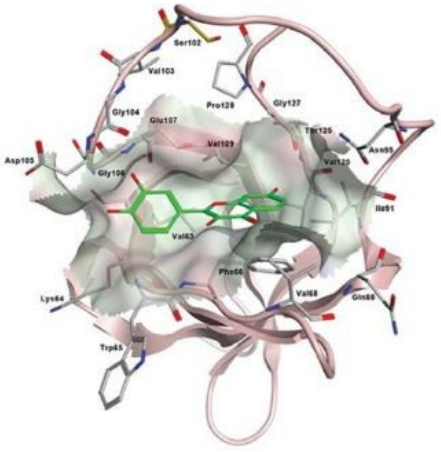

Figure 10: Fisetin (green) docking to CSD of YB-1.
Modified after (Khan et al. 2014).

Chapter 2

Aim of the study

YB-1 is a multifunctional oncoprotein that is overexpressed in different tumor entities and is implicated in different cancer hallmarks. YB-1 overexpression is linked to therapy resistance, leading to reduced OS. *KRAS* gain-of-function mutation and exposure to IR, induce YB-1 phosphorylation at S102. Previous research from our laboratory indicates that enhanced YB-1 phosphorylation at S102 stimulates the repair of IR-induced DSBs, thereby causing radioresistance. In addition, YB-1 is highly phosphorylated in *KRAS* mutated tumor cells, including TNBC and CRC cells.

One of the approaches to target YB-1 is by targeting its upstream signaling pathways. It has been shown that YB-1 phosphorylation at S102 in *KRAS* mutated cells, is mediated by RSK. Therefore, targeting RSK may be a promising approach, especially in cells with mutations in the RAS pathway. Previously, it has been reported that targeting RSK in breast cancer cells blocks YB-1 phosphorylation at S102 in both irradiated and non-irradiated cells. However, activation of AKT following RSK inhibition, or constitutive activation of AKT in cells with *PIK3CA* mutation, undermines the efficacy of RSK targeting. Interestingly, dual inhibition of both RSK and AKT has shown promising results, although toxicity issues need to be evaluated.

In the initial phase of the project, we aimed to utilize fisetin, known to interfere with RSK-mediated YB-1 phosphorylation in melanoma cells, to further validate this effect in TNBCs *in vitro*. Subsequently, we sought to combine fisetin with IR to determine whether we could enhance the radiosensitivity of the TNBCs and investigate the underlying mechanisms of fisetin-mediated radiosensitization.

In the second part of the thesis, our objectives were to further expand the therapeutic potential of fisetin in CRC cells *in vitro* and *ex vivo*, and to evaluate its benefits, particularly in *KRAS* mutated cells.

Chapter 3

Results and Discussion

3.1 Publication I: Fisetin induces DNA double-strand break and interferes with the repair of radiation-induced damage to radiosensitize triple negative breast cancer cells (Khozooei et al. J Exp Clin Cancer Res. 2022;41:256)

TNBC is an aggressive form of breast cancer that is associated with poor treatment outcomes. In addition to surgery, radiotherapy remains one of the main approaches for improving patient survival over the long term. However, following radiotherapy, tumors frequently become resistant thereby interfering with the efficacy of the therapy. Consequently, targeting the mechanisms involved in radioresistance in TNBCs along with radiotherapy may result in enhanced treatment response. YB-1, an oncoprotein, has been shown to play a critical role in different cancer hallmarks, particularly in cell death resistance mechanisms. YB-1 is regulated by two main kinases, namely RSK and AKT, which phosphorylate YB-1 at S102 (Lettau et al. 2021). This phosphorylation and subsequent activation of YB-1 result in its role in stimulating IR-induced DNA DSB repair (Lettau et al. 2021). It has been previously demonstrated that the single targeting of RSK leads to activation of AKT (Lettau et al. 2021; Maier et al. 2019). The activated AKT is known to be directly involved in the DSB repair by binding to DNA-PKcs (Toulany et al. 2008; Toulany et al. 2012; Toulany et al. 2015). This, in turn, serves to minimize the effect of RSK targeting. Therefore, dual targeting of both AKT and RSK has been investigated in breast cancer and CRC cells, showing that it is more effective in inhibiting cell proliferation and blocking the DNA DSB repair which in turn induces radiosensitization and chemosensitization (Lettau et al. 2021; Maier et al. 2019). However, due to toxicity issues regarding targeting AKT and RSK, an alternative approach to target YB-1 is necessary. Fisetin is a plant flavonoid compound

that has been shown to interrupt RSK-mediated YB-1 phosphorylation and activity. In this study, we sought to elucidate the potential targets of fisetin in TNBC cells and investigate the effect of fisetin on DSB repair and radiation response.

3.1.1 Fisetin inhibits YB-1 and AKT phosphorylation in a cell line-dependent manner

First of all, the cells were authenticated, confirming that all TNBCs tested were negative for ER and PR, unlike the MCF-7 and T47D cell lines, which are classified as ER+/PR+ (Fig. S1). The association between the phosphorylation levels of YB-1 (S102), RSK (T359/S363), and the total protein level of RSK2 is illustrated in Fig. S1. The association between the phosphorylation levels of YB-1 (S102), RSK (T359/S363), and the total protein level of RSK2 is illustrated in Fig. S1. It has been reported that fisetin interferes with RSK-mediated YB-1 phosphorylation at S102 in the range of 20 to 80 µM in melanoma cells. In this study, the impact of fisetin treatment with concentrations ranging from 12.5 to 75 µM on the phosphorylation levels of YB-1 (S102) and AKT (S473) was investigated in TNBC cells, including MDA-MB-231, MDA-MB-453, HS 578T, and MDA-MB-468, over a 24-hour period. Fisetin significantly reduced YB-1 S102 phosphorylation in MDA-MB-231 and MDA-MB-453 cells in a dose-dependent manner, without affecting the YB-1 expression level (Fig. 1). It is noteworthy that, in HS 578T cells, high concentrations of fisetin (50 and 75 µM) were observed to reduce both YB-1 phosphorylation at S102 and expression. This effect was not observed in MDA-MB-468 cells. Most importantly, fisetin did not induce AKT phosphorylation at S473 in any of the TNBCs compared to RSK inhibitor LJI308 (Lettau et al. 2021; Maier et al. 2019). However, AKT phosphorylation in MDA-MB-231 cells was even decreased. Notably, the effect of fisetin was specific to the TNBCs, with no impact on HSF-7 normal human fibroblast cells. In HSF-7 cells, YB-1 phosphorylation was decreased very slightly in fisetin concentrations of 25 and 50 µM (Fig. 1).

The TNBCs used in this study have distinct mutations in the PI3K/AKT and MAPK/RSK pathways, as detailed in Table S2. The analysis of the basal level of phosphorylation of YB-1, AKT, and RSK, in addition to the expression of RSK isoforms, indicates that the phosphorylation of YB-1 at S102 is linked to the expression of RSK1 and RSK2 isoforms as well as phosphorylation level of RSK at T359/S363 (Fig. S1). A comparative analysis of TNBCs, namely MDA-MB-231 and MDA-MB-468 cells, revealed that the phosphorylation level of RSK is higher in cells with elevated YB-1 phosphorylation. On the other hand, in MDA-MB-453 and HS578T cells, where AKT S473 is highly phosphorylated, YB-1 phosphorylation at S102 is low. These findings suggest that YB-1 is mainly regulated by RSK in TNBCs, emphasizing on RSK as a critical candidate for

YB-1 targeting. According to previous studies, fisetin inhibits YB-1 S102 in melanoma cancer cells (Sechi et al. 2018), and interferes with PI3K/AKT pathway in breast cancer cells (Sun et al. 2018). In the present study, fisetin was used as an alternative approach to target both AKT and RSK to inhibit YB-1 phosphorylation. Our data is in line with the reported study on the effect of fisetin on YB-1 phosphorylation (Sechi et al. 2018).

3.1.2 Fisetin mimics RSK pharmacological inhibitors in terms of inhibiting YB-1 phosphorylation

Given the lack of effect of fisetin on the reduction of YB-1 phosphorylation at S102 in MDA-MB-468 cells, we sought to investigate whether this is due to its lack of effect on RSK activity. To test this hypothesis, we treated the MDA-MB-468 cells with fisetin (75 µM) in addition to two RSK inhibitors, namely LJI308 (LJI) and BI-D1870 (BID), each at 2.5 µM for 24 h. For comparison, we also treated MDA-MB-231 cells where we had previously observed the effect of fisetin on YB-1 phosphorylation (Figs. 2A-B). Our data shows that fisetin, similar to the other two RSK inhibitors, reduced YB-1 phosphorylation at S102 in MDA-MB-231 cells. However, in MDA-MB-468 cells, fisetin similar to BID, could not reduce YB-1 S102 phosphorylation. Interestingly, LJI with lower IC50 compared to BID (Aronchik et al. 2014), inhibited YB-1 S102 slightly in both cytoplasm and nucleus (Figs. 2A-B). These findings suggest that RSK represents a primary target of fisetin. Moreover, fisetin exerts a similar effect on cells as that observed with RSK inhibitors. When the cells are exposed to IR, DNA DSB occurs leading to the phosphorylation of YB-1 at S102 (Lettau et al. 2021; Toulany et al. 2011). However, in cells harboring *KRAS* gain-of-function mutation or *PTEN* loss-of-function mutation, YB-1 is constitutively phosphorylated at S102 and this phosphorylation in these cells is not further induced (Toulany et al. 2011). Therefore, we aimed to investigate whether the effect of fisetin is altered in irradiated MDA-MB-231 with *KRAS* mutation and MDA-MB-468 cells with *PTEN* mutation (Jang et al. 2010). As shown in Fig. 2C, both cells represent a high level of YB-1 phosphorylation at S102, which is not induced more by IR. Interestingly, similar to the non-irradiated conditions, fisetin inhibited YB-1 phosphorylation at S102 only in MDA-MB-231 cells (Fig. 2C).

In MDA-MB-468 cells, fisetin, similar to RSK inhibitors, did not affect YB-1 phosphorylation at S102, showing that this phosphorylation is RSK-independent. In line with this observation, *PTEN* loss-of-function mutation in MDA-MB-468 cells, correlated with highly activated AKT making YB-1 phosphorylation at S102 to be AKT-dependent (Lettau et al. 2021).

3.1.3 Fisetin radiosensitizes TNBC cells, enhances the frequency of DSB in non-irradiated cells, and interferes with repair of IR-induced DSB

In a previous study conducted in our laboratory, it was shown that the dual targeting of AKT and RSK inhibits YB-1 phosphorylation at S102. This consequently interferes with the DNA DSB repair and radiosensitizes both TNBC and non-TNBC cells (Lettau et al. 2021). In this study, we sought to investigate whether interfering with YB-1 phosphorylation at S102 by fisetin is correlated with radiosensitization. The clonogenic assay was performed in three settings. (1) A single dose of 3 Gy was administered in conjunction with varying concentrations of fisetin in the range of 0 to 100 µM. (2) Different doses of IR from 0 to 4 Gy combined with 75 µM fisetin, and (3) fractionated IR (up to 5 fractions, 1 Gy per fraction) combined with fractionated fisetin concentration, (up to 5 fractions, each with 75 µM). The results show that fisetin radiosensitizes the TNBCs in all experimental settings (Fig. 3). Interestingly, fisetin alone in non-irradiated cells, is able to decrease the clonogenic activity of the MDA-MB-231 and MDA-MB.468 cells (Figs. S2A-B). According to the data obtained, we combined 75 µM of fisetin with fractionated irradiation. As data indicates in Fig. 3, fisetin enhanced radiosensitivity in all TNBCs in a cell line-dependent manner. IR induces RSK/YB-1 and PI3K/AKT prosurvival pathways, whereas, fisetin has the opposite effect, inhibiting RSK/YB-1 in melanoma (Sechi et al. 2018), PI3K/AKT in pancreatic cancer (Xiao et al. 2021), and YB-1 in TNBC (Fig. 1). It is therefore anticipated that the combination of fisetin and IR will result in reduction in clonogenic activity and radiosensitizing effect.

According to the data in Fig. 3, the most radioresistant cell line among the cells tested is HS 578T cells. When we compare the radiosensitization effect of fisetin in HS 578T cells in a fractionated setting with the single dose of IR, we conclude that in fractionation IR (where only 1 Gy is applied per day), HS 578T cells are able to repair the DSBs in a more efficient manner. However, when fisetin is combined with a higher dose of IR (4 Gy), the radiosensitization effect of fisetin is observed (Fig. S2C). It is important to note that fisetin when combined with IR, did not have a radiosensitizing effect on normal human fibroblast HSF-7 cells as illustrated in Fig. S2C.

YB-1, as an oncoprotein, has been shown to participate in DNA repair mechanisms through direct binding to several DNA repair proteins, namely MSH2, DNA polymerase delta, WRN, and Ku80. Alternatively, YB-1 has the ability to bind the DNA and RNA at the site of DNA damage. In addition, data from our laboratory show that blocking YB-1 S102 phosphorylation with a blocking peptide and knocking down of YB-1 with siRNA impairs the repair of IR-induced DSBs (Lettau et al. 2021; Toulany et al. 2011) (Fig. 4C). We thus sought to determine whether the disruption of S102 YB-1

phosphorylation by fisetin is associated with the inhibition of IR-induced DSB repair. TNBC cells were treated with different concentrations of fisetin ranging from 25 µM to 75 µM and the number of residual DSB was assessed 24 h after IR. The data in Figs. 4A-B indicate that fisetin increases the residual DSB when combined with IR in all TNBCs, independent of the effect of fisetin on YB-1 phosphorylation at S102, as fisetin was not effective in reducing YB-1 phosphorylation at S102 in MDA-MB-468 cells (Fig 1). This effect was related to the observed radiosensitization effect of fisetin (Fig. 3). More importantly, fisetin at the highest concentration (75 µM), did not block the repair of IR-induced DSB in HSF-7 cells. Conversely, at 25 µM fisetin stimulated DSB repair in HSF-7 cells. These results are consistent with the study showing that fisetin is able to exert radioprotective effects against γ -irradiation (Piao et al. 2013). Furthermore, fisetin was found to raise the levels of reduced glutathione (GSH), as a substrate for radical scavenging by glutathione peroxidase. Therefore, it protects the cells from H_2O_2-induced cell damage, thereby acting as an antioxidant in mouse hippocampal HT-22 and Chinese hamster lung fibroblast (V79-4) cells (Ishige et al. 2001; Kang et al. 2014).

To explore if fisetin affects DSB induction by IR, γH2AX foci, as a marker of DNA damage, were analyzed shortly after IR. In order to be able to count the γH2AX foci 30 min post IR, the cells were irradiated with 1 Gy rather than 4 Gy, thus reducing the level of damage to facilitate accurate counting. The data presented in Fig. S3A demonstrate that the pretreatment with 75 µM fisetin, increases γH2AX foci compared to mock-treated conditions. This suggests that fisetin may either induce DNA damage or block the repair of endogenous damages. These results are in line with the other studies, indicating the role of fisetin as a DNA damage inducer at concentrations similar to those used in this study, including in pancreatic cancer (50-100 µM) (Ding et al. 2020), hepatic cancer (60 µM) (Kim et al. 2010), and gastric cancer (50 µM) (Sabarwal et al. 2017). To better assess the interference of fisetin with DSB, the MDA-MB-231 and MDA-MB-468 cells were treated with fisetin at the concentrations of 25, 50, and 75 µM for 48 h, and the number of γH2AX foci was analyzed as shown in Fig. S3B. Fisetin induced DNA damage in both cells at the high concentration. Notably, lower concentrations (25 and 50 µM) also resulted in DNA damage induction in MDA-MB-468 cells, whereas no effect was observed in MDA-MB-231 cells. These data suggest that fisetin has a dual role of both inducing DNA damage in the cells and further impairing the repair of IR-induced DSB. To compare the effect of fisetin on the IR-induced DSB repair and to determine the extent to which this impact is dependent on YB-1, we knocked down YB-1 with siRNA and applied fisetin before IR. The impact of fisetin on DSB repair was more pronounced than that of YB-1 siRNA, and this effect was partially dependent on YB-1, as evidenced by the analysis of the number of γH2AX foci (Fig. 4C).

If damage is left unrepaired, it may result in chromosome aberrations during mitosis, which could ultimately lead to mitotic catastrophe. Therefore, we examined whether fisetin causes chromosomal aberrations in MDA-MB-231 and MDA-MB-468 cells where YB-1 phosphorylation at S102 is differentially affected. As demonstrated by three-color fluorescence *in situ* hybridization, fisetin treatment at a concentration of 75 µM for a period of 72 hours is similarly capable of causing chromosomal damage, as is IR at a dose of 2 Gy (Fig. 4D). A study by Klimaszewska-Wisniewska et al. (Klimaszewska-Wisniewska et al. 2016) showed that fisetin at a concentration of 10 µM can induce mitotic catastrophe when combined with paclitaxel. Interestingly, fisetin is known to be an antimitotic compound, which directly inhibits Aurora B kinase during the mitotic phase, ultimately leading to forced mitotic exit without cytokinesis (Salmela et al. 2009).

3.1.4 Fisetin inhibits DSB repair through interference with C-NHEJ and HR repair pathways

As previously outlined, DSBs are primarily repaired by HR, C-NHEJ, and Alt-NHEJ repair pathways. Here we investigated the underlying DSB repair pathway that is affected by fisetin. The MDA-MB-231 and MDA-MB-468 cells were treated with specific pathway inhibitors in combination with fisetin. The inhibitors of the C-NHEJ, HR, and Alt-NHEJ pathways were NU7441 (5 µM), a DNA-PKcs inhibitor; B02 (5 µM), a Rad51 inhibitor; and talazoparib (25 nM), a PARP inhibitor. The data presented in Fig. 5A indicate that treatment with fisetin and NU7441 resulted in substantial inhibition of DSB repair in both MDA-MB-231 and MDA-MB-468 cells following exposure to 4 Gy irradiation. Interestingly, B02 impeded DSB repair only in MDA-MB-468 cells (Fig. 5B). A combined treatment with fisetin and either Nu7441 (Fig. 5A) or B02 (Fig. 5B), in contrast to single treatments, did not result in an enhanced residual DSB. In addition, talazoparib increased the residual damage when applied as a single agent. However, the combination of fisetin with talazoparib demonstrated an additive effect in blocking the repair of IR-induced DSBs (Fig. 5C). It can thus be concluded that fisetin affects the repair of DSBs through its action on the HR and C-NHEJ pathways, with a minimal effect on Alt-NHEJ.

To provide additional evidence in support of the data obtained, the effect of fisetin on I-SceI-induced DSB was tested on osteosarcoma cell lines, namely U2OS cells, which harbor reporter constructs specific for each repair pathway (Gunn et al. 2012). Figs. 5D-F depicts the schematic of the DNA repair constructs for each cell line. Following DSB induction by I-SceI, DSBs are repaired and as a result, (green fluorescent protein) GFP protein is expressed and can be measured as a DNA repair efficiency. According to the data in Figs. 5E-F, fisetin similar to the data obtained in MDA-MB-231 and

MDA-MB-468 cells (Figs. 5A-C) reduces HR and C-NHEJ DNA repair efficiency which is not observed in Alt-NHEJ cells. In line with our data, a study by Huang et al. (Huang et al. 2022) has demonstrated that fisetin impairs HR in pancreatic cancer cells, through reduction in the level of m^6A on the PHF10 mRNA which plays a significant role in HR (Huang et al. 2022).

3.1.5 Effect of fisetin in combination with IR on apoptosis and autophagy

The accumulation of unrepaired DSBs leads to cell death through mitotic catastrophe, apoptosis and autophagy. Therefore, we then sought to investigate whether fisetin in combination with IR, increases apoptosis, as a mechanism of radiosensitization. We first evaluated the cell cycle profile for each condition and analyzed the number of cells in each cell cycle phase. In parallel, we examined the number of cells in the sub-G1 phase of the cell cycle as apoptotic cells. Based on the data shown in Fig. 6A, fisetin treatment (75 µM) for 72 h, reduced G1 cells in all TNBCs. In addition, sub-G1 cells were increased in MDA-MB-231 and MDA-MB-4453 cells. Radiation alone significantly reduced the number of G1 cells in MDA-MB-453 and MDA-MB-468 cells. In contrast to fisetin, irradiation did not increase apoptosis in all TNBCs tested. The combination of fisetin with irradiation could enhance apoptosis only in MDA-MB-468 cells compared to the single treatments (Fig. 6A). According to our previous data, fisetin radiosensitized all TNBCs tested in this study. However, since fisetin did not enhance apoptosis in these cells, therefore this radiosensitizing effect might not result from enhanced apoptosis. These data contradict the report by Chen et al. (Chen et al. 2010), where they showed that fisetin enhances apoptosis as a mechanism of action of radiosensitization in colorectal cancer cells. They compared the radiosensitization effect of HT-29 ($TP53^{mut}$) with HCT-116 ($TP53^{wt}$) and showed that fisetin is more effective in *TP53* mutated cells. Of note, there are a number of factors that affect cell death decisions, including, the complexity of DSB, the mutation status of the cells, and the signaling pathways involved in the cell death mechanisms. Based on our data, fisetin radiosensitized *TP53* mutated TNBCs. However, fisetin did not radiosensitize non-TNBC cell line T47D cells which have *TP53* mutation (data not shown), explaining that p53 is not a prerequisite for fisetin to be effective. In line with this, another study by Leu et al. (Leu et al. 2016) has been shown that fisetin radiosensitizes CT-26 xenograft tumors that have $TP53^{wt}$. These data show that there are other factors such as TNBC status might affect the response to fisetin. TNBCs lack the expression of

the receptors, which might be beneficial for fisetin treatment since they lack receptor-mediated resistant mechanisms and therefore they respond better. This remains to be elucidated.

It is known that IR increases protein unfolding as an indirect effect by generating ROS, thereby triggering unfolded protein response (UPR) within the endoplasmic reticulum (ER). Consequently, this results in ER stress. Interestingly, there is a close association between the UPR pathway and autophagy therefore, IR may induce autophagy indirectly. Autophagy is a lysosome-mediated catabolic process that degrades damaged organelles in response to stress signals (Roy et al. 2022). The role of autophagy in post-irradiation survival remains unclear. An increase in autophagy could be beneficial for certain cells when exposed to stress conditions. For example, it has been reported that ATM activation upon exposure to IR, results in reduction in autophagy. Consequently, cancer cells upregulate a number of miRNAs and proteins, including miRNA18a and WIP1 phosphatase, in order to inhibit ATM activity and thereby increase autophagy. Conversely, numerous studies have reported the role of ATM in promoting radioresistance. In this context, increased autophagy via the ATM-Chk2-BECN1 axis has been shown to be upregulated in irradiated tumor cells (Roy et al. 2022). These reports thus indicate that autophagy plays a dual role in cell survival after IR. To examine the pattern of autophagy in the TNBCs, the cells were treated with fisetin (75 µM, 72 h), IR (4 Gy), and a combination of both. The levels of LC3II and p62, as autophagy markers, were examined. Based on the data depicted in Fig. 6B, fisetin increased the expression of LC3II in MDA-MB-231 and MDA-MB-468 cells, however, it did not change the expression of p62. Interestingly, IR and a combination of IR and fisetin also did not induce autophagy (Fig. 6B).

As mentioned earlier, it is not clear how autophagy affects cell fate after IR. The role of autophagy in tumor development depends on the stage of the tumor. In the initial stages of tumor progression, autophagy is considered to be tumor-suppressive. However, as the tumor progresses to the later stages, autophagy is observed to contribute to the survival of tumor cells (Kocaturk et al. 2019; Russo et al. 2018). Several reports have indicated that the inhibition of autophagy causes radiosensitization in different cancer types including breast cancer, liver cancer, and esophageal squamous cell carcinomas (Chaachouay et al. 2011; Chen et al. 2011; Tseng et al. 2011). On the other hand, autophagy inducers such as rapamycin, temsirolimus and everolimus inhibit mTOR and enhance radiosensitization in glioma, renal cancer, and prostate cancer (Roy et al. 2022). In pancreatic cancer, fisetin has been shown to enhance autophagy (Jia et al. 2019), whereas it decreases autophagy in hepatocellular carcinoma HepG2 cells (Sundarraj et al. 2021). The present study shows that fisetin, when combined with IR, does not alter autophagy in comparison to radiation alone.

3.1.6 Fisetin modulates activation of DDR signaling cascades

As has been previously demonstrated, fisetin interferes with RSK-mediated YB-1 phosphorylation at S102 in melanoma cancer cells (Sechi et al. 2018). Here, we sought to investigate whether fisetin, in addition to its inhibitory effect on YB-1 phosphorylation at S102, affects the activation of alternative proteins or pathways involved in post-irradiation cell survival of TNBCs. Therefore, we mock-treated or treated MDA-MB-231 cells with fisetin (75 µM) and mock-irradiated or irradiated with 4 Gy IR. Thereafter, by applying a phospho-kinase array, we analyzed the number of different phosphoproteins 30 min and 24 h post IR. According to the data shown in Fig. 7, fisetin inhibits RSK1/2 phosphorylation at S221/S227. When fisetin was combined with IR, the phosphorylation level of p53 (S392), Src (Y419), and the expression of β-catenin were suppressed both 30 min and 24 h post IR (Fig. 7). The administration of fisetin for a period of 24 hours (in the 30-minute post-IR experiment) was observed to have a relatively mild effect. These data show that fisetin apart from RSK, targets other survival pathways, which may represent an additional mechanism of radiosensitization. In this context, β-catenin overexpression has been shown to be correlated with radioresistant Human Nasopharyngeal Carcinoma CNE-2 cells (He et al. 2018a). In accordance with the function of β-catenin in radiosensitization, Zhao et al. (Zhao et al. 2018) have demonstrated that Wnt/β-catenin pathway regulates high-mobility group box 1 protein (HMGB1), which is a chromatin remodeling protein involved in DNA repair. This subsequently results in radioresistance of esophageal squamous cell carcinoma (Zhao et al. 2018). In addition, it has been reported that AZD0530, a Src kinase inhibitor, radiosensitizes lung cancer cells *in vitro* (Purnell et al. 2009).

Next, we conducted a phosphoproteomics analysis on MDA-MB-231 and MDA-MB-468 cells to investigate the impact of pretreatment with fisetin, followed by irradiation with 4 Gy, on DDR signaling in comparison to irradiation alone. In MDA-MB-468 cells, where fisetin did not alter YB-1 phosphorylation at S102, we identified a total of 472 differentially regulated phosphoproteins out of 1564 phosphoproteins analyzed (Fig. 8A). Among the top 10 most significantly downregulated phosphoproteins, DEK (T13, S51), nucleolin (NCL) (S563), XRCC1 (S210), and TOP2A (S1106) were notably involved in DNA repair processes. Subsequently, we conducted a gene ontology (GO) enrichment analysis to determine if altered phosphosites are associated with DDR signaling, specifically DSB repair. As shown in Fig. 8B and Table S1, the genes exhibiting the greatest regulation are enriched in pathways associated with DSB repair. Interestingly, the GO analysis in both MDA-MB-231 (Fig. S5) and MDA-MB-468 (Fig. 8B) revealed similarities, indicating that DNA repair is among the primary pathways that fisetin affects in

irradiated cells. Therefore, our data demonstrate that fisetin inhibits YB-1 phosphorylation at S102 in all TNBCs, with the exception of MDA-MB-468 cells. However, fisetin inhibits the repair of IR-induced DSBs and radiosensitizes these cells. Furthermore, by knocking down YB-1 in MDA-MB-231 cells, we demonstrated that fisetin has an inhibitory effect on DSB repair, although to a lesser extent than the control condition. In light of these findings, it can be concluded that fisetin exerts its effects not only through YB-1 but also through multiple other targets, particularly in the context of DNA repair mechanisms. This could potentially influence the response of cancer cells to radiotherapy.

3.2 Publication II: Fisetin overcomes non-targetability of mutated KRAS induced YB-1 signaling in colorectal cancer cells and improves radiosensitivity by blocking repair of radiation-induced DNA double-strand breaks (Khozooei et al. Radiother Oncol. 2023;188:109867)

The treatment of advanced and metastatic CRCs typically involves the use of adjuvant and/or neoadjuvant chemotherapy or CRT regimens in conjunction with surgical resection (Aparicio et al. 2020). In addition, molecular-targeted therapy and immunotherapy are also administered. The location and the stage of the cancer, in addition to the health condition of the patients, determine the treatment plan. Despite advances in treatment strategies, the mortality rate of CRC remains high. However, these treatments are accompanied by drawbacks, as they may be non-specific and therefore, cytotoxic to the normal tissue (Kumar et al. 2023). Furthermore, patients may develop resistance to therapy, necessitating the development of combinational therapies to enhance treatment outcomes and overcome the resistant mechanisms in tumor cells. CRC is known to be heterogeneous, which results in multiple pathways being involved in tumorigenesis (Zhu et al. 2021). *KRAS* is one of the most frequently mutated genes, with approximately 44% of colorectal cancers, primarily in codons 12, 13, and 61 (Zhu et al. 2021). CRC patients with *KRAS* mutation have a poor prognosis and this mutation is associated with reduced survival. Additionally, the YB-1 oncoprotein is also highly expressed in *KRAS* mutated cells, which is also linked to decreased OS. As previously stated, YB-1 is mainly regulated by the PI3K/AKT and RAS/RSK pathway, and it is directly phosphorylated at S102 by RSK and AKT.

PAK proteins as a family of serine/threonine kinases with 6 isoforms, are involved in multiple survival pathways modulated by RAS oncogenes. Among them, PAK1 as a downstream of KRAS, has been shown to directly interact with PDK1, thereby enhancing AKT activity (King et al. 2000). In addition, PDKA can also phosphorylate and activate PAK1 (King et al. 2000). Therefore, PAK1 can be regulated by KRAS which can further control the activity of AKT. It is known that PAK1, activates ERK1/2 via MEK1/2, and in turn, ERK1/2 via MEK1/2 activates PAK1 in a positive loop (Wang et al. 2013). Hence, it is hypothesized that the PAK family members act as pivotal points in the interaction between AKT and RSK, which phosphorylate YB-1 at S102.

It is found that the expression and phosphorylation of YB-1 at S102 are critical for the repair of IR-induced DSBs and play a significant role in mediating radioresistance within breast cancer cells (Lettau et al. 2021; Toulany et al. 2011). In line with this,

the selective inhibition of YB-1 S102 phosphorylation through dual targeting of AKT and RSK has been demonstrated to be effective in impairing the repair of IR-induced DSBs in breast cancer cells (Lettau et al. 2021) and enhancing chemosensitization of CRC cells to 5-fluorouracil (5-Fu) (Maier et al. 2019). Additionally, Our previous study has shown that the flavonoid fisetin significantly inhibits YB-1 phosphorylation at S102, induces DSBs, and impairs the repair of IR-induced DSBs in TNBCs, which served as a potential candidate to overcome radiation resistance (Khozooei et al. 2022).

This study aimed to elucidate the impact of distinct treatment modalities on the phosphorylation status of YB-1 at S102. These include DT of AKT and RSK, PAK targeting, EGFR targeting, and fisetin. Furthermore, the effect of these therapeutic approaches on the DSB repair and consequently on the radiation response in CRC cells was investigated.

3.2.1 YB-1 is highly phosphorylated in CRC cells with an activating mutation in MAPK pathways

The cell lines used in our study carry different *KRAS* mutations. HCT-116 with heterozygous $KRAS^{G13D}$, SW48 with $KRAS^{wt}$, and CaCo2 cells with $KRAS^{wt}$. The CaCo2, which naturally contains $KRAS^{wt}$ and has been engineered to express $KRAS^{G12V}$ with a doxycycline-inducible construct (Möller et al. 2014). The doxycycline-inducible $KRAS^{G12V}$ expression system is comprised of two expression cassettes. The first cassette contains doxycycline-inducible mutant $KRAS^{G12V}$ and GFP with a Blasticidin S resistance gene. The second cassette includes constitutively expressed doxycycline-inducible system components, namely reverse tetracycline transactivator (rtTA) and tetracycline repressible transcriptional silencer (tTS) with a puromycin resistance gene (Möller et al. 2014; Roßner et al. 2016). The schematic below (Figs. 11A-B) illustrates the construct for BRAF expression and the construct for the KRAS was designed based on this expression system (Herr et al. 2011).

In this system, the constitutively expressed cassette expresses rtTA and tTS. In the absence of doxycycline (dox), the tTS binds to the tetracycline-binding element, thereby repressing the expression of the cassette and ensuring that there is no leakage of the expression in the absence of dox. In the presence of dox, the rtTA protein binds to the tetracycline-binding element, thereby initiating the expression of the cassette. In our system, the cassette is responsible for the expression of KRAS protein with G12V mutation. To be able to track the mutated KRAS, the construct contains a GFP which

is separated from the KRAS with an internal ribosomal entry site (IRES). This configuration ensures that the GFP is expressed along with the $KRAS^{G12V}$ mutation, but not as a fusion protein.

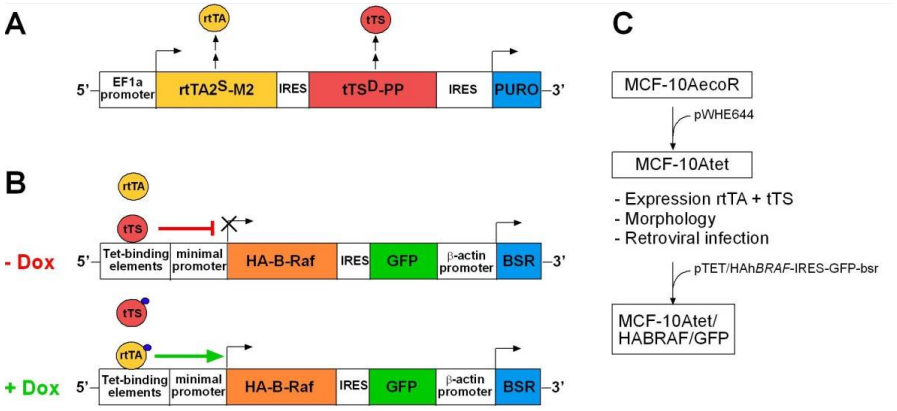

Figure 11: The expression cassettes used to generate doxycycline-inducible $KRAS^{G12V}$ expression. BSR Blasticidine resistance gene, Dox Doxycycline, EF1a Elongation factor 1a constitutive promoter, IRES Internal ribosomal entry site, Puro Puromycin resistance gene, rtTA Reverse tetracycline-regulated transactivator, tTS Tetracycline-repressible transcriptional silencer. Adapted from (Herr et al. 2011).

In order to assess the activity of the KRAS protein in these cells, we performed a Ras activity assay. As indicated in Fig. 1A, the level of KRAS bound to the RAS binding domain of Raf1 (Raf1-RBD) is higher in HCT-116 as heterozygous $KRAS^{G13D}$ cells compared to $KRAS^{wt}$ cells SW48 and CaCo2 cells, indicating that the KRAS activity in HCT-116 cells are higher. Upon induction of $KRAS^{G12V}$ expression in CaCo2 cells with 2 µg/ml dox for 72 h, an increase in KRAS activity was observed (Fig. 1A). Subsequently, the phosphorylation status of YB-1 at S102 in CRC cells with activating mutations in KRAS/MAPK pathway was determined, given that YB-1 is a downstream effector of KRAS. As illustrated in Fig. 1A, YB-1 exhibited increased phosphorylation at S102 in both $KRAS^{wt}$ SW48 cells and $KRAS^{mut}$ cells (Fig. 1A). In CaCo2 cells, treatment with dox resulted in the phosphorylation of YB-1 at S102 almost in three-fold change (Fig. 1A) These findings align with previous reports indicating that constitutive activation of KRAS leads to enhanced phosphorylation of YB-1 at S102 (Maier et al. 2019; Toulany et al. 2011). However, the elevated level of YB-1 phosphorylation in $KRAS^{wt}$ SW48 cells may be attributed to an activating mutation located in the cascade between KRAS and YB-1. In accordance with this, $KRAS^{wt}$ SW48 cells have been shown to possess a heterozygous mutation in *MEK1* at codon 56 $MEK1^{Q65P}$, which functions as an upstream of RSK, a kinase responsible for YB-1 S102 phosphorylation (Jing et al. 2019). Thus, activating mutations in *KRAS* and downstream of KRAS signaling lead to enhanced YB-1 phosphorylation at S102.

Next, the phosphorylation of YB-1 at S102 was assessed in a time kinetic experiment in CaCo2 cells after dox treatment. This was done to assess the dependency of YB-1 phosphorylation on *KRAS* mutation status. The data in Figs. 1B-C show that, YB-1 phosphorylation is induced along with KRAS in dox-treated cells in a time-dependent manner. This is evidenced by the increased GFP expression observed within six days. Furthermore, the data demonstrate that dox treatment results in increased phosphorylation of ERK1/2 and AKT, indicating that *KRAS* mutation leads to enhanced MAPK and PI3K/AKT signaling pathways. Apart from *KRAS* mutation, IR also has been shown to induce KRAS activity in $KRAS^{wt}$ cells (Toulany et al. 2007), as well as YB-1 phosphorylation at S102 in breast cancer cells (Lettau et al. 2021; Tiwari et al. 2018; Toulany et al. 2011). In line with this observation, as shown in Fig. S1, IR induced YB-1 phosphorylation at S102 in CaCo2 with $KRAS^{wt}$ but not in CaCo2 with $KRAS^{G12V}$ cells.

AKT and RSK have been shown to be involved in regulating YB-1 phosphorylation at S102 (Stratford et al. 2008; Sutherland et al. 2005). A previous report shows that the simultaneous targeting of AKT and RSK reduces YB-1 phosphorylation at S102 in SW48 and HCT-116 cells. Therefore, we sought to investigate how inhibiting RSK and AKT in the long term (72 h) as a single agent or as a combination, affects YB-1 phosphorylation at S102 in the isogenic CaCo2 parental and CaCo2 $KRAS^{G12V}$. As shown in Fig. 1D, the AKT inhibitor MK2206 at 5 µM for 72 h effectively blocked the phosphorylation of AKT at S473 in both $KRAS^{wt}$ and $KRAS^{G12V}$ CaCo2 cells. LJI308, as an RSK inhibitor, demonstrated inhibitory effects on RSK phosphorylation at T359/S363 when applied at a concentration of 10 µM for 72 h. However, this inhibition was observed only in the $KRAS^{G12V}$ CaCo2 cells. MK2206 reduced YB-1 phosphorylation at S102 in $KRAS^{wt}$ CaCo2 cells, with a more pronounced effect than that observed with LJI308 suggesting that YB-1 phosphorylation at S102 in CaCo2 parental cells is dependent on AKT. In contrast, in CaCo2 with $KRAS^{G12V}$ expression, YB-1 phosphorylation at S102 is dependent on RSK, as evidenced by the strong inhibitory effect of LJI308 on YB-1 phosphorylation at S102, which was not observed with the AKT inhibitor. Irrespective of the *KRAS* mutation status, DT of both kinases was the most effective approach to inhibit YB-1 phosphorylation (Fig. 1D). Our data is in line with the other report showing that the effectiveness of the kinases in regulating YB-1 phosphorylation at S102 depends on the mutation status of *KRAS*, where in $KRAS^{wt}$ cells, YB-1 phosphorylation is predominantly regulated by the PI3K/AKT pathway, but in $KRAS^{mut}$ cells, it is controlled by the MEK/ERK/RSK pathway (Tiwari et al. 2020). These observations are also in line with a report demonstrating that $KRAS^{mut}$ cells are addicted to the RAF and its downstream pathways (Lee et al. 2019).

Previous work demonstrated that in CRC cells, when RSK is inhibited under non-irradiated conditions, AKT becomes activated (Maier et al. 2019). AKT has been shown to be involved in the repair of IR-induced DSBs and due to the role of YB-1 in DDR signaling, we sought to investigate how the pattern of YB-1 phosphorylation at S102 is affected after IR in CRC cells pretreated with LJI380 and MK2206. As indicated in Fig. S1, in parental CaCo2 cells, MK2206 with the concentration of 5 µM for 72 h inhibited YB-1 phosphorylation at S102 post IR, but was not effective in $KRAS^{G12V}$ mutated CaCo2 cells. Furthermore, IR did not induce further YB-1 phosphorylation at S102 in $KRAS^{G12V}$ mutated CaCo2 cells. However, LJI308 with a concentration of 10 µM for 72 h reduced YB-1 phosphorylation at S102 in the mutated CaCo2 cells. Simultaneous targeting of both AKT and RSK was shown to be the most effective approach in blocking YB-1 phosphorylation following IR in both $KRAS^{mut}$ and $KRAS^{wt}$ cells (Fig. S1). In line with this, previous results also showed that dual inhibition of AKT and RSK could suppress chemotherapy-induced YB-1 phosphorylation at S102 in SW48 and HCT-116 cells (Maier et al. 2019).

3.2.2 Pathways in YB-1 phosphorylation *in vitro* and *Ex vivo*

As a consequence of the effective targeting of YB-1 phosphorylation at S102 by dual targeting of AKT and RSK, there is an implication of a potential cross-talk between these two pathways (Misale et al. 2019). In an effort to identify the critical point of interaction, we investigated the role of PAK proteins and we found that the PAK family members were the primary proteins involved. In line with this, PAKs have been described to be involved in phosphorylation and activation of multiple kinases in PI3K and MAPK pathways, including AKT (Higuchi et al. 2008), RAF (Beeser et al. 2005; Lu et al. 2017a), MEK (Beeser et al. 2005; Lu et al. 2017a; Eblen et al. 2002; Wang et al. 2013), and ERK (Beeser et al. 2005; Eblen et al. 2002; Wang et al. 2013). In addition, it is found that PAK family proteins can be phosphorylated and activated by kinases such as AKT (Tang et al. 2000), PDK1 (King et al. 2000), PI3K (Ebi et al. 2013; Thillai et al. 2017), and RAF (McCarty et al. 2014). Interestingly PAK is downstream of KRAS (Takács et al. 2020b) and has been shown to have a role in regulating protein kinase C (PKC) (Reina-Campos et al. 2019). The findings of these reports provide evidence to support the hypothesis that PAK functions as a mediator between kinase cascades. Accordingly, we sought to investigate whether the inhibition of PAK would result in the interference of YB-1 phosphorylation at S102. To test this hypothesis, CaCo2 cells expressing $KRAS^{wt}$ and $KRAS^{mut}$ were treated with FRAX486, as a PAK inhibitor, or DT. Furthermore, the cells were treated with erlotinib, an inhibitor of EGFR, as a control treatment. Given that in $KRAS^{mut}$ cells, EGFR does not control the

PI3K/AKT and MAPK/ERK pathways, the erlotinib treatment with 10 µM for 72 hours was observed not to impair YB-1 phosphorylation at S102 in CaCo2 $KRAS^{G12V}$ cells (Fig. 2A). Similar to DT, FRAX486 (10 µM, 72 hours) inhibited YB-1 phosphorylation at S102 regardless of *KRAS* mutation status and the long-term inhibition of PAK did not result in the reactivation of YB-1 phosphorylation at S102 (Fig. 2A and Fig. S2). It is noteworthy that the inhibition of YB-1 phosphorylation by FRAX486 following constitutive phosphorylation due to *KRAS* mutation or IR, was also observed in other CRC cells, including HCT116 and SW48 with varying *KRAS* mutation status. However, the effect was more pronounced in $KRAS^{wt}$ cells (Fig. S3).

In *ex vivo* settings, the DT of both RSK and AKT effectively reduced YB-1 phosphorylation at S102 in all tissues from four patients (Figs. 2B,D-F). However, the effect of FRAX486 and erlotinib was not similar in all samples. For instance, PAK inhibitor had no effect in reducing YB-1 phosphorylation in samples #1 and #4 (Figs. 2B,F), while inhibited in sample #3 (Fig. 2E). On the other hand, erlotinib reduced YB-1 phosphorylation in sample #2 and #3 (Fig. 2E), but not in sample #1 and #4 (Figs. 2B,F). Sequencing revealed that sample #1 has $KRAS^{G12V}$ mutation which was not observed in the other three samples (Fig. 2C). Interestingly, different patterns of YB-1 phosphorylation at S102 variations were observed between some of the replicates of the same tumor tissue after inhibitor treatments. In this context, in tissues #2 and #3, the pattern of IR-induced YB-1 phosphorylation at S102 is different (Figs. 2D-E). As an additional example to this variation, the inhibition of IR-induced YB-1 phosphorylation by MK2206 and FRAX486 in tissue #2 and by MK2206 in tissue #3 was observed to be in a different pattern between replicates (Figs. 2D-E). However, in terms of AKT phosphorylation at S473, IR induced this phosphorylation, but this was inhibited by MK2206, DT, and slightly by FRAX486 (Fig. 2D). Furthermore, in tissue #4, the pattern of IR-induced YB-1 and AKT phosphorylation is consistent between the two replicates after treatment with MK2206, DT, and FRAX486. However, this was not the case after erlotinib treatment (Fig. 2F), wherein one of the replicates, it did not affect YB-1 phosphorylation despite having $KRAS^{wt}$. It is important to note that tissue #4 has $KRAS^{wt}$, however, the allele frequency of the loss-of-function mutation in F-Box and WD Repeat Domain Containing 7 (*FBXW7*) gene is high. *FBXW7* is found to be mutated in almost 14% of CRC patients (Liu et al. 2023). This gene is considered a potential tumor suppressor gene which is a part of the SKP1-CUL1-F-box protein (SCF) complex, as an E3 ubiquitin ligase. It has been shown that FBXW7 is responsible for degrading multiple oncoproteins, including c-Myc, cyclin E, c-Jun, and Notch. Furthermore, FBXW7 also regulates p53 degradation (Liu et al. 2023). In addition to the aforementioned oncoproteins, FBXW7 is also involved in DNA repair mechanisms.

In this context, indeed it has been shown that FBXW7 promotes ubiquitination of multiple DNA repair proteins, including polo-like kinase (PLK), SOX9, and bloom (BLM) helicase (Lan et al. 2021). Therefore, loss-of-function mutations in *FBXW7* could potentially improve tumorigenesis. In this context, the most frequent mutations in *FBXW7* are found to be R505C, R465H, R465C, R278*, and S582L (Liu et al. 2023). All these mutations affect the substrate binding of FBXW7, therefore interfering with the ubiquitination of the target proteins (Lan et al. 2021). Once mutated, several oncogenes may accumulate in the cells, resulting in uncontrolled proliferation and tumor progression. Additionally, it has been reported that in esophageal squamous cell carcinoma cells, where a loss-of-function mutation in *FBXW7* is observed, the ERK1/2 activity is increased (Pan et al. 2023). Given that ERK1/2 is downstream of KRAS and upstream of RSK, it can be suggested that these cells with *FBXW7* mutation have $KRAS^{mut}$ phenotype. Interestingly, a recent report by Boretto et al. has shown that one of the substrates of FBXW7 is EGFR (Boretto et al. 2024). When *FBXW7* is mutated, EGFR can be accumulated on the cell surface, resulting in the ineffectiveness of erlotinib in inhibiting the signaling pathway despite being $KRAS^{wt}$. In $KRAS^{mut}$ tumor tissue, similar to the *in vitro* data, erlotinib did not affect YB-1 phosphorylation at S102 (Fig. 2B). While sample #2 also has a loss-of-function mutation in *FBXW7*, the frequency of allele of the mutation appears to be relatively low, which may also explain the observed heterogeneity between the of sample replicates of tissue #2. On the other hand, the patient #4 has two loss-of-function mutations in *FBXW7* gene. One of the mutations results in protein truncation, while the other renders the protein non-functional. Given the high allele frequency in tissue #4, the sample #4 shows $KRAS^{mut}$ characteristics. Therefore, in this tissue more uniform pattern of YB-1 and AKT phosphorylation is observed. Thus, given the heterogenicity of the tumors, combinational targeting for example, DT of both AKT and RSK could be beneficial. Although the number of tissues in our study was limited, however, based on our data, tumor heterogenicity and mutation status of the cells affect the therapy response to AKT, RSK, and PAK inhibition significantly.

Considering the potential influence of hypoxic regions within the tumor slices on signaling patterns, an experiment was conducted under both normoxic and hypoxic conditions. Unexpectedly, hypoxia led to reduced phosphorylation of RSK, AKT, and YB-1 in both the parental CaCo2 cells and those overexpressing $KRAS^{G12V}$ (Fig. S4). In *ex vivo* experiments, the expression level of HIF1α was not observed (Figs. 2B,D-F). However, differences in the tumor slices in the context of oxygenation level cannot be completely excluded. This has to be tested in more tissue samples.

3.2.3 Impact of targeting PAK and DT of RSK/AKT on NHEJ and HR repair pathways

Our previous data indicated that fisetin reduces YB-1 phosphorylation at S102 and impairs IR-induced DSB repair by interfering with C-NHEJ and HR DSB repair pathways (Khozooei et al. 2022). The objective of this study was to investigate whether pretreatment with DT of AKT (5 µM) and RSK (10 µM) and inhibition of PAK (10 µM) for 24 h would result in a reduction in the repair efficiency of I-SceI-induced DSBs in U2OS cells harboring different DNA repair constructs (Fig. 3A). Once the I-SceI-induced DSB has been repaired, the expression of GFP can be quantified (Fig. 3A). As demonstrated in Figs. 3B-C, the data illustrate that both the DT of AKT and RSK and FRAX486, resulted in a reduction in the repair efficiency of HR and Alt-NHEJ, as evidenced by a reduction in the number of GFP-positive cells. the efficiency of C-NHEJ was found to be reduced by FRAX586. However, the DT of AKT and RSK had a negligible impact on C-NHEJ (Figs. 3B-C). Since some compounds might have non-specific effects on GFP expression, U2OS cells transiently overexpressing enhanced GFP were treated with the inhibitors used, including DT of AKT and RSK and FRAX486. As indicated in Fig. 3 D, the DT of AKT and RSK did not alter the fluorescence intensity of the GFP reporter in any of the three U2OS cell lines. In contrast, the treatment with FRAX486 resulted in a notable reduction in the GFP expression. As depicted in Fig. 3E, the impact of DT of AKT and RSK and PAK inhibition on YB-1, AKT and RSK phosphorylation and protein expression in U2OS cells was elucidated following 30 min post 4 Gy. FRAX486 markedly inhibited YB-1, AKT and RSK1/2/3 protein level which is also associated with the significant decrease in their phosphorylation level in all three U2OS cells harboring distinct DSB repair pathway constructs (Fig. 3E).

Given the observed impact of these inhibitors on the DSB repair pathways in U2OS cells, we further sought to investigate the effect of DT of AKT and RSK, PAK inhibition, and fisetin treatment on IR-induced DSB repair, apoptosis, and radiosensitivity in CaCo2 parental and CaCo2 with $KRAS^{G12V}$ cells. Firstly, the effect of $KRAS^{G12V}$ on the IR-induced DSB repair was investigated. According to the data shown in Fig. 4A, the overexpression of $KRAS^{G12V}$ increased the number of γH2AX foci both in non-irradiated and irradiated conditions. In contrast to these data, previous report showed that knockdown of KRAS in $KRAS^{mut}$ breast cancer cells results in inhibition of repair of IR-induced DSBs (Toulany et al. 2011). In line with this, in another study the role of each $KRAS^{G12C}$, $KRAS^{G12D}$, or $KRAS^{G12V}$ in isogenic SW48 cell line as well as $KRAS^{G13D}$ in HCT-116 cells was tested and shown that once $KRAS$ is mutated, the cells become radioresistant (Yang et al. 2021). It has been reported that $KRAS^{mut}$ overexpression leads to reduced radiation-induced mitotic catastrophe and accelerated

exit from G2/M cell cycle arrest. In addition, the authors found that $KRAS^{mut}$ overexpression results in increased NRF2-mediated 53BP1 expression enhancing C-NHEJ repair. Interestingly, YB-1 upregulates the NRF2 expression (El-Naggar et al. 2019), which might suggest how the effect of $KRAS^{mut}$ in stimulating DSB repair is mediated by YB-1. The discrepancies between findings may be due to the use of different cell systems in different studies. In the study by Yang et al. (Yang et al. 2021), KRAS is stably overexpressed, allowing the cells to adapt to the replication stress mediated by KRAS. However, in our study, we transiently overexpressed KRAS in CaCo2 cells which may cause replication stress (Di Micco et al. 2006), leading to increased DNA damage and residual damage in both non-irradiated and irradiated conditions. Another explanation could be that, since CaCo2 cells have a *TP53* mutation (Liu et al. 2006), the cells rely on the G2/M checkpoint. Once KRAS is upregulated, it causes more replication stress that leads to G2/M cell cycle arrest as the most radiosensitive phase of the cell cycle (Hall et al. 2006; Landry et al. 2022; Seiwert et al. 2007). In contrast, SW48 and HCT-116 cells are $TP53^{wt}$ (Liu et al. 2006), and they may undergo arrest in S phase to repair the damage, making them more resistant to stress-induced damages.

Dual inhibition of AKT and RSK was shown to be effective in reducing YB-1 phosphorylation at S120 based on *in vitro* and *ex vivo* data (Fig. 1D, Fig. 2). Targeting AKT and RSK similar to PAK inhibition resulted in inhibition of IR-induced DSB repair only in CaCo2 parental cells (Figs. 4A-B, Figs. S6A-B). However, this effect was not associated with the radiosensitization, as dual inhibition of AKT and RSK did not radiosensitize both $KRAS^{wt}$ cells and $KRAS^{mut}$ cells. In contrast, targeting PAK with FRAX486, could slightly radiosensitize $KRAS^{wt}$ CaCo2 cells. As indicated in Fig. S5, erlotinib significantly reduced the residual breaks and therefore enhanced the DSB repair. As shown in Fig. 2A, erlotinib inhibited YB-1 phosphorylation at S102 in CaCo2 $KRAS^{wt}$ cells, however, it did not reduce AKT phosphorylation. Since AKT has a role in DNA DSB repair, the lack of effect of erlotinib on the CaCo2 cells could be due to the YB-1-independent effect of AKT on C-NEHJ and HR mechanisms of DSB repair (Bozulic et al. 2008; Mueck et al. 2017; Toulany et al. 2012), indicating that AKT, independent of YB-1, stimulates DSB repair and affect radiation response. In $KRAS^{G12V}$ CaCo2 cells, as they have endogenous $KRAS^{wt}$, inhibition of EGFR abolish survival signaling downstream of endogenous $KRAS^{wt}$, however, this could trigger a compensatory activation of pathways mediated by $KRAS^{mut}$ leading to enhancement of IR-induced DSB repair. In addition, there are reports showing that RAS is capable of dimer formation (Güldenhaupt et al. 2012; Lin et al. 2014; Spencer-Smith et al. 2017), which indeed recruits RAF effector that also need dimerization for its activation. KRAS dimerization leads to enhanced MAPK activation (Nan et al. 2015). Interestingly, Ambrogio et al. showed that, in the lung cancer cells having $KRAS^{wt}$, overexpression of $KRAS^{mut}$in

these cells leads to the formation of $KRAS^{wt}$ and mutated KRAS dimers (Ambrogio et al. 2018). It has been shown that these cells are resistant to MEK inhibition as ERK might be activated by different pathways. On the other hand, in cells lacking $KRAS^{wt}$, mutated KRAS forms homodimers which results in high activation of the MAPK pathway and the cells become sensitive to MEK inhibition since the cells only rely on MAPK for survival (Ambrogio et al. 2018). Therefore, the formation of dimer between $KRAS^{wt}$ and $KRAS^{mut}$, reduces oncogenic signaling activation. In our cell model when dox induces expression of $KRAS^{G12V}$, the endogenous $KRAS^{wt}$ remains, and they might form a dimer leading to enhanced ERK activation despite EGFR inhibition, which is why in erlotinib treated condition we see stimulation of DSB repair.

It is known that fisetin interferes with the RSK-mediated YB-1 phosphorylation at S102 in melanoma cancer (Sechi et al. 2018). Previously, we demonstrated that fisetin can also inhibit YB-1 phosphorylation at S102 in TNBCs (Khozooei et al. 2022). This effect was associated with inducing DNA damage, blocking the repair of IR-induced DSBs, and consequently radiosensitizing TNBCs (Khozooei et al. 2022). In this study, we aimed to investigate the effect of fisetin on CRC cells. As shown in Fig. 4C, fisetin treatment for 24 h at a concentration of 75 µM inhibited YB-1 and RSK phosphorylation in both CaCo2 $KRAS^{wt}$ and CaCo2 $KRAS^{G12V}$ cells. In contrast, the effect of fisetin on ERK phosphorylation differed between two cell lines: in CaCo2 $KRAS^{wt}$, it was inhibited, whereas in CaCo2 $KRAS^{G12V}$ cells, ERK phosphorylation was increased. It is interesting to note that in both cell lines, phosphorylated AKT is not induced following fisetin treatment (Fig. 4C).

Next, the effect of fisetin on the repair of IR-induced DSBs was investigated as shown in Fig. 4D, Fig. S6C. Both CaCo2 $KRAS^{wt}$ and CaCo2 $KRAS^{G12V}$ cells pretreated with fisetin, showed significantly increased residual damages compared to control conditions. As investigated before, fisetin impacts on a variety of different proteins involved in DNA repair mechanisms in TNBCs (Khozooei et al. 2022), and therefore, this effect might be also partially dependent on YB-1 as also indicated in Fig. 5. In addition, fisetin radiosensitized CaCo2 cells regardless of *KRAS* mutation status, however, this effect was more pronounced in $KRAS^{G12V}$ compared to $KRAS^{wt}$ cells. In addition, fisetin enhanced the residual damages in SW48 cells when combined with IR (Fig. S8A), which was also correlated to the radiosensitization effect as shown in Fig S8B. In line with this data, we previously have shown that fisetin interferes with the repair of DSBs in TNBCs regardless of KRAS mutation status via suppression of C-NHEJ and HR pathways (Khozooei et al. 2022). Interestingly, it is known that in *KRAS* mutated cells, the C-NHEJ pathway is enhanced through the NRF2/53BP1 axis. Thus, C-NHEJ pathways could play a pivotal role in these cells. Based on our data in U2OS cells

harboring $KRAS^{wt}$, dual inhibition of AKT and RSK significantly reduced HR and A-NHEJ efficiency, however, it did not markedly decrease C-NHEJ (Figs. 3B-C). Similar to DT of AKT and RSK, inhibition of PAK, resulted in a sharp decrease in all three repair pathways (Figs. 3B-C). Of note, FRAX486 significantly suppressed GFP expression or fluorescence intensity of the cells (Fig. 3D), this implies that the part of the observed effect of FRAX486 on the repair efficiencies might be due to this reason. This effect was in line with the absence of the effect of DT and FRAX in CaCo2 $KRAS^{G12V}$ cells (Figs. 4A-B).

As one of the mechanisms underlying the inhibition of clonogenic activity and subsequent radiosensitization is related to unrepaired damages leading to apoptosis, we next investigated whether fisetin enhances apoptosis. To this aim, we analyzed the number of sub-G1 cells, a marker of apoptosis, in CaCo2 $KRAS^{G12V}$ cells. We found that fisetin alone increased sub-G1 cells, but did not increase IR-induced apoptosis (Fig. S9). Interestingly, irradiation did not enhance apoptotic cells and therefore, the combination of fisetin and IR did not further increase apoptosis (Fig. S9). Similarly, we evaluated the apoptosis after targeting PAK and dual inhibition of AKT and RSK. Based on the data in Fig. S10, FRAX486 enhanced IR-induced apoptosis. Interestingly, while PAK inhibition slightly radiosensitized the cells (Fig. S7), it did not affect the DSB repair (Fig. 4B). In contrast, dual inhibition of AKT and RSK neither increased IR-induced apoptosis (Fig. S10), nor did it radiosensitize the cells (Fig. S7) or impair the DSB repair (Fig. 4A).

In conclusion, our data for the first time shows that fisetin can be a potential candidate that may enhance therapeutic response in CRC by overcoming CRT regardless of *KRAS* mutation status.

3.3 Publication III: YB-1 activating cascades as potential targets in KRAS-mutated tumors (Khozooei et al. Strahlenther Onkol. 2023 Dec;199(12):1110-1127.)

Due to our expertise in YB-1 and *KRAS* mutations, we were invited by the Strahlentherapie und Onkologie journal to write a comprehensive review on this topic. In this review, we focused on the biology of YB-1 and its role in different cellular processes. We compiled evidence highlighting the prognostic role of YB-1 in *KRAS* mutated cancers and explored the association between *KRAS* mutation and the oncogenic functions of YB-1. Furthermore, we outlined how YB-1 is regulated by the different signaling pathways. Finally, we discussed how targeting the KRAS/YB-1 axis by introducing multiple approaches could be beneficial for *KRAS* mutated tumors that could potentially improve CRT outcome.

Chapter 4

Conclusive remarks and future perspectives

YB-1, a multifunctional oncoprotein, is known to be highly activated and overexpressed, contributing to CRT resistance. Intriguingly, YB-1 is also found to be involved in DNA repair mechanisms. The overexpression of YB-1 is associated with *KRAS* mutation, where YB-1 is known to be regulated by KRAS/RSK pathway. Therefore, targeting YB-1, especially in $KRAS^{mut}$ tumors, represents a promising strategy to overcome CRT resistance.

Targeting YB-1 directly, due to lack of kinase activity, is still challenging. However, several strategies have been proposed, most of which are still in the preclinical phase. In our study, we showed that fisetin, as a flavonoid natural compound, interferes with YB-1 phosphorylation at S102 in TNBCs and CRC cells *in vitro*. Interestingly, fisetin impairs the repair of IR-induced DSBs by interfering with C-NHEJ and HR pathways partially through its effect on YB-1. However, our data show that YB-1 is not the sole target of fisetin, as fisetin affects multiple proteins, particularly those involved in DNA damage and repair pathways.

In addition, fisetin as an alternative to dual inhibition of AKT and RSK and PAK can be a strong candidate, due to the fewer associated toxicities, that is able to exert its anti-cancer effects in both $KRAS^{wt}$ and $KRAS^{mut}$ cells. This study opens a new avenue for treating $KRAS^{mut}$ cancers and highlights the potential of fisetin as an anti-cancer agent, with the possibility of entering animal studies.

Mechanistically, the exact role of YB-1 in DSB repair is not fully understood. However, YB-1 is an RNA and DNA binding protein that plays a crucial role in DNA repair mechanisms. Upon activation in the nucleus, YB-1 interacts with DNA repair proteins

to facilitate the repair processes. Recent studies have highlighted the significance of RNAs and their interactions with both DNA and proteins in DSB signaling and repair. In particular, long and short non-coding RNAs have been identified as direct regulators of the DSB repair pathway. These RNAs may be connected to RNA-binding proteins, such as YB-1, within the DSB response network. Therefore, further investigation is needed to clarify the precise role of YB-1 in DSB repair.

Bibliography

Adan, A. and Y. Baran (2015). "The pleiotropic effects of fisetin and hesperetin on human acute promyelocytic leukemia cells are mediated through apoptosis, cell cycle arrest, and alterations in signaling networks". In: *Tumour Biol* 36.11, pp. 8973–84. ISSN: 1010-4283. DOI: 10.1007/s13277-015-3597-6.

Ambrogio, Chiara, Jens Köhler, Zhi-Wei Zhou, Haiyun Wang, Raymond Paranal, Jiaqi Li, Marzia Capelletti, Cristina Caffarra, Shuai Li, Qi Lv, Sudershan Gondi, John C. Hunter, Jia Lu, Roberto Chiarle, David Santamaría, Kenneth D. Westover, and Pasi A. Jänne (2018). "KRAS Dimerization Impacts MEK Inhibitor Sensitivity and Oncogenic Activity of Mutant KRAS". In: *Cell* 172.4, 857–868.e15. ISSN: 0092-8674. DOI: https://doi.org/10.1016/j.cell.2017.12.020. URL: https://www.sciencedirect.com/science/article/pii/S0092867417315003.

Aparicio, Jorge, Francis Esposito, Sara Serrano, Esther Falco, Pilar Escudero, Ana Ruiz-Casado, Hermini Manzano, and Ana Fernandez-Montes (2020). "Metastatic Colorectal Cancer. First Line Therapy for Unresectable Disease". In: *Journal of Clinical Medicine* 9.12, p. 3889. ISSN: 2077-0383. URL: https://www.mdpi.com/2077-0383/9/12/3889.

Aronchik, I., B. A. Appleton, S. E. Basham, K. Crawford, M. Del Rosario, L. V. Doyle, W. F. Estacio, J. Lan, M. K. Lindvall, C. A. Luu, E. Ornelas, E. Venetsanakos, C. M. Shafer, and A. B. Jefferson (2014). "Novel potent and selective inhibitors of p90 ribosomal S6 kinase reveal the heterogeneity of RSK function in MAPK-driven cancers". In: *Mol Cancer Res* 12.5, pp. 803–12. ISSN: 1541-7786. DOI: 10.1158/1541-7786.Mcr-13-0595.

Bader, A. G. and P. K. Vogt (2008). "Phosphorylation by Akt disables the anti-oncogenic activity of YB-1". In: *Oncogene* 27.8, pp. 1179–1182. ISSN: 1476-5594. DOI: 10.1038/sj.onc.1210719. URL: https://doi.org/10.1038/sj.onc.1210719.

Beeser, A., Z. M. Jaffer, C. Hofmann, and J. Chernoff (2005). "Role of group A p21-activated kinases in activation of extracellular-regulated kinase by growth factors". In: *J Biol Chem* 280.44, pp. 36609–15. ISSN: 0021-9258 (Print) 0021-9258 (Linking). DOI: 10.1074/jbc.M502306200. URL: https://www.ncbi.nlm.nih.gov/pubmed/16129686.

Boretto, Matteo, Maarten H. Geurts, Shashank Gandhi, Ziliang Ma, Nadzeya Staliarova, Martina Celotti, Sangho Lim, Gui-Wei He, Rosemary Millen, Else Driehuis, Harry Begthel, Lidwien Smabers, Jeanine Roodhart, Johan van Es, Wei Wu, and Hans Clevers (2024). "Epidermal growth factor receptor (EGFR) is a target of the tumor-suppressor E3 ligase FBXW7". In: *Proceedings of the National Academy of Sciences* 121.12, e2309902121. DOI: doi:10.1073/pnas.2309902121. URL: https://www.pnas.org/doi/abs/10.1073/pnas.2309902121.

Borrego-Soto, G., R. Ortiz-López, and A. Rojas-Martínez (2015). "Ionizing radiation-induced DNA injury and damage detection in patients with breast cancer". In: *Genet Mol Biol* 38.4, pp. 420–32. ISSN: 1415-4757 (Print) 1415-4757. DOI: 10.1590/s1415-475738420150019.

Bozulic, Lana, Banu Surucu, Debby Hynx, and Brian A. Hemmings (2008). "PKBx3b1;/Akt1 Acts Downstream of DNA-PK in the DNA Double-Strand Break Response and Promotes Survival". In: *Molecular Cell* 30.2, pp. 203–213. ISSN: 1097-2765. DOI: 10.1016/j.molcel.2008.02.024. URL: https://doi.org/10.1016/j.molcel.2008.02.024.

Bray, Freddie, Mathieu Laversanne, Hyuna Sung, Jacques Ferlay, Rebecca L. Siegel, Isabelle Soerjomataram, and Ahmedin Jemal (2024). "Global cancer statistics 2022: GLOBOCAN estimates of incidence and mortality worldwide for 36 cancers in 185 countries". In: *CA: A Cancer Journal for Clinicians* 74.3, pp. 229–263. ISSN: 0007-9235. DOI: https://doi.org/10.3322/caac.21834. URL: https://acsjournals.onlinelibrary.wiley.com/doi/abs/10.3322/caac.21834.

Buhrman, G., G. Wink, and C. Mattos (2007). "Transformation efficiency of RasQ61 mutants linked to structural features of the switch regions in the presence of Raf". In: *Structure* 15.12, pp. 1618–29. ISSN: 0969-2126 (Print) 0969-2126. DOI: 10.1016/j.str.2007.10.011.

Chaachouay, H., P. Ohneseit, M. Toulany, R. Kehlbach, G. Multhoff, and H. P. Rodemann (2011). "Autophagy contributes to resistance of tumor cells to ionizing radiation". In: *Radiother Oncol* 99.3, pp. 287–92. ISSN: 0167-8140. DOI: 10.1016/j.radonc.2011.06.002.

Chang, Howard H. Y., Go Watanabe, Christina A. Gerodimos, Takashi Ochi, Tom L. Blundell, Stephen P. Jackson, and Michael R. Lieber (2016). "Different DNA End Configurations Dictate Which NHEJ Components Are Most Important for Joining Efficiency *¡sup¿ ¡/sup¿". In: *Journal of Biological Chemistry* 291.47, pp. 24377–24389. ISSN: 0021-9258. DOI: 10.1074/jbc.M116.752329. URL: https://doi.org/10.1074/jbc.M116.752329.

Chao, Hsiao-Mei, Hong-Xuan Huang, Po-Hsiang Chang, Kuo-Chang Tseng, Atsushi Miyajima, and Edward Chern (2016). "Y-box binding protein-1 promotes hepatocellular carcinoma-initiating cell progression and tumorigenesis via Wnt/-catenin pathway". In: *Oncotarget* 8.2. ISSN: 1949-2553. URL: https://www.oncotarget.com/article/13733/text/.

Chatterjee, M., C. Rancso, T. Stühmer, N. Eckstein, M. Andrulis, C. Gerecke, H. Lorentz, H. D. Royer, and R. C. Bargou (2008). "The Y-box binding protein YB-1 is associated with progressive disease and mediates survival and drug resistance in multiple myeloma". In: *Blood* 111.7, pp. 3714–22. ISSN: 0006-4971 (Print) 0006-4971. DOI: 10.1182/blood-2007-05-089151.

Chen, C. C., T. K. Er, Y. Y. Liu, J. K. Hwang, M. J. Barrio, M. Rodrigo, E. Garcia-Toro, and M. Herreros-Villanueva (2013). "Computational analysis of KRAS mutations: implications for different effects on the KRAS p.G12D and p.G13D mutations". In: *PLoS One* 8.2, e55793. ISSN: 1932-6203 (Electronic) 1932-6203 (Linking). DOI: 10.1371/journal.pone.0055793. URL: https://www.ncbi.nlm.nih.gov/pubmed/23437064.

Chen, W. S., Y. J. Lee, Y. C. Yu, C. H. Hsaio, J. H. Yen, S. H. Yu, Y. J. Tsai, and S. J. Chiu (2010). "Enhancement of p53-mutant human colorectal cancer cells radiosensitivity by flavonoid fisetin". In: *Int J Radiat Oncol Biol Phys* 77.5, pp. 1527–35. ISSN: 0360-3016. DOI: 10.1016/j.ijrobp.2010.02.043.

Chen, Y. S., H. X. Song, Y. Lu, X. Li, T. Chen, Y. Zhang, J. X. Xue, H. Liu, B. Kan, G. Yang, and T. Fu (2011). "Autophagy inhibition contributes to radiation sensitization of esophageal squamous carcinoma cells". In: *Dis Esophagus* 24.6, pp. 437–43. ISSN: 1120-8694. DOI: 10.1111/j.1442-2050.2010.01156.x.

Chida, K., D. Kotani, T. Masuishi, T. Kawakami, Y. Kawamoto, K. Kato, K. Fushiki, K. Sawada, R. Kumanishi, H. Shirasu, Y. Matsubara, S. Yuki, Y. Komatsu, K. Yamazaki, and T. Yoshino (2021). "The Prognostic Impact of KRAS G12C Mutation in Patients with Metastatic Colorectal Cancer: A Multicenter Retrospective Observational Study". In: *Oncologist* 26.10, pp. 845–853. ISSN: 1549-490X (Electronic) 1083-7159 (Print) 1083-7159 (Linking). DOI: 10.1002/onco.13870. URL: https://www.ncbi.nlm.nih.gov/pubmed/34232546.

Chu, Po-Chen, Peng-Chan Lin, Hsing-Yu Wu, Kuen-Tyng Lin, Christina Wu, Tanios Bekaii-Saab, Yih-Jyh Lin, Chung-Ta Lee, Jeng-Chang Lee, and Ching-Shih Chen (2018). "Mutant KRAS promotes liver metastasis of colorectal cancer, in part, by upregulating the MEK-Sp1-DNMT1-miR-137-YB-1-IGF-IR signaling pathway". In: *Oncogene* 37.25, pp. 3440–3455. ISSN: 1476-5594. DOI: 10.1038/s41388-018-0222-3. URL: https://doi.org/10.1038/s41388-018-0222-3.

Dahl, Edgar, Abdelaziz En-Nia, Frank Wiesmann, Renate Krings, Sonja Djudjaj, Elisabeth Breuer, Thomas Fuchs, Peter J. Wild, Arndt Hartmann, Sandra E. Dunn, and

Peter R. Mertens (2009). "Nuclear detection of Y-boxprotein-1 (YB-1) closely associates with progesterone receptor negativity and is a strong adverse survival factor in human breast cancer". In: *BMC Cancer* 9.1, p. 410. ISSN: 1471-2407. DOI: 10.1186/1471-2407-9-410. URL: https://doi.org/10.1186/1471-2407-9-410.

Dai, M., R. Jahanzaib, Y. Liao, F. Yao, J. Li, X. Teng, K. Chen, and W. Cheng (2022). "Prognostic value of KRAS subtype in patients with PDAC undergoing radical resection". In: *Front Oncol* 12, p. 1074538. ISSN: 2234-943X (Print) 2234-943X (Electronic) 2234-943X (Linking). DOI: 10.3389/fonc.2022.1074538. URL: https://www.ncbi.nlm.nih.gov/pubmed/36582783.

Di Micco, R., M. Fumagalli, A. Cicalese, S. Piccinin, P. Gasparini, C. Luise, C. Schurra, M. Garre, P. G. Nuciforo, A. Bensimon, R. Maestro, P. G. Pelicci, and F. d'Adda di Fagagna (2006). "Oncogene-induced senescence is a DNA damage response triggered by DNA hyper-replication". In: *Nature* 444.7119, pp. 638–42. ISSN: 0028-0836. DOI: 10.1038/nature05327.

Ding, Guoping, Xiaodong Xu, Dan Li, Yuhao Chen, Weimin Wang, Dongnan Ping, Shengnan Jia, and Liping Cao (2020). "Fisetin inhibits proliferation of pancreatic adenocarcinoma by inducing DNA damage via RFXAP/KDM4A-dependent histone H3K36 demethylation". In: *Cell Death Disease* 11.10, p. 893. ISSN: 2041-4889. DOI: 10.1038/s41419-020-03019-2. URL: https://doi.org/10.1038/s41419-020-03019-2.

Dolfini, D. and R. Mantovani (2013). "Targeting the Y/CCAAT box in cancer: YB-1 (YBX1) or NF-Y?" In: *Cell Death Differentiation* 20.5, pp. 676–685. ISSN: 1476-5403. DOI: 10.1038/cdd.2013.13. URL: https://doi.org/10.1038/cdd.2013.13.

Dong, Shengli, Hassan Yousefi, Isabella Van Savage, Samuel C. Okpechi, Maryl K. Wright, Margarite D. Matossian, Bridgette M. Collins-Burow, Matthew E. Burow, and Suresh K. Alahari (2022). "Ceritinib is a novel triple negative breast cancer therapeutic agent". In: *Molecular Cancer* 21.1, p. 138. ISSN: 1476-4598. DOI: 10.1186/s12943-022-01601-0. URL: https://doi.org/10.1186/s12943-022-01601-0.

Dueva, Rositsa and George Iliakis (2013a). "Alternative pathways of non-homologous end joining (NHEJ) in genomic instability and cancer". In: *Translational Cancer Research* 2.3. ISSN: 2219-6803. URL: https://tcr.amegroups.org/article/view/1152.

– (2013b). "Alternative pathways of non-homologous end joining (NHEJ) in genomic instability and cancer". In: *Translational Cancer Research* 2.3, pp. 163–177. ISSN: 2219-6803. URL: https://tcr.amegroups.org/article/view/1152.

Ebi, H., C. Costa, A. C. Faber, M. Nishtala, H. Kotani, D. Juric, P. Della Pelle, Y. Song, S. Yano, M. Mino-Kenudson, C. H. Benes, and J. A. Engelman (2013). "PI3K regulates MEK/ERK signaling in breast cancer via the Rac-GEF, P-Rex1". In: *Proc Natl Acad Sci U S A* 110.52, pp. 21124–9. ISSN: 1091-6490 (Electronic) 0027-8424

(Print) 0027-8424 (Linking). DOI: 10.1073/pnas.1314124110. URL: https://www.ncbi.nlm.nih.gov/pubmed/24327733.

Eblen, S. T., J. K. Slack, M. J. Weber, and A. D. Catling (2002). "Rac-PAK signaling stimulates extracellular signal-regulated kinase (ERK) activation by regulating formation of MEK1-ERK complexes". In: *Mol Cell Biol* 22.17, pp. 6023–33. ISSN: 0270-7306 (Print) 1098-5549 (Electronic) 0270-7306 (Linking). DOI: 10.1128/MCB.22.17.6023-6033.2002. URL: https://www.ncbi.nlm.nih.gov/pubmed/12167697.

El Hage, Krystel, Nicolas Babault, Olek Maciejak, Bénédicte Desforges, Pierrick Craveur, Emilie Steiner, Juan Carlos Rengifo-Gonzalez, Hélène Henrie, Marie-Jeanne Clement, Vandana Joshi, Ahmed Bouhss, Liya Wang, Cyril Bauvais, and David Pastré (2023). "Targeting RNA:protein interactions with an integrative approach leads to the identification of potent YBX1 inhibitors". In: *eLife* 12, e80387. ISSN: 2050-084X. DOI: 10.7554/eLife.80387. URL: https://doi.org/10.7554/eLife.80387.

Elbanna, M., N. N. Chowdhury, R. Rhome, and M. L. Fishel (2021). "Clinical and Preclinical Outcomes of Combining Targeted Therapy With Radiotherapy". In: *Front Oncol* 11, p. 749496. ISSN: 2234-943X (Print) 2234-943x. DOI: 10.3389/fonc.2021.749496.

Eser, S., A. Schnieke, G. Schneider, and D. Saur (2014). "Oncogenic KRAS signalling in pancreatic cancer". In: *Br J Cancer* 111.5, pp. 817–22. ISSN: 0007-0920 (Print) 0007-0920. DOI: 10.1038/bjc.2014.215.

Evdokimova, V., P. Ruzanov, M. S. Anglesio, A. V. Sorokin, L. P. Ovchinnikov, J. Buckley, T. J. Triche, N. Sonenberg, and P. H. Sorensen (2006). "Akt-mediated YB-1 phosphorylation activates translation of silent mRNA species". In: *Mol Cell Biol* 26.1, pp. 277–92. URL: http://www.ncbi.nlm.nih.gov/entrez/query.fcgi?cmd=Retrieve&db=PubMed&dopt=Citation&list_uids=16354698.

Evdokimova, V., C. Tognon, T. Ng, P. Ruzanov, N. Melnyk, D. Fink, A. Sorokin, L. P. Ovchinnikov, E. Davicioni, T. J. Triche, and P. H. Sorensen (2009). "Translational activation of snail1 and other developmentally regulated transcription factors by YB-1 promotes an epithelial-mesenchymal transition". In: *Cancer Cell* 15.5, pp. 402–15. ISSN: 1535-6108. DOI: 10.1016/j.ccr.2009.03.017.

Evdokimova, Valentina M., Elizaveta A. Kovrigina, Dmitry V. Nashchekin, Elena K. Davydova, John W. B. Hershey, and Lev P. Ovchinnikov (1998). "The Major Core Protein of Messenger Ribonucleoprotein Particles (p50) Promotes Initiation of Protein Biosynthesis in Vitro *". In: *Journal of Biological Chemistry* 273.6, pp. 3574–3581. ISSN: 0021-9258. DOI: https://doi.org/10.1074/jbc.273.6.3574. URL: https://www.sciencedirect.com/science/article/pii/S002192581893766X.

Evdokimova, Valentina M., Chia-Lin Wei, Albert S. Sitikov, Peter N. Simonenko, Oleg A. Lazarev, Konstantin S. Vasilenko, Valentin A. Ustinov, John W. B. Hershey, and Lev P. Ovchinnikov (1995). "The Major Protein of Messenger Ribonucleoprotein Particles

in Somatic Cells Is a Member of the Y-box Binding Transcription Factor Family ()". In: *Journal of Biological Chemistry* 270.7, pp. 3186–3192. ISSN: 0021-9258. DOI: https://doi.org/10.1074/jbc.270.7.3186. URL: https://www.sciencedirect.com/science/article/pii/S002192581882909X.

Fan, W. H., F. L. Wang, Z. H. Lu, Z. Z. Pan, L. R. Li, Y. H. Gao, G. Chen, X. J. Wu, P. R. Ding, Z. F. Zeng, and D. S. Wan (2015). "Surgery with versus without preoperative concurrent chemoradiotherapy for mid/low rectal cancer: an interim analysis of a prospective, randomized trial". In: *Chin J Cancer* 34.9, pp. 394–403. ISSN: 1000-467X (Print) 1944-446x. DOI: 10.1186/s40880-015-0024-8.

Fujiwara-Okada, Y., Y. Matsumoto, J. Fukushi, N. Setsu, S. Matsuura, S. Kamura, T. Fujiwara, K. Iida, M. Hatano, A. Nabeshima, H. Yamada, M. Ono, Y. Oda, and Y. Iwamoto (2013). "Y-box binding protein-1 regulates cell proliferation and is associated with clinical outcomes of osteosarcoma". In: *British Journal of Cancer* 108.4, pp. 836–847. ISSN: 1532-1827. DOI: 10.1038/bjc.2012.579. URL: https://doi.org/10.1038/bjc.2012.579.

Fushimi, Fumiyoshi, Kenichi Taguchi, Hiroto Izumi, Kimitoshi Kohno, Michihiko Kuwano, Mayumi Ono, Yutaka Nakashima, Tetsuro Takesue, Seiji Naito, and Yoshinao Oda (2013). "Peroxiredoxins, thioredoxin, and Y-box-binding protein-1 are involved in the pathogenesis and progression of dialysis-associated renal cell carcinoma". In: *Virchows Archiv* 463.4, pp. 553–562. ISSN: 1432-2307. DOI: 10.1007/s00428-013-1460-y. URL: https://doi.org/10.1007/s00428-013-1460-y.

Gaudreault, Isabelle, David Guay, and Michel Lebel (2004). "YB-1 promotes strand separation in vitro of duplex DNA containing either mispaired bases or cisplatin modifications, exhibits endonucleolytic activities and binds several DNA repair proteins". In: *Nucleic Acids Research* 32.1, pp. 316–327. ISSN: 0305-1048. DOI: 10.1093/nar/gkh170. URL: https://doi.org/10.1093/nar/gkh170.

Gessner, C., C. Woischwill, A. Schumacher, U. Liebers, H. Kuhn, P. Stiehl, K. Jurchott, H. D. Royer, C. Witt, and G. Wolff (2004). "Nuclear YB-1 expression as a negative prognostic marker in nonsmall cell lung cancer". In: *Eur Respir J* 23.1, pp. 14–9. ISSN: 0903-1936 (Print) 0903-1936 (Linking). DOI: 10.1183/09031936.03.00033203. URL: https://www.ncbi.nlm.nih.gov/pubmed/14738225.

Ghosh, Dipayan and Sathees C. Raghavan (2021). "Nonhomologous end joining: new accessory factors fine tune the machinery". In: *Trends in Genetics* 37.6, pp. 582–599. ISSN: 0168-9525. DOI: 10.1016/j.tig.2021.03.001. URL: https://doi.org/10.1016/j.tig.2021.03.001.

Gieseler-Halbach, Steffi, Stefan Meltendorf, Mandy Pierau, Soenke Weinert, Florian H. Heidel, Thomas Fischer, Juliane Handschuh, Ruediger C. Braun-Dullaeus, Martin Schrappe, Jonathan A. Lindquist, Peter R. Mertens, Ulrich Thomas, and Monika C. Brunner-Weinzierl (2017). "RSK-mediated nuclear accumulation of the cold-shock

Y-box protein-1 controls proliferation of T cells and T-ALL blasts". In: *Cell Death Differentiation* 24.2, pp. 371–383. ISSN: 1476-5403. DOI: 10.1038/cdd.2016.141. URL: https://doi.org/10.1038/cdd.2016.141.

Gort, Eelke, Melissa Lynne Johnson, Jimmy J. Hwang, Shubham Pant, Ulrich Dünzinger, Kathrin Riemann, Thomas Kitzing, and Pasi A. Janne (2020). "A phase I, open-label, dose-escalation trial of BI 1701963 as monotherapy and in combination with trametinib in patients with KRAS mutated advanced or metastatic solid tumors". In: *Journal of Clinical Oncology* 38.15$_s$*uppl*, TPS3651–TPS3651. DOI: 10.1200/JCO.2020.38.15_suppl.TPS3651. URL: https://ascopubs.org/doi/abs/10.1200/JCO.2020.38.15_suppl.TPS3651.

Grynkiewicz, Grzegorz and Oleg M Demchuk (Oct. 2019). "New perspectives for fisetin". en. In: *Front. Chem.* 7, p. 697.

Guay, David, Audrey-Ann Evoy, Éric Paquet, Chantal Garand, Magdalena Bachvarova, Dimcho Bachvarov, and Michel Lebel (2008). "The strand separation and nuclease activities associated with YB-1 are dispensable for cisplatin resistance but overexpression of YB-1 in MCF7 and MDA-MB-231 breast tumor cells generates several chemoresistance signatures". In: *The International Journal of Biochemistry Cell Biology* 40.11, pp. 2492–2507. ISSN: 1357-2725. DOI: https://doi.org/10.1016/j.biocel.2008.04.011. URL: https://www.sciencedirect.com/science/article/pii/S1357272508001799.

Güldenhaupt, Jörn, Till Rudack, Peter Bachler, Daniel Mann, Gemma Triola, Herbert Waldmann, Carsten Kötting, and Klaus Gerwert (2012). "N-Ras forms dimers at POPC membranes". In: *Biophysical journal* 103.7, pp. 1585–1593. ISSN: 0006-3495.

Gunasekaran, V. P., K. Nishi, D. Sivakumar, T. Sivaraman, and G. Mathan (2018). "Identification of 2,4-dihydroxy-5-pyrimidinyl imidothiocarbomate as a novel inhibitor to Y box binding protein-1 (YB-1) and its therapeutic actions against breast cancer". In: *Eur J Pharm Sci* 116, pp. 2–14. ISSN: 0928-0987. DOI: 10.1016/j.ejps.2017.09.019.

Gunn, A. and J. M. Stark (2012). "I-SceI-based assays to examine distinct repair outcomes of mammalian chromosomal double strand breaks". In: *Methods Mol Biol* 920, pp. 379–91. ISSN: 1064-3745. DOI: 10.1007/978-1-61779-998-3_27.

Hahn, S. M., E. J. Bernhard, W. Regine, M. Mohiuddin, D. G. Haller, J. P. Stevenson, D. Smith, B. Pramanik, J. Tepper, T. F. DeLaney, K. D. Kiel, B. Morrison, P. Deutsch, R. J. Muschel, and W. G. McKenna (2002). "A Phase I trial of the farnesyltransferase inhibitor L-778,123 and radiotherapy for locally advanced lung and head and neck cancer". In: *Clin Cancer Res* 8.5, pp. 1065–72. ISSN: 1078-0432 (Print) 1078-0432 (Linking). URL: https://www.ncbi.nlm.nih.gov/pubmed/12006520.

Haigis, K. M. (2017). "KRAS Alleles: The Devil Is in the Detail". In: *Trends Cancer* 3.10, pp. 686–697. ISSN: 2405-8033 (Print) 2405-8025. DOI: 10.1016/j.trecan.2017.08.006.

Hall, Eric J and Amato J Giaccia (2006). *Radiobiology for the Radiologist*. Vol. 6. Philadelphia.

Hamon, Loïc, Karina Budkina, and David Pastré (2022). "YB-1 Structure/Function Relationship in the Packaging of mRNPs and Consequences for Translation Regulation and Stress Granule Assembly in Cells". In: *Biochemistry (Moscow)* 87.1, S20–S31. ISSN: 1608-3040. DOI: 10.1134/S0006297922140036. URL: https://doi.org/10.1134/S0006297922140036.

Hasegawa, Susan L., Paul W. Doetsch, Krista K. Hamilton, Amy M. Martin, Sharon A. Okenquist, Jack Lenz, and Jeremy M. Boss (1991). "DNA binding properties of YB-1 and dbpA: binding to doublestranded, single-stranded, and abasic site containing DNAs". In: *Nucleic Acids Research* 19.18, pp. 4915–4920. ISSN: 0305-1048. DOI: 10.1093/nar/19.18.4915. URL: https://doi.org/10.1093/nar/19.18.4915.

He, H., K. Lin, Y. Su, S. Lin, C. Zou, J. Pan, Y. Zhou, and C. Chen (2018a). "Overexpression of -Catenin Decreases the Radiosensitivity of Human Nasopharyngeal Carcinoma CNE-2 Cells". In: *Cell Physiol Biochem* 50.5, pp. 1929–1944. ISSN: 1015-8987. DOI: 10.1159/000494873.

He, Ming Yuan, Chloé Rancoule, Amel Rehailia-Blanchard, Sophie Espenel, Jane-Chloé Trone, Emilie Bernichon, Elodie Guillaume, Alexis Vallard, and Nicolas Magné (2018b). "Radiotherapy in triple-negative breast cancer: Current situation and upcoming strategies". In: *Critical Reviews in Oncology/Hematology* 131, pp. 96–101. ISSN: 1040-8428. DOI: https://doi.org/10.1016/j.critrevonc.2018.09.004. URL: https://www.sciencedirect.com/science/article/pii/S1040842817304080.

Hemmings, B. A. and D. F. Restuccia (2012). "PI3K-PKB/Akt pathway". In: *Cold Spring Harb Perspect Biol* 4.9, a011189. ISSN: 1943-0264. DOI: 10.1101/cshperspect.a011189.

Herr, Ricarda, Franziska U Wöhrle, Christina Danke, Christian Berens, and Tilman Brummer (July 2011). "A novel MCF-10A line allowing conditional oncogene expression in 3D culture". en. In: *Cell Commun. Signal.* 9.1, p. 17.

Higashi, K., Y. Tomigahara, H. Shiraki, K. Miyata, T. Mikami, T. Kimura, T. Moro, Y. Inagaki, and H. Kaneko (2011). "A novel small compound that promotes nuclear translocation of YB-1 ameliorates experimental hepatic fibrosis in mice". In: *J Biol Chem* 286.6, pp. 4485–92. ISSN: 0021-9258 (Print) 0021-9258. DOI: 10.1074/jbc.M110.151936.

Higuchi, M., K. Onishi, C. Kikuchi, and Y. Gotoh (2008). "Scaffolding function of PAK in the PDK1-Akt pathway". In: *Nat Cell Biol* 10.11, pp. 1356–64. ISSN: 1476-4679

(Electronic) 1465-7392 (Linking). DOI: 10.1038/ncb1795. URL: https://www.ncbi.nlm.nih.gov/pubmed/18931661.

Hoendervangers, S., J. P. M. Burbach, M. M. Lacle, M. Koopman, W. M. U. van Grevenstein, M. P. W. Intven, and H. M. Verkooijen (2020). "Pathological Complete Response Following Different Neoadjuvant Treatment Strategies for Locally Advanced Rectal Cancer: A Systematic Review and Meta-analysis". In: *Annals of Surgical Oncology* 27.11, pp. 4319–4336. ISSN: 1534-4681. DOI: 10.1245/s10434-020-08615-2. URL: https://doi.org/10.1245/s10434-020-08615-2.

Huang, C., S. Zhou, C. Zhang, Y. Jin, G. Xu, L. Zhou, G. Ding, T. Pang, S. Jia, and L. Cao (2022). "ZC3H13-mediated N6-methyladenosine modification of PHF10 is impaired by fisetin which inhibits the DNA damage response in pancreatic cancer". In: *Cancer Lett* 530, pp. 16–28. ISSN: 0304-3835. DOI: 10.1016/j.canlet.2022.01.013.

Hubbard, S. R. and W. T. Miller (2007). "Receptor tyrosine kinases: mechanisms of activation and signaling". In: *Curr Opin Cell Biol* 19.2, pp. 117–23. ISSN: 0955-0674 (Print) 0955-0674. DOI: 10.1016/j.ceb.2007.02.010.

Hunter, John C., Anuj Manandhar, Martin A. Carrasco, Deepak Gurbani, Sudershan Gondi, and Kenneth D. Westover (2015). "Biochemical and Structural Analysis of Common Cancer-Associated KRAS Mutations". In: *Molecular Cancer Research* 13.9, pp. 1325–1335. ISSN: 1541-7786. DOI: 10.1158/1541-7786.Mcr-15-0203. URL: https://doi.org/10.1158/1541-7786.MCR-15-0203.

Ihle, N. T., L. A. Byers, E. S. Kim, P. Saintigny, J. J. Lee, G. R. Blumenschein, A. Tsao, S. Liu, J. E. Larsen, J. Wang, L. Diao, K. R. Coombes, L. Chen, S. Zhang, M. F. Abdelmelek, X. Tang, V. Papadimitrakopoulou, J. D. Minna, S. M. Lippman, W. K. Hong, R. S. Herbst, II Wistuba, J. V. Heymach, and G. Powis (2012). "Effect of KRAS oncogene substitutions on protein behavior: implications for signaling and clinical outcome". In: *J Natl Cancer Inst* 104.3, pp. 228–39. ISSN: 1460-2105 (Electronic) 0027-8874 (Print) 0027-8874 (Linking). DOI: 10.1093/jnci/djr523. URL: https://www.ncbi.nlm.nih.gov/pubmed/22247021.

Ise, T., G. Nagatani, T. Imamura, K. Kato, H. Takano, M. Nomoto, H. Izumi, H. Ohmori, T. Okamoto, T. Ohga, T. Uchiumi, M. Kuwano, and K. Kohno (1999). "Transcription factor Y-box binding protein 1 binds preferentially to cisplatin-modified DNA and interacts with proliferating cell nuclear antigen". In: *Cancer Res* 59.2, pp. 342–6. ISSN: 0008-5472 (Print) 0008-5472.

Ishige, K., D. Schubert, and Y. Sagara (2001). "Flavonoids protect neuronal cells from oxidative stress by three distinct mechanisms". In: *Free Radic Biol Med* 30.4, pp. 433–46. ISSN: 0891-5849 (Print) 0891-5849. DOI: 10.1016/s0891-5849(00)00498-6.

Izumi, H., T. Imamura, G. Nagatani, T. Ise, T. Murakami, H. Uramoto, T. Torigoe, H. Ishiguchi, Y. Yoshida, M. Nomoto, T. Okamoto, T. Uchiumi, M. Kuwano, K. Funa, and K. Kohno (2001). "Y box-binding protein-1 binds preferentially to single-stranded

nucleic acids and exhibits 3'–¿5' exonuclease activity". In: *Nucleic Acids Res* 29.5, pp. 1200–7. ISSN: 0305-1048 (Print) 0305-1048. DOI: 10.1093/nar/29.5.1200.

Jang, K., M. Kim, H. S. Seo, and I. Shin (2010). "PTEN sensitizes MDA-MB-468 cells to inhibition of MEK/Erk signaling for the blockade of cell proliferation". In: *Oncol Rep* 24.3, pp. 787–93. ISSN: 1021-335x. DOI: 10.3892/or_00000922.

Jayavelu, Ashok Kumar, Tina M. Schnöder, Florian Perner, Carolin Herzog, Arno Meiler, Gurumoorthy Krishnamoorthy, Nicolas Huber, Juliane Mohr, Bärbel Edelmann-Stephan, Rebecca Austin, Sabine Brandt, Francesca Palandri, Nicolas Schröder, Berend Isermann, Frank Edlich, Amit U. Sinha, Martin Ungelenk, Christian A. Hübner, Robert Zeiser, Susann Rahmig, Claudia Waskow, Iain Coldham, Thomas Ernst, Andreas Hochhaus, Stefanie Jilg, Philipp J. Jost, Ann Mullally, Lars Bullinger, Peter R. Mertens, Steven W. Lane, Matthias Mann, and Florian H. Heidel (2020). "Splicing factor YBX1 mediates persistence of JAK2-mutated neoplasms". In: *Nature* 588.7836, pp. 157–163. ISSN: 1476-4687. DOI: 10.1038/s41586-020-2968-3. URL: https://doi.org/10.1038/s41586-020-2968-3.

Jia, S., X. Xu, S. Zhou, Y. Chen, G. Ding, and L. Cao (2019). "Fisetin induces autophagy in pancreatic cancer cells via endoplasmic reticulum stress- and mitochondrial stress-dependent pathways". In: *Cell Death Dis* 10.2, p. 142. DOI: 10.1038/s41419-019-1366-y.

Jia, Y., T. Jiang, X. Li, C. Zhao, L. Zhang, S. Zhao, X. Liu, M. Qiao, J. Luo, J. Shi, H. Yang, Y. Wang, L. Xi, S. Zhang, G. Gao, C. Su, S. Ren, and C. Zhou (2017). "Characterization of distinct types of KRAS mutation and its impact on first-line platinum-based chemotherapy in Chinese patients with advanced non-small cell lung cancer". In: *Oncol Lett* 14.6, pp. 6525–6532. ISSN: 1792-1074 (Print) 1792-1082 (Electronic) 1792-1074 (Linking). DOI: 10.3892/ol.2017.7016. URL: https://www.ncbi.nlm.nih.gov/pubmed/29163686.

Jiang, L., G. L. Yuan, Q. L. Liang, H. J. Zhang, J. Huang, S. A. Cheng, and X. X. Peng (2017). "Positive expression of Y-box binding protein 1 and prognosis in non-small cell lung cancer: a meta-analysis". In: *Oncotarget* 8.33, pp. 55613–55621. ISSN: 1949-2553. DOI: 10.18632/oncotarget.14732.

Jing, Changwen, Huizi Li, Yuanyuan Du, Haixia Cao, Siwen Liu, Zhuo Wang, Rong Ma, Jifeng Feng, and Jianzhong Wu (2019). "MEK inhibitor enhanced the antitumor effect of oxaliplatin and 5-fluorouracil in MEK1 Q56P-mutant colorectal cancer cells". In: *Mol Med Rep* 19.2, pp. 1092–1100. ISSN: 1791-2997 1791-3004. DOI: 10.3892/mmr.2018.9730. URL: https://doi.org/10.3892/mmr.2018.9730.

Jurchott, K., S. Bergmann, U. Stein, W. Walther, M. Janz, I. Manni, G. Piaggio, E. Fietze, M. Dietel, and H. D. Royer (2003). "YB-1 as a cell cycle-regulated transcription factor facilitating cyclin A and cyclin B1 gene expression". In: *J Biol Chem* 278.30, pp. 27988–96. ISSN: 0021-9258 (Print) 0021-9258. DOI: 10.1074/jbc.M212966200.

Kang, Kyoung Ah, Mei Jing Piao, Ki Cheon Kim, Ji Won Cha, Jian Zheng, Cheng Wen Yao, Sungwook Chae, and Jin Won Hyun (2014). "Fisetin attenuates hydrogen peroxide-induced cell damage by scavenging reactive oxygen species and activating protective functions of cellular glutathione system". In: *In Vitro Cellular Developmental Biology. Animal* 50.1, pp. 66–74. ISSN: 10712690, 1543706X. URL: http://www.jstor.org/stable/24596438.

Khan, M. I., V. M. Adhami, R. K. Lall, M. Sechi, D. C. Joshi, O. M. Haidar, D. N. Syed, I. A. Siddiqui, S. Y. Chiu, and H. Mukhtar (2014). "YB-1 expression promotes epithelial-to-mesenchymal transition in prostate cancer that is inhibited by a small molecule fisetin". In: *Oncotarget* 5.9, pp. 2462–74. ISSN: 1949-2553. DOI: 10.18632/oncotarget.1790.

Khatri, A., J. J. Gu, C. M. McKernan, X. Xu, and A. M. Pendergast (2019). "ABL kinase inhibition sensitizes primary lung adenocarcinomas to chemotherapy by promoting tumor cell differentiation". In: *Oncotarget* 10.20, pp. 1874–1886. ISSN: 1949-2553. DOI: 10.18632/oncotarget.26740.

Khozooei, Shayan, Konstanze Lettau, Francesca Barletta, Tina Jost, Simone Rebholz, Soundaram Veerappan, Mirita Franz-Wachtel, Boris Macek, George Iliakis, Luitpold V. Distel, Daniel Zips, and Mahmoud Toulany (2022). "Fisetin induces DNA double-strand break and interferes with the repair of radiation-induced damage to radiosensitize triple negative breast cancer cells". In: *Journal of Experimental Clinical Cancer Research* 41.1, p. 256. ISSN: 1756-9966. DOI: 10.1186/s13046-022-02442-x. URL: https://doi.org/10.1186/s13046-022-02442-x.

Khozooei, Shayan, Soundaram Veerappan, and Mahmoud Toulany (2023). "YB-1 activating cascades as potential targets in KRAS-mutated tumors". In: *Strahlentherapie und Onkologie* 199.12, pp. 1110–1127. ISSN: 1439-099X. DOI: 10.1007/s00066-023-02092-8. URL: https://doi.org/10.1007/s00066-023-02092-8.

Kim, E. R., A. A. Selyutina, I. A. Buldakov, V. Evdokimova, L. P. Ovchinnikov, and A. V. Sorokin (2013). "The proteolytic YB-1 fragment interacts with DNA repair machinery and enhances survival during DNA damaging stress". In: *Cell Cycle* 12.24, pp. 3791–803. ISSN: 1538-4101 (Print) 1551-4005. DOI: 10.4161/cc.26670.

Kim, J. Y., Y. K. Jeon, W. Jeon, and M. J. Nam (2010). "Fisetin induces apoptosis in Huh-7 cells via downregulation of BIRC8 and Bcl2L2". In: *Food Chem Toxicol* 48.8-9, pp. 2259–64. ISSN: 0278-6915. DOI: 10.1016/j.fct.2010.05.058.

King, C. C., E. M. Gardiner, F. T. Zenke, B. P. Bohl, A. C. Newton, B. A. Hemmings, and G. M. Bokoch (2000). "p21-activated kinase (PAK1) is phosphorylated and activated by 3-phosphoinositide-dependent kinase-1 (PDK1)". In: *J Biol Chem* 275.52, pp. 41201–9. ISSN: 0021-9258 (Print) 0021-9258. DOI: 10.1074/jbc.M006553200.

Klimaszewska-Wisniewska, Anna, Marta Halas-Wisniewska, Tadeusz Tadrowski, Maciej Gagat, Dariusz Grzanka, and Alina Grzanka (2016). "Paclitaxel and the dietary

flavonoid fisetin: a synergistic combination that induces mitotic catastrophe and autophagic cell death in A549 non-small cell lung cancer cells". In: *Cancer Cell International* 16.1, p. 10. ISSN: 1475-2867. DOI: 10.1186/s12935-016-0288-3. URL: https://doi.org/10.1186/s12935-016-0288-3.

Kocaturk, N. M., Y. Akkoc, C. Kig, O. Bayraktar, D. Gozuacik, and O. Kutlu (2019). "Autophagy as a molecular target for cancer treatment". In: *Eur J Pharm Sci* 134, pp. 116–137. ISSN: 0928-0987. DOI: 10.1016/j.ejps.2019.04.011.

Koike, Koji, Takeshi Uchiumi, Takefumi Ohga, Satoshi Toh, Morimasa Wada, Kimitoshi Kohno, and Michihiko Kuwano (1997). "Nuclear translocation of the Y-box binding protein by ultraviolet irradiation". In: *FEBS Letters* 417.3, pp. 390–394. ISSN: 0014-5793. DOI: https://doi.org/10.1016/S0014-5793(97)01296-9. URL: https://www.sciencedirect.com/science/article/pii/S0014579397012969.

Kolch, Walter, Dénes Berta, and Edina Rosta (2023). "Dynamic regulation of RAS and RAS signaling". In: *Biochemical Journal* 480.1, pp. 1–23. ISSN: 0264-6021. DOI: 10.1042/bcj20220234. URL: https://doi.org/10.1042/BCJ20220234.

Korzeniecki, Claudia and Ronny Priefer (2021). "Targeting KRAS mutant cancers by preventing signaling transduction in the MAPK pathway". In: *European Journal of Medicinal Chemistry* 211, p. 113006. ISSN: 0223-5234. DOI: https://doi.org/10.1016/j.ejmech.2020.113006. URL: https://www.sciencedirect.com/science/article/pii/S0223523420309788.

Kumar, A., V. Gautam, A. Sandhu, K. Rawat, A. Sharma, and L. Saha (2023). "Current and emerging therapeutic approaches for colorectal cancer: A comprehensive review". In: *World J Gastrointest Surg* 15.4, pp. 495–519. ISSN: 1948-9366 (Print). DOI: 10.4240/wjgs.v15.i4.495.

Kumar, R., A. E. Gururaj, and C. J. Barnes (2006). "p21-activated kinases in cancer". In: *Nat Rev Cancer* 6.6, pp. 459–71. ISSN: 1474-175X (Print) 1474-175x. DOI: 10.1038/nrc1892.

Kuntz, S., U. Wenzel, and H. Daniel (1999). "Comparative analysis of the effects of flavonoids on proliferation, cytotoxicity, and apoptosis in human colon cancer cell lines". In: *Eur J Nutr* 38.3, pp. 133–42. ISSN: 1436-6207 (Print) 1436-6207. DOI: 10.1007/s003940050054.

Lall, Rahul K., Vaqar Mustafa Adhami, and Hasan Mukhtar (2016). "Dietary flavonoid fisetin for cancer prevention and treatment". In: *Molecular Nutrition Food Research* 60.6, pp. 1396–1405. ISSN: 1613-4125. DOI: https://doi.org/10.1002/mnfr.201600025. URL: https://onlinelibrary.wiley.com/doi/abs/10.1002/mnfr.201600025.

Lan, Huiyin and Yi Sun (2021). "Tumor Suppressor FBXW7 and Its Regulation of DNA Damage Response and Repair". In: *Frontiers in Cell and Developmental Biology* 9. ISSN: 2296-634X. DOI: 10.3389/fcell.2021.751574. URL: https://www.

frontiersin.org/journals/cell-and-developmental-biology/articles/10.3389/fcell.2021.751574.

Landry, Madeleine, Dylan Nelson, Eunseo Choi, Allison DuRoss, and Conroy Sun (2022). "Development of a G2/M arrest high-throughput screening method identifies potent radiosensitizers". In: *Translational Oncology* 16, p. 101336. ISSN: 1936-5233. DOI: https://doi.org/10.1016/j.tranon.2021.101336. URL: https://www.sciencedirect.com/science/article/pii/S1936523321003272.

Lanman, B. A., J. R. Allen, J. G. Allen, A. K. Amegadzie, K. S. Ashton, S. K. Booker, J. J. Chen, N. Chen, M. J. Frohn, G. Goodman, D. J. Kopecky, L. Liu, P. Lopez, J. D. Low, V. Ma, A. E. Minatti, T. T. Nguyen, N. Nishimura, A. J. Pickrell, A. B. Reed, Y. Shin, A. C. Siegmund, N. A. Tamayo, C. M. Tegley, M. C. Walton, H. L. Wang, R. P. Wurz, M. Xue, K. C. Yang, P. Achanta, M. D. Bartberger, J. Canon, L. S. Hollis, J. D. McCarter, C. Mohr, K. Rex, A. Y. Saiki, T. San Miguel, L. P. Volak, K. H. Wang, D. A. Whittington, S. G. Zech, J. R. Lipford, and V. J. Cee (2020). "Discovery of a Covalent Inhibitor of KRAS(G12C) (AMG 510) for the Treatment of Solid Tumors". In: *J Med Chem* 63.1, pp. 52–65. ISSN: 1520-4804 (Electronic) 0022-2623 (Linking). DOI: 10.1021/acs.jmedchem.9b01180. URL: https://www.ncbi.nlm.nih.gov/pubmed/31820981.

Lasham, A., W. Samuel, H. Cao, R. Patel, R. Mehta, J. L. Stern, G. Reid, A. G. Woolley, L. D. Miller, M. A. Black, A. N. Shelling, C. G. Print, and A. W. Braithwaite (2012). "YB-1, the E2F pathway, and regulation of tumor cell growth". In: *J Natl Cancer Inst* 104.2, pp. 133–46. ISSN: 0027-8874 (Print) 0027-8874. DOI: 10.1093/jnci/djr512.

Law, Jennifer H., Yvonne Li, Karen To, Michelle Wang, Arezoo Astanehe, Karen Lambie, Jaspreet Dhillon, Steven J. M. Jones, Martin E. Gleave, Connie J. Eaves, and Sandra E. Dunn (2010). "Molecular Decoy to the Y-Box Binding Protein-1 Suppresses the Growth of Breast and Prostate Cancer Cells whilst Sparing Normal Cell Viability". In: *PLOS ONE* 5.9, e12661. DOI: 10.1371/journal.pone.0012661. URL: https://doi.org/10.1371/journal.pone.0012661.

Lee, C. S., L. C. Lee, T. L. Yuan, S. Chakka, C. Fellmann, S. W. Lowe, N. J. Caplen, F. McCormick, and J. Luo (2019). "MAP kinase and autophagy pathways cooperate to maintain RAS mutant cancer cell survival". In: *Proc Natl Acad Sci U S A* 116.10, pp. 4508–4517. ISSN: 1091-6490 (Electronic) 0027-8424 (Print) 0027-8424 (Linking). DOI: 10.1073/pnas.1817494116. URL: https://www.ncbi.nlm.nih.gov/pubmed/30709910.

Lettau, K., D. Zips, and M. Toulany (2021). "Simultaneous Targeting of RSK and AKT Efficiently Inhibits YB-1-Mediated Repair of Ionizing Radiation-Induced DNA Double-Strand Breaks in Breast Cancer Cells". In: *Int J Radiat Oncol Biol Phys* 109.2, pp. 567–580. ISSN: 0360-3016. DOI: 10.1016/j.ijrobp.2020.09.005.

Leu, J. D., B. S. Wang, S. J. Chiu, C. Y. Chang, C. C. Chen, F. D. Chen, S. Avirmed, and Y. J. Lee (2016). "Combining fisetin and ionizing radiation suppresses the growth of mammalian colorectal cancers in xenograft tumor models". In: *Oncol Lett* 12.6, pp. 4975–4982. ISSN: 1792-1074 (Print) 1792-1074. DOI: 10.3892/ol.2016.5345.

Li, J., Y. Cheng, W. Qu, Y. Sun, Z. Wang, H. Wang, and B. Tian (2011). "Fisetin, a dietary flavonoid, induces cell cycle arrest and apoptosis through activation of p53 and inhibition of NF-kappa B pathways in bladder cancer cells". In: *Basic Clin Pharmacol Toxicol* 108.2, pp. 84–93. ISSN: 1742-7835. DOI: 10.1111/j.1742-7843.2010.00613.x.

Li, J., X. Ma, D. Chakravarti, S. Shalapour, and R. A. DePinho (2021). "Genetic and biological hallmarks of colorectal cancer". In: *Genes Dev* 35.11-12, pp. 787–820. ISSN: 0890-9369 (Print) 0890-9369. DOI: 10.1101/gad.348226.120.

Lin, Wan-Chen, Lars Iversen, Hsiung-Lin Tu, Christopher Rhodes, Sune M Christensen, Jeffrey S Iwig, Scott D Hansen, William YC Huang, and Jay T Groves (2014). "H-Ras forms dimers on membrane surfaces via a protein–protein interface". In: *Proceedings of the National Academy of Sciences* 111.8, pp. 2996–3001. ISSN: 0027-8424.

Lin, Y., R. Shi, X. Wang, and H. M. Shen (2008). "Luteolin, a flavonoid with potential for cancer prevention and therapy". In: *Curr Cancer Drug Targets* 8.7, pp. 634–46. ISSN: 1568-0096 (Print) 1568-0096. DOI: 10.2174/156800908786241050.

Lindquist, Jonathan A. and Peter R. Mertens (2018). "Cold shock proteins: from cellular mechanisms to pathophysiology and disease". In: *Cell Communication and Signaling* 16.1, p. 63. ISSN: 1478-811X. DOI: 10.1186/s12964-018-0274-6. URL: https://doi.org/10.1186/s12964-018-0274-6.

Liu, Y. and W. F. Bodmer (2006). "Analysis of P53 mutations and their expression in 56 colorectal cancer cell lines". In: *Proc Natl Acad Sci U S A* 103.4, pp. 976–81. ISSN: 0027-8424 (Print) 0027-8424. DOI: 10.1073/pnas.0510146103.

Liu, Yang, Yueting Hu, Jinqi Xue, Jingying Li, Jiang Yi, Jiawen Bu, Zhenyong Zhang, Peng Qiu, and Xi Gu (2023). "Advances in immunotherapy for triple-negative breast cancer". In: *Molecular Cancer* 22.1, p. 145. ISSN: 1476-4598. DOI: 10.1186/s12943-023-01850-7. URL: https://doi.org/10.1186/s12943-023-01850-7.

Lu, H., S. Liu, G. Zhang, Wu Bin, Y. Zhu, D. T. Frederick, Y. Hu, W. Zhong, S. Randell, N. Sadek, W. Zhang, G. Chen, C. Cheng, J. Zeng, L. W. Wu, J. Zhang, X. Liu, W. Xu, C. Krepler, K. Sproesser, M. Xiao, B. Miao, J. Liu, C. D. Song, J. Y. Liu, G. C. Karakousis, L. M. Schuchter, Y. Lu, G. Mills, Y. Cong, J. Chernoff, J. Guo, G. M. Boland, R. J. Sullivan, Z. Wei, J. Field, R. K. Amaravadi, K. T. Flaherty, M. Herlyn, X. Xu, and W. Guo (2017a). "PAK signalling drives acquired drug resistance to MAPK inhibitors in BRAF-mutant melanomas". In: *Nature* 550.7674, pp. 133–136. ISSN: 1476-4687 (Electronic) 0028-0836 (Print) 0028-0836 (Linking). DOI: 10.1038/nature24040. URL: https://www.ncbi.nlm.nih.gov/pubmed/28953887.

Lu, J., X. Li, F. Wang, Y. Guo, Y. Huang, H. Zhu, Y. Wang, Y. Lu, and Z. Wang (2017b). "YB-1 expression promotes pancreatic cancer metastasis that is inhibited by microRNA-216a". In: *Exp Cell Res* 359.2, pp. 319–326. ISSN: 1090-2422 (Electronic) 0014-4827 (Linking). DOI: 10.1016/j.yexcr.2017.07.039. URL: https://www.ncbi.nlm.nih.gov/pubmed/28782557.

Lyabin, Dmitry N., Irina A. Eliseeva, and Lev P. Ovchinnikov (2014). "YB-1 protein: functions and regulation". In: *WIREs RNA* 5.1, pp. 95–110. ISSN: 1757-7004. DOI: https://doi.org/10.1002/wrna.1200. URL: https://wires.onlinelibrary.wiley.com/doi/abs/10.1002/wrna.1200.

Ma, Jui-Wen, Chao-Ming Hung, Ying-Chao Lin, Chi-Tang Ho, Jung-Yie Kao, and Tzong-Der Way (2016). "Aloe-emodin inhibits HER-2 expression through the down-regulation of Y-box binding protein-1 in HER-2-overexpressing human breast cancer cells". In: *Oncotarget* 7.37. ISSN: 1949-2553. URL: https://www.oncotarget.com/article/10410/text/.

Maier, E., F. Attenberger, A. Tiwari, K. Lettau, S. Rebholz, B. Fehrenbacher, M. Schaller, C. Gani, and M. Toulany (2019). "Dual Targeting of Y-Box Binding Protein-1 and Akt Inhibits Proliferation and Enhances the Chemosensitivity of Colorectal Cancer Cells". In: *Cancers (Basel)* 11.4. ISSN: 2072-6694 (Print) 2072-6694. DOI: 10.3390/cancers11040562.

Manser, E., T. Leung, H. Salihuddin, Z. S. Zhao, and L. Lim (1994). "A brain serine/threonine protein kinase activated by Cdc42 and Rac1". In: *Nature* 367.6458, pp. 40–6. ISSN: 0028-0836 (Print) 0028-0836. DOI: 10.1038/367040a0.

Manzi, J., C. O. Hoff, R. Ferreira, A. Pimentel, J. Datta, A. S. Livingstone, R. Vianna, and P. Abreu (2023). "Targeted Therapies in Colorectal Cancer: Recent Advances in Biomarkers, Landmark Trials, and Future Perspectives". In: *Cancers (Basel)* 15.11. ISSN: 2072-6694 (Print) 2072-6694. DOI: 10.3390/cancers15113023.

Martin, N. E., T. B. Brunner, K. D. Kiel, T. F. DeLaney, W. F. Regine, M. Mohiuddin, E. F. Rosato, D. G. Haller, J. P. Stevenson, D. Smith, B. Pramanik, J. Tepper, W. K. Tanaka, B. Morrison, P. Deutsch, A. K. Gupta, R. J. Muschel, W. G. McKenna, E. J. Bernhard, and S. M. Hahn (2004). "A phase I trial of the dual farnesyltransferase and geranylgeranyltransferase inhibitor L-778,123 and radiotherapy for locally advanced pancreatic cancer". In: *Clin Cancer Res* 10.16, pp. 5447–54. ISSN: 1078-0432 (Print) 1078-0432 (Linking). DOI: 10.1158/1078-0432.CCR-04-0248. URL: https://www.ncbi.nlm.nih.gov/pubmed/15328183.

Matsumoto, Ken and Alan P. Wolffe (1998). "Gene regulation by Y-box proteins: coupling control of transcription and translation". In: *Trends in Cell Biology* 8.8, pp. 318–323. ISSN: 0962-8924. DOI: https://doi.org/10.1016/S0962-8924(98)01300-2. URL: https://www.sciencedirect.com/science/article/pii/S0962892498013002.

Mavragani, I. V., Z. Nikitaki, S. A. Kalospyros, and A. G. Georgakilas (2019). "Ionizing Radiation and Complex DNA Damage: From Prediction to Detection Challenges and Biological Significance". In: *Cancers (Basel)* 11.11. ISSN: 2072-6694 (Print) 2072-6694. DOI: 10.3390/cancers11111789.

McCarty, S. K., M. Saji, X. Zhang, C. M. Knippler, L. S. Kirschner, S. Fernandez, and M. D. Ringel (2014). "BRAF activates and physically interacts with PAK to regulate cell motility". In: *Endocr Relat Cancer* 21.6, pp. 865–77. ISSN: 1479-6821 (Electronic) 1351-0088 (Print) 1351-0088 (Linking). DOI: 10.1530/ERC-14-0424. URL: https://www.ncbi.nlm.nih.gov/pubmed/25228413.

McCormick, F. (2020). "Sticking it to KRAS: Covalent Inhibitors Enter the Clinic". In: *Cancer Cell* 37.1, pp. 3–4. ISSN: 1535-6108 (Print) 1535-6108. DOI: 10.1016/j.ccell.2019.12.009.

Mehta, S., C. McKinney, M. Algie, C. S. Verma, S. Kannan, R. Harfoot, T. K. Bartolec, P. Bhatia, A. J. Fisher, M. L. Gould, K. Parker, A. J. Cesare, H. E. Cunliffe, S. B. Cohen, T. Kleffmann, A. W. Braithwaite, and A. G. Woolley (2020). "Dephosphorylation of YB-1 is Required for Nuclear Localisation During G(2) Phase of the Cell Cycle". In: *Cancers (Basel)* 12.2. ISSN: 2072-6694 (Print) 2072-6694. DOI: 10.3390/cancers12020315.

Minich, W. B., I. P. Maidebura, and L. P. Ovchinnikov (1993). "Purification and characterization of the major 50-kDa repressor protein from cytoplasmic mRNP of rabbit reticulocytes". In: *Eur J Biochem* 212.3, pp. 633–8. ISSN: 0014-2956 (Print) 0014-2956. DOI: 10.1111/j.1432-1033.1993.tb17701.x.

Misale, Sandra, Jackson P. Fatherree, Eliane Cortez, Chendi Li, Samantha Bilton, Daria Timonina, David T. Myers, Dana Lee, Maria Gomez-Caraballo, Max Greenberg, Varuna Nangia, Patricia Greninger, Regina K. Egan, Joseph McClanaghan, Giovanna T. Stein, Ellen Murchie, Patrick P. Zarrinkar, Matthew R. Janes, Lian-Sheng Li, Yi Liu, Aaron N. Hata, and Cyril H. Benes (2019). "KRAS G12C NSCLC Models Are Sensitive to Direct Targeting of KRAS in Combination with PI3K Inhibition". In: *Clinical Cancer Research* 25.2, pp. 796–807. ISSN: 1078-0432. DOI: 10.1158/1078-0432.Ccr-18-0368. URL: https://doi.org/10.1158/1078-0432.CCR-18-0368.

Mladenov, Emil, Simon Magin, Aashish Soni, and George Iliakis (2013). "DNA Double-Strand Break Repair as Determinant of Cellular Radiosensitivity to Killing and Target in Radiation Therapy". In: *Frontiers in Oncology* 3. ISSN: 2234-943X. DOI: 10.3389/fonc.2013.00113. URL: https://www.frontiersin.org/journals/oncology/articles/10.3389/fonc.2013.00113.

Mladenov, Emil, Veronika Mladenova, Martin Stuschke, and George Iliakis (2023). "New Facets of DNA Double Strand Break Repair: Radiation Dose as Key Determinant of HR versus c-NHEJ Engagement". In: *International Journal of Molecular Sciences*

24.19, p. 14956. ISSN: 1422-0067. URL: https://www.mdpi.com/1422-0067/24/19/14956.

Möller, Yvonne, Martin Siegemund, Sven Beyes, Ricarda Herr, Daniele Lecis, Domenico Delia, Roland Kontermann, Tilman Brummer, Klaus Pfizenmaier, and Monilola A. Olayioye (2014). "EGFR-Targeted TRAIL and a Smac Mimetic Synergize to Overcome Apoptosis Resistance in KRAS Mutant Colorectal Cancer Cells". In: *PLOS ONE* 9.9, e107165. DOI: 10.1371/journal.pone.0107165. URL: https://doi.org/10.1371/journal.pone.0107165.

Moodie, S. A., B. M. Willumsen, M. J. Weber, and A. Wolfman (1993). "Complexes of Ras.GTP with Raf-1 and mitogen-activated protein kinase kinase". In: *Science* 260.5114, pp. 1658–61. ISSN: 0036-8075 (Print) 0036-8075. DOI: 10.1126/science.8503013.

Mozaffari, Nour L., Fabio Pagliarulo, and Alessandro A. Sartori (2021). "Human CtIP: A 'double agent' in DNA repair and tumorigenesis". In: *Seminars in Cell Developmental Biology* 113, pp. 47–56. ISSN: 1084-9521. DOI: https://doi.org/10.1016/j.semcdb.2020.09.001. URL: https://www.sciencedirect.com/science/article/pii/S1084952119300953.

Mueck, Katharina, Simone Rebholz, Mozhgan Dehghan Harati, H. Peter Rodemann, and Mahmoud Toulany (2017). "Akt1 Stimulates Homologous Recombination Repair of DNA Double-Strand Breaks in a Rad51-Dependent Manner". In: *International Journal of Molecular Sciences* 18.11, p. 2473. ISSN: 1422-0067. URL: https://www.mdpi.com/1422-0067/18/11/2473.

Muñoz-Maldonado, C., Y. Zimmer, and M. Medová (2019). "A Comparative Analysis of Individual RAS Mutations in Cancer Biology". In: *Front Oncol* 9, p. 1088. ISSN: 2234-943X (Print) 2234-943x. DOI: 10.3389/fonc.2019.01088.

Mylona, E., S. Melissaris, I. Giannopoulou, I. Theohari, C. Papadimitriou, A. Keramopoulos, and L. Nakopoulou (2014). "Y-box-binding protein 1 (YB1) in breast carcinomas: Relation to aggressive tumor phenotype and identification of patients at high risk for relapse". In: *European Journal of Surgical Oncology (EJSO)* 40.3, pp. 289–296. ISSN: 0748-7983. DOI: https://doi.org/10.1016/j.ejso.2013.09.008. URL: https://www.sciencedirect.com/science/article/pii/S0748798313007798.

Nadal, E., G. Chen, J. R. Prensner, H. Shiratsuchi, C. Sam, L. Zhao, G. P. Kalemkerian, D. Brenner, J. Lin, R. M. Reddy, A. C. Chang, G. Capella, F. Cardenal, D. G. Beer, and N. Ramnath (2014). "KRAS-G12C mutation is associated with poor outcome in surgically resected lung adenocarcinoma". In: *J Thorac Oncol* 9.10, pp. 1513–22. ISSN: 1556-1380 (Electronic) 1556-0864 (Linking). DOI: 10.1097/JTO.0000000000000305. URL: https://www.ncbi.nlm.nih.gov/pubmed/25170638.

El-Naggar, A. M., C. J. Veinotte, H. Cheng, T. G. Grunewald, G. L. Negri, S. P. Somasekharan, D. P. Corkery, F. Tirode, J. Mathers, D. Khan, A. H. Kyle, J. H. Baker,

N. E. LePard, S. McKinney, S. Hajee, M. Bosiljcic, G. Leprivier, C. E. Tognon, A. I. Minchinton, K. L. Bennewith, O. Delattre, Y. Wang, G. Dellaire, J. N. Berman, and P. H. Sorensen (2015). "Translational Activation of HIF1 by YB-1 Promotes Sarcoma Metastasis". In: *Cancer Cell* 27.5, pp. 682–97. ISSN: 1535-6108. DOI: 10.1016/j.ccell.2015.04.003.

El-Naggar, Amal M, Syam Prakash Somasekharan, Yemin Wang, Hongwei Cheng, Gian Luca Negri, Melvin Pan, Xue Qi Wang, Alberto Delaidelli, Bo Rafn, Jordan Cran, Fan Zhang, Haifeng Zhang, Shane Colborne, Martin Gleave, Anna Mandinova, Nancy Kedersha, Christopher S Hughes, Didier Surdez, Olivier Delattre, Yuzhuo Wang, David G Huntsman, Gregg B Morin, and Poul H Sorensen (Dec. 2019). "Class I HDAC inhibitors enhance YB-1 acetylation and oxidative stress to block sarcoma metastasis". en. In: *EMBO Rep.* 20.12, e48375.

Nan, Xiaolin, Tanja M Tamgüney, Eric A Collisson, Li-Jung Lin, Cameron Pitt, Jacqueline Galeas, Sophia Lewis, Joe W Gray, Frank McCormick, and Steven Chu (2015). "Ras-GTP dimers activate the mitogen-activated protein kinase (MAPK) pathway". In: *Proceedings of the National Academy of Sciences* 112.26, pp. 7996–8001. ISSN: 0027-8424.

Nishio, Shin, Kimio Ushijima, Tomohiko Yamaguchi, Yuko Sasajima, Hitoshi Tsuda, Takahiro Kasamatsu, Masayoshi Kage, Mayumi Ono, Michihiko Kuwano, and Toshiharu Kamura (2014). "Nuclear Y-box-binding protein-1 is a poor prognostic marker and related to epidermal growth factor receptor in uterine cervical cancer". In: *Gynecologic Oncology* 132.3, pp. 703–708. ISSN: 0090-8258. DOI: https://doi.org/10.1016/j.ygyno.2014.01.045. URL: https://www.sciencedirect.com/science/article/pii/S009082581400105X.

Nöthen, Till, Mohsen Abdi Sarabi, Sönke Weinert, Werner Zuschratter, Ronnie Morgenroth, Peter R. Mertens, Ruediger C. Braun-Dullaeus, and Senad Medunjanin (2023). "DNA-Dependent Protein Kinase Mediates YB-1 (Y-Box Binding Protein)-Induced Double Strand Break Repair". In: *Arteriosclerosis, Thrombosis, and Vascular Biology* 43.2, pp. 300–311. DOI: doi:10.1161/ATVBAHA.122.317922. URL: https://www.ahajournals.org/doi/abs/10.1161/ATVBAHA.122.317922.

Ohishi, T., M. K. Kaneko, Y. Yoshida, A. Takashima, Y. Kato, and M. Kawada (2023). "Current Targeted Therapy for Metastatic Colorectal Cancer". In: *Int J Mol Sci* 24.2. ISSN: 1422-0067. DOI: 10.3390/ijms24021702.

Pan, Yunzhi, Jing Liu, Yingyin Gao, Yuqing Guo, Changxing Wang, Zhipan Liang, Meiying Wu, Yulan Qian, Yinyan Li, Jingyi Shen, Chenchen Lu, and Sai Ma (2023). "FBXW7 loss of function promotes esophageal squamous cell carcinoma progression via elevating MAP4 and ERK phosphorylation". In: *Journal of Experimental Clinical Cancer Research* 42.1, p. 75. ISSN: 1756-9966. DOI: 10.1186/s13046-023-02630-3. URL: https://doi.org/10.1186/s13046-023-02630-3.

Parikh, Aparna R., Annamaria Szabolcs, Jill N. Allen, Jeffrey W. Clark, Jennifer Y. Wo, Michael Raabe, Hannah Thel, David Hoyos, Arnav Mehta, Sanya Arshad, David J. Lieb, Lorraine C. Drapek, Lawrence S. Blaszkowsky, Bruce J. Giantonio, Colin D. Weekes, Andrew X. Zhu, Lipika Goyal, Ryan D. Nipp, Jon S. Dubois, Emily E. Van Seventer, Bronwen E. Foreman, Lauren E. Matlack, Leilana Ly, Jessica A. Meurer, Nir Hacohen, David P. Ryan, Beow Y. Yeap, Ryan B. Corcoran, Benjamin D. Greenbaum, David T. Ting, and Theodore S. Hong (2021). "Radiation therapy enhances immunotherapy response in microsatellite stable colorectal and pancreatic adenocarcinoma in a phase II trial". In: *Nature Cancer* 2.11, pp. 1124–1135. ISSN: 2662-1347. DOI: 10.1038/s43018-021-00269-7. URL: https://doi.org/10.1038/s43018-021-00269-7.

Park, E. R., S. T. Eblen, and A. D. Catling (2007). "MEK1 activation by PAK: a novel mechanism". In: *Cell Signal* 19.7, pp. 1488–96. ISSN: 0898-6568 (Print) 0898-6568 (Linking). DOI: 10.1016/j.cellsig.2007.01.018. URL: https://www.ncbi.nlm.nih.gov/pubmed/17314031.

Park, H. E., S. Y. Yoo, N. Y. Cho, J. M. Bae, S. W. Han, H. S. Lee, K. J. Park, T. Y. Kim, and G. H. Kang (2021). "Tumor microenvironment-adjusted prognostic implications of the KRAS mutation subtype in patients with stage III colorectal cancer treated with adjuvant FOLFOX". In: *Sci Rep* 11.1, p. 14609. ISSN: 2045-2322 (Electronic) 2045-2322 (Linking). DOI: 10.1038/s41598-021-94044-4. URL: https://www.ncbi.nlm.nih.gov/pubmed/34272423.

Patel, Grisma, Alison Prince, and Mark Harries (2024). "Advanced Triple-Negative Breast Cancer". In: *Seminars in Oncology Nursing* 40.1, p. 151548. ISSN: 0749-2081. DOI: https://doi.org/10.1016/j.soncn.2023.151548. URL: https://www.sciencedirect.com/science/article/pii/S0749208123002231.

Piao, M. J., K. C. Kim, S. Chae, Y. S. Keum, H. S. Kim, and J. W. Hyun (2013). "Protective Effect of Fisetin (3,7,3',4'-Tetrahydroxyflavone) against -Irradiation-Induced Oxidative Stress and Cell Damage". In: *Biomol Ther (Seoul)* 21.3, pp. 210–5. ISSN: 1976-9148 (Print) 1976-9148. DOI: 10.4062/biomolther.2013.017.

Prior, I. A., F. E. Hood, and J. L. Hartley (2020). "The Frequency of Ras Mutations in Cancer". In: *Cancer Res* 80.14, pp. 2969–2974. ISSN: 1538-7445 (Electronic) 0008-5472 (Linking). DOI: 10.1158/0008-5472.CAN-19-3682. URL: https://www.ncbi.nlm.nih.gov/pubmed/32209560.

Purnell, P. R., P. C. Mack, C. G. Tepper, C. P. Evans, T. P. Green, P. H. Gumerlock, P. N. Lara, D. R. Gandara, H. J. Kung, and O. Gautschi (2009). "The Src inhibitor AZD0530 blocks invasion and may act as a radiosensitizer in lung cancer cells". In: *J Thorac Oncol* 4.4, pp. 448–54. ISSN: 1556-0864 (Print) 1556-0864. DOI: 10.1097/JTO.0b013e31819c78fb.

Rahmani, Arshad Husain, Ahmad Almatroudi, Khaled S. Allemailem, Amjad Ali Khan, and Saleh A. Almatroodi (2022). "The Potential Role of Fisetin, a Flavonoid in Cancer Prevention and Treatment". In: *Molecules* 27.24, p. 9009. ISSN: 1420-3049. URL: https://www.mdpi.com/1420-3049/27/24/9009.

Rauen, Thomas, Bjoern C. Frye, Jialin Wang, Ute Raffetseder, Christina Alidousty, Abdelaziz En-Nia, Jürgen Floege, and Peter R. Mertens (2016). "Cold shock protein YB-1 is involved in hypoxia-dependent gene transcription". In: *Biochemical and Biophysical Research Communications* 478.2, pp. 982–987. ISSN: 0006-291X. DOI: https://doi.org/10.1016/j.bbrc.2016.08.064. URL: https://www.sciencedirect.com/science/article/pii/S0006291X16313201.

Reina-Campos, M., M. T. Diaz-Meco, and J. Moscat (2019). "The Dual Roles of the Atypical Protein Kinase Cs in Cancer". In: *Cancer Cell* 36.3, pp. 218–235. ISSN: 1535-6108 (Print) 1535-6108. DOI: 10.1016/j.ccell.2019.07.010.

Reipas, Kristen M., Jennifer H. Law, Nicole Couto, Sumaiya Islam, Yvonne Li, Huifang Li, Artem Cherkasov, Karen Jung, Amarpal S. Cheema, Steven J.M. Jones, John A. Hassell, and Sandra E. Dunn (2013). "Luteolin is a novel p90 ribosomal S6 kinase (RSK) inhibitor that suppresses Notch4 signaling by blocking the activation of Y-box binding protein-1 (YB-1)". In: *Oncotarget* 4.2. ISSN: 1949-2553. URL: https://www.oncotarget.com/article/834/text/.

Ridouane, Y., G. Lopes, G. Ku, H. Masud, and B. Haaland (2017). "Targeted first-line therapies for advanced colorectal cancer: a Bayesian meta-analysis". In: *Oncotarget* 8.39, pp. 66458–66466. ISSN: 1949-2553. DOI: 10.18632/oncotarget.20185.

Rodriguez, J., R. Zarate, E. Bandres, A. Viudez, A. Chopitea, J. García-Foncillas, and I. Gil-Bazo (2007). "Combining chemotherapy and targeted therapies in metastatic colorectal cancer". In: *World J Gastroenterol* 13.44, pp. 5867–76. ISSN: 1007-9327 (Print) 1007-9327. DOI: 10.3748/wjg.v13.i44.5867.

Rodriguez-Viciana, P., P. H. Warne, A. Khwaja, B. M. Marte, D. Pappin, P. Das, M. D. Waterfield, A. Ridley, and J. Downward (1997). "Role of phosphoinositide 3-OH kinase in cell transformation and control of the actin cytoskeleton by Ras". In: *Cell* 89.3, pp. 457–67. ISSN: 0092-8674 (Print) 0092-8674. DOI: 10.1016/s0092-8674(00)80226-3.

Roeyen, Claudia R. C. van, Florian G. Scurt, Sabine Brandt, Vanessa A. Kuhl, Sandra Martinkus, Sonja Djudjaj, Ute Raffetseder, Hans-Dieter Royer, Ioannis Stefanidis, Sandra E. Dunn, Steven Dooley, Honglei Weng, Thomas Fischer, Jonathan A. Lindquist, and Peter R. Mertens (2013). "Cold shock Y-box protein-1 proteolysis autoregulates its transcriptional activities". In: *Cell Communication and Signaling* 11.1, p. 63. ISSN: 1478-811X. DOI: 10.1186/1478-811X-11-63. URL: https://doi.org/10.1186/1478-811X-11-63.

Roßner, F., C. Gieseler, M. Morkel, H. D. Royer, M. Rivera, H. Bläker, M. Dietel, R. Schäfer, and C. Sers (2016). "Uncoupling of EGFR–RAS signaling and nuclear localization of YBX1 in colorectal cancer". In: *Oncogenesis* 5.1, e187–e187. ISSN: 2157-9024. DOI: 10.1038/oncsis.2015.51. URL: https://doi.org/10.1038/oncsis.2015.51.

Roy, A., S. Bera, L. Saso, and B. S. Dwarakanath (2022). "Role of autophagy in tumor response to radiation: Implications for improving radiotherapy". In: *Front Oncol* 12, p. 957373. ISSN: 2234-943X (Print) 2234-943x. DOI: 10.3389/fonc.2022.957373.

Rudolph, Joachim, James J. Crawford, Klaus P. Hoeflich, and Weiru Wang (2015). "Inhibitors of p21-Activated Kinases (PAKs)". In: *Journal of Medicinal Chemistry* 58.1, pp. 111–129. ISSN: 0022-2623. DOI: 10.1021/jm501613q. URL: https://doi.org/10.1021/jm501613q.

Russo, M. and G. L. Russo (2018). "Autophagy inducers in cancer". In: *Biochem Pharmacol* 153, pp. 51–61. ISSN: 0006-2952. DOI: 10.1016/j.bcp.2018.02.007.

Sabarwal, A., R. Agarwal, and R. P. Singh (2017). "Fisetin inhibits cellular proliferation and induces mitochondria-dependent apoptosis in human gastric cancer cells". In: *Mol Carcinog* 56.2, pp. 499–514. ISSN: 0899-1987. DOI: 10.1002/mc.22512.

Sakuno, T. and Y. Watanabe (2015). "Phosphorylation of cohesin Rec11/SA3 by casein kinase 1 promotes homologous recombination by assembling the meiotic chromosome axis". In: *Dev Cell* 32.2, pp. 220–30. ISSN: 1534-5807. DOI: 10.1016/j.devcel.2014.11.033.

Salmela, Anna-Leena, Jeroen Pouwels, Asta Varis, Anu M. Kukkonen, Pauliina Toivonen, Pasi K. Halonen, Merja Perälä, Olli Kallioniemi, Gary J. Gorbsky, and Marko J. Kallio (2009). "Dietary flavonoid fisetin induces a forced exit from mitosis by targeting the mitotic spindle checkpoint". In: *Carcinogenesis* 30.6, pp. 1032–1040. ISSN: 0143-3334. DOI: 10.1093/carcin/bgp101. URL: https://doi.org/10.1093/carcin/bgp101.

Sartori, A. A., C. Lukas, J. Coates, M. Mistrik, S. Fu, J. Bartek, R. Baer, J. Lukas, and S. P. Jackson (2007). "Human CtIP promotes DNA end resection". In: *Nature* 450.7169, pp. 509–14. ISSN: 0028-0836 (Print) 0028-0836. DOI: 10.1038/nature06337.

Schwartz, Stephen M (2024). "Epidemiology of Cancer". In: *Clinical Chemistry* 70.1, pp. 140–149. ISSN: 0009-9147. DOI: 10.1093/clinchem/hvad202. URL: https://doi.org/10.1093/clinchem/hvad202.

Sechi, M., R. K. Lall, S. O. Afolabi, A. Singh, D. C. Joshi, S. Y. Chiu, H. Mukhtar, and D. N. Syed (2018). "Fisetin targets YB-1/RSK axis independent of its effect on ERK signaling: insights from in vitro and in vivo melanoma models". In: *Sci Rep* 8.1, p. 15726. ISSN: 2045-2322. DOI: 10.1038/s41598-018-33879-w.

Seiwert, Tanguy Y, Joseph K Salama, and Everett E Vokes (2007). "The concurrent chemoradiation paradigm—general principles". In: *Nature clinical practice Oncology* 4.2, pp. 86–100. ISSN: 1743-4254.

Sheridan, C. M., T. R. Grogan, H. G. Nguyen, C. Galet, M. B. Rettig, A. C. Hsieh, and D. Ruggero (2015). "YB-1 and MTA1 protein levels and not DNA or mRNA alterations predict for prostate cancer recurrence". In: *Oncotarget* 6.10, pp. 7470–80. ISSN: 1949-2553. DOI: 10.18632/oncotarget.3477.

Shi, Xiang, Jingjing Wang, Yu Lei, Caofan Cong, Dailin Tan, and Xianrong Zhou (2019). "Research progress on the PI3K/AKT signaling pathway in gynecological cancer (Review)". In: *Mol Med Rep* 19.6, pp. 4529–4535. ISSN: 1791-2997 1791-3004. DOI: 10.3892/mmr.2019.10121. URL: https://doi.org/10.3892/mmr.2019.10121.

Shibahara, Kotaro, Kenji Sugio, Toshihiro Osaki, Takeshi Uchiumi, Yoshihiko Maehara, Kimitoshi Kohno, Kosei Yasumoto, Keizo Sugimachi, and Michihiko Kuwano (2001). "Nuclear Expression of the Y-Box Binding Protein, YB-1, as a Novel Marker of Disease Progression in Non-Small Cell Lung Cancer1". In: *Clinical Cancer Research* 7.10, pp. 3151–3155. ISSN: 1078-0432.

Shibata, Tomohiro, Kosuke Watari, Akihiko Kawahara, Tomoya Sudo, Satoshi Hattori, Yuichi Murakami, Hiroto Izumi, Junji Itou, Masakazu Toi, Jun Akiba, Yoshito Akagi, Maki Tanaka, Michihiko Kuwano, and Mayumi Ono (2020). "Targeting Phosphorylation of Y-Box–Binding Protein YBX1 by TAS0612 and Everolimus in Overcoming Antiestrogen Resistance". In: *Molecular Cancer Therapeutics* 19.3, pp. 882–894. ISSN: 1535-7163. DOI: 10.1158/1535-7163.Mct-19-0690. URL: https://doi.org/10.1158/1535-7163.MCT-19-0690.

Shimazaki, N. and M. R. Lieber (2008). "DNA-PKcs at 7 angstrom: insights for DNA repair". In: *Structure* 16.3, pp. 334–6. ISSN: 0969-2126 (Print) 0969-2126. DOI: 10.1016/j.str.2008.02.003.

Shinkai, K., K. Nakano, L. Cui, Y. Mizuuchi, H. Onishi, Y. Oda, S. Obika, M. Tanaka, and M. Katano (2016). "Nuclear expression of Y-box binding protein-1 is associated with poor prognosis in patients with pancreatic cancer and its knockdown inhibits tumor growth and metastasis in mice tumor models". In: *Int J Cancer* 139.2, pp. 433–45. ISSN: 1097-0215 (Electronic) 0020-7136 (Linking). DOI: 10.1002/ijc.30075. URL: https://www.ncbi.nlm.nih.gov/pubmed/26939718.

Shiraiwa, Sachiko, Tetsushi Kinugasa, Akihiko Kawahara, Tomoaki Mizobe, Takafumi Ohchi, Kotaro Yuge, Shinya Fujino, Mitsuhiro Katagiri, Susumu Shimomura, Kensuke Tajiri, Tomoya Sudo, Masayoshi Kage, Michihiko Kuwano, and Yoshito Akagi (July 2016). "Nuclear Y-Box-binding protein-1 expression predicts poor clinical outcome in stage III colorectal cancer". en. In: *Anticancer Res.* 36.7, pp. 3781–3788.

Singhal, Anupriya, Bob T. Li, and Eileen M. O'Reilly (2024). "Targeting KRAS in cancer". In: *Nature Medicine* 30.4, pp. 969–983. ISSN: 1546-170X. DOI: 10.1038/s41591-024-02903-0. URL: https://doi.org/10.1038/s41591-024-02903-0.

Sinnberg, T., B. Sauer, P. Holm, B. Spangler, S. Kuphal, A. Bosserhoff, and B. Schittek (2012). "MAPK and PI3K/AKT mediated YB-1 activation promotes melanoma cell proliferation which is counteracted by an autoregulatory loop". In: *Exp Dermatol* 21.4, pp. 265–70. ISSN: 0906-6705. DOI: 10.1111/j.1600-0625.2012.01448.x.

Smith, M. J., B. G. Neel, and M. Ikura (2013). "NMR-based functional profiling of RASopathies and oncogenic RAS mutations". In: *Proc Natl Acad Sci U S A* 110.12, pp. 4574–9. ISSN: 1091-6490 (Electronic) 0027-8424 (Print) 0027-8424 (Linking). DOI: 10.1073/pnas.1218173110. URL: https://www.ncbi.nlm.nih.gov/pubmed/23487764.

Sogorina, Ekaterina M., Ekaterina R. Kim, Alexey V. Sorokin, Dmitry N. Lyabin, Lev P. Ovchinnikov, Daria A. Mordovkina, and Irina A. Eliseeva (2022). "YB-1 Phosphorylation at Serine 209 Inhibits Its Nuclear Translocation". In: *International Journal of Molecular Sciences* 23.1, p. 428. ISSN: 1422-0067. URL: https://www.mdpi.com/1422-0067/23/1/428.

Song, Y. H., M. Shiota, A. Yokomizo, T. Uchiumi, K. Kiyoshima, K. Kuroiwa, Y. Oda, and S. Naito (2014). "Twist1 and Y-box-binding protein-1 are potential prognostic factors in bladder cancer". In: *Urol Oncol* 32.1, 31.e1–7. ISSN: 1078-1439. DOI: 10.1016/j.urolonc.2012.11.003.

Spencer-Smith, Russell, Akiko Koide, Yong Zhou, Raphael R Eguchi, Fern Sha, Priyanka Gajwani, Dianicha Santana, Ankit Gupta, Miranda Jacobs, and Erika Herrero-Garcia (2017). "Inhibition of RAS function through targeting an allosteric regulatory site". In: *Nature chemical biology* 13.1, pp. 62–68. ISSN: 1552-4450.

Stratford, A. L., C. J. Fry, C. Desilets, A. H. Davies, Y. Y. Cho, Y. Li, Z. Dong, I. M. Berquin, P. P. Roux, and S. E. Dunn (2008). "Y-box binding protein-1 serine 102 is a downstream target of p90 ribosomal S6 kinase in basal-like breast cancer cells". In: *Breast Cancer Res* 10.6, R99. URL: http://www.ncbi.nlm.nih.gov/entrez/query.fcgi?cmd=Retrieve&db=PubMed&dopt=Citation&list_uids=19036157.

Suh, Y., F. Afaq, N. Khan, J. J. Johnson, F. H. Khusro, and H. Mukhtar (2010). "Fisetin induces autophagic cell death through suppression of mTOR signaling pathway in prostate cancer cells". In: *Carcinogenesis* 31.8, pp. 1424–33. ISSN: 0143-3334 (Print) 0143-3334. DOI: 10.1093/carcin/bgq115.

Sun, X., X. Ma, Q. Li, Y. Yang, X. Xu, J. Sun, M. Yu, K. Cao, L. Yang, G. Yang, G. Zhang, and X. Wang (2018). "Anti-cancer effects of fisetin on mammary carcinoma cells via regulation of the PI3K/Akt/mTOR pathway: In vitro and in vivo studies". In: *Int J Mol Med* 42.2, pp. 811–820. ISSN: 1107-3756 (Print) 1107-3756. DOI: 10.3892/ijmm.2018.3654.

Sundarraj, K., A. Raghunath, L. Panneerselvam, and E. Perumal (2021). "Fisetin Inhibits Autophagy in HepG2 Cells via PI3K/Akt/mTOR and AMPK Pathway". In: *Nutr Cancer* 73.11-12, pp. 2502–2514. ISSN: 0163-5581. DOI: 10.1080/01635581.2020.1836241.

Sutherland, Brent W., Jill Kucab, Joyce Wu, Cathy Lee, Maggie C. U. Cheang, Erika Yorida, Dmitry Turbin, Shoukat Dedhar, Colleen Nelson, Michael Pollak, H. Leighton Grimes, Kathy Miller, Sunil Badve, David Huntsman, C. Blake-Gilks, Min Chen, Catherine J. Pallen, and Sandra E. Dunn (2005). "Akt phosphorylates the Y-box binding protein 1 at Ser102 located in the cold shock domain and affects the anchorage-independent growth of breast cancer cells". In: *Oncogene* 24.26, pp. 4281–4292. ISSN: 1476-5594. DOI: 10.1038/sj.onc.1208590. URL: https://doi.org/10.1038/sj.onc.1208590.

Tailor, Dhanir, Angel Resendez, Fernando Jose Garcia-Marques, Mallesh Pandrala, Catherine C. Going, Abel Bermudez, Vineet Kumar, Marjan Rafat, Dhanya K. Nambiar, Alexander Honkala, Quynh-Thu Le, George W. Sledge, Edward Graves, Sharon J. Pitteri, and Sanjay V. Malhotra (2021). "Y box binding protein 1 inhibition as a targeted therapy for ovarian cancer". In: *Cell Chemical Biology* 28.8, 1206–1220.e6. ISSN: 2451-9456. DOI: https://doi.org/10.1016/j.chembiol.2021.02.014. URL: https://www.sciencedirect.com/science/article/pii/S2451945621000994.

Takács, T., G. Kudlik, A. Kurilla, B. Szeder, L. Buday, and V. Vas (2020a). "The effects of mutant Ras proteins on the cell signalome". In: *Cancer Metastasis Rev* 39.4, pp. 1051–1065. ISSN: 0167-7659 (Print) 0167-7659. DOI: 10.1007/s10555-020-09912-8.

Takács, Tamás, Gyöngyi Kudlik, Anita Kurilla, Bálint Szeder, László Buday, and Virag Vas (Dec. 2020b). "The effects of mutant Ras proteins on the cell signalome". en. In: *Cancer Metastasis Rev.* 39.4, pp. 1051–1065.

Tanaka, Toru, Hiroaki Saito, Shinichi Miyairi, and Shunsuke Kobayashi (2021). "7-Hydorxyindirubin is capable of specifically inhibiting anticancer drug-induced YB-1 nuclear translocation without showing cytotoxicity in HepG2 hepatocellular carcinoma cells". In: *Biochemical and Biophysical Research Communications* 544, pp. 15–21. ISSN: 0006-291X. DOI: https://doi.org/10.1016/j.bbrc.2021.01.048. URL: https://www.sciencedirect.com/science/article/pii/S0006291X2100084X.

Tang, K. J., J. D. Constanzo, N. Venkateswaran, M. Melegari, M. Ilcheva, J. C. Morales, F. Skoulidis, J. V. Heymach, D. A. Boothman, and P. P. Scaglioni (2016). "Focal Adhesion Kinase Regulates the DNA Damage Response and Its Inhibition Radiosensitizes Mutant KRAS Lung Cancer". In: *Clin Cancer Res* 22.23, pp. 5851–5863. ISSN: 1078-0432 (Print) 1078-0432. DOI: 10.1158/1078-0432.Ccr-15-2603.

Tang, Y., H. Zhou, A. Chen, R. N. Pittman, and J. Field (2000). "The Akt proto-oncogene links Ras to Pak and cell survival signals". In: *J Biol Chem* 275.13, pp. 9106–

9. ISSN: 0021-9258 (Print) 0021-9258 (Linking). DOI: 10.1074/jbc.275.13.9106. URL: https://www.ncbi.nlm.nih.gov/pubmed/10734042.

Thillai, K., H. Lam, D. Sarker, and C. M. Wells (2017). "Deciphering the link between PI3K and PAK: An opportunity to target key pathways in pancreatic cancer?" In: *Oncotarget* 8.8, pp. 14173–14191. ISSN: 1949-2553 (Electronic) 1949-2553 (Linking). DOI: 10.18632/oncotarget.13309. URL: https://www.ncbi.nlm.nih.gov/pubmed/27845911.

Tiwari, A., M. Iida, C. Kosnopfel, M. Abbariki, A. Menegakis, B. Fehrenbacher, J. Maier, M. Schaller, S. Y. Brucker, D. L. Wheeler, P. M. Harari, U. Rothbauer, B. Schittek, D. Zips, and M. Toulany (2020). "Blocking Y-Box Binding Protein-1 through Simultaneous Targeting of PI3K and MAPK in Triple Negative Breast Cancers". In: *Cancers (Basel)* 12.10. ISSN: 2072-6694 (Print) 2072-6694. DOI: 10.3390/cancers12102795.

Tiwari, A., S. Rebholz, E. Maier, M. Dehghan Harati, D. Zips, C. Sers, H. P. Rodemann, and M. Toulany (2018). "Stress-Induced Phosphorylation of Nuclear YB-1 Depends on Nuclear Trafficking of p90 Ribosomal S6 Kinase". In: *Int J Mol Sci* 19.8. ISSN: 1422-0067 (Electronic) 1422-0067 (Linking). DOI: 10.3390/ijms19082441. URL: https://www.ncbi.nlm.nih.gov/pubmed/30126195.

Toulany, K. J. Lee, K. R. Fattah, Y. F. Lin, B. Fehrenbacher, M. Schaller, B. P. Chen, D. J. Chen, and H. P. Rodemann (2012). "Akt promotes post-irradiation survival of human tumor cells through initiation, progression, and termination of DNA-PKcs-dependent DNA double-strand break repair". In: *Mol Cancer Res* 10.7, pp. 945–57. ISSN: 1541-7786. DOI: 10.1158/1541-7786.Mcr-11-0592.

Toulany, M., M. Iida, S. Keinath, F. F. Iyi, K. Mueck, B. Fehrenbacher, W. Y. Mansour, M. Schaller, D. L. Wheeler, and H. P. Rodemann (2016). "Dual targeting of PI3K and MEK enhances the radiation response of K-RAS mutated non-small cell lung cancer". In: *Oncotarget* 7.28, pp. 43746–43761. ISSN: 1949-2553 (Electronic) 1949-2553 (Linking). DOI: 10.18632/oncotarget.9670. URL: https://www.ncbi.nlm.nih.gov/pubmed/27248324.

Toulany, M., R. Kehlbach, U. Florczak, A. Sak, S. Wang, J. Chen, M. Lobrich, and H. P. Rodemann (2008). "Targeting of AKT1 enhances radiation toxicity of human tumor cells by inhibiting DNA-PKcs-dependent DNA double-strand break repair". In: *Mol Cancer Ther* 7.7, pp. 1772–81. ISSN: 1535-7163 (Print) 1535-7163. DOI: 10.1158/1535-7163.Mct-07-2200.

Toulany, M., M. Minjgee, M. Saki, M. Holler, F. Meier, W. Eicheler, and H. P. Rodemann (2014). "ERK2-dependent reactivation of Akt mediates the limited response of tumor cells with constitutive K-RAS activity to PI3K inhibition". In: *Cancer Biol Ther* 15.3, pp. 317–28. ISSN: 1538-4047. DOI: 10.4161/cbt.27311. URL: https://www.ncbi.nlm.nih.gov/pmc/articles/PMC3974833/pdf/cbt-15-317.pdf.

Toulany, M. and H. P. Rodemann (2015). "Phosphatidylinositol 3-kinase/Akt signaling as a key mediator of tumor cell responsiveness to radiation". In: *Semin Cancer Biol* 35, pp. 180–90. ISSN: 1044-579x. DOI: 10.1016/j.semcancer.2015.07.003.

Toulany, M., T. A. Schickfluss, W. Eicheler, R. Kehlbach, B. Schittek, and H. P. Rodemann (2011). "Impact of oncogenic K-RAS on YB-1 phosphorylation induced by ionizing radiation". In: *Breast Cancer Res* 13.2, R28. ISSN: 1465-5411. DOI: 10.1186/bcr2845.

Toulany, Mahmoud, Michael Baumann, and H. Peter Rodemann (2007). "Stimulated PI3K-AKT Signaling Mediated through Ligand or Radiation-Induced EGFR Depends Indirectly, but not Directly, on Constitutive K-Ras Activity". In: *Molecular Cancer Research* 5.8, pp. 863–872. ISSN: 1541-7786. DOI: 10.1158/1541-7786.Mcr-06-0297. URL: https://doi.org/10.1158/1541-7786.MCR-06-0297.

Tsakiridis, T., C. Taha, S. Grinstein, and A. Klip (1996). "Insulin activates a p21-activated kinase in muscle cells via phosphatidylinositol 3-kinase". In: *J Biol Chem* 271.33, pp. 19664–7. ISSN: 0021-9258 (Print) 0021-9258. DOI: 10.1074/jbc.271.33.19664.

Tseng, H. C., W. S. Liu, Y. S. Tyan, H. C. Chiang, W. H. Kuo, and F. P. Chou (2011). "Sensitizing effect of 3-methyladenine on radiation-induced cytotoxicity in radio-resistant HepG2 cells in vitro and in tumor xenografts". In: *Chem Biol Interact* 192.3, pp. 201–8. ISSN: 0009-2797. DOI: 10.1016/j.cbi.2011.03.011.

Ushijima, Miho, Masaki Shiota, Takashi Matsumoto, Eiji Kashiwagi, Junichi Inokuchi, and Masatoshi Eto (2022). "An oral first-in-class small molecule RSK inhibitor suppresses AR variants and tumor growth in prostate cancer". In: *Cancer Science* 113.5, pp. 1731–1738. ISSN: 1347-9032. DOI: https://doi.org/10.1111/cas.15280. URL: https://onlinelibrary.wiley.com/doi/abs/10.1111/cas.15280.

Vanhaesebroeck, Bart, Julie Guillermet-Guibert, Mariona Graupera, and Benoit Bilanges (2010). "The emerging mechanisms of isoform-specific PI3K signalling". In: *Nature reviews Molecular cell biology* 11.5, pp. 329–341. ISSN: 1471-0072.

Wagle, Marie-Claire, Daniel Kirouac, Christiaan Klijn, Bonnie Liu, Shilpi Mahajan, Melissa Junttila, John Moffat, Mark Merchant, Ling Huw, and Matthew Wongchenko (2018). "A transcriptional MAPK Pathway Activity Score (MPAS) is a clinically relevant biomarker in multiple cancer types". In: *NPJ precision oncology* 2.1, p. 7. ISSN: 2397-768X.

Wang, Jialin, Lydia Gibbert, Sonja Djudjaj, Christina Alidousty, Thomas Rauen, Uta Kunter, Andreas Rembiak, Dieter Enders, Vera Jankowski, Gerald S. Braun, Jürgen Floege, Tammo Ostendorf, and Ute Raffetseder (2016). "Therapeutic nuclear shuttling of YB-1 reduces renal damage and fibrosis". In: *Kidney International* 90.6, pp. 1226–1237. ISSN: 0085-2538. DOI: https://doi.org/10.1016/j.kint.2016.07.008. URL: https://www.sciencedirect.com/science/article/pii/S0085253816303428.

Wang, X., S. Allen, J. F. Blake, V. Bowcut, D. M. Briere, A. Calinisan, J. R. Dahlke, J. B. Fell, J. P. Fischer, R. J. Gunn, J. Hallin, J. Laguer, J. D. Lawson, J. Medwid, B. Newhouse, P. Nguyen, J. M. O'Leary, P. Olson, S. Pajk, L. Rahbaek, M. Rodriguez, C. R. Smith, T. P. Tang, N. C. Thomas, D. Vanderpool, G. P. Vigers, J. G. Christensen, and M. A. Marx (2022). "Identification of MRTX1133, a Noncovalent, Potent, and Selective KRAS(G12D) Inhibitor". In: *J Med Chem* 65.4, pp. 3123–3133. ISSN: 0022-2623. DOI: 10.1021/acs.jmedchem.1c01688.

Wang, Z., M. Fu, L. Wang, J. Liu, Y. Li, C. Brakebusch, and Q. Mei (2013). "p21-activated kinase 1 (PAK1) can promote ERK activation in a kinase-independent manner". In: *J Biol Chem* 288.27, pp. 20093–9. ISSN: 1083-351X (Electronic) 0021-9258 (Linking). DOI: 10.1074/jbc.M112.426023. URL: https://www.ncbi.nlm.nih.gov/pubmed/23653349.

Wee, S., Z. Jagani, K. X. Xiang, A. Loo, M. Dorsch, Y. M. Yao, W. R. Sellers, C. Lengauer, and F. Stegmeier (2009). "PI3K pathway activation mediates resistance to MEK inhibitors in KRAS mutant cancers". In: *Cancer Res* 69.10, pp. 4286–93. ISSN: 1538-7445 (Electronic) 0008-5472 (Linking). DOI: 10.1158/0008-5472.CAN-08-4765. URL: http://www.ncbi.nlm.nih.gov/pubmed/19401449.

Woolley, Adele G., Michael Algie, Weini Samuel, Rhodri Harfoot, Anna Wiles, Noelyn A. Hung, Puay-Hoon Tan, Peter Hains, Valentina A. Valova, Lily Huschtscha, Janice A. Royds, David Perez, Han-Seung Yoon, Scott B. Cohen, Phillip J. Robinson, Boon-Huat Bay, Annette Lasham, and Antony W. Braithwaite (2011). "Prognostic Association of YB-1 Expression in Breast Cancers: A Matter of Antibody". In: *PLOS ONE* 6.6, e20603. DOI: 10.1371/journal.pone.0020603. URL: https://doi.org/10.1371/journal.pone.0020603.

Wu, Joyce, Cathy Lee, Daniel Yokom, Helen Jiang, Maggie C.U. Cheang, Erika Yorida, Dmitry Turbin, Isabelle M. Berquin, Peter R. Mertens, Thomas Iftner, C. Blake Gilks, and Sandra E. Dunn (2006). "Disruption of the Y-Box Binding Protein-1 Results in Suppression of the Epidermal Growth Factor Receptor and HER-2". In: *Cancer Research* 66.9, pp. 4872–4879. ISSN: 0008-5472. DOI: 10.1158/0008-5472.Can-05-3561. URL: https://doi.org/10.1158/0008-5472.CAN-05-3561.

Xiao, Y., Y. Liu, Z. Gao, X. Li, M. Weng, C. Shi, C. Wang, and L. Sun (2021). "Fisetin inhibits the proliferation, migration and invasion of pancreatic cancer by targeting PI3K/AKT/mTOR signaling". In: *Aging (Albany NY)* 13.22, pp. 24753–24767. ISSN: 1945-4589. DOI: 10.18632/aging.203713.

Yan, X., L. Yan, J. Zhou, S. Liu, Z. Shan, C. Jiang, Y. Tian, and Z. Jin (2014). "High expression of Y-box-binding protein 1 is associated with local recurrence and predicts poor outcome in patients with colorectal cancer". In: *Int J Clin Exp Pathol* 7.12, pp. 8715–23. ISSN: 1936-2625.

Yang, Linlin, Changxian Shen, Adriana Estrada-Bernal, Ryan Robb, Moumita Chatterjee, Nikhil Sebastian, Amy Webb, Xiaokui Mo, Wei Chen, Sunil Krishnan, and Terence M Williams (2021). "Oncogenic KRAS drives radioresistance through upregulation of NRF2-53BP1-mediated non-homologous end-joining repair". In: *Nucleic Acids Research* 49.19, pp. 11067–11082. ISSN: 0305-1048. DOI: 10.1093/nar/gkab871. URL: https://doi.org/10.1093/nar/gkab871.

Yang, P. M., H. H. Tseng, C. W. Peng, W. S. Chen, and S. J. Chiu (2012). "Dietary flavonoid fisetin targets caspase-3-deficient human breast cancer MCF-7 cells by induction of caspase-7-associated apoptosis and inhibition of autophagy". In: *Int J Oncol* 40.2, pp. 469–78. ISSN: 1019-6439. DOI: 10.3892/ijo.2011.1203.

Yang, Xiao-Juan, Hong Zhu, Shi-Rong Mu, Wen-Juan Wei, Xun Yuan, Meng Wang, Yanchao Liu, Jingyi Hui, and Ying Huang (2019). "Crystal structure of a Y-box binding protein 1 (YB-1)–RNA complex reveals key features and residues interacting with RNA". In: *Journal of Biological Chemistry* 294.28, pp. 10998–11010. ISSN: 0021-9258. DOI: https://doi.org/10.1074/jbc.RA119.007545. URL: https://www.sciencedirect.com/science/article/pii/S0021925820301988.

Ying, T. H., S. F. Yang, S. J. Tsai, S. C. Hsieh, Y. C. Huang, D. T. Bau, and Y. H. Hsieh (2012). "Fisetin induces apoptosis in human cervical cancer HeLa cells through ERK1/2-mediated activation of caspase-8-/caspase-3-dependent pathway". In: *Arch Toxicol* 86.2, pp. 263–73. ISSN: 0340-5761. DOI: 10.1007/s00204-011-0754-6.

Zhan, Yuting, Xianyong Chen, Hongmei Zheng, Jiadi Luo, Yang Yang, Yue Ning, Haihua Wang, Yuting Zhang, Ming Zhou, Weiyuan Wang, and Songqing Fan (2022). "YB1 associates with oncogenetic roles and poor prognosis in nasopharyngeal carcinoma". In: *Scientific Reports* 12.1, p. 3699. ISSN: 2045-2322. DOI: 10.1038/s41598-022-07636-z. URL: https://doi.org/10.1038/s41598-022-07636-z.

Zhang, Haiping, Lijun Jiang, Xinyi Du, Zhen Qian, Guizhu Wu, Ying Jiang, and Zhiyong Mao (2024). "The cGAS-Ku80 complex regulates the balance between two end joining subpathways". In: *Cell Death Differentiation* 31.6, pp. 792–803. ISSN: 1476-5403. DOI: 10.1038/s41418-024-01296-4. URL: https://doi.org/10.1038/s41418-024-01296-4.

Zhang, X. F., J. Settleman, J. M. Kyriakis, E. Takeuchi-Suzuki, S. J. Elledge, M. S. Marshall, J. T. Bruder, U. R. Rapp, and J. Avruch (1993). "Normal and oncogenic p21ras proteins bind to the amino-terminal regulatory domain of c-Raf-1". In: *Nature* 364.6435, pp. 308–13. ISSN: 0028-0836 (Print) 0028-0836. DOI: 10.1038/364308a0.

Zhang, Y., S. R. Reng, L. Wang, L. Lu, Z. H. Zhao, Z. K. Zhang, X. D. Feng, X. D. Ding, J. Wang, G. Feng, T. Z. Dai, J. Pu, and X. B. Du (2012). "Overexpression of Y-box binding protein-1 in cervical cancer and its association with the pathological response rate to chemoradiotherapy". In: *Med Oncol* 29.3, pp. 1992–7. ISSN: 1357-0560. DOI: 10.1007/s12032-011-0062-2.

Zhang, Y., P. W. Zhao, G. Feng, G. Xie, A. Q. Wang, Y. H. Yang, D. Wang, and X. B. Du (2015). "The expression level and prognostic value of Y-box binding protein-1 in rectal cancer". In: *PLoS One* 10.3, e0119385. ISSN: 1932-6203. DOI: 10.1371/journal.pone.0119385.

Zhao, Bailin, Eli Rothenberg, Dale A. Ramsden, and Michael R. Lieber (2020). "The molecular basis and disease relevance of non-homologous DNA end joining". In: *Nature Reviews Molecular Cell Biology* 21.12, pp. 765–781. ISSN: 1471-0080. DOI: 10.1038/s41580-020-00297-8. URL: https://doi.org/10.1038/s41580-020-00297-8.

Zhao, Yuanyuan, Jun Yi, Leilei Tao, Guichun Huang, Xiaoyuan Chu, Haizhu Song, and Longbang Chen (2018). "Wnt signaling induces radioresistance through upregulating HMGB1 in esophageal squamous cell carcinoma". In: *Cell Death Disease* 9.4, p. 433. ISSN: 2041-4889. DOI: 10.1038/s41419-018-0466-4. URL: https://doi.org/10.1038/s41419-018-0466-4.

Zhu, Gongmin, Lijiao Pei, Hongwei Xia, Qiulin Tang, and Feng Bi (2021). "Role of oncogenic KRAS in the prognosis, diagnosis and treatment of colorectal cancer". In: *Molecular Cancer* 20.1, p. 143. ISSN: 1476-4598. DOI: 10.1186/s12943-021-01441-4. URL: https://doi.org/10.1186/s12943-021-01441-4.

Zhuo, W., L. Zhang, Y. Zhu, B. Zhu, and Z. Chen (2015). "Fisetin, a dietary bioflavonoid, reverses acquired Cisplatin-resistance of lung adenocarcinoma cells through MAPK/-Survivin/Caspase pathway". In: *Am J Transl Res* 7.10, pp. 2045–52. ISSN: 1943-8141 (Print) 1943-8141.

Appendix

Appendix A

Publication I

Khozooei *et al. J Exp Clin Cancer Res (2022) 41:256*
https://doi.org/10.1186/s13046-022-02442-x

Journal of Experimental & Clinical Cancer Research

RESEARCH Open Access

Fisetin induces DNA double-strand break and interferes with the repair of radiation-induced damage to radiosensitize triple negative breast cancer cells

Shayan Khozooei[1,2], Konstanze Lettau[1,2], Francesca Barletta[3], Tina Jost[4,5], Simone Rebholz[1,2], Soundaram Veerappan[1,2], Mirita Franz-Wachtel[6], Boris Macek[6], George Iliakis[7], Luitpold V. Distel[4,5], Daniel Zips[1,2] and Mahmoud Toulany[1,2*]

Abstract

Background: Triple-negative breast cancer (TNBC) is associated with aggressiveness and a poor prognosis. Besides surgery, radiotherapy serves as the major treatment modality for TNBC. However, response to radiotherapy is limited in many patients, most likely because of DNA damage response (DDR) signaling mediated radioresistance. Y-box binding protein-1 (YB-1) is a multifunctional protein that regulates the cancer hallmarks among them resisting to radiotherapy-induced cell death. Fisetin, is a plant flavonol of the flavonoid family of plant polyphenols that has anti-cancer properties, partially through inhibition of p90 ribosomal S6 kinase (RSK)-mediated YB-1 phosphorylation. The combination of fisetin with radiotherapy has not yet been investigated.

Methods: Activation status of the RSK signaling pathway in total cell lysate and in the subcellular fractions was analyzed by Western blotting. Standard clonogenic assay was applied to test post-irradiation cell survival. γH2AX foci assay and 3 color fluorescence in situ hybridization analyses were performed to study frequency of double-strand breaks (DSB) and chromosomal aberrations, respectively. The underlying repair pathways targeted by fisetin were studied in cells expressing genomically integrated reporter constructs for the DSB repair pathways via quantifying the expression of green fluorescence protein by flow cytometry. Flow cytometric quantification of sub-G1 cells and the protein expression of LC3-II were employed to measure apoptosis and autophagy, respectively. Kinase array and phosphoproteomics were performed to study the effect of fisetin on DDR response signaling.

Results: We showed that the effect of fisetin on YB-1 phosphorylation in TNBC cells is comparable to the effect of the RSK pharmacological inhibitors. Similar to ionizing radiation (IR), fisetin induces DSB. Additionally, fisetin impairs repair of IR-induced DSB through suppressing the classical non-homologous end-joining and homologous recombination repair pathways, leading to chromosomal aberration as tested by metaphase analysis. Effect of fisetin on DSB repair was partially dependent on YB-1 expression. Phosphoproteomic analysis revealed that fisetin inhibits DDR signaling,

*Correspondence: mahmoud.toulany@uni-tuebingen.de

[1] Division of Radiobiology and Molecular Environmental Research, Department of Radiation Oncology, University of Tuebingen, Roentgenweg 11, 72076 Tuebingen, Germany
Full list of author information is available at the end of the article

which leads to radiosensitization in TNBC cells, as shown in combination with single dose or fractionated doses irradiation.

Conclusion: Fisetin acts as a DSB-inducing agent and simultaneously inhibits repair of IR-induced DSB. Thus, fisetin may serve as an effective therapeutic strategy to improve TNBC radiotherapy outcome.

Keywords: Triple negative breast cancer, Y-box binding protein-1, Fisetin, Double strand break repair, Radiosensitization

Background

Triple negative breast cancer (TNBC) does not express estrogen receptor (ER) and progesterone receptor (PR) and is characterized by the absence of HER2 overexpression/ amplification [1]. TNBC is one of the most aggressive subtypes of breast cancer that accounts for about 20% of breast cancers. Since the three receptors are the major target of most hormone therapies, treating patients with TNBC remains challenging. Radiotherapy, as an important treatment approach for breast cancer patients, improves locoregional control both after breast conserving surgery and mastectomy [2], with a positive impact in high-risk patients for long-term survival [1]. Tumor radioresistance comprised of acquired radioresistance as well as intrinsic radioresistance is the major cause of a diminished radiotherapy outcome.

Y-box binding protein 1 (YB-1), is a member of the cold-shock protein superfamily. The protein contains a cold-shock domain (CSD) that enables it to bind to DNA and RNA [3]. YB-1 is overexpressed in different tumor types and is involved in nearly all cancer hallmarks described to date [4], particularly cell death resistance after exposure to ionizing radiation (IR) [5, 6]. In breast cancers, expression of YB-1 plays an important role in cancer progression from the early-stage; this identifies YB-1 as a potential target for breast cancer treatment [7]. Clinical studies revealed that YB-1 expression diminishes response to radiochemotherapy in different tumor entities [8–10], is crucial in acquired drug resistance development [11] and is associated with tumor recurrence [12]. DNA double-strand break (DSB) is the major cause of radiation-induced cell death. YB-1 knockdown interferes with DSB repair and mediates radiosensitization [5, 6]. In support of the role of YB-1 in DNA repair, YB-1 was found in a complex with MSH2 and Ku80 as well as with WRN proteins, involved in mismatch repair and DSB repair, respectively [13]. In line with the proposed role of YB-1 in DNA repair, namely DSB repair, previous reports have shown that in YB-1 knockdown breast cancer cells, the frequency of residual DSB is increased and the cells become radiosensitized [5, 6]. Because YB-1 lacks a kinase domain, direct molecular targeting by applying pharmacological inhibitors is not plausible. Thus, investigations have focused on targeting p90 ribosomal S6 kinase (RSK) as the most important kinase stimulating YB-1 phosphorylation [14] to interfere with its pro-survival effect. Recently, we demonstrated that in breast cancer cells application of the RSK inhibitor LJI308 effectively blocks YB-1 phosphorylation in non-irradiated as well as in irradiated cells [6]. However, compared to the YB-1-siRNA approach, the effect of LJI308 on inhibition of DSB repair was minimal and it did not induce radiosensitization although YB-1 activity was blocked [6]. Mechanistically, we demonstrated that activation of AKT after RSK inhibition or constitutive activation of AKT in cells with mutation in genes such as *PIK3CA* or *PTEN* stimulates DSB repair and leads to the failure of RSK inhibitors to induce radiosensitization. Supporting these results, we were able to show that the dual inhibition of AKT and RSK is able to induce sensitivity to IR in breast cancer cells independent of TNBC status [6]. The toxicity issue of this approach remains to be investigated in further in vivo studies.

Although successful targeting of YB-1 by other approaches, *i.e.*, RNAi approaches and blocking peptides has been reported, the applicability of these approaches in vivo remains a major issue. Recently, the effect of the plant flavonoid fisetin has been investigated on the activation of YB-1 in tumor cells from different entities [15]. It has been shown that fisetin interferes with binding of RSK2 to YB-1 and that it thus blocks YB-1 phosphorylation [16]. According to the described role of S102 phosphorylated YB-1 in DSB repair [6], fisetin in combination with IR might improve radiation response of TNBC. YB-1 independent targets of fisetin, *e.g.*, demethylating histone H3K36 [17], inhibition of AKT [18] and modulating autophagy [19] may also affect radiation response, independently of its effect on YB-1. In the present study, the effect of fisetin on phosphorylation of proteins inside and outside the YB-1 cascade was analyzed in TNBC cells. YB-1-dependent and YB-1-independent effect of fisetin in DSB repair were investigated. The obtained data demonstrated that fisetin induces DSB and has a strong anti-clonogenic activity in TNBC cells when applied as monotherapy. Likewise, fisetin strongly blocked DSB repair after irradiation and improved radiosensitivity in a combined therapy.

Materials and methods

Cell lines

TNBC cell lines; MDA-MB-231 (ATCC HTB-26), MDA-MB-468 (ATCC HTB-132), MDA-MB-453 (ATCC HTB-131) and HS 578T (ATCC HTB-126) as well as non-TNBC cell lines MCF-7 and T47D were used. Single nucleotide polymorphism (SNP) profiling was used to verify the authenticity of the cells (Multiplexion, Heidelberg, Germany). Normal human skin fibroblasts (HSF-7 cells) were included in the study as healthy control cells. The cells, except MCF-7, were cultured in DMEM containing 10% fetal calf serum (FCS) and 1% penicillin–streptomycin (PS) and incubated in a humidified atmosphere of 93% air and 7% CO2 at 37 °C. MCF-7 cells were culture in RPMI medium containing 10% FCS and 1% PS. U2OS osteosarcoma cells expressing genomically integrated reporter constructs for homologous recombination (HR), classical non-homologous end joining (C-NHEJ) and alternative NHEJ (Alt-NHEJ) repair pathways, engineered in Dr. Jeremy Stark's lab [20] were cultured in DMEM containing 10% FCS, 1% PS and 2 µg/ml of puromycin.

Antibodies and reagents

Primary antibodies against YB-1 (#42,042), phospho-YB-1 (S102) (#2900), phospho-RSK (T359/S363) (#9344), RSK1/RSK2/RSK3 (#9355), phospho-AKT (S473) (#9271) and p62 (#8025) were purchased from Cell Signaling Technology (Frankfurt, Germany). All these antibodies were used at the dilution of 1:1000. LC3 antibody was purchased from Nanotools (Teningen, Germany, dilution 1:150). The β-actin antibody (#A2066, dilution 1:1000) and Triamzinolonacetonid (#8056) were purchased from Sigma-Aldrich (Taufkirchen, Germany). The anti-phospho-H2AX antibody (S139) (#05–636, dilution 1:300) was purchased from Merck (Darmstadt, Germany). The RSK inhibitor LJI308 (#S7871) and fisetin (#S2298) were purchased from Selleckchem (#S7871) (Munich, Germany). BI-D1870 (#BML-EI407) was purchased from Enzo (Lörrach, Germany). Rad51 inhibitor B02 (#S8434) was purchased from Absource (Munich, Germany). Small interfering RNA (siRNA) against YB-1 (#M-010213) and nontargeting siRNA (#D-001810) were purchased from Darmacon (Frankfurt, Germany). Lipofectamine RNAiMAX transfection reagent and opti-MEM were purchased from Invitrogen (Darmstadt, Germany). I-SceI-GR-RFP expression plasmid was a gift from Tom Misteli (Addgene plasmid #17,654, USA).

Inhibitor treatment

The RSK inhibitors LJI308 (LJI) and BI-D1870 (BID) were dissolved in dimethyl sulfoxide (DMSO). For treatment, stock solutions of the inhibitors were diluted in culture medium and applied to the cells. Control cells received equivalent DMSO concentrations.

Irradiation

Irradiation was performed at 37 °C using a Gulmay RS225 X-ray machine (Gulmay Limited, Chertsey, UK) at a dose rate of 1 Gy/min operated at 200 kVp, 15 mA and 0.5 mm copper filter.

Cellular fractionation and immunoblotting analysis

Cytoplasmic and nuclear protein fractions were separated as previously described [21]. Cells were harvested in lysis buffer as described previously [22]. Protein was quantified with Biorad DC Protein Assay Reagent and 100 µg of protein were loaded to SDS-PAGE. Afterwards, proteins were transferred to a nitrocellulose membrane, incubated with the corresponding primary antibodies at 4 °C overnight, followed by 3 washes and then incubated with the corresponding secondary antibodies for 1 h at room temperature. PVDF (polyvinylidene fluoride) was used to detect LC3 I/II proteins. LI-COR Biosciences system (Bad Homburg, Germany) and ECL detection kits (GE Healthcare or Cell Signaling) were used to detect chemiluminescence.

Clonogenic assay

Clonogenic assay was performed to investigate potential radiosensitizing effect of fisetin in all TNBC and HSF-7 cells. Briefly, log phase cells in T12.5 flasks were treated with DMSO (0.1%) control (10 flasks) or 75 µM of Fisetin (10 flasks) for 24 h. Thereafter, cells were clustered in 4 groups, *i.e.*, control, IR, fisetin and fisetin + IR, with 5 flasks/group. Cells were either mock irradiated (control and fisetin groups) or irradiated with one fraction of 1 Gy (IR and IR + fisetin groups). From each group, one flask was trypsinized immediately after irradiation or mock irradiation and plated in 6-well plates in medium containing 20% FCS without additional treatment. The medium was changed for the rest of the cells (16 flasks), with the fresh medium containing DMSO (0.1%) or fisetin for the next fraction of irradiation the following day. The same procedure was repeated on day 2 and the following days. In the experiments with single dose irradiation, cells were treated either with DMSO (0.07%) or fisetin (75 µM). Twenty-four hours later, cells were mock irradiated or irradiated with 0 to 4 Gy. Cells were trypsinized immediately after irradiation or mock irradiation and plated in 6-well plates. Depending on the cell lines, 10 to 15 days later, cultures were stained and colonies with more than 50 cells were scored as survivors. Plating efficiency (PE) in each condition was calculated by dividing number of colonies to the number of seeded cells. The survival fraction for each radiation dose was

calculated by dividing the PE of irradiated cells with the PE of non-irradiated DMSO control or non-irradiated fisetin control. Survival curves were graphed based on the calculated survival fractions by using Sigma Plot and Microsoft Excel software.

γH2AX assay

To determine residual DNA DSB after IR, TNBC and HSF-7 cell lines were irradiated with the indicated dose of X-ray in each experiment. Either thirty minutes or 24 h after irradiation, cells were fixed with 70% ethanol and followed by staining with phospho-H2AX (S139) antibody as described before [23]. The foci were counted using FoCo software [24] and the average foci number per nuclei were determined and graphed.

SiRNA transfection

SiRNA transfection was performed as described previously [5,]. Cells were transfected with 50 nM of non-target siRNA or YB-1 siRNA. Twenty-four hours after transfection, cells were treated according to the required experimental procedure.

Three-color fluorescence in situ hybridization

The effect of fisetin on chromosomal aberration was studied with three-color fluorescence in situ hybridization as described before [25] in MDA-MB-231 and MDA-MB-468 cells with differential effect of fisetin on YB-1 phosphorylation. Cells were seeded in T175 culture flasks and 24 h later were treated with DMSO (0.07%) or fisetin (75 μM) for 72 h hours. In the IR condition, the cells were irradiated with 2 Gy and after 48 h, a mitotic shake off was performed to detach the currently dividing cells with condensed chromosomes mitotic cells. After cell lysis, pellets were resuspended in 0.02% potassium chloride solution (Sigma Aldrich, München, Germany) and a 3:1 methanol:acetic acid (Sigma Aldrich, München, Germany) solution. DNA was transferred to glass slides and treated with RNase (Roche, Penzberg, Germany) and pepsin (Sigma Aldrich, München, Germany) to remove cell debris. Afterwards, DNA was fixated with formaldehyde-buffer (Merck, Darmstadt, Germany), denatured with formamide-buffer (Merck, Darmstadt, Germany) at 72 °C and hybridization was performed by incubating DNA with a mixture of probes for chromosome #1, #2 and #4 at 37 °C for 72 h. Finally, glass slides were stained with FITC (Merck, Darmstadt, Germany) and anti-avidin/rhodamin (Merck, Darmstadt, Germany) and microscopic images were taken using a Zeiss Axioplan 2 fluorescence microscope. The Metasystems software (Metafer 4 V3.10.1, Altlussheim, Germany) was used to search chromosome metaphases automatically at 100 × magnification and an image of each metaphase was acquired at a magnification of 630 × . For each metaphase, black and white images of each color (red, green and blue) were acquired and used for evaluation.

DSB repair pathway analysis

The DSB repair pathway analysis was performed in U2OS cells expressing genomically integrated reporter constructs for HR, C-NHEJ and Alt-NHEJ repair pathways [20]. Cells (5×10^5) were transfected with 800 ng/ml of inducible I-SceI expression plasmid [26] and were treated with fisetin (75 μM) after 24 h. Twenty-four hours after the fisetin treatment, the cells were treated with 100 ng/ml of triamcinolonacetonid (TA) to induce nuclear translocation of I-SceI. After an additional 24 h, cells were analyzed for GFP expression by BD FACSCanto System using Flowing software.

Flow cytometric analysis of apoptosis

To analyze the effect of fisetin on apoptosis and cell cycle progression, all TNBC cell lines were seeded 24 h before treatment with DMSO (0.07%) or fisetin (75 μM). After twenty-four hours, cultures were mock irradiated or irradiated with 4 Gy. Cells were trypsinized and fixed with 70% ethanol 48 h after irradiation. Propidium iodide staining and cell preparation for cell cycle analysis were performed as described before [27] using BD FACSCanto System and the data were analyzed by FlowJo software.

Phospho-kinase proteome profiler array

MDA-MB-231 cells were treated with DMSO (0.07%) or fisetin (75 μM) for 72 h and followed by mock irradiation or irradiation with 4 Gy. Protein samples were extracted at 30 min and 24 h after irradiation. Phospho-kinase proteome array was performed according to the manufacturer's protocol (R&D Systems, Minneapolis, MN, USA).

SILAC-based phosphoproteomics analysis

Quantitative phosphoproteomics using Stable Isotope Labeling by Amino Acids in Cell Culture (SILAC) was done in 6 samples distributed in two experimental groups in biological triplicates for MDA-MB-468 as follow: 1) IR (4 Gy) ("light" and "medium" labelled); 2) IR plus Fisetin (75 μM) (IR + Fisetin) ("heavy labelled). Similar treatments were performed in MDA-MB-231 with the exception of labelling IR condition with "light" medium. Briefly, MDA-MB-231 and MDA-MB-468 cell lines were grown in 3 different media containing"light" (Lys0, Arg0), "medium-heavy" ($^{13}C_6{}^{14}N_4$-L-arginine/Arg6, 4,4,5,5-D4-L-lysine/Lys4) and "heavy" ($^{13}C_6{}^{15}N_4$-L arginine/Arg10,$^{13}C_6{}^{15}N_2$-L-Lysine/Lys8) amino acids. Cells were cultured for 10 passages to ensure the incorporation of labeled amino acids was higher than 97% in all

cases. Afterwards, IR treatment was applied for 30 min and cells were lysed in lysis buffer [28] for 30 min at room temperature and then sonified for 1 min on ice (Bandelin SONOPULS HD 200, Program MS73D). Protein extracts were precipitated with ice-cold acetone-methanol at -20 °C overnight. The proteins were pelleted by centrifugation (2000 × *g*, 20 min, 4 °C) and washed three times with 80% ice-cold acetone. Dried proteins were resolved in digestion buffer (6 M urea, 2 M thiourea, 10 mM Tris, pH 8.0). The samples were mixed in 1:1:1 ratio according to measured protein amounts in two pools, each of them containing a "light- ", "heavy-medium- " and "heavy-SILAC" sample. Afterwards, 600 µg of the mixture was digested in solution with trypsin as described previously [29] and 3% of the resulting peptides were directly desalted with C_{18} StageTips [30].

The rest of the peptide mixture was purified on Sep-Pak 18 cartridges (Waters) and subjected to phosphopeptide enrichment by MagReSyn Ti-IMAC (ReSyn Bioscience) as described previously [29] with minor modifications: approximately 60 µl of magnetic bead suspension per mix and enrichment round was washed two times for 5 min with 70% ethanol, followed by washing for 10 min with 1% NH_4OH. Before peptide loading, beads were equilibrated three times with loading buffer (1 M glycolic acid and 5% TFA in 80% ACN). Elution from the beads was performed three times with 100 µl of 1% NH_4OH. The pooled eluates were further purified by C_{18} StageTips. Peptide mixes were subjected to three consecutive rounds of enrichment. LC–MS analyses of peptides and enriched phosphopeptides were performed on an EASY-nLC 1200 UHPLC coupled to a quadrupole Orbitrap Exploris 480 mass spectrometer (both Thermo Scientific).

Separations of the peptide mixtures and enriched phosphopeptides were performed as described previously [31] with slight modifications: the peptides were injected onto the column in HPLC solvent A (0.1% formic acid) at a flow rate of 500 nl/min and subsequently eluted with a 127 or 57 min segmented gradient of 10–33-50–90% of HPLC solvent B (80% acetonitrile in 0.1% formic acid) at a flow rate of 200 nl/min. The mass spectrometer was operated in data dependent mode, collecting MS spectra in the Orbitrap mass analyzer (60,000 resolution, 300–1750 m/*z* range) with an automatic gain control (AGC) set to standard and a maximum ion injection time set to automatic. The 20 most intense precursor ions were sequentially fragmented with a normalized collision energy of 28 in each scan cycle using higher energy collisional dissociation (HCD) fragmentation. In all proteome and phosphoproteome measurements, sequenced precursor masses were excluded from further selection for 30 s. MS/MS spectra were recorded with a resolution of 15,000 and 30,000, respectively, whereby AGC was set to standard and fill time was set to automatic.

MS data were processed using default parameters of the MaxQuant software (v1.5.2.8) [32]. Extracted peak lists were submitted to a database search using the Andromeda search engine [33] to query a target-decoy [34] database of *homo sapiens* (97,795 entries, downloaded on 7th of October 2020) and 285 commonly observed contaminants.

In the database search, full tryptic specificity was required and up to two missed cleavages were allowed. Protein N-terminal acetylation, oxidation of methionine, and phosphorylation of serine, threonine, and tyrosine were set as variable modifications, whereas no fixed modification was defined. Initial precursor mass tolerance was set to 4.5 ppm, and 20 ppm at the fragment ion level. Peptide, protein and modification site identifications were filtered at a false discovery rate (FDR) of 0.01. For protein group quantitation a minimum of two quantified non-phosphorylated peptides were required, for phosphorylation sites at least one quantitation event was required. Quantified phosphorylation sites were further normalized for changes on the proteome level by dividing the site ratio by the corresponding protein group ratio. The normalization was done in R v. 4.1.2 (R Development Core Team (2012).

Bioinformatics

Downstream statistical analysis of proteomics and phosphoproteomics was performed in R (version 3.6.0). The R package proteus (version 0.2.14) was used to analyze MaxQuant's Proteomics output file "proteinGroups_SILAC.txt" and the phosphoproteomics output file "Phospho (STY)Sites.txt". Differential expression (DE) analysis was performed with the R package Limma (version 3.42.2) outside of the package Proteus. As cut-off for statistical significance a multiple adjusted p value (p.adj value) < 0.05 was chosen, which is corrected for multiple testing to control the false discovery rate (FDR). In a first step the SILAC ratios were quantile normalized and log2 transformed. In order to identify differentially expressed proteins a linear model was then fitted to each protein/phosphosite as follows: exp = ~ condition with "exp" representing expression of a protein and condition representing the ratios from fisetin treatment vs control. Using as null hypothesis log fisetin/control = 0 above formula was analyzed for the intercept term only, which is defined as the mean response value when all explanatory variables (here "condition") were set to zero. For graphical visualization heatmaps and a volcano plot showing statistical significance -log10(p-value) versus log2 FC were produced. The same procedure was done for phosphosites and afterwards the phosphosite table was compared

against the protein table to exclude phosphosites that were different due to differential expression at the protein level.

For a pathway and GO analysis in MDA-MB-468 cells, the g:Profiler tool (https://biit.cs.ut.ee/gprofiler/gost) (version e101_eg48_p14_baf17f0) was used. The protein IDs corresponding to the DE phosphosites and proteins with p.adj < 0.05 were copied into the g:Profiler tool. Homo sapiens was selected as the species and for the advanced options the following parameters were considered: only annotated genes, g:SCS threshold, 0.05 threshold and ENTREZGENE_ACC; before clicking on Run query. For GO analysis in MDA-MB-231 cells, DAVID 2021 (https://david.ncifcrf.gov/) was used. The protein IDs related to the DE phosphosites with significance B < 0.01 were copied into the DAVID tool. Homo sapiens was selected as the species and the most enriched pathways in DNA damage and repair pathways were selected and plotted.

Statistics and densitometry

A densitometry analysis of the Western blots was performed by using LI-COR *Odyssey Fc* with Image Studio Lite software version 5.2. (Bad Homburg v. d. Hoeh, Germany). Student's *t*-test was applied to test a significant difference on the expected endpoint according to each experiment between two groups. The non-parametric Mann–Whitney U test was performed to analyze a significant difference on the number of chromosomal aberrations per metaphase induced by irradiation or fisetin treatment. $p < 0.05$ was considered statistically significant (* $p < 0.05$, ** $p < 0.01$, *** $p < 0.001$***, $p < 0.0001$).

Results

Inhibition of YB1 and AKT phosphorylation by fisetin is cell line dependent

Cell authentication confirmed the lack of ER and PR in all TNBC cell lines in comparison with the MCF-7 and T47D classified as ER+/PR+ (Fig. S1). In addition, it also suggested an association between the levels of phosphorylation of YB-1 (S102), RSK (T359/S363) and the expression of RSK2 (Fig. S1). Fisetin is a plant flavonoid with anticancer properties that inhibits RSK-mediated YB-1 S102 phosphorylation in the range of 20 to 80 μM by inhibiting the interaction of RSK1 and RSK2 to YB-1 in melanoma cells [16]. Here, we evaluated the effects of fisetin at the concentrations of 12.5, 25, 50 and 75 μM on phosphorylation of YB-1 (S102) and AKT (S473) in TNBC cells 24 h after treatment. We analyzed phosphorylation status of YB-1, AKT and RSK in TNBC cell lines; MDA-MB-231, MDA-MB-453, HS 578T and MDA-MB-468.

Fisetin showed a cell line dependent inhibition effect (Fig. 1). It strongly reduced YB-1 (S102) phosphorylation in MDA-MB-231 and MDA-MB-453 cells in a dose-dependent manner without an effect on YB-1 protein expression. In HS 578T cells, fisetin reduced not only 50% YB-1 (S102) phosphorylation at the concentrations of 50 and 75 μM, but also YB-1 protein expression. In MDA-MB-468 cells, none of the fisetin concentrations inhibited YB-1 (S102) phosphorylation. Regarding AKT, fisetin failed to stimulate AKT (S473) phosphorylation in comparison to the RSK inhibitor LJI308 [6, 35] in all tested cell lines. However, it inhibited AKT (S473) phosphorylation in MDA-MB-231, with relatively lower levels of AKT phosphorylation shown in Fig. S1 and reported before [36]. In HSF-7 normal human fibroblast, fisetin slightly inhibited YB-1 (S102) phosphorylation only at concentrations of 25 and 50 μM (Fig. 1).

Fisetin mimics RSK pharmacological inhibitors in terms of inhibiting YB-1 (S102) phosphorylation

Since fisetin inhibited YB-1 phosphorylation at S102 in MDA-MB-231 but not in MDA-MB-468 cells, we inquired whether this is due to the difference in inhibiting RSK activity or due to the divergent effects of fisetin on YB-1 (S102) phosphorylation. To this aim, we compared the effects of fisetin (75 μM, 24 h) with the those of two RSK pharmacological inhibitors LJI308 (LJI) and BI-D1870 (BID), both at concentrations of 2.5 μM administered for 24 h. The data shown in Fig. 2A and the related densitometry in Fig. 2B indicate that fisetin (75 μM) mimics two RSK inhibitors that could markedly inhibit YB-1 phosphorylation at S102 in both cytoplasmic and nuclear fractions of MDA-MB-231. Similar to the data shown in Fig. 1, fisetin did not inhibit YB-1 phosphorylation in cytoplasmic and nuclear fractions of MDA-MB-468. Interestingly and similar to the fisetin effect, both RSK pharmacological inhibitors inhibited YB-1 phosphorylation in MDA-MB-231 cells. In MDA-MB-468 cells, fisetin as well as the RSK inhibitor BID did not affect YB-1 phosphorylation. While LJI with a lower IC50 values [37] slightly reduced YB-1 phosphorylation in MDA-MB-468 cells in both cytoplasmic and nuclear fractions (Figs. 2A-B). This data indicates that RSK is one of the major targets of fisetin. It is known that IR, along with inducing DNA DSB, stimulates YB-1 phosphorylation in wild-type cells [5, 6]. In cells with mutations, e.g., gain of function mutation in *KRAS* or loss of function mutation in *PTEN*, YB-1 is highly phosphorylated and this is not further enhanced by IR [5,]. Here, we inquired whether pattern of the effect of fisetin on YB-1 phosphorylation will be changed after irradiation in KRAS-mutated MDA-MB-231 and in PTEN-mutated MDA-MB-468 cells. As expected,

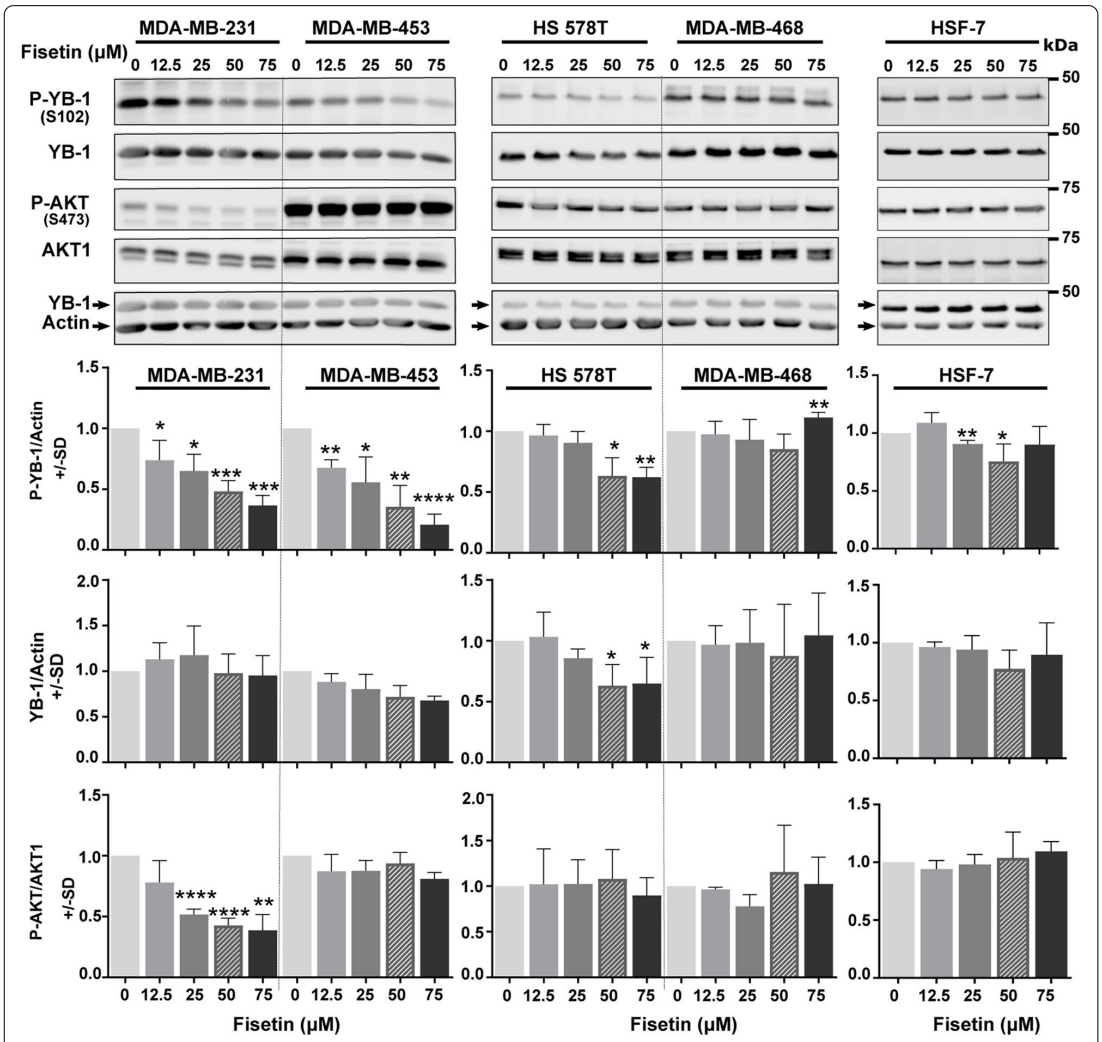

Fig. 1 Effect of fisetin on phosphorylation of YB-1 and AKT is cell line dependent. The TNBC cells were treated with indicated concentrations of fisetin for 24 h. Thereafter, protein samples were extracted and loaded into a SDS-PAGE. The level of phosphorylation of YB-1 (S102) and AKT (S473) were detected by Western blotting. Blots were stripped and incubated with antibody against YB-1 and AKT1, respectively. Actin was detected from the YB-1 detected membrane without stripping as a loading control. The histograms represent the mean densitometry values ± SD of phospho-YB-1 to actin, YB-1 to actin and phospho-AKT to AKT1 normalized to 0 μM condition from 3 independent experiments. The asterisks indicate significant fisetin mediated changes on YB-1 and AKT phosphorylation (*$p < 0.05$, **$p < 0.01$, ***$p < 0.001$), ****$p < 0.0001$; students t-test). SD: standard deviation

both cell lines presented high level of YB-1 phosphorylation at S102, which was not further stimulated by IR (Fig. 2C). Intriguingly, the effect of fisetin on YB-1 phosphorylation at 15 min and 30 min after 4 Gy irradiation remained unchanged, *i.e.*, inhibited in MDA-MB-231 cells and not affected in MDA-MB-468 (Fig. 2C).

Fisetin radiosensitizes TNBC cells

Inhibiting YB-1 phosphorylation on S102 by dual targeting of RSK and AKT was shown to be an efficient approach to block DSB repair and induce radiosensitization in breast cancer cells, independent of TNBC status [6]. We performed a clonogenic assay to investigate

whether the inhibition of YB-1 phosphorylation by fisetin correlates with radiosensitization in the cell lines tested. To this aim, clonogenic assay was tested in 3 different combination settings, *i.e.*, one dose of IR (3 Gy) combined with multiple concentrations of fisetin (0 to 100 μM), multiple doses of IR (0 to 4 Gy) combined with one concentration of fisetin (75 μM) and fractionated irradiation (1 to 5 fractions of 1 Gy) combined with fractionated fisetin treatment (1 to 5 fractions of 75 μM). The data obtained from these experiments showed that fisetin induces radiosensitivity under all tested conditions. Fisetin at different concentrations induced radiosensitization in MDA-MB-231 cells irradiated with 3 Gy (Fig. S2A), in accordance with the inhibition of YB-1 phosphorylation shown in Fig. 1. Fisetin in non-irradiated cells (0 Gy) strongly inhibited clonogenic activity as well (Fig. S2A).

In a separate experiment we compared the effect of fisetin (0 to 100 μM) with irradiation (0 to 4 Gy) in MDA-MB-231 and MDA-MB-468 on clonogenic activity and showed that, similar to IR, fisetin inhibits clonogenic activity in both of the cell lines tested (Fig. S2B). Based on this data in the further experiments we applied fisetin at 75 μM in combination with fractionated irradiation and investigated its radiosensitization in all 4 TNBC lines including MDA-MB-231 cells. Data shown in Fig. 3 indicates that fisetin induces radiosensitization in all TNBC lines, however the effect was cell line dependent.

Among the cell lines tested, HS 578T was the most radioresistant cell line and the radiosensitizing effect of fisetin started appearing in fraction 4. From this data we proposed that DSB repair machinery effectively repairs damages induced by 1 Gy fraction and that the potential radiosensitizing effect of fisetin might be observed when combined with a single dose of irradiation. We confirmed this hypothesis by performing a clonogenic assay in combination with fisetin (75 μM) and a single dose of irradiation of 0 to 4 Gy. Data obtained from this experiment confirmed the radiosensitizing effect of fisetin in HS 578T cells (Fig. S2C). Very interestingly, fisetin (75 μM) did not radiosensitize normal human fibroblast HSF-7 cells when combined with single dose irradiation 0 to 4 Gy (Fig. S2C).

Fisetin blocks repair of IR-induced DSB

It is known that YB-1 stimulates repair of IR-induced DSB [5, 6]. Thus, we investigated whether fisetin affects the repair of DSB in association with the inhibition of YB-1 phosphorylation at S102. Analyzing residual DSB 24 h after irradiation revealed that the fisetin pretreatment at concentrations of 25, 50 and 75 μM for 24 h inhibits repair of DSB in all 4 TNBC cell lines tested, independent of its effect on YB-1 phosphorylation at S102 (Fig. 4A-B). Fisetin (75 μM) did not affect IR-induced DSB repair in HSF-7 cells, while at the concentration of 25 μM it stimulated DSB repair (Fig. 4A-B), which is in favor of future clinical applications of the drug. To analyze whether induction of damage is different in the presence and absence of fisetin, the number of γH2AX foci was analyzed 30 min after irradiation with 1 Gy in cells pretreated with and without fisetin (75 μM). The data presented in Fig. S3A indicates that the frequency of γH2AX foci in fisetin treated cells is higher than in control cells at either the 0 Gy or 1 Gy irradiation condition, which indicates that fisetin can induce DSB. Functions of fisetin as an inhibitor of the repair of IR-induced DSB and as an inducer of DSB when applied as a single treatment was tested in MDA-MB-231 and MDA-MB-468 cells after treatment with 0, 25, 50 and 75 μM for 48 h. Data shown in Fig. S3B indicates that fisetin at a concentration of 75 μM induced DSB in both cell lines. However, fisetin at lower concentrations, *i.e.*, 25 and 50 μM did not induce DSB in MDA-MB-231 cells. The frequency of residual DSB was higher when these concentrations of fisetin were combined with IR, indicating inhibition of repair of IR-induced DSB (Fig. 4A-B). By applying YB-1-siRNA in MDA-MB-231 cells, we were able to show that the inhibitory effect of fisetin on DSB repair is much stronger than the effect of YB-1 knockdown (Fig. 4C). These data indicate that fisetin blocks the repair of IR-induced DSB and that this effect is only partially dependent on YB-1.

Residual DSB in proliferating cells result in a variety of chromosomal aberrations that lead to cell death. We investigated whether fisetin induces chromosomal aberration in MDA-MB-231 and MDA-MB-468 cells, in which YB-1 phosphorylation was differentially affected by fisetin, *i.e.*, inhibited in MDA-MB-231 cells and not affected in MDA-MB-468 cells. Fisetin (75 μM, 72 h)

(See figure on next page.)

Fig. 2 Fisetin and RSK inhibitors have similar effect on YB-1 phosphorylation. **A** The indicated cells were treated with fisetin (75 μM), LJI308 (LJI) (2.5 μM) or BI-D1870 (BID) (2.5 μM). Cytoplasmic and nuclear protein fractions were isolated after 24 h and subjected to SDS-PAGE. Phospho-YB-1, total YB-1, phospho-AKT and total AKT1 were detected by Western blotting. α-Tubulin and lamin A/C were used as cytoplasmic and nuclear markers, respectively. Actin was detected as loading control. **B** The histograms represent the mean densitometry values ± SD of P-YB-1 to actin and YB-1 to actin from 3 independent experiments normalized to DMSO treated control (Ctrl) condition. The asterisks indicate significant fisetin mediated changes on YB-1 phosphorylation (*$p < 0.05$, **$p < 0.01$, ***$p < 0.001$), ****$p < 0.0001$; students t-test). **C** Cells were treated with and without fisetin (75 μM, 24 h) and mock irradiated or irradiated 4 Gy. Cytoplasmic and nuclear protein fractions were isolated at the indicated times after IR and subjected to SDS-PAGE. Phospho-YB-1 and total YB-1 were detected by Western blotting. α-Tubulin and lamin A/C were used as cytoplasmic and nuclear markers, respectively. Actin was detected as loading control

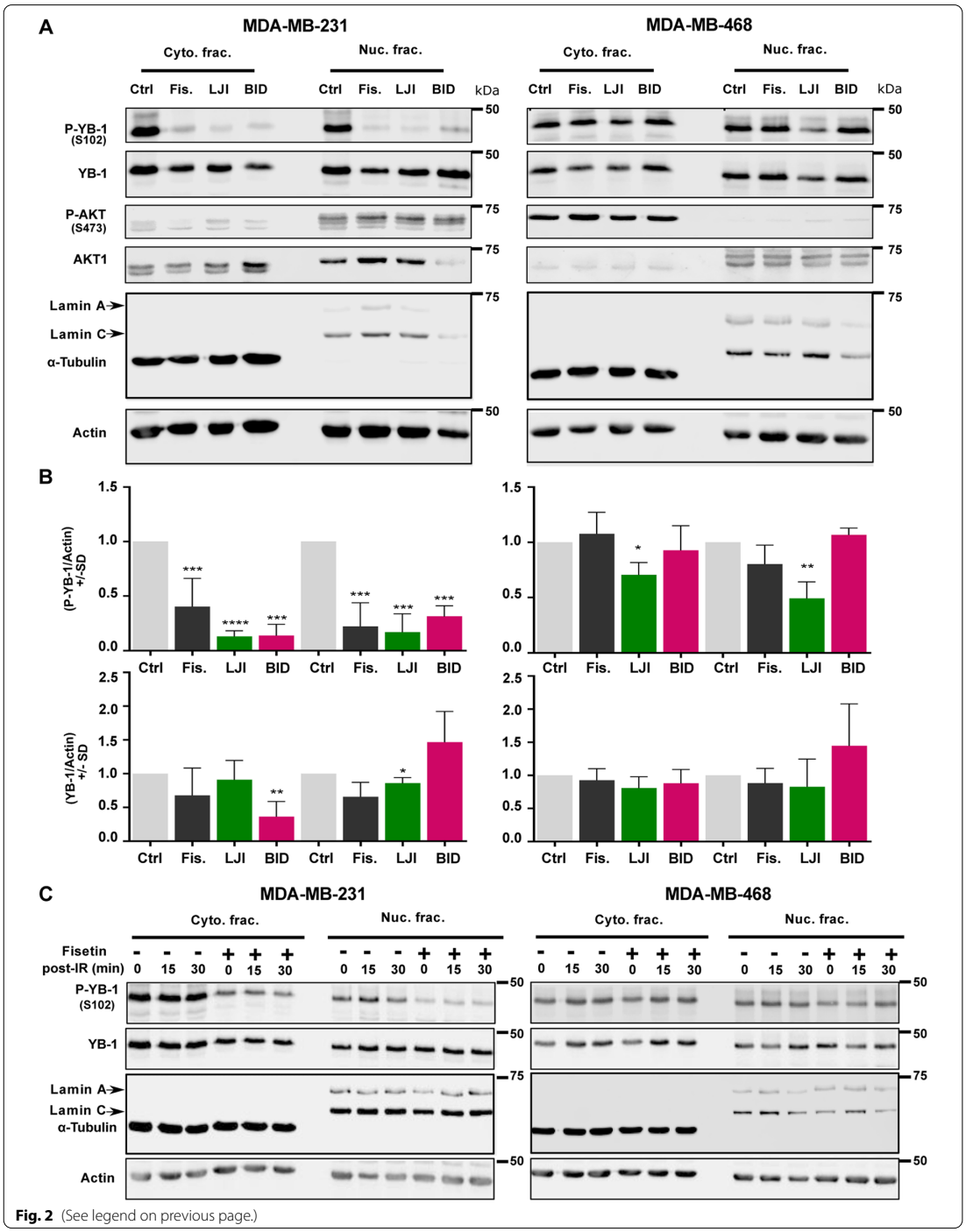

Fig. 2 (See legend on previous page.)

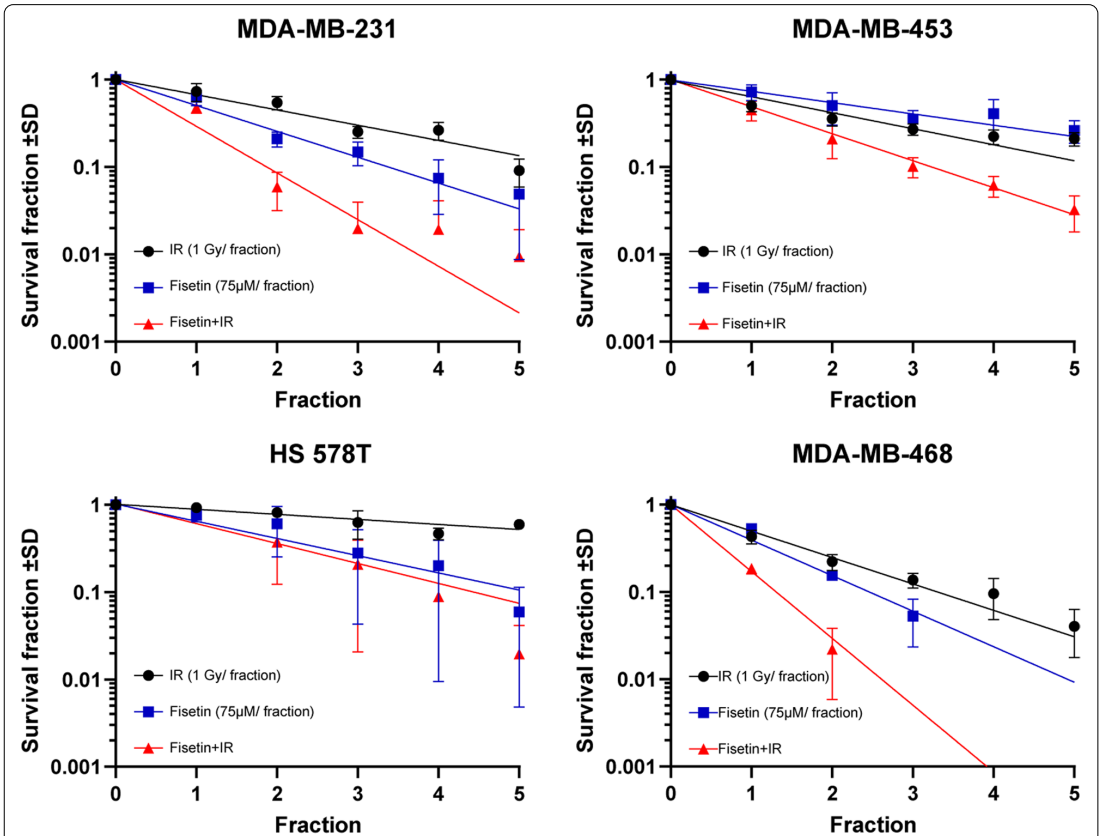

Fig. 3 Fisetin radiosensitizes TNBC cells. The cells were treated with a vehicle (DMSO) or fisetin (75 μM) for 24 h, irradiated with a fractionated irradiation of 1 Gy and clonogenic assay was performed as described in the *Methods* section. The data points represent the mean surviving fraction ± SD of 12 data from 2 independent experiments (MDA-MB-231, MDA-MB-453, HS 578T) and 6 data from one experiment (MDA-MB-468)

induced chromosomal aberration in MDA-MB-231. In MDA-MB-468 cells, the frequency of aberration was also slightly but not significantly enhanced (Fig. 4D). In both cell lines, IR (2 Gy) induced chromosomal aberration (Fig. 4D).

Fisetin inhibits DSB repair through interference with C-NHEJ and HR repair pathways

IR-induced DSB are repaired either by C-NHEJ or Alt-NHEJ throughout the cell cycle and by HR during the S and G2 phases. We investigated which DSB repair pathway was inhibited by fisetin by combining fisetin with a specific inhibitor of each repair pathway. To this end, DNA-PKcs inhibitor NU7441 (5 μM), Rad51 inhibitor B02 (5 μM) and PARP inhibitor Talazoparib (25 nM) were used as the inhibitors of C-NHEJ, HR and Alt-NHEJ repair pathways, respectively. Data shown in Fig. 5A revealed that treatment with fisetin and NU7441 significantly inhibited DSB repair in MDA-MB-231 and MDA-MB-468 cells after 4 Gy irradiation. B02 inhibited DSB repair in MDA-MB-468 but not in MDA-MB-231 cells (Fig. 5B). A combination of fisetin neither with Nu7441 (Fig. 5A) nor B02 (Fig. 5B) enhanced residual DSB compared to single treatments. Similar to fisetin, talazoparib as a PARP inhibitor, induced DSB as monotherapy and inhibited repair of IR-induced DSB in both cell lines (Fig. 5C). A combination of fisetin with talazoparib resulted in an additive effect after irradiation in both cell lines (Fig. 5C).

To support the data by pharmacological inhibitors of the specific DSB repair pathways, the effect of fisetin on I-SceI-induced DSB was tested in osteosarcoma cell lines U2OS cells harboring reporter constructs specific for the individual repair pathways. Schematic figures demonstrating

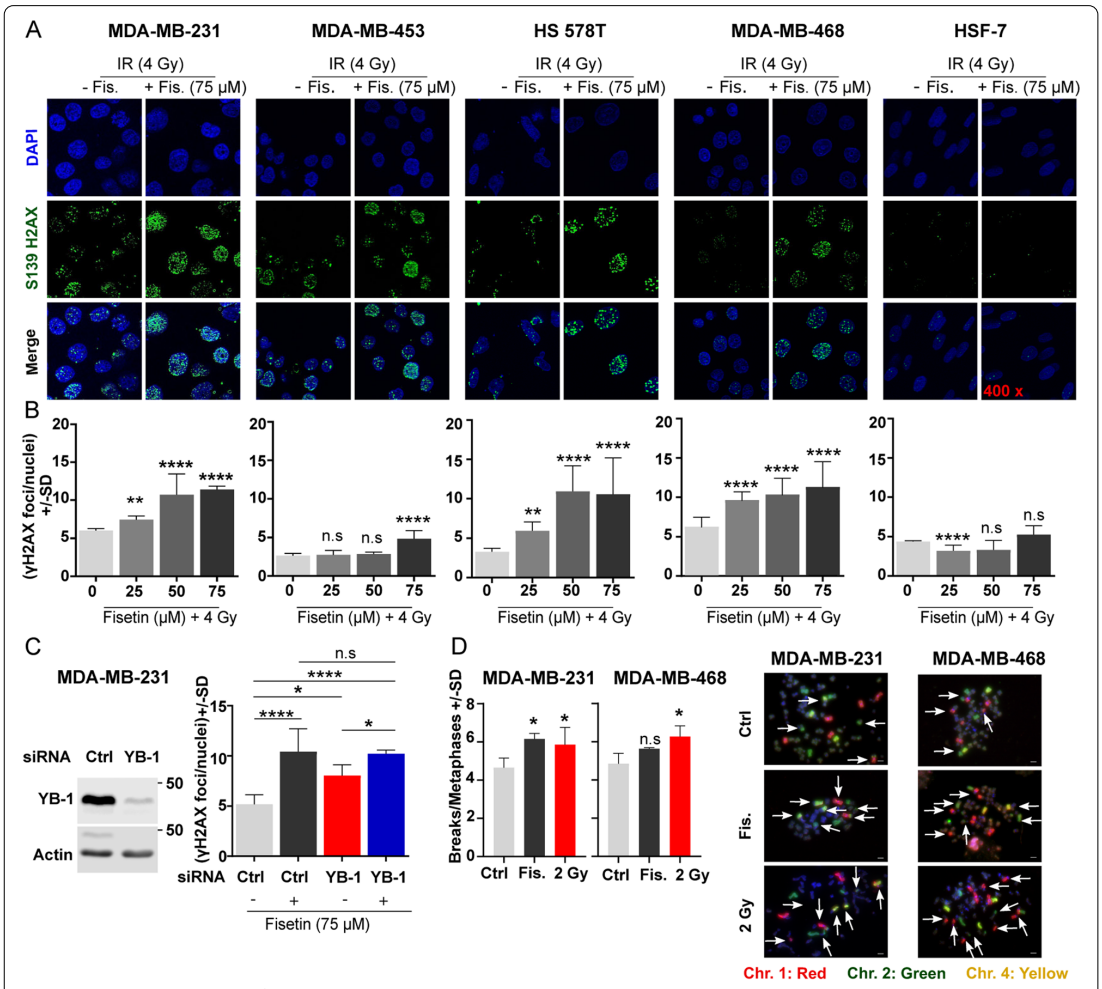

Fig. 4 Fisetin inhibits the repair of IR-induced DSB, which leads to chromosomal aberration in TNBC cells. **A**, **B** The cells were treated with the indicated concentrations of fisetin for 24 h and irradiated with 4 Gy. Twenty-four hours after irradiation γH2AX foci assay was performed as described in the *Methods* section. **A** The representative immunofluorescent images of γH2AX foci used for analyses. **B** Asterisks indicate significant inhibition of DSB repair shown by increased mean residual γH2AX ± SD after fisetin treatment compared to DMSO treated/ 4 Gy irradiated control (Ctrl) condition in 500 nuclei in MDA-MB-231 cells, 700 nuclei in MDA-MB-453 cells, 600 nuclei in MDA-MB-468 cells, 500 nuclei in HS 578T cells and 440 nuclei in HSF-7 cells, from 3 independent experiments. **C** MDA-MB-231 were transfected with 50 nM indicated siRNA and protein samples were isolated 72 h after transfection to analyze knockdown efficiency by Western blotting. In the parallel cultures, 24 h after transfection cells were treated with DMSO or fisetin (75 μM) for additional 24 h and irradiated with 4 Gy. γH2AX was performed 24 h after irradiation (72 h after transfection) and counted using FoCo software. The asterisks indicate significant difference in mean γH2AX ± SD between the indicated conditions (*$p < 0.05$, **$p < 0.01$, ***$p < 0.001$), ****$p < 0.0001$; students t-test) analyzed in 444 cells, from 3 independent experiments. The DMSO concentration in the cells treated with different concentrations of fisetin was kept similar. **D** The mean number of chromosomal aberrations analyzed in at least 50 metaphases 48 h after irradiation (2 Gy) or 72 h after treatment with fisetin (75 μM). (*$p < 0.05$, Mann–Whitney U test): n.s. = non-significant. Chr.: Chromosome

the constructs for the repair pathways they report have been outlined in Fig. 5D-F. The data obtained using these cells indicate that pretreatment with fisetin (75 μM) inhibits I-SceI-induced DSB repair in cells reporting HR and C-NHEJ but not Alt-NHEJ as shown by the FACS plots (Fig. 5E) as well as the mean percentage of GFP positive cells (Figs. 5F).

Effect of fisetin in combination with IR on apoptosis and autophagy

As an alternative to residual DSB mediated cell death by mitotic catastrophe, enhanced apoptosis by the combination of fisetin and radiation might be a potential mechanism of radiosensitization by fisetin. Here, using flowcytometry analysis, it was shown that fisetin (75 µM) treatment for 72 h (24 h before and 48 h after IR) generally reduces the percentage of cells in G1 phase (Fig. 6A). Fisetin significantly enhanced sub-G1 population as an indication of apoptosis only in MDA-MB-231 and MDA-MB-453 cells. Radiation (4 Gy) did significantly reduce the G1 population only in MDA-MB-453 and MDA-MB-468 cells. Irradiation did not induce apoptosis in either of 4 TNBC cell lines. Interestingly, a combination of fisetin with IR enhanced apoptosis compared to fisetin or radiation alone only in MDA-MB-468 cells (Figs. 6A).

Controversial data has been reported regarding the effect of fisetin on autophagy. It is not known how the level of autophagy is changed in TNBC cells after a fisetin treatment in combination with irradiation. In this study, we investigated if there was a correlation between the expression pattern of LC3-II and p62 as autophagy markers and radiosensitizing effect of fisetin. Our data demonstrated that fisetin (75 µM, 72 h) markedly induced the expression of LC3-II in MDA-MB-231 and MDA-MB-468 cells without changes on the expression level of p62. Neither IR nor the combination of IR with fisetin induced the expression of autophagy markers, as shown by Western blotting (Fig. 6B). However, similar to a 24 h treatment, treatment with fisetin for 72 h induced radiosensitization in MDA-MB-231 cells when combined with single dose irradiation of 3 Gy (Fig. S2A) or IR doses of 1 to 4 Gy (data not shown). Together, the data presented for DSB repair, autophagy and apoptosis indicates that the combination of fisetin with radiation leads to radiosensitization due to enhanced residual DSB that results in mitotic catastrophe but not stimulating apoptosis or regulating autophagy in TNBC cells.

Fisetin modulates activation of DDR signaling cascades

Fisetin in the range of 20 to 80 µM interacts with RSK1 and RSK2 to inhibits YB-1 phosphorylation at S102 in melanoma cells [16]. By applying a short scale phosphokinase array in irradiated MDA-MB-231 cells we could show that fisetin (75 µM) inhibits phosphorylation of RSK1/2 (S221/S227) as the major kinases involved in YB-1 phosphorylation. However, fisetin in combination with IR markedly inhibited p53 phosphorylation (S392), phosphorylation of Src kinase (Y419) and suppressed the expression of ß-catenin, analyzed at 30 min as well as 24 h post-IR (Fig. 7). The inhibitory effect of fisetin alone in non-irradiated condition in the 30-min post-IR experiment was mild. This data indicated that fisetin may affect multiple pathways involved in cell survival.

To analyze a possible effect of fisetin on DDR signaling, a large scale phosphoproteomic study was performed in fisetin pre-treated and irradiated cells compared to irradiation alone. In MDA-MB-468 cells, in which fisetin does not inhibit YB-1 phosphorylation, a total of 472 phosphosites from 1564 analyzed phosphosites were found to be up- or down regulated (Fig. 8A, Fig. S4). DEK (T13, S51), nucleolin (NCL) (S563), XRCC1 (S210) and TOP2A (S1106) were among the top 10 inhibited phosphorylation sites involved in DNA repair. Next, we performed a gene ontology (GO) enrichment analysis to verify if deregulated phosphosites are involved in DDR signaling, *i.e.*, DSB repair. The GO data presented in Fig. 8B and Table S1 indicates that gene products involved in DSB repair are among the most frequently inhibited targets participating in DDR signaling. Interestingly, the GO biological process analysis in irradiated MDA-MB-231 cells presented in Fig. S5 was similar to the data obtained in MDA-MB-468 cells indicating the importance of DNA repair gene products as the most important targets of fisetin in irradiated cells (Fig. S5).

(See figure on next page.)

Fig. 5 Fisetin inhibits DSB through the HR and C-NHEJ repair pathways. **A**-**C** MDA-MB-231 and MDA-MB-468 cells were treated with or without fisetin (75 µM) for 22 h and followed by treatment with or without DNA-PKcs inhibitor (NU7441, 5 µM), Rad51 inhibitor (B02, 5 µM) or PARP inhibitor (Talazoparib, 25 nM) for 2 h. The DMSO concentration in cells treated with different inhibitors was kept similar. Thereafter, cells were mock irradiated or irradiated 4 Gy and γH2AX was performed 24 h after IR. γH2AX foci per nuclei were counted using FoCo software. The data are presented as the mean number of foci per nuclei ± S.D. The asterisks indicate significant inhibition of DSB repair shown by increased mean residual γH2AX ± SD after treatment with indicated inhibitors compared to DMSO treated/ 4 Gy irradiated control condition or compared between indicated groups from at least 300 nuclei in MDA-MB-231 cells and MDA-MB-468 cells from at least 3 independent experiments (*$p < 0.05$, **$p < 0.01$, ***$p < 0.001$), ****$p < 0.0001$; students t-test). **D** U2OS cells harboring different DNA repair constructs including HR, C-NHEJ and Alt-NHEJ were used. **E** The cells were either transiently transfected with an inducible endonuclease I-SceI plasmid (800 ng/ml) or not transfected as a negative control. Twenty-four hours after transfection, cells were treated with or without fisetin (75 µM, 24 h). Nuclear translocation of I-SceI was induced by 100 ng/ml triamzinolonacetonid and twenty-four hours later the percentage of GFP positive cells were determined using FACS. **F** The bar graphs show the mean percentage of GFP positive cells ± SD from 4 independent experiments normalized to DMSO treated control condition. Asterisks indicate inhibition of the indicated repair pathway by fisetin treatment (*$p < 0.05$, **$p < 0.01$; students t-test). The data shown for GFP-negative control cells is the mean from 2 independent experiments

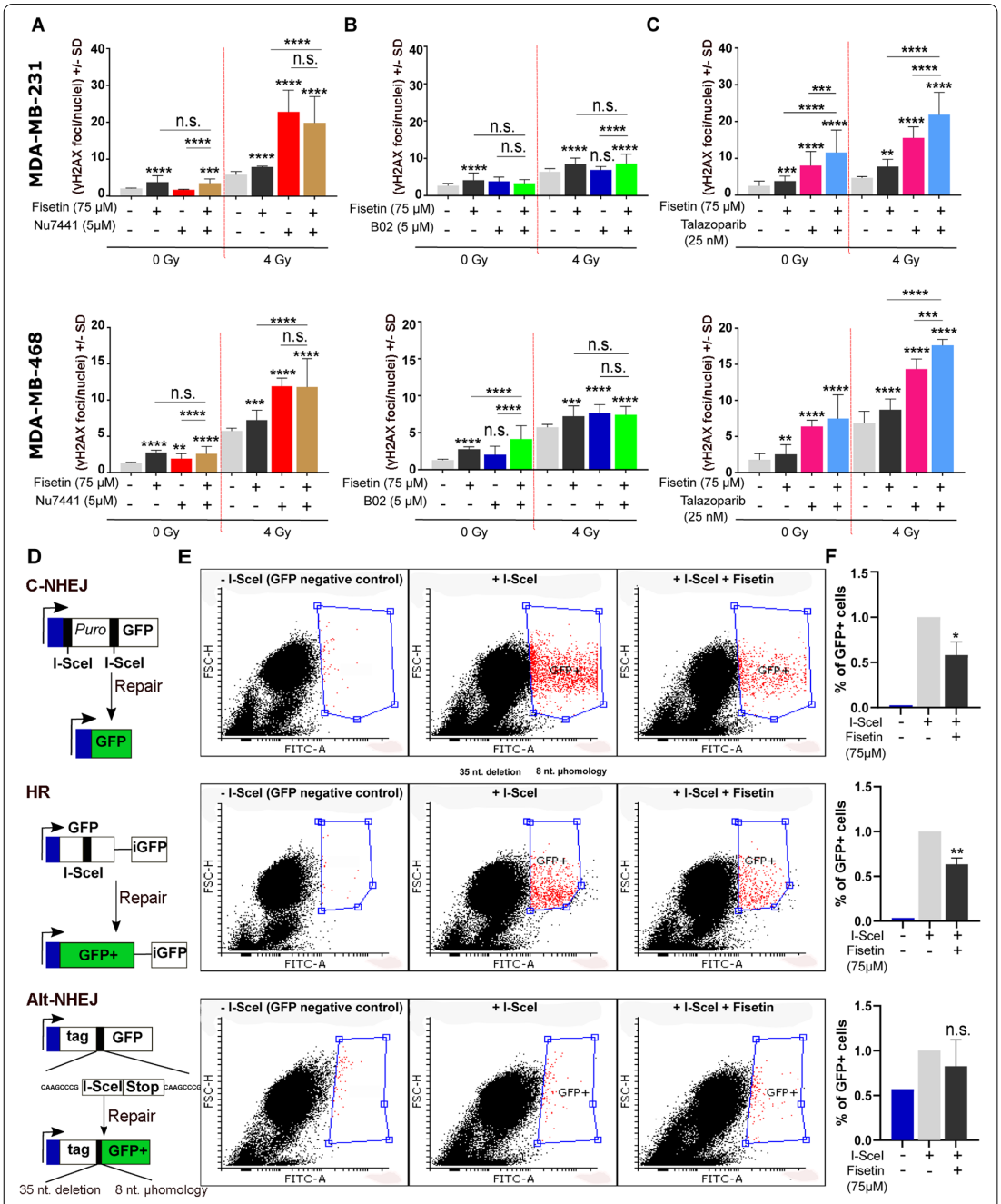

Fig. 5 (See legend on previous page.)

Discussion

TNBC is an aggressive type of breast cancer with poor outcomes. Beside surgery, radiotherapy is the main treatment option for TNBCs; unfortunately, radioresistance frequently occurs and diminishes the results of the therapy outcome. YB-1 as a multi-functional oncoprotein is overexpressed in different tumor types and plays a pivotal role in cell death resistance mechanisms. Fisetin is a plant flavonoid compound that interferes with RSK mediated YB-1 activity. In this study, we uncovered potential targets of fisetin in TNBC cells and investigated effect of fisetin on DSB repair and radiation response. The data obtained demonstrates that fisetin induces radiosensitization in association with inhibiting DSB repair in TNBC cells but not in normal human skin fibroblast. Fisetin inhibited DSB repair by inhibiting the HR and C-NHEJ repair pathways.

Fisetin interferes with the DDR signaling RSK and AKT pathways

RSK and AKT are the main kinases phosphorylating YB-1 at S102 [38], prerequisite for the effect of YB-1 in stimulating repair of IR induced DSB [6]. AKT, besides its role in YB-1 phosphorylation, stimulates repair of IR-induced DSB by directly binding to DNA-PKcs [27, 39, 40]. Thus, due to the compensatory role of AKT, inhibiting YB-1 activity by solely targeting RSK is not an effective approach to inhibit DSB repair and induce radiosensitization [6]. To this aim, it was previously shown that co-targeting of RSK and AKT was more effective than single targeting of each kinase in terms of inhibiting cell proliferation [35], blocking DSB repair and inducing chemosensitivity [35] as well as radiosensitivity [6]. TNBC cell lines in this study harbor the key mutations (Table S2) that stimulate the PI3K/AKT and MAPK/RSK pathways, as underlying pathways involved in phosphorylation of YB-1 at S102. Analyzing basal phosphorylation of YB-1, AKT and RSK and the expression of RSK1 and RSK2 revealed that phosphorylation of YB-1 at S102 is mainly associated with the expression of RSK1 and RSK2 as well as the phosphorylation of RSK (T359/S363) (see Fig. S1). RSK and YB-1 are highly phosphorylated in MDA-MB-231 and MDA-MB-468 cells while MDA-MB-453 and HS 578T cells present high phosphorylation of AKT (S473) and low phosphorylation of YB-1. According to this data, phosphorylation of YB-1 is mainly stimulated by RSK, suggesting that RSK targeting is necessary to efficiently inhibit YB-1 phosphorylation and YB-1-dependent cellular functions. Fisetin is known to block YB-1 phosphorylation in melanoma cells by binding mainly to RSK2 and to a lesser degree to RSK1 [16]. Likewise, fisetin inhibits the PI3K/AKT pathway in breast cancer cells [18]. In the present study, we applied fisetin as an alternative approach to AKT/RSK dual targeting strategy to block YB-1 phosphorylation. Our data in TNBC cells supports the reported effect of fisetin on YB-1 phosphorylation in melanoma cells [16]. Fisetin mimicked the effect of RSK inhibitors on YB-1 phosphorylation, indicating that fisetin interfered with RSK in TNBC cells. It inhibited YB-1 phosphorylation in 3 out of the 4 TNBC cell lines tested. In MDA-MB-468 cells, in which fisetin did not affect YB-1 phosphorylation at S102, the lack of an effect was also observed by two well-described RSK inhibitors, in the presence or absence or irradiation. This set of data indicates that S102 phosphorylation of YB-1 in MDA-MB-468 cells is mainly RSK independent. In line with this conclusion, MDA-MB-468 cells lack the expression of PTEN [41], which results in hyperactivation of AKT and, consequently, AKT-dependent YB-1 phosphorylation [6].

Fisetin induces DSB and interferes with DSB repair after IR

Nuclear localization of YB-1 is linked to a poor prognosis in different tumors, as reviewed elsewhere [38]. Binding of YB-1 to DNA repair proteins MSH2, DNA polymerase delta, Ku80 and WRN proteins has been described before [13]. In this context, our previous studies demonstrated that a genetic knockdown of YB-1 or blocking S102 phosphorylation of YB-1 using a specific peptide impairs the repair of IR-induced DSB [5, 6]. Here, we could show that fisetin inhibits YB-1 phosphorylation at S102 in 3 out of 4 TNBC cell lines tested, indicating the potential of fisetin to block the repair of DSB after irradiation. Interestingly, in all cell lines tested, including MDA-MB-468 cells, which lack a response to the effect of fisetin on YB-1 S102 phosphorylation, the frequency of residual DSB shown by γH2AX was enhanced in the combination of fisetin with IR compared to IR alone. This

(See figure on next page.)

Fig. 6 Fisetin in combination with irradiation does not affect cell cycle progression and autophagy. **A** log-phase cells were treated with fisetin (75 μM) for 24 h and irradiated with 4 Gy. Forty-eight hours after irradiation, cells were collected and fluorescence-activated cell sorting analysis was performed as described before [27]. The percentage of cells in different cell cycles as mean ± SD was calculated from at least 3 independent experiments and graphed. The asterisks indicate significant differences in individual treatment groups compared to the DMSO treated control (Ctrl) condition or between the arrows indicated conditions (*$p < 0.05$, **$p < 0.01$, ***$p < 0.001$; students t-test). **B** The cells were treated with a vehicle or fisetin (75 μM) for 65 h and mock irradiated or irradiated with 4 Gy. Protein samples were isolated 7 h after irradiation and subjected to SDS-PAGE. The level of LC3I/II and p62 were detected using Western blotting. The experiments were repeated at least 3 times and similar results were obtained. Actin was detected as the loading control. Bar graphs represent the mean densitometry of LC3-II to actin from at least 3 independent experiments normalized to 1 in control condition. The asterisks indicate significant differences in mean LC3-II/actin between the indicated conditions or compared to untreated control (*$p < 0.05$, **$p < 0.01$; students t-test)

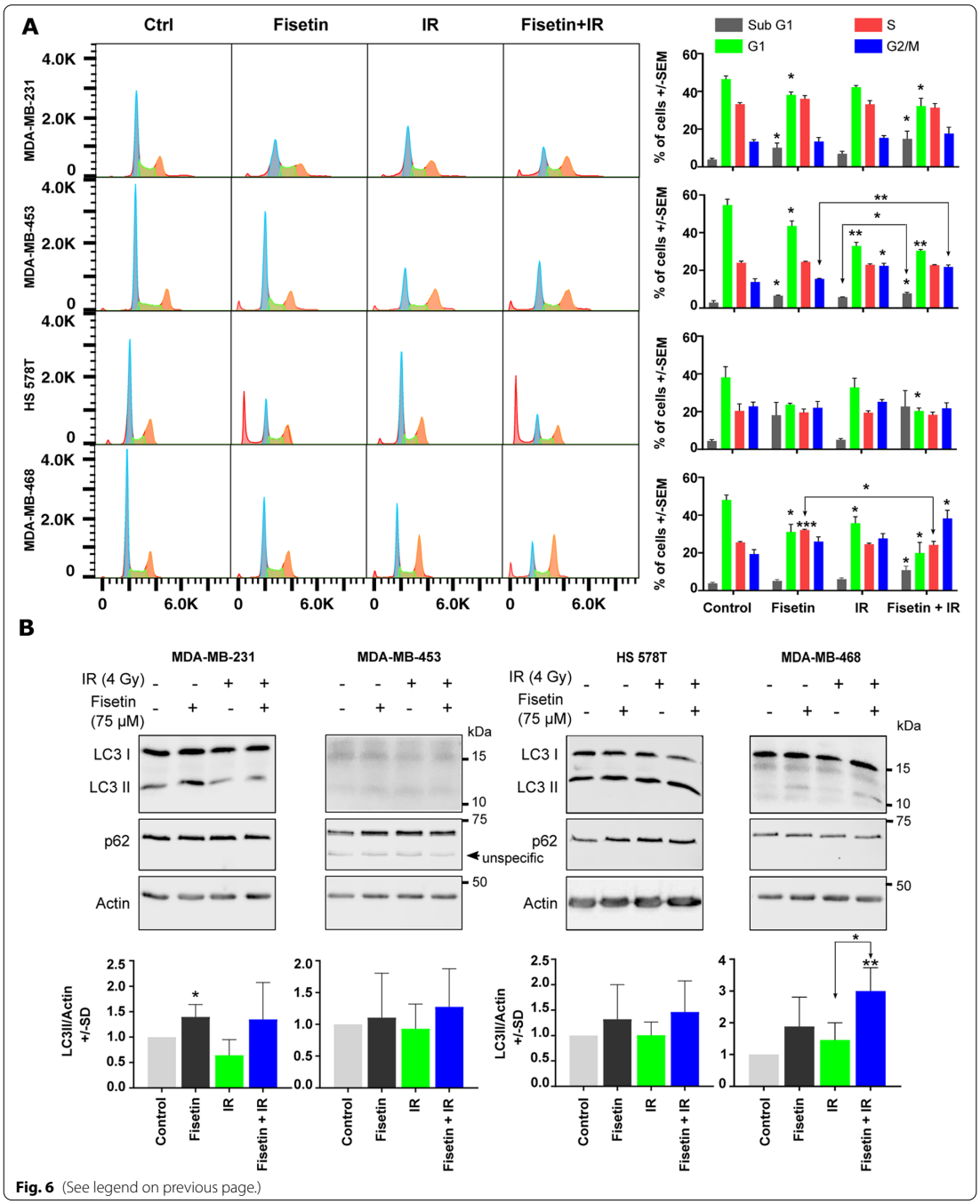

Fig. 6 (See legend on previous page.)

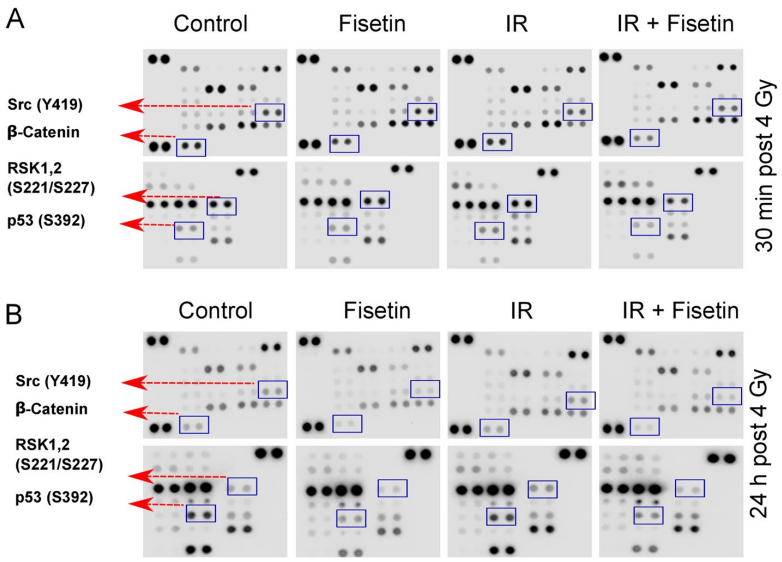

Fig. 7 Effect of fisetin om multiple Kinases in MDA-MB-231 cells after irradiation. MDA-MB-231 cells were treated with fisetin (75 µM) for 72 h and irradiated with 4 Gy. Protein samples were isolated either 30 min (**A**) or 24 h after irradiation (**B**). A phospho-kinase proteome analysis was performed according to the manufacturer's protocol after the described treatments

effect was associated with radiosensitization in all tumor cells tested but not in normal fibroblasts. As expected, fisetin did not affect DSB repair in normal fibroblasts. In line with this observation, Piao et al. reported that fisetin has a protective effect against γ-irradiation-induced oxidative stress and cell damage in Chinese hamster lung fibroblasts [42]. Interestingly, fisetin alone was shown to function as a DNA damage inducing agent when applied at 75 µM in all TNBC cells tested. This effect of fisetin in TNBC cells correlates with the previous reports from other laboratories indicating DNA damage induced in three tumor entities by fisetin at different concentrations, *i.e.*, in hepatic cancer (60 µM) [43], gastric cancer (50 µM) [44] and pancreatic cancers (50 and 100 µM) [17]. In the current study, applying fisetin at the concentrations of 25 and 50 µM did not induce DNA damage as shown in MDA-MB-231 (Fig. S3) but inhibited repair of IR-induced DSB at these as well as a concentration of 75 µM (Fig. 4). This data supports the effect of fisetin on DDR signaling. Thus, fisetin can potentially function as a double-edged sword in irradiated TNBC cells. Similar to IR, it functions as a DSB inducing agent, but simultaneously inhibits repair of DSB that are induced by IR. At present, it is not known whether the quality and complexity of DSB induced by fisetin and IR are similar. This is a topic that remains to be investigated.

DSB is the major type of DNA damage involved in radiotherapy-induced cell death. Activation of signaling pathways such as RSK/YB-1 and PI3K/AKT by irradiation stimulates DSB repair and diminishes the effect of radiotherapy. [6, 39]. So far existing data indicates that fisetin inhibits survival signaling pathways in different tumors, e.g., RSK/YB-1 in melanoma [16], PI3K/AKT in pancreatic cancer [45] and YB-1 in TNBC cells as shown in the present study. The inhibition of prosurvival pathways by fisetin contrasts with the effect of IR, which is known to stimulate these pathways [5, 6, 46]. Thus, fisetin treatment is expected to block clonogenic activity. Comparing the effect of single doses of fisetin with the effect of single doses of IR on clonogenic

(See figure on next page.)

Fig. 8 DDR are the major target of fisetin in irradiated cells. A phosphoproteomic study was performed in MDA-MB-468 cells, treated with or without fisetin (75 µM) for 24 h and irradiated with 4 Gy. Thirty minutes after irradiation cells were isolated and phosphoproteomics was performed as described in the *Material & Methods* section. **A** A total of 472 deregulated phosphosites (320 downregulated and 152 upregulated) and 47 deregulated total proteins were identified. **B** The gene ontology analysis indicates that phospho-proteins involved in DDR are the most frequently downregulated ones by fisetin in irradiated cells. The asterisks indicate significant deregulation ($N=3$, $*p<0.05$, $**p<0.01$, $***p<0.001$; values extracted from g:profiler analysis). **C** The proposed signaling pathway targeted by fisetin to interfere with repair of IR-induced DS

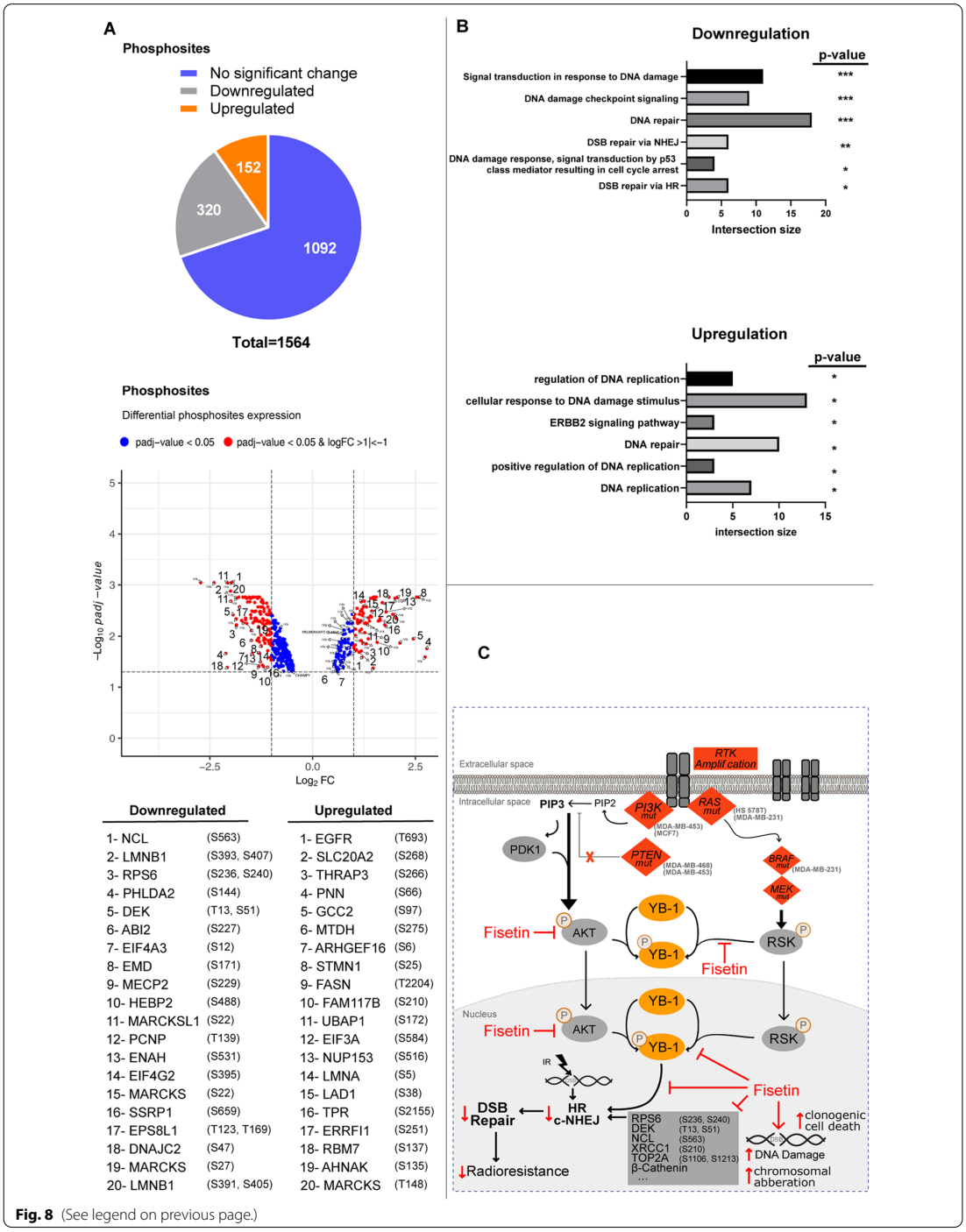

Fig. 8 (See legend on previous page.)

activity of MDA-MB-231 and MDA-MB-468 cells supports this conclusion (Fig. S2B). The anti-clonogenic activity of fisetin in MDA-MB-468 cells was stronger compared to that in MDA-MB-231 cells. This might be due to the stronger effect of fisetin in DSB induction in MDA-MB-468 compared to that in MDA-MB-231 cells (Fig. S3B). Our results from the present study indicate that fisetin in combination with IR inhibits the major DSB repair pathway, *i.e.*, C-NHEJ and HR (see Figs. 5). The data on the effect of fisetin on HR is also supported by a recent report from Huang et al., who showed that HR repair efficiency in pancreatic cancer cells is diminished by fisetin treatment [47]. In this study, the authors demonstrate that fisetin inhibiting HR is due to a modification of N6-methyladenosine [47]. However, gene ontology from our phosphoproteomic study revealed that a variety of phosphosites involved in DDR are inhibited by fisetin treatment in irradiated cells. Among them, gene products involved in DNA repair, chromatin binding and DNA replication are the most affected. DEK (T13, S51) [48], nucleolin (S563) [49], XRCC1 (S210) [50] and TOP2A (S1106) [51] were found to be among the top 20 fisetin inhibited phospho-proteins that have been reported to be involved in DDR signaling, *i.e.,* DSB repair. Thus, we suggest that fisetin affects DDR at multiple levels rather than blocking it at a specific stage by affecting/inhibiting a single target.

Radiosensitization of TNBC by fisetin results from boosting DSB but not modulating autophagy and apoptosis

Non-repaired DSB leads to cell death by different mechanisms, *i.e.,* mitotic catastrophe, apoptosis and autophagy. So far, published data indicates that fisetin induces cell death by stimulating apoptosis. Here, we were able to show a significant enhancement of apoptosis by fisetin treatment in two out of the 4 TNBC cell lines. IR did not induce apoptosis in any of the cell lines tested. Importantly, a combination of fisetin with radiation slightly stimulated apoptosis in only one cell line (MDA-MB-468). However, the radiosensitizing effect of fisetin was observed in all TNBC cells but not in normal human fibroblast. The lack of enhanced apoptosis in TNBC cells after combination of fisetin with irradiation is in conflict with the report by Chen et al., who described that fisetin radiosensitizes *TP53* mutated HT-29 colorectal cancer cells through stimulating apoptosis [52]. The initiation of apoptosis or alternative types of cell death depends on a variety of parameters. Complexity of DSB, expression of the components of the underlying signaling pathways involved in a certain type of cell death and the mutation status of these components are the most crucial parameters, which vary in different cell lines. Thus, the conflicting results might be due to the different in cell lines investigated. Although, all the TNBC cell lines tested so far in our study are mutated in *TP53* and radiosensitized by fisetin, *TP53* mutation is not a prerequisite for fisetin-mediated radiosensitization since fisetin did not radiosensitize the *TP53* mutated non-TNBC cell line T74D (data not shown). Additionally, fisetin has been reported to improve radiotherapy outcome of *TP53* wild-type CT-26 xenograft tumors [53]. Thus, this data may indicate that the radiosensitizing effect of fisetin in breast cancer cells is dependent on the TNBC status, *i.e.,* the expression of HER2, estrogen and progesterone receptors. Radiation induces autophagy in breast cancer cells [54] however contradictory results exist in terms of the effect of autophagy on post-irradiation cell survival. It has been shown that the inhibition of autophagy by pharmacological inhibitors radiosensitizes breast cancer cells, liver cancer cells and esophageal squamous cell carcinomas [54–56]. In contrast, a genetic knockdown of ATG5 and Beclin 1 was shown to mediate radioresistance in prostate cancer cells [57]. The differential effect of fisetin on autophagy has been reported as well. The induction of autophagy by fisetin was described in pancreatic cancer cells [58], whereas fisetin inhibited autophagy in hepatocellular carcinoma HepG2 cells [19]. Independent of the function of autophagy in post-irradiation cell survival, as well as the effect of fisetin on autophagy induction, in the present study we could show that fisetin in combination with radiation does not change autophagy levels when compared to radiation alone.

Conclusion

The application of fisetin may improve the radiotherapy outcome of TNBC patients through interference with signaling pathways involved in DSB repair (Fig. 8C) and consequently mitotic catastrophe.

Abbreviations

A-NHEJ: Alternative non-homologous end joining; BID: BI-D1870; C-NHEJ: Classical non-homologous end joining; CSD: Cold-shock domain; DDR: DNA damage response; DE: Differential expression; DSB: Double-strand breaks; ER: Estrogen receptor; GFP: Green fluorescence protein; GO: Gene ontology; Gy: Grey; HR: Homologous recombination; IR: Ionizing radiation; LJI: LJI308; PE: Plating efficiency; PR: Progesterone receptor; SF: Survival fraction; SILAC: Stable Isotope Labeling by Amino Acids in Cell Culture; TA: Triamcinolonacetonid; TNBC: Triple-negative breast cancer; YB-1: Y-box binding protein-1.

Supplementary Information

The online version contains supplementary material available at https://doi.org/10.1186/s13046-022-02442-x.

Additional file 1: Table S1. The GO indicating modified gene products involved in DSB repair.

Additional file 2: Table S2. Mutation status on KRAS , HRAS, PTEN and TP53 in the TNBC cell lines under study.

Additional file 3: Fig. S1 The pattern of expression of the estrogen-, progesterone- and HER2 receptors, as well as the activation status of YB-1, AKT and RSK in the indicated cell lines under study. **Fig. S2** The radiosensitizing effect of fisetin in combination with single dose irradiation. **Fig. S3** Frequency of DSB induction after fisetin, IR and the combination of fisetin and ITR. **Fig. S4** Heat map, gene ontology and pathway analysis of phosphosites in MDA-MB-468 cells. **Fig. S5** Gene ontology analysis of MDA-MB-231 after pretreatment with fisetin.

Acknowledgements
We thank Nikan Toulany, Medical Faculty University Hospital Tuebingen, Tuebingen, Germany for assisting in the analysis of γH2AX-foci; Paula Rahm, B.Sc. University of Ottawa, Canada for proofreading the manuscript; Dr. Christial Gille and Dr. Marco Ginzel, Department of Neonatology, University Children's Hospital Tuebingen, Tuebingen, Germany for assisting in FACS experiments and Dr. André Koch, Department of Gynecology and Obstetrics, Research Centre for Women's Health, University Hospital Tuebingen, Tuebingen, Germany, for providing MDA-MB-468, HS 578T and T47D cell lines. We acknowledge support by Open Access Publishing Fund of University of Tübingen.

Authors' contributions
SK performed the experiments, analyzed and interpreted data, prepared figures and wrote the manuscript. KL, and SV performed experiments and helped with the figures preparation. SR performed experiments. MFW and BM performed phosphoprotemic study and interpreted the data. FB performed bioinformatics data analysis and edited the manuscript. TJ and LVD performed 3 color fluorescence in situ hybridization analysis, interpreted the data and prepared the figure to that. GI and DZ provided material and conceptual support. MT supervised the project, conceptualized the research, analyzed and interpreted data, wrote, reviewed and edited the manuscript. The authors read and approved the final manuscript.

Funding
Open Access funding enabled and organized by Projekt DEAL. This research was supported by a grant from the German Research Council (DFG, Deutsche Forschungsgemeinschaft) (TO 685/2–3).

Availability of data and materials
All data in our study are available upon request.

Declarations

Ethics approval and consent to participate
Not applicable.

Consent for publication
All authors have given their consent for publication.

Competing interests
The authors declare no competing financial interests.

Author details
[1]Division of Radiobiology and Molecular Environmental Research, Department of Radiation Oncology, University of Tuebingen, Roentgenweg 11, 72076 Tuebingen, Germany. [2]German Cancer Consortium (DKTK), partner site Tuebingen, German Cancer Research Center (DKFZ), Heidelberg, Germany. [3]Quantitative Biology Center (QBiC), University of Tuebingen, Auf der Morgenstelle 10, 72076 Tuebingen, Germany. [4]Department of Radiation Oncology, Universitätsklinikum Erlangen, Friedrich-Alexander-Universität Erlangen-Nürnberg, Erlangen, Germany. [5]Comprehensive Cancer Center Erlangen-EMN (CCC ER-EMN), Universitätsklinikum Erlangen, Friedrich-Alexander-Universität Erlangen-Nürnberg, Erlangen, Germany. [6]Proteome Center Tuebingen, University of Tuebingen, Tuebingen, Germany. [7]Divison of Experimental Radiation Oncology, Department of Radiation Oncology, Institutsgruppe 1, Bauteil A, 4.038, University of Duisburg-Essen, Hufelandstr. 55, 45122 Essen, Germany.

Received: 25 April 2022 Accepted: 18 July 2022
Published online: 22 August 2022

References

1. He MY, Rancoule C, Rehailia-Blanchard A, Espenel S, Trone JC, Bernichon E, Guillaume E, Vallard A, Magne N. Radiotherapy in triple-negative breast cancer: Current situation and upcoming strategies. Crit Rev Oncol Hematol. 2018;131:96–101.
2. Xu Y, Wu Y, Zhang S, Ma P, Jin X, Wang Z, Yao M, Zhang E, Tao B, Qin Y, et al. A Tumor-Specific Super-Enhancer Drives Immune Evasion by Guiding Synchronous Expression of PD-L1 and PD-L2. Cell Rep. 2019;29(11):3435-3447.e3434.
3. Lasham A, Print Cristin G, Woolley Adele G, Dunn Sandra E, Braithwaite Antony W. YB-1: oncoprotein, prognostic marker and therapeutic target? Biochem J. 2012;449(1):11–23.
4. Hanahan D, Weinberg Robert A. Hallmarks of Cancer: The Next Generation. Cell. 2011;144(5):646–74.
5. Toulany M, Schickfluß T-A, Eicheler W, Kehlbach R, Schittek B, Rodemann HP. Impact of oncogenic K-RASon YB-1 phosphorylation induced by ionizing radiation. Breast Cancer Res. 2011;13(2):R28.
6. Lettau K, Zips D, Toulany M. Simultaneous Targeting of RSK and AKT Efficiently Inhibits YB-1-Mediated Repair of Ionizing Radiation-Induced DNA Double-Strand Breaks in Breast Cancer Cells. Int J Radiat Oncol Biol Phys. 2021;109(2):567–80.
7. Bansal T, Tanveer N, Singh UR, Sharma S, Kaur N. Y-Box binding protein 1 expression in breast cancer and its correlation with hormone receptors and other prognostic markers. J Lab Physicians. 2018;10(4):420–5.
8. Kolk A, Jubitz N, Mengele K, Mantwill K, Bissinger O, Schmitt M, Kremer M, Holm PS. Expression of Y-box-binding protein YB-1 allows stratification into long- and short-term survivors of head and neck cancer patients. Br J Cancer. 2011;105(12):1864–73.
9. Fujiwara-Okada Y, Matsumoto Y, Fukushi J, Setsu N, Matsuura S, Kamura S, Fujiwara T, Iida K, Hatano M, Nabeshima A, et al. Y-box binding protein-1 regulates cell proliferation and is associated with clinical outcomes of osteosarcoma. Br J Cancer. 2013;108(4):836–47.
10. Zhang Y, Reng SR, Wang L, Lu L, Zhao ZH, Zhang ZK, Feng XD, Ding XD, Wang J, Feng G, et al. Overexpression of Y-box binding protein-1 in cervical cancer and its association with the pathological response rate to chemoradiotherapy. Med Oncol. 2012;29(3):1992–7.
11. D'Costa NM, Lowerison MR, Raven PA, Tan Z, Roberts ME, Shrestha R, Urban MW, Monjaras-Avila CU, Oo HZ, Hurtado-Coll A, et al. Y-box binding protein-1 is crucial in acquired drug resistance development in metastatic clear-cell renal cell carcinoma. J Exp Clin Cancer Res. 2020;39(1):33.
12. Tay WL, Yip GWC, Tan PH, Matsumoto K, Yeo R, Ng TP, Kumar SD, Tsujimoto M, Bay BH. Y-Box-binding protein-1 is a promising predictive marker of radioresistance and chemoradioresistance in nasopharyngeal cancer. Mod Pathol. 2009;22(2):282–90.
13. Gaudreault I, Guay D, Lebel M. YB-1 promotes strand separation in vitro of duplex DNA containing either mispaired bases or cisplatin modifications, exhibits endonucleolytic activities and binds several DNA repair proteins. Nucleic Acids Res. 2004;32(1):316–27.
14. Stratford AL, Fry CJ, Desilets C, Davies AH, Cho YY, Li Y, Dong Z, Berquin IM, Roux PP, Dunn SE. Y-box binding protein-1 serine 102 is a downstream target of p90 ribosomal S6 kinase in basal-like breast cancer cells. Breast Cancer Res. 2008;10(6):R99.
15. Khan N, Syed DN, Ahmad N, Mukhtar H. Fisetin: a dietary antioxidant for health promotion. Antioxid Redox Signal. 2013;19(2):151–62.
16. Sechi M, Lall RK, Afolabi SO, Singh A, Joshi DC, Chiu SY, Mukhtar H, Syed DN. Fisetin targets YB-1/RSK axis independent of its effect on ERK signaling: insights from in vitro and in vivo melanoma models. Sci Rep. 2018;8(1):15726.
17. Ding G, Xu X, Li D, Chen Y, Wang W, Ping D, Jia S, Cao L. Fisetin inhibits proliferation of pancreatic adenocarcinoma by inducing DNA damage via RFXAP/KDM4A-dependent histone H3K36 demethylation. Cell Death Dis. 2020;11(10):893.
18. Sun X, Ma X, Li Q, Yang Y, Xu X, Sun J, Yu M, Cao K, Yang L, Yang G, et al. Anticancer effects of fisetin on mammary carcinoma cells via regulation of the PI3K/Akt/mTOR pathway: In vitro and in vivo studies. Int J Mol Med. 2018;42(2):811–20.

19. Sundarraj K, Raghunath A, Panneerselvam L, Perumal E. Fisetin Inhibits Autophagy in HepG2 Cells via PI3K/Akt/mTOR and AMPK Pathway. Nutr Cancer. 2021;73(11-12):2502–14.
20. Gunn A, Stark JM. I-SceI-based assays to examine distinct repair outcomes of mammalian chromosomal double strand breaks. Methods Mol Biol. 2012;920:379–91.
21. Iida M, Brand TM, Campbell DA, Li C, Wheeler DL. Yes and Lyn play a role in nuclear translocation of the epidermal growth factor receptor. Oncogene. 2013;32(6):759–67.
22. Toulany M, Dittmann K, Baumann M, Rodemann HP. Radiosensitization of Ras-mutated human tumor cells in vitro by the specific EGF receptor antagonist BIBX1382BS. Radiother Oncol. 2005;74(2):117–29.
23. Toulany M, Kasten-Pisula U, Brammer I, Wang S, Chen J, Dittmann K, Baumann M, Dikomey E, Rodemann HP. Blockage of epidermal growth factor receptor-phosphatidylinositol 3-kinase-AKT signaling increases radiosensitivity of K-RAS mutated human tumor cells in vitro by affecting DNA repair. Clin Cancer Res. 2006;12(13):4119–26.
24. Lapytsko A, Kollarovic G, Ivanova L, Studencka M, Schaber J. FoCo: a simple and robust quantification algorithm of nuclear foci. BMC Bioinformatics. 2015;16:392–392.
25. Ulrike K, Markus H, Thomas H, Ellen H, Barbara S, Rainer F, Distel LV. NNRTI-based antiretroviral therapy may increase risk of radiation induced side effects in HIV-1-infected patients. Radiother Oncol. 2015;116(2):323–30.
26. Soutoglou E, Dorn JF, Sengupta K, Jasin M, Nussenzweig A, Ried T, Danuser G, Misteli T. Positional stability of single double-strand breaks in mammalian cells. Nat Cell Biol. 2007;9(6):675–82.
27. Toulany M, Kehlbach R, Florczak U, Sak A, Wang S, Chen J, Lobrich M, Rodemann HP. Targeting of AKT1 enhances radiation toxicity of human tumor cells by inhibiting DNA-PKcs-dependent DNA double-strand break repair. Mol Cancer Ther. 2008;7(7):1772–81.
28. Franz-Wachtel M, Eisler SA, Krug K, Wahl S, Carpy A, Nordheim A, Pfizenmaier K, Hausser A, Macek B. Global detection of protein kinase D-dependent phosphorylation events in nocodazole-treated human cells. Mol Cell Proteomics. 2012;11(5):160–70.
29. Zittlau KI, Lechado-Terradas A, Nalpas N, Geisler S, Kahle PJ, Macek B. Temporal Analysis of Protein Ubiquitylation and Phosphorylation During Parkin-Dependent Mitophagy. Mol Cell Proteomics. 2022;21(2):100191.
30. Rappsilber J, Mann M, Ishihama Y. Protocol for micro-purification, enrichment, pre-fractionation and storage of peptides for proteomics using StageTips. Nat Protoc. 2007;2(8):1896–906. PMID: 17703201.
31. Bekker-Jensen DB, Martínez-Val A, Steigerwald S, Rüther P, Fort KL, Arrey TN, Harder A, Makarov A, Olsen JV. A Compact Quadrupole-Orbitrap Mass Spectrometer with FAIMS Interface Improves Proteome Coverage in Short LC Gradients. Mol Cell Proteomics. 2020;19(4):716–29.
32. Cox J, Mann M. MaxQuant enables high peptide identification rates, individualized p.p.b.-range mass accuracies and proteome-wide protein quantification. Nat Biotechnol. 2008;26(12):1367–72. PMID: 19029910.
33. Cox J, Neuhauser N, Michalski A, Scheltema RA, Olsen JV, Mann M. J. Andromeda: a peptide search engine integrated into the MaxQuant environment. Proteome Res. 2011;10(4):1794–805. PMID: 21254760.
34. Elias JE, Gygi SP. Target-decoy search strategy for increased confidence in large-scale protein identifications by mass spectrometry. Nat Methods. 2007;4(3):207–14. PMID: 17327847.
35. Maier E, Attenberger F, Tiwari A, Lettau K, Rebholz S, Fehrenbacher B, Schaller M, Gani C, Toulany M. Dual Targeting of Y-Box Binding Protein-1 and Akt Inhibits Proliferation and Enhances the Chemosensitivity of Colorectal Cancer Cells. Cancers (Basel). 2019;11(4):562.
36. Tiwari A, Iida M, Kosnopfel C, Abbariki M, Menegakis A, Fehrenbacher B, Maier J, Schaller M, Brucker SY, Wheeler DL, et al. Blocking Y-Box Binding Protein-1 through Simultaneous Targeting of PI3K and MAPK in Triple Negative Breast Cancers. Cancers (Basel). 2020;12(10):2795.
37. Aronchik I, Appleton BA, Basham SE, Crawford K, Del Rosario M, Doyle LV, Estacio WF, Lan J, Lindvall MK, Luu CA, et al. Novel potent and selective inhibitors of p90 ribosomal S6 kinase reveal the heterogeneity of RSK function in MAPK-driven cancers. Mol Cancer Res. 2014;12(5):803–12.
38. Lettau K, Khozooei S, Kosnopfel C, Zips D, Schittek B, Toulany M. Targeting the Y-box Binding Protein-1 Axis to Overcome Radiochemotherapy Resistance in Solid Tumors. Int J Radiat Oncol Biol Phys. 2021;111(4):1072–87.
39. Toulany M, Lee KJ, Fattah KR, Lin YF, Fehrenbacher B, Schaller M, Chen BP, Chen DJ, Rodemann HP. Akt promotes post-irradiation survival of human tumor cells through initiation, progression, and termination of DNA-PKcs-dependent DNA double-strand break repair. Mol Cancer Res. 2012;10(7):945–57.
40. Toulany M, Rodemann HP. Phosphatidylinositol 3-kinase/Akt signaling as a key mediator of tumor cell responsiveness to radiation. Semin Cancer Biol. 2015;35:180–90.
41. Jang K, Kim M, Seo HS, Shin I. PTEN sensitizes MDA-MB-468 cells to inhibition of MEK/Erk signaling for the blockade of cell proliferation. Oncol Rep. 2010;24(3):787–93.
42. Piao MJ, Kim KC, Chae S, Keum YS, Kim HS, Hyun JW. Protective Effect of Fisetin (3,7,3',4'-Tetrahydroxyflavone) against gamma-Irradiation-Induced Oxidative Stress and Cell Damage. Biomol Ther (Seoul). 2013;21(3):210–5.
43. Kim JY, Jeon YK, Jeon W, Nam MJ. Fisetin induces apoptosis in Huh-7 cells via downregulation of BIRC8 and Bcl2L2. Food Chem Toxicol. 2010;48(8–9):2259–64.
44. Sabarwal A, Agarwal R, Singh RP. Fisetin inhibits cellular proliferation and induces mitochondria-dependent apoptosis in human gastric cancer cells. Mol Carcinog. 2017;56(2):499–514.
45. Xiao Y, Liu Y, Gao Z, Li X, Weng M, Shi C, Wang C, Sun L. Fisetin inhibits the proliferation, migration and invasion of pancreatic cancer by targeting PI3K/AKT/mTOR signaling. Aging (Albany NY). 2021;13(22):24753–67.
46. Toulany M, Baumann M, Rodemann HP. Stimulated PI3K-AKT signaling mediated through ligand or radiation-induced EGFR depends indirectly, but not directly, on constitutive K-Ras activity. Mol Cancer Res. 2007;5(8):863–72.
47. Huang C, Zhou S, Zhang C, Jin Y, Xu G, Zhou L, Ding G, Pang T, Jia S, Cao L. ZC3H13-mediated N6-methyladenosine modification of PHF10 is impaired by fisetin which inhibits the DNA damage response in pancreatic cancer. Cancer Lett. 2022;530:16–28.
48. Smith EA, Gole B, Willis NA, Soria R, Starnes LM, Krumpelbeck EF, Jegga AG, Ali AM, Guo H, Meetei AR, et al. DEK is required for homologous recombination repair of DNA breaks. Sci Rep. 2017;7:44662.
49. Kawamura K, Qi F, Meng Q, Hayashi I, Kobayashi J. Nucleolar protein nucleolin functions in replication stress-induced DNA damage responses. J Radiat Res. 2019;60(3):281–8.
50. Chou WC, Wang HC, Wong FH, Ding SL, Wu PE, Shieh SY, Shen CY. Chk2-dependent phosphorylation of XRCC1 in the DNA damage response promotes base excision repair. EMBO J. 2008;27(23):3140–50.
51. de Campos-Nebel M, Larripa I, Gonzalez-Cid M. Topoisomerase II-mediated DNA damage is differently repaired during the cell cycle by non-homologous end joining and homologous recombination. PLoS One. 2010;5(9):e12541.
52. Chen WS, Lee YJ, Yu YC, Hsaio CH, Yen JH, Yu SH, Tsai YJ, Chiu SJ. Enhancement of P53-Mutant Human Colorectal Cancer Cells Radiosensitivity by Flavonoid Fisetin. Int J Radiat Oncol Biol Phys. 2010;77(5):1527–35.
53. Leu JD, Wang BS, Chiu SJ, Chang CY, Chen CC, Chen FD, Avirmed S, Lee YJ. Combining fisetin and ionizing radiation suppresses the growth of mammalian colorectal cancers in xenograft tumor models. Oncol Lett. 2016;12(6):4975–82.
54. Chaachouay H, Ohneseit P, Toulany M, Kehlbach R, Multhoff G, Rodemann HP. Autophagy contributes to resistance of tumor cells to ionizing radiation. Radiother Oncol. 2011;99(3):287–92.
55. Chen YS, Song HX, Lu Y, Li X, Chen T, Zhang Y, Xue JX, Liu H, Kan B, Yang G, et al. Autophagy inhibition contributes to radiation sensitization of esophageal squamous carcinoma cells. Dis Esophagus. 2011;24(6):437–43.
56. Tseng HC, Liu WS, Tyan YS, Chiang HC, Kuo WH, Chou FP. Sensitizing effect of 3-methyladenine on radiation-induced cytotoxicity in radioresistant HepG2 cells in vitro and in tumor xenografts. Chem Biol Interact. 2011;192(3):201–8.

57. Cao C, Subhawong T, Albert JM, Kim KW, Geng L, Sekhar KR, Gi YJ, Lu B. Inhibition of mammalian target of rapamycin or apoptotic pathway induces autophagy and radiosensitizes PTEN null prostate cancer cells. Cancer Res. 2006;66(20):10040–7.
58. Jia S, Xu X, Zhou S, Chen Y, Ding G, Cao L. Fisetin induces autophagy in pancreatic cancer cells via endoplasmic reticulum stress- and mitochondrial stress-dependent pathways. Cell Death Dis. 2019;10(2):142.

Publisher's Note

table S1

Cluster 1 **Enriched phosphosites upregulation**

p_value	intersectio	term_id	source	term_name
0.000180446	19	GO:0016071	GO:BP	mRNA metabolic process
0.000511117	14	GO:0006397	GO:BP	mRNA processing
0.000511117	19	GO:0016032	GO:BP	viral process
0.00297448	7	GO:0007266	GO:BP	Rho protein signal transduction
0.00297448	17	GO:1903047	GO:BP	mitotic cell cycle process
0.004094478	10	GO:0007265	GO:BP	Ras protein signal transduction
0.004094478	10	GO:0006913	GO:BP	nucleocytoplasmic transport
0.004094478	10	GO:0051169	GO:BP	nuclear transport
0.00420302	26	GO:0033554	GO:BP	cellular response to stress
0.005101079	3	GO:0045657	GO:BP	positive regulation of monocyte differentiation
0.005707275	10	GO:1903311	GO:BP	regulation of mRNA metabolic process
0.005763146	8	GO:0019080	GO:BP	viral gene expression
0.006404935	17	GO:0000278	GO:BP	mitotic cell cycle
0.006743806	4	GO:0030224	GO:BP	monocyte differentiation
0.006743806	20	GO:0007010	GO:BP	cytoskeleton organization
0.008999052	11	GO:0007264	GO:BP	small GTPase mediated signal transduction
0.008999052	3	GO:2001224	GO:BP	positive regulation of neuron migration
0.008999052	44	GO:0048523	GO:BP	negative regulation of cellular process
0.008999052	5	GO:0006970	GO:BP	response to osmotic stress
0.009584774	2	GO:0060327	GO:BP	cytoplasmic actin-based contraction involved in cell motility
0.011473659	6	GO:0050684	GO:BP	regulation of mRNA processing
0.013095388	21	GO:0046907	GO:BP	intracellular transport
0.013095388	6	GO:0051028	GO:BP	mRNA transport
0.013358335	22	GO:0007049	GO:BP	cell cycle
0.013419969	6	GO:0006606	GO:BP	protein import into nucleus
0.015683597	15	GO:0006396	GO:BP	RNA processing
0.016026322	46	GO:0006139	GO:BP	nucleobase-containing compound metabolic process
0.016026322	3	GO:0045655	GO:BP	regulation of monocyte differentiation
0.016026322	7	GO:0032869	GO:BP	cellular response to insulin stimulus
0.016026322	47	GO:0046483	GO:BP	heterocycle metabolic process
0.016026322	18	GO:0022402	GO:BP	cell cycle process
0.017002407	13	GO:0030029	GO:BP	actin filament-based process
0.017002407	5	GO:0006275	GO:BP	regulation of DNA replication
0.017489487	7	GO:0015931	GO:BP	nucleobase-containing compound transport
0.017489487	5	GO:0006406	GO:BP	mRNA export from nucleus
0.017489487	5	GO:0071427	GO:BP	mRNA-containing ribonucleoprotein complex export from nucleus
0.017489487	6	GO:0051170	GO:BP	import into nucleus
0.017489487	47	GO:0006725	GO:BP	cellular aromatic compound metabolic process
0.020591715	46	GO:0048519	GO:BP	negative regulation of biological process
0.020814213	6	GO:0050657	GO:BP	nucleic acid transport
0.020814213	6	GO:0050658	GO:BP	RNA transport
0.020951169	5	GO:0060147	GO:BP	regulation of posttranscriptional gene silencing
0.02115331	6	GO:0051236	GO:BP	establishment of RNA localization
0.02115331	5	GO:0060966	GO:BP	regulation of gene silencing by RNA
0.023170942	9	GO:0008380	GO:BP	RNA splicing
0.023170942	6	GO:0007052	GO:BP	mitotic spindle organization
0.023170942	11	GO:0000226	GO:BP	microtubule cytoskeleton organization
0.023170942	19	GO:0019220	GO:BP	regulation of phosphate metabolic process
0.023170942	8	GO:0000375	GO:BP	RNA splicing, via transesterification reactions
0.023170942	8	GO:0000377	GO:BP	RNA splicing, via transesterification reactions with bulged adenosine as nucleophile
0.023170942	8	GO:0000398	GO:BP	mRNA splicing, via spliceosome
0.023170942	5	GO:0006405	GO:BP	RNA export from nucleus
0.023170942	2	GO:0016479	GO:BP	negative regulation of transcription by RNA polymerase I
0.023170942	5	GO:0071166	GO:BP	ribonucleoprotein complex localization
0.023170942	16	GO:0051336	GO:BP	regulation of hydrolase activity
0.023170942	19	GO:0051174	GO:BP	regulation of phosphorus metabolic process
0.023170942	42	GO:0090304	GO:BP	nucleic acid metabolic process
0.023170942	8	GO:0032386	GO:BP	regulation of intracellular transport
0.023170942	5	GO:0071426	GO:BP	ribonucleoprotein complex export from nucleus
0.023238408	13	GO:0006974	GO:BP	cellular response to DNA damage stimulus
0.023238408	3	GO:0038128	GO:BP	ERBB2 signaling pathway
0.023238408	6	GO:0051168	GO:BP	nuclear export
0.026581021	4	GO:0016925	GO:BP	protein sumoylation
0.026642234	47	GO:1901360	GO:BP	organic cyclic compound metabolic process
0.026642234	5	GO:0060968	GO:BP	regulation of gene silencing
0.027783052	7	GO:0032868	GO:BP	response to insulin
0.028243078	6	GO:1902850	GO:BP	microtubule cytoskeleton organization involved in mitosis
0.028243078	10	GO:0006281	GO:BP	DNA repair
0.028243078	8	GO:0019058	GO:BP	viral life cycle

0.028434248	13	GO:0007017	GO:BP	microtubule-based process
0.02884127	29	GO:0065009	GO:BP	regulation of molecular function
0.029765128	31	GO:0051641	GO:BP	cellular localization
0.030099528	6	GO:0017038	GO:BP	protein import
0.030991025	11	GO:0030036	GO:BP	actin cytoskeleton organization
0.030991025	5	GO:0006997	GO:BP	nucleus organization
0.030991025	6	GO:0006403	GO:BP	RNA localization
0.030991025	24	GO:0050790	GO:BP	regulation of catalytic activity
0.030991025	4	GO:0035023	GO:BP	regulation of Rho protein signal transduction
0.032267839	3	GO:0045740	GO:BP	positive regulation of DNA replication
0.032452809	5	GO:0030048	GO:BP	actin filament-based movement
0.03303235	14	GO:0009894	GO:BP	regulation of catabolic process
0.03303235	3	GO:0071276	GO:BP	cellular response to cadmium ion
0.03303235	26	GO:0051649	GO:BP	establishment of localization in cell
0.03303235	8	GO:1901653	GO:BP	cellular response to peptide
0.035787051	16	GO:0051094	GO:BP	positive regulation of developmental process
0.037533657	48	GO:0034641	GO:BP	cellular nitrogen compound metabolic process
0.037533657	19	GO:0044093	GO:BP	positive regulation of molecular function
0.039040916	26	GO:0071310	GO:BP	cellular response to organic substance
0.040754602	3	GO:2001222	GO:BP	regulation of neuron migration
0.041194753	5	GO:0061572	GO:BP	actin filament bundle organization
0.041194753	4	GO:0019886	GO:BP	antigen processing and presentation of exogenous peptide antigen via MHC class II
0.041194753	34	GO:0006996	GO:BP	organelle organization
0.043547952	6	GO:0043488	GO:BP	regulation of mRNA stability
0.043547952	2	GO:0090557	GO:BP	establishment of endothelial intestinal barrier
0.043918283	7	GO:0071375	GO:BP	cellular response to peptide hormone stimulus
0.043918283	15	GO:0009628	GO:BP	response to abiotic stimulus
0.043918283	7	GO:0006260	GO:BP	DNA replication
0.044764395	4	GO:0002495	GO:BP	antigen processing and presentation of peptide antigen via MHC class II
0.045006088	48	GO:0016043	GO:BP	cellular component organization
0.046073642	26	GO:0035556	GO:BP	intracellular signal transduction
0.046073642	8	GO:0007015	GO:BP	actin filament organization
0.046073642	6	GO:0061013	GO:BP	regulation of mRNA catabolic process
0.046073642	6	GO:0007051	GO:BP	spindle organization
0.046073642	4	GO:0002504	GO:BP	antigen processing and presentation of peptide or polysaccharide antigen via MHC class II
0.046073642	2	GO:0002566	GO:BP	somatic diversification of immune receptors via somatic mutation
0.046073642	4	GO:0031124	GO:BP	mRNA 3'-end processing
0.048333614	6	GO:0043487	GO:BP	regulation of RNA stability
0.049659881	8	GO:1901990	GO:BP	regulation of mitotic cell cycle phase transition
0.049710058	4	GO:0048024	GO:BP	regulation of mRNA splicing, via spliceosome
3.52E-06	53	GO:0005829	GO:CC	cytosol
6.00E-06	18	GO:0099513	GO:CC	polymeric cytoskeletal fiber
2.02E-05	62	GO:0005634	GO:CC	nucleus
2.02E-05	91	GO:0005622	GO:CC	intracellular anatomical structure
2.02E-05	19	GO:0099512	GO:CC	supramolecular fiber
2.02E-05	22	GO:0099080	GO:CC	supramolecular complex
2.02E-05	19	GO:0099081	GO:CC	supramolecular polymer
0.000147372	16	GO:0070161	GO:CC	anchoring junction
0.000211611	28	GO:0005856	GO:CC	cytoskeleton
0.000217435	12	GO:0005911	GO:CC	cell-cell junction
0.000319707	11	GO:0005874	GO:CC	microtubule
0.000319707	45	GO:0043228	GO:CC	non-membrane-bounded organelle
0.000322048	41	GO:0031981	GO:CC	nuclear lumen
0.000322048	39	GO:0005654	GO:CC	nucleoplasm
0.000364774	14	GO:0048471	GO:CC	perinuclear region of cytoplasm
0.000364774	7	GO:0005875	GO:CC	microtubule associated complex
0.000364774	86	GO:0043226	GO:CC	organelle
0.000515617	44	GO:0043232	GO:CC	intracellular non-membrane-bounded organelle
0.000687159	82	GO:0043229	GO:CC	intracellular organelle
0.000756863	5	GO:0032432	GO:CC	actin filament bundle
0.002040834	8	GO:0031965	GO:CC	nuclear membrane
0.002040834	3	GO:0035145	GO:CC	exon-exon junction complex
0.002352466	81	GO:0043227	GO:CC	membrane-bounded organelle
0.002979127	6	GO:0005912	GO:CC	adherens junction
0.002979127	9	GO:0016607	GO:CC	nuclear speck
0.003268316	44	GO:0070013	GO:CC	intracellular organelle lumen
0.003268316	44	GO:0043233	GO:CC	organelle lumen
0.003268316	44	GO:0031974	GO:CC	membrane-enclosed lumen
0.003268316	10	GO:0015629	GO:CC	actin cytoskeleton
0.004628163	4	GO:0097517	GO:CC	contractile actin filament bundle
0.004628163	4	GO:0001725	GO:CC	stress fiber
0.005741579	22	GO:0030054	GO:CC	cell junction
0.005888994	9	GO:0005635	GO:CC	nuclear envelope

0.006684073	4	GO:0042641	GO:CC	actomyosin
0.01089827	74	GO:0043231	GO:CC	intracellular membrane-bounded organelle
0.015834227	10	GO:0030424	GO:CC	axon
0.01868173	15	GO:0015630	GO:CC	microtubule cytoskeleton
0.019097421	41	GO:0032991	GO:CC	protein-containing complex
0.022277989	2	GO:0099092	GO:CC	postsynaptic density, intracellular component
0.023405452	12	GO:0005730	GO:CC	nucleolus
0.024269511	14	GO:0140513	GO:CC	nuclear protein-containing complex
0.024269511	4	GO:0005884	GO:CC	actin filament
0.024269511	3	GO:0043657	GO:CC	host cell
0.024269511	3	GO:0018995	GO:CC	host cellular component
0.027258468	72	GO:0005737	GO:CC	cytoplasm
0.02972019	2	GO:0099091	GO:CC	postsynaptic specialization, intracellular component
0.02972019	4	GO:0030018	GO:CC	Z disc
0.034502938	1	GO:0097489	GO:CC	multivesicular body, internal vesicle lumen
0.034502938	2	GO:0005868	GO:CC	cytoplasmic dynein complex
0.034502938	7	GO:0005925	GO:CC	focal adhesion
0.034502938	1	GO:0016938	GO:CC	kinesin I complex
0.035694718	4	GO:0031674	GO:CC	I band
0.035694718	7	GO:0030055	GO:CC	cell-substrate junction
0.039563811	4	GO:0043296	GO:CC	apical junction complex
0.043704954	2	GO:0030057	GO:CC	desmosome
0.045267414	10	GO:0016604	GO:CC	nuclear body
2.54E-06	31	GO:0003723	GO:MF	RNA binding
2.97E-05	12	GO:0045296	GO:MF	cadherin binding
7.78E-05	44	GO:0003676	GO:MF	nucleic acid binding
7.78E-05	14	GO:0050839	GO:MF	cell adhesion molecule binding
0.000186227	93	GO:0005515	GO:MF	protein binding
0.0021403	25	GO:0019899	GO:MF	enzyme binding
0.002969474	16	GO:0008092	GO:MF	cytoskeletal protein binding
0.006984406	50	GO:1901363	GO:MF	heterocyclic compound binding
0.007998595	50	GO:0097159	GO:MF	organic cyclic compound binding
0.007998595	16	GO:0098772	GO:MF	molecular function regulator
0.018982513	9	GO:0003779	GO:MF	actin binding
0.019265637	3	GO:0071889	GO:MF	14-3-3 protein binding
0.024980835	13	GO:0030234	GO:MF	enzyme regulator activity
0.027460148	3	GO:0043531	GO:MF	ADP binding
0.03679647	3	GO:0019894	GO:MF	kinesin binding
0.038244415	96	GO:0005488	GO:MF	binding
0.000611345	8	KEGG:03013	KEGG	RNA transport
0.032815165	4	KEGG:04012	KEGG	ErbB signaling pathway
0.032815165	4	KEGG:05210	KEGG	Colorectal cancer
0.032815165	6	KEGG:04510	KEGG	Focal adhesion
0.032815165	6	KEGG:05205	KEGG	Proteoglycans in cancer
0.041680853	6	KEGG:05132	KEGG	Salmonella infection
0.041680853	4	KEGG:03015	KEGG	mRNA surveillance pathway
0.008324969	3	REAC:R-HSA-9	REAC	Signaling by ERBB2 ECD mutants
0.008324969	3	REAC:R-HSA-5	REAC	Constitutive Signaling by EGFRvIII
0.008324969	3	REAC:R-HSA-5	REAC	Signaling by EGFRvIII in Cancer
0.008324969	7	REAC:R-HSA-9	REAC	HCMV Infection
0.008950406	3	REAC:R-HSA-5	REAC	Signaling by Ligand-Responsive EGFR Variants in Cancer
0.008950406	3	REAC:R-HSA-1	REAC	Constitutive Signaling by Ligand-Responsive EGFR Cancer Variants
0.008950406	6	REAC:R-HSA-9	REAC	HCMV Early Events
0.014779479	3	REAC:R-HSA-9	REAC	Signaling by ERBB2 KD Mutants
0.015149541	3	REAC:R-HSA-1	REAC	Signaling by ERBB2 in Cancer
0.01561579	3	REAC:R-HSA-1	REAC	Signaling by EGFR in Cancer
0.022223142	20	REAC:R-HSA-1	REAC	Disease
0.027479275	9	REAC:R-HSA-1	REAC	Signaling by Rho GTPases
0.027479275	2	REAC:R-HSA-5	REAC	Signaling by FGFR4 in disease
0.027479275	4	REAC:R-HSA-1	REAC	Antiviral mechanism by IFN-stimulated genes
0.027479275	2	REAC:R-HSA-8	REAC	Signaling by FGFR3 fusions in cancer
0.027479275	4	REAC:R-HSA-7	REAC	Transport of Mature Transcript to Cytoplasm
0.027479275	6	REAC:R-HSA-9	REAC	Interferon Signaling
0.027479275	2	REAC:R-HSA-2	REAC	EGFR Transactivation by Gastrin
0.027479275	3	REAC:R-HSA-4	REAC	SUMOylation of SUMOylation proteins
0.027479275	9	REAC:R-HSA-9	REAC	Signaling by Rho GTPases, Miro GTPases and RHOBTB3
0.027479275	3	REAC:R-HSA-3	REAC	SUMOylation of ubiquitinylation proteins
0.027479275	4	REAC:R-HSA-1	REAC	Transport of Mature mRNA derived from an Intron-Containing Transcript
0.036639123	3	REAC:R-HSA-3	REAC	SUMOylation of transcription cofactors
0.036639123	13	REAC:R-HSA-5	REAC	Infectious disease
0.036656095	2	REAC:R-HSA-1	REAC	GRB2 events in EGFR signaling
0.037144357	3	REAC:R-HSA-4	REAC	SUMOylation of RNA binding proteins
0.037144357	3	REAC:R-HSA-4	REAC	SUMOylation of DNA replication proteins

0.039129446	2	REAC:R-HSA-1 REAC	SHC1 events in EGFR signaling
0.040513845	2	REAC:R-HSA-1 REAC	PI3K events in ERBB2 signaling
0.040513845	3	REAC:R-HSA-1 REAC	Signaling by ERBB2
0.040513845	2	REAC:R-HSA-1 REAC	GRB2 events in ERBB2 signaling
0.040513845	3	REAC:R-HSA-2 REAC	Nuclear Envelope Breakdown
0.041735127	3	REAC:R-HSA-1 REAC	Signaling by EGFR
0.044632777	5	REAC:R-HSA-3 REAC	SUMO E3 ligases SUMOylate target proteins

table S1

Cluster 2 **Enriched phosphosites downregulation**

p_value	intersectio	term_id	source	term_name
2.21E-11	37	GO:0016071	GO:BP	mRNA metabolic process
6.81E-11	83	GO:0006996	GO:BP	organelle organization
1.54E-09	109	GO:0071840	GO:BP	cellular component organization or biogenesis
6.03E-09	105	GO:0016043	GO:BP	cellular component organization
6.03E-09	49	GO:0007049	GO:BP	cell cycle
6.03E-09	22	GO:1903311	GO:BP	regulation of mRNA metabolic process
9.74E-09	21	GO:0000377	GO:BP	RNA splicing, via transesterification reactions with bulged adenosine as nucleophile
9.74E-09	21	GO:0000398	GO:BP	mRNA splicing, via spliceosome
1.01E-08	21	GO:0000375	GO:BP	RNA splicing, via transesterification reactions
1.14E-08	38	GO:0033043	GO:BP	regulation of organelle organization
1.45E-08	23	GO:0008380	GO:BP	RNA splicing
1.45E-08	33	GO:1903047	GO:BP	mitotic cell cycle process
2.06E-08	40	GO:0022402	GO:BP	cell cycle process
2.77E-08	67	GO:0044085	GO:BP	cellular component biogenesis
3.66E-08	24	GO:0006397	GO:BP	mRNA processing
4.81E-08	63	GO:0022607	GO:BP	cellular component assembly
7.11E-08	37	GO:0051276	GO:BP	chromosome organization
8.42E-08	34	GO:0000278	GO:BP	mitotic cell cycle
6.70E-07	31	GO:0006396	GO:BP	RNA processing
7.30E-07	91	GO:0048522	GO:BP	positive regulation of cellular process
1.99E-06	96	GO:0048518	GO:BP	positive regulation of biological process
3.49E-06	23	GO:0010638	GO:BP	positive regulation of organelle organization
4.07E-06	50	GO:0051128	GO:BP	regulation of cellular component organization
4.07E-06	21	GO:0051493	GO:BP	regulation of cytoskeleton organization
7.38E-06	55	GO:0035556	GO:BP	intracellular signal transduction
8.22E-06	10	GO:0048024	GO:BP	regulation of mRNA splicing, via spliceosome
8.22E-06	36	GO:0007010	GO:BP	cytoskeleton organization
1.25E-05	22	GO:0051301	GO:BP	cell division
1.42E-05	11	GO:0050684	GO:BP	regulation of mRNA processing
1.80E-05	31	GO:0051130	GO:BP	positive regulation of cellular component organization
1.80E-05	16	GO:0140014	GO:BP	mitotic nuclear division
2.09E-05	11	GO:0043484	GO:BP	regulation of RNA splicing
3.73E-05	27	GO:0006259	GO:BP	DNA metabolic process
3.92E-05	22	GO:0044770	GO:BP	cell cycle phase transition
4.42E-05	60	GO:0009892	GO:BP	negative regulation of metabolic process
4.42E-05	67	GO:0065008	GO:BP	regulation of biological quality
4.46E-05	29	GO:0051726	GO:BP	regulation of cell cycle
4.46E-05	79	GO:0090304	GO:BP	nucleic acid metabolic process
5.21E-05	13	GO:0043488	GO:BP	regulation of mRNA stability
5.86E-05	34	GO:0009057	GO:BP	macromolecule catabolic process
6.34E-05	16	GO:0006402	GO:BP	mRNA catabolic process
6.65E-05	13	GO:0061013	GO:BP	regulation of mRNA catabolic process
6.65E-05	19	GO:0048285	GO:BP	organelle fission
6.65E-05	25	GO:0006974	GO:BP	cellular response to DNA damage stimulus
6.67E-05	14	GO:0033044	GO:BP	regulation of chromosome organization
6.72E-05	35	GO:0045934	GO:BP	negative regulation of nucleobase-containing compound metabolic process
6.72E-05	18	GO:0000280	GO:BP	nuclear division
7.23E-05	13	GO:0043487	GO:BP	regulation of RNA stability
8.29E-05	15	GO:0007059	GO:BP	chromosome segregation
8.47E-05	77	GO:0048523	GO:BP	negative regulation of cellular process
8.58E-05	30	GO:0044265	GO:BP	cellular macromolecule catabolic process
8.58E-05	48	GO:0051172	GO:BP	negative regulation of nitrogen compound metabolic process
8.58E-05	10	GO:0010212	GO:BP	response to ionizing radiation
8.58E-05	56	GO:0010605	GO:BP	negative regulation of macromolecule metabolic process
9.00E-05	145	GO:0065007	GO:BP	biological regulation
0.000100961	135	GO:0050794	GO:BP	regulation of cellular process
0.000100961	26	GO:0044087	GO:BP	regulation of cellular component biogenesis
0.000104319	42	GO:0033554	GO:BP	cellular response to stress
0.000114471	11	GO:2001252	GO:BP	positive regulation of chromosome organization
0.000114471	11	GO:0042770	GO:BP	signal transduction in response to DNA damage
0.000119463	23	GO:0010564	GO:BP	regulation of cell cycle process
0.00013209	26	GO:0016032	GO:BP	viral process
0.000137048	27	GO:0009894	GO:BP	regulation of catabolic process
0.000137048	11	GO:0071478	GO:BP	cellular response to radiation
0.000137048	19	GO:0044772	GO:BP	mitotic cell cycle phase transition
0.000154997	16	GO:0006401	GO:BP	RNA catabolic process
0.000157299	82	GO:0006139	GO:BP	nucleobase-containing compound metabolic process
0.000158484	8	GO:1903312	GO:BP	negative regulation of mRNA metabolic process
0.000160573	139	GO:0050789	GO:BP	regulation of biological process
0.000160737	11	GO:0051168	GO:BP	nuclear export
0.000160814	83	GO:0048519	GO:BP	negative regulation of biological process
0.000169225	13	GO:0072331	GO:BP	signal transduction by p53 class mediator
0.000173659	14	GO:0006260	GO:BP	DNA replication
0.000181656	15	GO:0051052	GO:BP	regulation of DNA metabolic process
0.000190765	15	GO:1902903	GO:BP	regulation of supramolecular fiber organization
0.000191556	49	GO:0031324	GO:BP	negative regulation of cellular metabolic process
0.000207483	7	GO:0071479	GO:BP	cellular response to ionizing radiation
0.000243792	9	GO:0000077	GO:BP	DNA damage checkpoint signaling
0.000247481	11	GO:0000819	GO:BP	sister chromatid segregation
0.000247481	8	GO:0044773	GO:BP	mitotic DNA damage checkpoint signaling
0.00028418	14	GO:0051169	GO:BP	nuclear transport
0.000307257	16	GO:0009314	GO:BP	response to radiation
0.000307257	70	GO:0016070	GO:BP	RNA metabolic process
0.00030946	8	GO:0044774	GO:BP	mitotic DNA integrity checkpoint signaling

0.00030946	35	GO:0046907	GO:BP	intracellular transport
0.000310157	14	GO:0010639	GO:BP	negative regulation of organelle organization
0.000310157	17	GO:0007264	GO:BP	small GTPase mediated signal transduction
0.00032041	6	GO:0035196	GO:BP	production of miRNAs involved in gene silencing by miRNA
0.000340702	9	GO:0031570	GO:BP	DNA integrity checkpoint signaling
0.000372103	18	GO:0006281	GO:BP	DNA repair
0.000377554	5	GO:0050686	GO:BP	negative regulation of mRNA processing
0.000415449	82	GO:0046483	GO:BP	heterocycle metabolic process
0.000415449	85	GO:1901360	GO:BP	organic cyclic compound metabolic process
0.00041598	6	GO:0031050	GO:BP	dsRNA processing
0.00041598	6	GO:0070918	GO:BP	production of small RNA involved in gene silencing by RNA
0.000420843	13	GO:0009895	GO:BP	negative regulation of catabolic process
0.000435023	9	GO:0070507	GO:BP	regulation of microtubule cytoskeleton organization
0.000472121	17	GO:1901987	GO:BP	regulation of cell cycle phase transition
0.000472121	12	GO:0006302	GO:BP	double-strand break repair
0.000472121	23	GO:0031329	GO:BP	regulation of cellular catabolic process
0.000520975	82	GO:0006725	GO:BP	cellular aromatic compound metabolic process
0.00055633	10	GO:0000075	GO:BP	cell cycle checkpoint signaling
0.000594097	23	GO:0010608	GO:BP	posttranscriptional regulation of gene expression
0.000615777	9	GO:0007093	GO:BP	mitotic cell cycle checkpoint signaling
0.000635027	13	GO:0104004	GO:BP	cellular response to environmental stimulus
0.000635027	13	GO:0071214	GO:BP	cellular response to abiotic stimulus
0.000655643	11	GO:0032886	GO:BP	regulation of microtubule-based process
0.000673837	12	GO:0098813	GO:BP	nuclear chromosome segregation
0.000682661	17	GO:1903827	GO:BP	regulation of cellular protein localization
0.000682661	4	GO:0009299	GO:BP	mRNA transcription
0.000743374	59	GO:0051252	GO:BP	regulation of RNA metabolic process
0.000743374	7	GO:0071709	GO:BP	membrane assembly
0.000744935	62	GO:0019219	GO:BP	regulation of nucleobase-containing compound metabolic process
0.000797568	51	GO:0033036	GO:BP	macromolecule localization
0.000849637	30	GO:0051253	GO:BP	negative regulation of RNA metabolic process
0.000852009	33	GO:2000113	GO:BP	negative regulation of cellular macromolecule biosynthetic process
0.000852009	13	GO:0006913	GO:BP	nucleocytoplasmic transport
0.000958151	33	GO:0010558	GO:BP	negative regulation of macromolecule biosynthetic process
0.00097207	8	GO:0019079	GO:BP	viral genome replication
0.001007059	10	GO:1902850	GO:BP	microtubule cytoskeleton organization involved in mitosis
0.001017992	30	GO:0010629	GO:BP	negative regulation of gene expression
0.001033916	7	GO:0044091	GO:BP	membrane biogenesis
0.001041184	21	GO:0006325	GO:BP	chromatin organization
0.001057777	51	GO:0065009	GO:BP	regulation of molecular function
0.001057777	19	GO:0030036	GO:BP	actin cytoskeleton organization
0.001113581	36	GO:0045935	GO:BP	positive regulation of nucleobase-containing compound metabolic process
0.001139281	90	GO:0023052	GO:BP	signaling
0.001194117	10	GO:0007163	GO:BP	establishment or maintenance of cell polarity
0.001234902	55	GO:0010604	GO:BP	positive regulation of macromolecule metabolic process
0.001330879	4	GO:0048025	GO:BP	negative regulation of mRNA splicing, via spliceosome
0.001330879	42	GO:0050790	GO:BP	regulation of catalytic activity
0.001430273	15	GO:0045786	GO:BP	negative regulation of cell cycle
0.001483574	87	GO:0032502	GO:BP	developmental process
0.001695935	8	GO:1903313	GO:BP	positive regulation of mRNA metabolic process
0.001786082	20	GO:0030029	GO:BP	actin filament-based process
0.001808859	4	GO:0070920	GO:BP	regulation of production of small RNA involved in gene silencing by RNA
0.001808859	33	GO:0031327	GO:BP	negative regulation of cellular biosynthetic process
0.001808859	4	GO:1903798	GO:BP	regulation of production of miRNAs involved in gene silencing by miRNA
0.00182133	11	GO:0110053	GO:BP	regulation of actin filament organization
0.001969537	8	GO:0006997	GO:BP	nucleus organization
0.002003832	7	GO:0030330	GO:BP	DNA damage response, signal transduction by p53 class mediator
0.002010679	10	GO:0090068	GO:BP	positive regulation of cell cycle process
0.002053404	10	GO:0032271	GO:BP	regulation of protein polymerization
0.002053404	4	GO:0051220	GO:BP	cytoplasmic sequestering of protein
0.002203987	9	GO:0007052	GO:BP	mitotic spindle organization
0.002241121	14	GO:1901990	GO:BP	regulation of mitotic cell cycle phase transition
0.002284704	16	GO:0034655	GO:BP	nucleobase-containing compound catabolic process
0.002369796	55	GO:0023051	GO:BP	regulation of signaling
0.00237496	33	GO:0009890	GO:BP	negative regulation of biosynthetic process
0.002428976	8	GO:0031056	GO:BP	regulation of histone modification
0.002433354	14	GO:0043254	GO:BP	regulation of protein-containing complex assembly
0.002582028	26	GO:0009628	GO:BP	response to abiotic stimulus
0.002619717	4	GO:0033119	GO:BP	negative regulation of RNA splicing
0.002619717	32	GO:0065003	GO:BP	protein-containing complex assembly
0.002702484	9	GO:0051054	GO:BP	positive regulation of DNA metabolic process
0.002739234	12	GO:0007265	GO:BP	Ras protein signal transduction
0.002753057	6	GO:0032204	GO:BP	regulation of telomere maintenance
0.002753057	9	GO:1901796	GO:BP	regulation of signal transduction by p53 class mediator
0.002792143	53	GO:0051641	GO:BP	cellular localization
0.002884496	3	GO:0051574	GO:BP	positive regulation of histone H3-K9 methylation
0.002884496	3	GO:1903800	GO:BP	positive regulation of production of miRNAs involved in gene silencing by miRNA
0.002884496	4	GO:2000637	GO:BP	positive regulation of gene silencing by miRNA
0.00295174	97	GO:0051716	GO:BP	cellular response to stimulus
0.00295174	21	GO:0070925	GO:BP	organelle assembly
0.003113948	12	GO:0071103	GO:BP	DNA conformation change
0.003224297	5	GO:0031468	GO:BP	nuclear membrane reassembly
0.003224297	4	GO:0060148	GO:BP	positive regulation of posttranscriptional gene silencing
0.003248827	25	GO:0051248	GO:BP	negative regulation of protein metabolic process
0.003338049	17	GO:0000226	GO:BP	microtubule cytoskeleton organization
0.003434766	88	GO:0007154	GO:BP	cell communication
0.003505733	12	GO:0032956	GO:BP	regulation of actin cytoskeleton organization

0.003555012	10	GO:0000082	GO:BP	G1/S transition of mitotic cell cycle
0.0038754	15	GO:0044089	GO:BP	positive regulation of cellular component biogenesis
0.003912091	44	GO:0051649	GO:BP	establishment of localization in cell
0.003912091	10	GO:0031330	GO:BP	negative regulation of cellular catabolic process
0.003912091	35	GO:0043933	GO:BP	protein-containing complex subunit organization
0.003912091	32	GO:0051254	GO:BP	positive regulation of RNA metabolic process
0.003988357	11	GO:0045787	GO:BP	positive regulation of cell cycle
0.003992375	16	GO:0007346	GO:BP	regulation of mitotic cell cycle
0.004053072	11	GO:0045930	GO:BP	negative regulation of mitotic cell cycle
0.004256207	48	GO:0051173	GO:BP	positive regulation of nitrogen compound metabolic process
0.004304086	16	GO:0046700	GO:BP	heterocycle catabolic process
0.004329092	56	GO:0009893	GO:BP	positive regulation of metabolic process
0.004329092	3	GO:0071481	GO:BP	cellular response to X-ray
0.004720687	16	GO:0044270	GO:BP	cellular nitrogen compound catabolic process
0.004751708	9	GO:0006403	GO:BP	RNA localization
0.004805444	39	GO:0044248	GO:BP	cellular catabolic process
0.004805444	10	GO:0044839	GO:BP	cell cycle G2/M phase transition
0.004805444	4	GO:0010165	GO:BP	response to X-ray
0.004832298	6	GO:0031058	GO:BP	positive regulation of histone modification
0.005039412	13	GO:0051656	GO:BP	establishment of organelle localization
0.005039412	11	GO:1901988	GO:BP	negative regulation of cell cycle phase transition
0.005039412	2	GO:0150007	GO:BP	clathrin-dependent synaptic vesicle endocytosis
0.005039412	9	GO:2001020	GO:BP	regulation of response to DNA damage stimulus
0.005218505	13	GO:0007015	GO:BP	actin filament organization
0.005218505	22	GO:0000902	GO:BP	cell morphogenesis
0.005323234	82	GO:0007165	GO:BP	signal transduction
0.005553706	16	GO:0019439	GO:BP	aromatic compound catabolic process
0.005891484	79	GO:0048856	GO:BP	anatomical structure development
0.005891484	8	GO:0050658	GO:BP	RNA transport
0.005891484	8	GO:0050657	GO:BP	nucleic acid transport
0.005891484	20	GO:0032880	GO:BP	regulation of protein localization
0.005925317	24	GO:0010628	GO:BP	positive regulation of gene expression
0.005925317	6	GO:0006303	GO:BP	double-strand break repair via nonhomologous end joining
0.005925317	15	GO:0022411	GO:BP	cellular component disassembly
0.005925317	83	GO:0034641	GO:BP	cellular nitrogen compound metabolic process
0.006184997	8	GO:0000070	GO:BP	mitotic sister chromatid segregation
0.006229142	5	GO:0031571	GO:BP	mitotic G1 DNA damage checkpoint signaling
0.006233636	9	GO:0046777	GO:BP	protein autophosphorylation
0.006233636	60	GO:0006950	GO:BP	response to stress
0.006291233	8	GO:0051236	GO:BP	establishment of RNA localization
0.00632363	19	GO:0060341	GO:BP	regulation of cellular localization
0.006334015	10	GO:0044843	GO:BP	cell cycle G1/S phase transition
0.006435997	12	GO:0010948	GO:BP	negative regulation of cell cycle process
0.006435997	7	GO:0030010	GO:BP	establishment of cell polarity
0.006441976	5	GO:0044819	GO:BP	mitotic G1/S transition checkpoint signaling
0.006478623	43	GO:0009056	GO:BP	catabolic process
0.006554037	6	GO:0061640	GO:BP	cytoskeleton-dependent cytokinesis
0.006908362	12	GO:0032970	GO:BP	regulation of actin filament-based process
0.006939568	23	GO:0034622	GO:BP	cellular protein-containing complex assembly
0.007083004	4	GO:0031112	GO:BP	positive regulation of microtubule polymerization or depolymerization
0.007083004	16	GO:0051640	GO:BP	organelle localization
0.007083004	32	GO:0010557	GO:BP	positive regulation of macromolecule biosynthetic process
0.007113865	19	GO:0097435	GO:BP	supramolecular fiber organization
0.007631834	49	GO:0031325	GO:BP	positive regulation of cellular metabolic process
0.007631834	48	GO:0009966	GO:BP	regulation of signal transduction
0.007777064	16	GO:1901361	GO:BP	organic cyclic compound catabolic process
0.0079131	61	GO:0048869	GO:BP	cellular developmental process
0.0079131	21	GO:0061024	GO:BP	membrane organization
0.0079131	8	GO:0050821	GO:BP	protein stabilization
0.008074335	12	GO:0043547	GO:BP	positive regulation of GTPase activity
0.008074335	9	GO:0015931	GO:BP	nucleobase-containing compound transport
0.008074335	9	GO:0006323	GO:BP	DNA packaging
0.008210942	2	GO:1900114	GO:BP	positive regulation of histone H3-K9 trimethylation
0.008210942	2	GO:0002309	GO:BP	T cell proliferation involved in immune response
0.008252823	52	GO:0010646	GO:BP	regulation of cell communication
0.008337087	32	GO:1902531	GO:BP	regulation of intracellular signal transduction
0.008383229	7	GO:0051028	GO:BP	mRNA transport
0.008413051	10	GO:0031647	GO:BP	regulation of protein stability
0.009436194	10	GO:1903829	GO:BP	positive regulation of cellular protein localization
0.009436194	10	GO:0051258	GO:BP	protein polymerization
0.009436194	10	GO:0048511	GO:BP	rhythmic process
0.009584939	5	GO:0071763	GO:BP	nuclear membrane organization
0.009584939	42	GO:0051246	GO:BP	regulation of protein metabolic process
0.009584939	13	GO:0060249	GO:BP	anatomical structure homeostasis
0.009584939	41	GO:0008104	GO:BP	protein localization
0.009584939	5	GO:0000281	GO:BP	mitotic cytokinesis
0.009731764	67	GO:0048731	GO:BP	system development
0.009765172	78	GO:0010467	GO:BP	gene expression
0.009978936	9	GO:0007051	GO:BP	spindle organization
0.010321326	3	GO:0046827	GO:BP	positive regulation of protein export from nucleus
0.010576241	13	GO:0043087	GO:BP	regulation of GTPase activity
0.010576241	5	GO:0000380	GO:BP	alternative mRNA splicing, via spliceosome
0.010690582	17	GO:0051129	GO:BP	negative regulation of cellular component organization
0.010882436	68	GO:0010468	GO:BP	regulation of gene expression
0.010882436	9	GO:1901991	GO:BP	negative regulation of mitotic cell cycle phase transition
0.010950915	7	GO:0001837	GO:BP	epithelial to mesenchymal transition
0.011179025	31	GO:0034613	GO:BP	cellular protein localization

0.011273174	7	GO:0051017	GO:BP	actin filament bundle assembly
0.011518886	33	GO:0009891	GO:BP	positive regulation of biosynthetic process
0.011518886	5	GO:0072332	GO:BP	intrinsic apoptotic signaling pathway by p53 class mediator
0.011926645	2	GO:0030263	GO:BP	apoptotic chromosome condensation
0.011926645	2	GO:1905605	GO:BP	positive regulation of blood-brain barrier permeability
0.011926645	5	GO:1901983	GO:BP	regulation of protein acetylation
0.011926645	2	GO:0110011	GO:BP	regulation of basement membrane organization
0.011926645	2	GO:2001197	GO:BP	basement membrane assembly involved in embryonic body morphogenesis
0.011926645	2	GO:1904261	GO:BP	positive regulation of basement membrane assembly involved in embryonic body morphogenesis
0.011926645	2	GO:1904259	GO:BP	regulation of basement membrane assembly involved in embryonic body morphogenesis
0.012048779	13	GO:0006417	GO:BP	regulation of translation
0.012048779	8	GO:1902749	GO:BP	regulation of cell cycle G2/M phase transition
0.012048779	31	GO:0070727	GO:BP	cellular macromolecule localization
0.012048779	7	GO:0061572	GO:BP	actin filament bundle organization
0.012247477	22	GO:0032269	GO:BP	negative regulation of cellular protein metabolic process
0.01258021	8	GO:1902905	GO:BP	positive regulation of supramolecular fiber organization
0.012909249	4	GO:0035722	GO:BP	interleukin-12-mediated signaling pathway
0.012913975	36	GO:1901575	GO:BP	organic substance catabolic process
0.013217033	59	GO:0030154	GO:BP	cell differentiation
0.013518417	14	GO:0034248	GO:BP	regulation of cellular amide metabolic process
0.013546976	72	GO:0007275	GO:BP	multicellular organism development
0.013709165	10	GO:0051056	GO:BP	regulation of small GTPase mediated signal transduction
0.013709165	7	GO:0051494	GO:BP	negative regulation of cytoskeleton organization
0.013709165	7	GO:0000723	GO:BP	telomere maintenance
0.013709165	11	GO:0032535	GO:BP	regulation of cellular component size
0.014204416	3	GO:0150105	GO:BP	protein localization to cell-cell junction
0.014396554	74	GO:0051171	GO:BP	regulation of nitrogen compound metabolic process
0.014534555	4	GO:0071349	GO:BP	cellular response to interleukin-12
0.014637718	59	GO:0048583	GO:BP	regulation of response to stimulus
0.014637718	5	GO:0050000	GO:BP	chromosome localization
0.014657363	8	GO:1902275	GO:BP	regulation of chromatin organization
0.014912369	56	GO:0010556	GO:BP	regulation of macromolecule biosynthetic process
0.015054766	27	GO:0042981	GO:BP	regulation of apoptotic process
0.015187749	5	GO:0006998	GO:BP	nuclear envelope organization
0.015258609	4	GO:0070671	GO:BP	response to interleukin-12
0.015258609	32	GO:0031328	GO:BP	positive regulation of cellular biosynthetic process
0.015263877	78	GO:0031323	GO:BP	regulation of cellular metabolic process
0.015525358	7	GO:0000910	GO:BP	cytokinesis
0.015558517	16	GO:0080135	GO:BP	regulation of cellular response to stress
0.015570733	81	GO:0060255	GO:BP	regulation of macromolecule metabolic process
0.015631424	5	GO:0035023	GO:BP	regulation of Rho protein signal transduction
0.015727045	2	GO:0048205	GO:BP	COPI coating of Golgi vesicle
0.015727045	2	GO:0035964	GO:BP	COPI-coated vesicle budding
0.015727045	2	GO:0048200	GO:BP	Golgi transport vesicle coating
0.015727045	26	GO:0032270	GO:BP	positive regulation of cellular protein metabolic process
0.015839007	4	GO:0101024	GO:BP	mitotic nuclear membrane organization
0.015839007	4	GO:0007084	GO:BP	mitotic nuclear membrane reassembly
0.015839007	39	GO:0032268	GO:BP	regulation of cellular protein metabolic process
0.015906167	8	GO:0032388	GO:BP	positive regulation of intracellular transport
0.015966514	6	GO:0006405	GO:BP	RNA export from nucleus
0.016439966	29	GO:0010941	GO:BP	regulation of cell death
0.016768814	4	GO:0032206	GO:BP	positive regulation of telomere maintenance
0.016817749	3	GO:1901984	GO:BP	negative regulation of protein acetylation
0.017467834	51	GO:0048513	GO:BP	animal organ development
0.017778667	4	GO:0010458	GO:BP	exit from mitosis
0.017778667	4	GO:0006984	GO:BP	ER-nucleus signaling pathway
0.017799641	8	GO:0051495	GO:BP	positive regulation of cytoskeleton organization
0.018119812	5	GO:0031110	GO:BP	regulation of microtubule polymerization or depolymerization
0.0181421	6	GO:1905269	GO:BP	positive regulation of chromatin organization
0.018505687	3	GO:0048026	GO:BP	positive regulation of mRNA splicing, via spliceosome
0.018505687	3	GO:0051570	GO:BP	regulation of histone H3-K9 methylation
0.019111417	27	GO:0120036	GO:BP	plasma membrane bounded cell projection organization
0.01913199	7	GO:0032200	GO:BP	telomere organization
0.019635015	75	GO:0080090	GO:BP	regulation of primary metabolic process
0.019843366	4	GO:0035065	GO:BP	regulation of histone acetylation
0.019887507	6	GO:0007266	GO:BP	Rho protein signal transduction
0.020044922	27	GO:0043067	GO:BP	regulation of programmed cell death
0.020093298	2	GO:0090240	GO:BP	positive regulation of histone H4 acetylation
0.020093298	2	GO:0036466	GO:BP	synaptic vesicle recycling via endosome
0.020093298	2	GO:2000210	GO:BP	positive regulation of anoikis
0.020093298	3	GO:0034063	GO:BP	stress granule assembly
0.020093298	2	GO:0052428	GO:BP	modulation by host of symbiont molecular function
0.02028181	16	GO:0000904	GO:BP	cell morphogenesis involved in differentiation
0.020911716	5	GO:0006903	GO:BP	vesicle targeting
0.021410499	107	GO:0050896	GO:BP	response to stimulus
0.021844047	4	GO:0031113	GO:BP	regulation of microtubule polymerization
0.021844047	4	GO:0006977	GO:BP	DNA damage response, signal transduction by p53 class mediator resulting in cell cycle arrest
0.022055785	19	GO:0030163	GO:BP	protein catabolic process
0.02214635	6	GO:0000724	GO:BP	double-strand break repair via homologous recombination
0.022194562	15	GO:0010942	GO:BP	positive regulation of cell death
0.022687193	6	GO:0045727	GO:BP	positive regulation of translation
0.022687193	34	GO:0071705	GO:BP	nitrogen compound transport
0.022687193	8	GO:0016197	GO:BP	endosomal transport
0.022817895	4	GO:0044380	GO:BP	protein localization to cytoskeleton
0.022830918	7	GO:0008064	GO:BP	regulation of actin polymerization or depolymerization
0.023175237	5	GO:0051205	GO:BP	protein insertion into membrane
0.023237196	6	GO:0000725	GO:BP	recombinational repair

0.023242707	7	GO:1902115	GO:BP	regulation of organelle assembly
0.023242707	7	GO:0030832	GO:BP	regulation of actin filament length
0.023962632	5	GO:0090559	GO:BP	regulation of membrane permeability
0.024317774	16	GO:0007420	GO:BP	brain development
0.024317774	8	GO:0043543	GO:BP	protein acylation
0.02475283	2	GO:1904354	GO:BP	negative regulation of telomere capping
0.02475283	2	GO:1990414	GO:BP	replication-born double-strand break repair via sister chromatid exchange
0.02475283	2	GO:1905603	GO:BP	regulation of blood-brain barrier permeability
0.02475283	27	GO:0030030	GO:BP	cell projection organization
0.02475283	2	GO:0071169	GO:BP	establishment of protein localization to chromatin
0.024836253	4	GO:0000381	GO:BP	regulation of alternative mRNA splicing, via spliceosome
0.02491965	13	GO:0061919	GO:BP	process utilizing autophagic mechanism
0.02491965	13	GO:0006914	GO:BP	autophagy
0.025813585	65	GO:0009059	GO:BP	macromolecule biosynthetic process
0.026072184	18	GO:0043066	GO:BP	negative regulation of apoptotic process
0.027313436	7	GO:0031032	GO:BP	actomyosin structure organization
0.027826363	3	GO:0045070	GO:BP	positive regulation of viral genome replication
0.028720311	7	GO:0071897	GO:BP	DNA biosynthetic process
0.029300286	11	GO:0043161	GO:BP	proteasome-mediated ubiquitin-dependent protein catabolic process
0.029300286	7	GO:0046578	GO:BP	regulation of Ras protein signal transduction
0.029300286	54	GO:2000112	GO:BP	regulation of cellular macromolecule biosynthetic process
0.029300286	26	GO:0051247	GO:BP	positive regulation of protein metabolic process
0.029933087	7	GO:0006413	GO:BP	translational initiation
0.029944543	2	GO:0099159	GO:BP	regulation of modification of postsynaptic structure
0.029944543	2	GO:0052205	GO:BP	modulation of molecular function in other organism involved in symbiotic interaction
0.029944543	4	GO:0045995	GO:BP	regulation of embryonic development
0.029944543	4	GO:2000756	GO:BP	regulation of peptidyl-lysine acetylation
0.029944543	2	GO:0044359	GO:BP	modulation of molecular function in other organism
0.029944543	2	GO:0070973	GO:BP	protein localization to endoplasmic reticulum exit site
0.029944543	2	GO:1901203	GO:BP	positive regulation of extracellular matrix assembly
0.029944833	5	GO:0120034	GO:BP	positive regulation of plasma membrane bounded cell projection assembly
0.030850277	7	GO:0040029	GO:BP	regulation of gene expression, epigenetic
0.030853045	16	GO:0032989	GO:BP	cellular component morphogenesis
0.031170412	4	GO:0046824	GO:BP	positive regulation of nucleocytoplasmic transport
0.031170412	4	GO:0051310	GO:BP	metaphase plate congression
0.031277069	8	GO:0000086	GO:BP	G2/M transition of mitotic cell cycle
0.031277069	7	GO:0006473	GO:BP	protein acetylation
0.031370656	6	GO:0051053	GO:BP	negative regulation of DNA metabolic process
0.031579452	15	GO:0034330	GO:BP	cell junction organization
0.031579452	5	GO:0061157	GO:BP	mRNA destabilization
0.031579452	40	GO:0009653	GO:BP	anatomical structure morphogenesis
0.031579452	5	GO:0006900	GO:BP	vesicle budding from membrane
0.031739194	18	GO:0043069	GO:BP	negative regulation of programmed cell death
0.032018318	4	GO:0043489	GO:BP	RNA stabilization
0.032018318	4	GO:0090307	GO:BP	mitotic spindle assembly
0.032018318	10	GO:0019058	GO:BP	viral life cycle
0.032388114	12	GO:0090066	GO:BP	regulation of anatomical structure size
0.032388114	16	GO:0006412	GO:BP	translation
0.032424533	8	GO:0031334	GO:BP	positive regulation of protein-containing complex assembly
0.033231685	27	GO:0031399	GO:BP	regulation of protein modification process
0.033231685	5	GO:1903008	GO:BP	organelle disassembly
0.033231685	4	GO:0030261	GO:BP	chromosome condensation
0.033231685	4	GO:0035794	GO:BP	positive regulation of mitochondrial membrane permeability
0.033244406	3	GO:0046825	GO:BP	regulation of protein export from nucleus
0.034299725	5	GO:0061014	GO:BP	positive regulation of mRNA catabolic process
0.034299725	5	GO:0098781	GO:BP	ncRNA transcription
0.034447457	2	GO:0099532	GO:BP	synaptic vesicle endosomal processing
0.034447457	2	GO:1904779	GO:BP	regulation of protein localization to centrosome
0.034447457	32	GO:0048468	GO:BP	cell development
0.034447457	2	GO:0048194	GO:BP	Golgi vesicle budding
0.034712764	38	GO:0071702	GO:BP	organic substance transport
0.035128095	5	GO:0050779	GO:BP	RNA destabilization
0.035244132	3	GO:0031116	GO:BP	positive regulation of microtubule polymerization
0.035244132	3	GO:0044818	GO:BP	mitotic G2/M transition checkpoint
0.035244132	3	GO:0009303	GO:BP	rRNA transcription
0.035414506	84	GO:0019222	GO:BP	regulation of metabolic process
0.035578631	16	GO:0060322	GO:BP	head development
0.035589375	4	GO:0006901	GO:BP	vesicle coating
0.0356266	34	GO:0008219	GO:BP	cell death
0.035795855	5	GO:2000278	GO:BP	regulation of DNA biosynthetic process
0.037029543	6	GO:0018393	GO:BP	internal peptidyl-lysine acetylation
0.03707515	4	GO:0031060	GO:BP	regulation of histone methylation
0.03707515	7	GO:0006261	GO:BP	DNA-dependent DNA replication
0.037199713	18	GO:0033365	GO:BP	protein localization to organelle
0.037199713	3	GO:1905508	GO:BP	protein localization to microtubule organizing center
0.037199713	3	GO:0035633	GO:BP	maintenance of blood-brain barrier
0.037199713	3	GO:0050685	GO:BP	positive regulation of mRNA processing
0.037867859	5	GO:1901989	GO:BP	positive regulation of cell cycle phase transition
0.038249018	56	GO:0009889	GO:BP	regulation of biosynthetic process
0.038249018	4	GO:1904377	GO:BP	positive regulation of protein localization to cell periphery
0.038249018	7	GO:0007623	GO:BP	circadian rhythm
0.038249018	9	GO:0032984	GO:BP	protein-containing complex disassembly
0.038249018	6	GO:0006475	GO:BP	internal protein amino acid acetylation
0.038748834	5	GO:0051225	GO:BP	spindle assembly
0.038769812	8	GO:0017148	GO:BP	negative regulation of translation
0.039103528	2	GO:0030953	GO:BP	astral microtubule organization
0.039103528	3	GO:0040001	GO:BP	establishment of mitotic spindle localization

0.039103528	3	GO:1901030	GO:BP	positive regulation of mitochondrial outer membrane permeabilization involved in apoptotic signaling pathway
0.039103528	2	GO:1905214	GO:BP	regulation of RNA binding
0.039103528	2	GO:0010172	GO:BP	embryonic body morphogenesis
0.039268992	4	GO:1905710	GO:BP	positive regulation of membrane permeability
0.040117658	7	GO:0008154	GO:BP	actin polymerization or depolymerization
0.040117658	13	GO:0043065	GO:BP	positive regulation of apoptotic process
0.040641294	5	GO:0060964	GO:BP	regulation of gene silencing by miRNA
0.040641294	11	GO:0022613	GO:BP	ribonucleoprotein complex biogenesis
0.040759023	4	GO:0048199	GO:BP	vesicle targeting, to, from or within Golgi
0.040759023	16	GO:0043043	GO:BP	peptide biosynthetic process
0.040759023	63	GO:0034645	GO:BP	cellular macromolecule biosynthetic process
0.040949404	3	GO:0000289	GO:BP	nuclear-transcribed mRNA poly(A) tail shortening
0.040949404	3	GO:0032205	GO:BP	negative regulation of telomere maintenance
0.040949404	3	GO:0043516	GO:BP	regulation of DNA damage response, signal transduction by p53 class mediator
0.040949404	3	GO:0010661	GO:BP	positive regulation of muscle cell apoptotic process
0.040949404	3	GO:1904358	GO:BP	positive regulation of telomere maintenance via telomere lengthening
0.040949404	3	GO:0051294	GO:BP	establishment of spindle orientation
0.041192013	5	GO:0007569	GO:BP	cell aging
0.042320081	55	GO:0031326	GO:BP	regulation of cellular biosynthetic process
0.04240059	5	GO:0060147	GO:BP	regulation of posttranscriptional gene silencing
0.04240059	5	GO:0051261	GO:BP	protein depolymerization
0.043565025	2	GO:0010826	GO:BP	negative regulation of centrosome duplication
0.043565025	2	GO:1900112	GO:BP	regulation of histone H3-K9 trimethylation
0.043565025	2	GO:0046606	GO:BP	negative regulation of centrosome cycle
0.043565025	2	GO:0019042	GO:BP	viral latency
0.043565025	30	GO:0006915	GO:BP	apoptotic process
0.043565025	3	GO:0032506	GO:BP	cytokinetic process
0.043565025	3	GO:0051567	GO:BP	histone H3-K9 methylation
0.043565025	2	GO:0070816	GO:BP	phosphorylation of RNA polymerase II C-terminal domain
0.043565025	5	GO:0060966	GO:BP	regulation of gene silencing by RNA
0.043565025	2	GO:0090557	GO:BP	establishment of endothelial intestinal barrier
0.043565025	2	GO:0098974	GO:BP	postsynaptic actin cytoskeleton organization
0.04425645	6	GO:0034250	GO:BP	positive regulation of cellular amide metabolic process
0.044530855	4	GO:1902369	GO:BP	negative regulation of RNA catabolic process
0.045086202	91	GO:0032501	GO:BP	multicellular organismal process
0.0452114	6	GO:0018394	GO:BP	peptidyl-lysine acetylation
0.045491948	3	GO:0033120	GO:BP	positive regulation of RNA splicing
0.045753317	19	GO:0031401	GO:BP	positive regulation of protein modification process
0.045821114	17	GO:0007017	GO:BP	microtubule-based process
0.046549661	5	GO:0042177	GO:BP	negative regulation of protein catabolic process
0.046549661	13	GO:0043068	GO:BP	positive regulation of programmed cell death
0.046549661	5	GO:0031109	GO:BP	microtubule polymerization or depolymerization
0.046684956	39	GO:0071310	GO:BP	cellular response to organic substance
0.046962273	6	GO:0030833	GO:BP	regulation of actin filament polymerization
0.047684211	4	GO:0033077	GO:BP	T cell differentiation in thymus
0.049468016	2	GO:0006983	GO:BP	ER overload response
0.049468016	2	GO:1905244	GO:BP	regulation of modification of synaptic structure
0.049468016	2	GO:0071712	GO:BP	ER-associated misfolded protein catabolic process
0.049527479	22	GO:0045892	GO:BP	negative regulation of transcription, DNA-templated
1.83E-23	113	GO:0043228	GO:CC	non-membrane-bounded organelle
2.05E-22	111	GO:0043232	GO:CC	intracellular non-membrane-bounded organelle
6.90E-19	98	GO:0031981	GO:CC	nuclear lumen
6.90E-19	94	GO:0005654	GO:CC	nucleoplasm
2.21E-17	173	GO:0005622	GO:CC	intracellular anatomical structure
3.42E-15	164	GO:0043229	GO:CC	intracellular organelle
8.56E-15	103	GO:0070013	GO:CC	intracellular organelle lumen
8.56E-15	103	GO:0043233	GO:CC	organelle lumen
8.56E-15	103	GO:0031974	GO:CC	membrane-enclosed lumen
2.29E-14	122	GO:0005634	GO:CC	nucleus
6.22E-14	167	GO:0043226	GO:CC	organelle
1.84E-10	92	GO:0005829	GO:CC	cytosol
5.02E-10	55	GO:0005856	GO:CC	cytoskeleton
1.38E-09	148	GO:0005737	GO:CC	cytoplasm
6.56E-09	38	GO:0099080	GO:CC	supramolecular complex
1.01E-08	29	GO:0016604	GO:CC	nuclear body
1.96E-08	31	GO:0005730	GO:CC	nucleolus
3.45E-08	18	GO:0005938	GO:CC	cell cortex
7.07E-08	28	GO:0070161	GO:CC	anchoring junction
8.80E-07	45	GO:0030054	GO:CC	cell junction
2.04E-06	9	GO:0071013	GO:CC	catalytic step 2 spliceosome
4.08E-06	141	GO:0043231	GO:CC	intracellular membrane-bounded organelle
4.67E-06	12	GO:0005681	GO:CC	spliceosomal complex
5.41E-06	31	GO:0140513	GO:CC	nuclear protein-containing complex
5.84E-06	19	GO:0015629	GO:CC	actin cytoskeleton
6.25E-06	149	GO:0043227	GO:CC	membrane-bounded organelle
7.42E-06	22	GO:1990904	GO:CC	ribonucleoprotein complex
1.29E-05	81	GO:0032991	GO:CC	protein-containing complex
3.27E-05	37	GO:0005694	GO:CC	chromosome
6.12E-05	9	GO:0034399	GO:CC	nuclear periphery
6.15E-05	12	GO:0035770	GO:CC	ribonucleoprotein granule
6.51E-05	10	GO:0005912	GO:CC	adherens junction
6.74E-05	25	GO:0099512	GO:CC	supramolecular fiber
7.52E-05	25	GO:0099081	GO:CC	supramolecular polymer
9.23E-05	15	GO:0016607	GO:CC	nuclear speck
0.000102561	21	GO:0099513	GO:CC	polymeric cytoskeletal fiber
0.000106102	8	GO:0016363	GO:CC	nuclear matrix
0.000106102	15	GO:0005925	GO:CC	focal adhesion

0.000120012	15	GO:0031252	GO:CC	cell leading edge
0.000120319	15	GO:0030055	GO:CC	cell-substrate junction
0.000145009	4	GO:0031616	GO:CC	spindle pole centrosome
0.000154581	11	GO:0036464	GO:CC	cytoplasmic ribonucleoprotein granule
0.000161509	16	GO:0005911	GO:CC	cell-cell junction
0.000184854	8	GO:0030863	GO:CC	cortical cytoskeleton
0.000258704	28	GO:0015630	GO:CC	microtubule cytoskeleton
0.000517028	39	GO:0120025	GO:CC	plasma membrane bounded cell projection
0.00054955	5	GO:0099738	GO:CC	cell cortex region
0.000812531	6	GO:0010494	GO:CC	cytoplasmic stress granule
0.000863136	17	GO:0098794	GO:CC	postsynapse
0.000863136	17	GO:0030425	GO:CC	dendrite
0.000863136	2	GO:0002944	GO:CC	cyclin K-CDK12 complex
0.000875144	17	GO:0097447	GO:CC	dendritic tree
0.001108416	14	GO:0005635	GO:CC	nuclear envelope
0.001175638	39	GO:0042995	GO:CC	cell projection
0.001363803	27	GO:0043005	GO:CC	neuron projection
0.003279079	6	GO:0016605	GO:CC	PML body
0.003914483	11	GO:0098978	GO:CC	glutamatergic synapse
0.004159254	10	GO:0031965	GO:CC	nuclear membrane
0.004159254	8	GO:0030496	GO:CC	midbody
0.00434924	2	GO:0005638	GO:CC	lamin filament
0.0058203	12	GO:0005874	GO:CC	microtubule
0.006510676	3	GO:0035145	GO:CC	exon-exon junction complex
0.00675489	2	GO:0045180	GO:CC	basal cortex
0.00675489	2	GO:0030981	GO:CC	cortical microtubule cytoskeleton
0.007354621	7	GO:0000922	GO:CC	spindle pole
0.007516015	11	GO:0005819	GO:CC	spindle
0.008667732	18	GO:0036477	GO:CC	somatodendritic compartment
0.008876474	10	GO:0014069	GO:CC	postsynaptic density
0.009341727	2	GO:0097427	GO:CC	microtubule bundle
0.009705893	17	GO:0005815	GO:CC	microtubule organizing center
0.009705893	10	GO:0032279	GO:CC	asymmetric synapse
0.010195387	10	GO:0098687	GO:CC	chromosomal region
0.011270566	5	GO:0030864	GO:CC	cortical actin cytoskeleton
0.01163683	3	GO:0071782	GO:CC	endoplasmic reticulum tubular network
0.01163683	7	GO:0043197	GO:CC	dendritic spine
0.01163683	24	GO:1902494	GO:CC	catalytic complex
0.012252049	7	GO:0044309	GO:CC	neuron spine
0.012845946	10	GO:0099572	GO:CC	postsynaptic specialization
0.014323337	2	GO:0032541	GO:CC	cortical endoplasmic reticulum
0.014323337	2	GO:0045293	GO:CC	mRNA editing complex
0.014323337	10	GO:0098984	GO:CC	neuron to neuron synapse
0.014323337	2	GO:0008024	GO:CC	cyclin/CDK positive transcription elongation factor complex
0.014323337	2	GO:0036396	GO:CC	RNA N6-methyladenosine methyltransferase complex
0.016595919	4	GO:0005637	GO:CC	nuclear inner membrane
0.016595919	7	GO:0030027	GO:CC	lamellipodium
0.021142411	8	GO:0099568	GO:CC	cytoplasmic region
0.021556532	6	GO:0000781	GO:CC	chromosome, telomeric region
0.022046692	4	GO:0035861	GO:CC	site of double-strand break
0.025055502	2	GO:0005652	GO:CC	nuclear lamina
0.025055502	4	GO:0005844	GO:CC	polysome
0.025055502	4	GO:0005905	GO:CC	clathrin-coated pit
0.025055502	21	GO:0000785	GO:CC	chromatin
0.029160908	4	GO:0000792	GO:CC	heterochromatin
0.029160908	2	GO:0019908	GO:CC	nuclear cyclin-dependent protein kinase holoenzyme complex
0.031633285	4	GO:0032432	GO:CC	actin filament bundle
0.032742964	4	GO:0042641	GO:CC	actomyosin
0.034158195	6	GO:0001726	GO:CC	ruffle
0.034969479	7	GO:0000793	GO:CC	condensed chromosome
0.038103573	6	GO:0030426	GO:CC	growth cone
0.040993532	13	GO:0030424	GO:CC	axon
0.041570093	31	GO:0070062	GO:CC	extracellular exosome
0.041912216	2	GO:0099092	GO:CC	postsynaptic density, intracellular component
0.042541083	6	GO:0030427	GO:CC	site of polarized growth
0.044936996	1	GO:0009330	GO:CC	DNA topoisomerase type II (double strand cut, ATP-hydrolyzing) complex
0.044936996	1	GO:0042564	GO:CC	NLS-dependent protein nuclear import complex
0.044936996	1	GO:0097489	GO:CC	multivesicular body, internal vesicle lumen
0.044936996	1	GO:0031592	GO:CC	centrosomal corona
0.044936996	1	GO:1905720	GO:CC	cytoplasmic microtubule bundle
0.048779479	7	GO:0045111	GO:CC	intermediate filament cytoskeleton
0.049292515	6	GO:0000775	GO:CC	chromosome, centromeric region
0.049292515	2	GO:0099524	GO:CC	postsynaptic cytosol
0.049450943	4	GO:0090734	GO:CC	site of DNA damage
4.08E-18	30	GO:0045296	GO:MF	cadherin binding
4.57E-16	62	GO:0003723	GO:MF	RNA binding
1.94E-14	32	GO:0050839	GO:MF	cell adhesion molecule binding
6.58E-10	82	GO:0003676	GO:MF	nucleic acid binding
9.58E-10	172	GO:0005515	GO:MF	protein binding
1.77E-08	50	GO:0019899	GO:MF	enzyme binding
2.51E-08	33	GO:0008092	GO:MF	cytoskeletal protein binding
3.74E-08	24	GO:0003729	GO:MF	mRNA binding
5.72E-06	178	GO:0005488	GO:MF	binding
1.37E-05	92	GO:1901363	GO:MF	heterocyclic compound binding
1.44E-05	18	GO:0003779	GO:MF	actin binding
1.66E-05	18	GO:0005096	GO:MF	GTPase activator activity
2.02E-05	92	GO:0097159	GO:MF	organic cyclic compound binding

2.18E-05	20	GO:0003682	GO:MF	chromatin binding
2.38E-05	19	GO:0060589	GO:MF	nucleoside-triphosphatase regulator activity
2.94E-05	18	GO:0030695	GO:MF	GTPase regulator activity
5.63E-05	25	GO:0030234	GO:MF	enzyme regulator activity
5.72E-05	31	GO:0044877	GO:MF	protein-containing complex binding
0.000198987	11	GO:0005085	GO:MF	guanyl-nucleotide exchange factor activity
0.000290412	21	GO:0019900	GO:MF	kinase binding
0.000290412	8	GO:0047485	GO:MF	protein N-terminus binding
0.00046174	11	GO:0042393	GO:MF	histone binding
0.000467349	26	GO:0098772	GO:MF	molecular function regulator
0.000476597	20	GO:0008047	GO:MF	enzyme activator activity
0.000514663	5	GO:0036002	GO:MF	pre-mRNA binding
0.000514663	19	GO:0019901	GO:MF	protein kinase binding
0.000581729	16	GO:0003712	GO:MF	transcription coregulator activity
0.001595472	16	GO:0008134	GO:MF	transcription factor binding
0.002466023	11	GO:0031625	GO:MF	ubiquitin protein ligase binding
0.00383636	5	GO:1990841	GO:MF	promoter-specific chromatin binding
0.00383636	11	GO:0044389	GO:MF	ubiquitin-like protein ligase binding
0.004315797	2	GO:0061649	GO:MF	ubiquitin modification-dependent histone binding
0.004710911	12	GO:0015631	GO:MF	tubulin binding
0.005583753	4	GO:0042162	GO:MF	telomeric DNA binding
0.006157168	9	GO:0140297	GO:MF	DNA-binding transcription factor binding
0.007266518	5	GO:0003684	GO:MF	damaged DNA binding
0.007600682	10	GO:0051020	GO:MF	GTPase binding
0.007820172	7	GO:0043021	GO:MF	ribonucleoprotein complex binding
0.007820172	8	GO:0061629	GO:MF	RNA polymerase II-specific DNA-binding transcription factor binding
0.008626439	4	GO:0061980	GO:MF	regulatory RNA binding
0.008772051	8	GO:0008022	GO:MF	protein C-terminus binding
0.009000368	3	GO:0070064	GO:MF	proline-rich region binding
0.010150787	3	GO:0051010	GO:MF	microtubule plus-end binding
0.010150787	7	GO:0140030	GO:MF	modification-dependent protein binding
0.011638099	8	GO:0051015	GO:MF	actin filament binding
0.011711804	39	GO:0003677	GO:MF	DNA binding
0.017912113	10	GO:0060090	GO:MF	molecular adaptor activity
0.026472501	7	GO:0003730	GO:MF	mRNA 3'-UTR binding
0.032536439	15	GO:0019904	GO:MF	protein domain specific binding
0.032536439	3	GO:0035198	GO:MF	miRNA binding
0.032851391	11	GO:0004674	GO:MF	protein serine/threonine kinase activity
0.035677133	6	GO:0045182	GO:MF	translation regulator activity
0.036711968	8	GO:0031267	GO:MF	small GTPase binding
0.036711968	2	GO:0098505	GO:MF	G-rich strand telomeric DNA binding
0.039709047	4	GO:0002039	GO:MF	p53 binding
0.042997499	2	GO:0140036	GO:MF	ubiquitin-dependent protein binding
0.044144077	5	GO:0042826	GO:MF	histone deacetylase binding
0.04866785	2	GO:0008353	GO:MF	RNA polymerase II CTD heptapeptide repeat kinase activity
0.04866785	2	GO:0043047	GO:MF	single-stranded telomeric DNA binding
0.049094775	8	GO:0003713	GO:MF	transcription coactivator activity
0.002258104	9	KEGG:03040	KEGG	Spliceosome
6.65E-05	25	REAC:R-HSA-16	REAC	Cell Cycle
0.00163073	11	REAC:R-HSA-7	REAC	mRNA Splicing - Major Pathway
0.001658379	11	REAC:R-HSA-7	REAC	mRNA Splicing
0.002292894	12	REAC:R-HSA-7	REAC	Processing of Capped Intron-Containing Pre-mRNA
0.005777492	20	REAC:R-HSA-8	REAC	Metabolism of RNA
0.010459625	7	REAC:R-HSA-6	REAC	G2/M DNA damage checkpoint
0.010796726	9	REAC:R-HSA-3	REAC	SUMO E3 ligases SUMOylate target proteins
0.010796726	17	REAC:R-HSA-6	REAC	Cell Cycle, Mitotic
0.011941863	9	REAC:R-HSA-2	REAC	SUMOylation
0.014569222	6	REAC:R-HSA-5	REAC	DNA Double Strand Break Response
0.014569222	6	REAC:R-HSA-5	REAC	Recruitment and ATM-mediated phosphorylation of repair and signaling proteins at DNA double strand breaks
0.025683383	8	REAC:R-HSA-5	REAC	DNA Double-Strand Break Repair
0.025683383	13	REAC:R-HSA-6	REAC	M Phase
0.025683383	12	REAC:R-HSA-3	REAC	Transcriptional Regulation by TP53
0.025683383	5	REAC:R-HSA-6	REAC	TP53 Regulates Transcription of DNA Repair Genes
0.025683383	3	REAC:R-HSA-1	REAC	Signaling by cytosolic FGFR1 fusion mutants
0.025683383	8	REAC:R-HSA-1	REAC	Apoptosis
0.025683383	4	REAC:R-HSA-1	REAC	Apoptotic cleavage of cellular proteins
0.025683383	8	REAC:R-HSA-6	REAC	G2/M Checkpoints
0.025683383	2	REAC:R-HSA-4	REAC	Localization of the PINCH-ILK-PARVIN complex to focal adhesions
0.025871543	4	REAC:R-HSA-8	REAC	Gene and protein expression by JAK-STAT signaling after Interleukin-12 stimulation
0.025871543	4	REAC:R-HSA-8	REAC	Transcriptional regulation by the AP-2 (TFAP2) family of transcription factors
0.028488207	3	REAC:R-HSA-3	REAC	SUMOylation of transcription factors
0.028488207	3	REAC:R-HSA-4	REAC	Cell-extracellular matrix interactions
0.029917479	6	REAC:R-HSA-8	REAC	Cargo recognition for clathrin-mediated endocytosis
0.030289158	8	REAC:R-HSA-5	REAC	Programmed Cell Death
0.031158409	2	REAC:R-HSA-8	REAC	TFAP2A acts as a transcriptional repressor during retinoic acid induced cell differentiation
0.037437602	2	REAC:R-HSA-9	REAC	Replication of the SARS-CoV-1 genome
0.037437602	2	REAC:R-HSA-9	REAC	Replication of the SARS-CoV-2 genome
0.037437602	2	REAC:R-HSA-9	REAC	SARS-CoV-1 Genome Replication and Transcription
0.037437602	2	REAC:R-HSA-9	REAC	SARS-CoV-2 Genome Replication and Transcription
0.037437602	4	REAC:R-HSA-9	REAC	Interleukin-12 signaling
0.037437602	10	REAC:R-HSA-6	REAC	Cell Cycle Checkpoints
0.037437602	3	REAC:R-HSA-6	REAC	TP53 regulates transcription of additional cell cycle genes whose exact role in the p53 pathway remain uncertain
0.042465139	4	REAC:R-HSA-6	REAC	TP53 Regulates Transcription of Cell Cycle Genes
0.047866207	4	REAC:R-HSA-7	REAC	Apoptotic execution phase
0.049195183	3	REAC:R-HSA-4	REAC	Deadenylation of mRNA

Table S2: Mutation status on KRA, HRAS, PTEN and TP53 in the TNBC cell lines under study.

Cell lines	KRAS	HRAS	PTEN	TP53
MDA-MB-231	mut [1]	wt	wt	mut [6]
MDA-MB-453	mut [2]	wt	mut[3]	mut [7]
MDA-MB-468	wt	wt	mut [5]	mut [8]
HS 578T	wt	mut [4]	wt	mut [9]

1. Kozma SC, Bogaard ME, Buser K, Saurer SM, Bos JL, Groner B, Hynes NE: The human c-Kirsten ras gene is activated by a novel mutation in codon 13 in the breast carcinoma cell line MDA-MB231. *Nucleic Acids Res* 1987, 15(15):5963-5971.
2. Vranic, S., Z. Gatalica, and Z.Y. Wang, *Update on the molecular profile of the MDA-MB-453 cell line as a model for apocrine breast carcinoma studies.* Oncol Lett, 2011. 2(6): p. 1131-1137.
3. Singh, G., et al., *Characterization of a novel PTEN mutation in MDA-MB-453 breast carcinoma cell line.* BMC Cancer, 2011. 11: p. 490.
4. Kraus, M.H., Y. Yuasa, and S.A. Aaronson, *A position 12-activated H-ras oncogene in all HS578T mammary carcinosarcoma cells but not normal mammary cells of the same patient.* Proc Natl Acad Sci U S A, 1984. 81(17): p. 5384-8.
5. Jang, K., et al., *PTEN sensitizes MDA-MB-468 cells to inhibition of MEK/Erk signaling for the blockade of cell proliferation.* Oncol Rep, 2010. 24(3): p. 787-93.
6. Hui, L., et al., *Mutant p53 in MDA-MB-231 breast cancer cells is stabilized by elevated phospholipase D activity and contributes to survival signals generated by phospholipase D.* Oncogene, 2006. **25**(55): p. 7305-10.
7. Runnebaum, I.B., et al., *Mutations in p53 as potential molecular markers for human breast cancer.* Proc Natl Acad Sci U S A, 1991. **88**(23): p. 10657-61.
8. Peng, J., et al., *Targeting Mutated p53 Dependency in Triple-Negative Breast Cancer Cells Through CDK7 Inhibition.* Front Oncol, 2021. **11**: p. 664848.
9. Huovinen, M., et al., *Characterization of human breast cancer cell lines for the studies on p53 in chemical carcinogenesis.* Toxicol In Vitro, 2011. **25**(5): p. 1007-17.

Supplementary data

Fisetin induces DNA double strand break and interferes with the repair of radiation-induced damage to radiosensitize triple negative breast cancer cells

Shayan Khozooei[1,2], Konstanze Lettau[1,2], Francesca Barletta[3], Tina Jost[4,5], Simone Rebholz[1,2], Soundaram Veerappan[1,2], Mirita Franz-Wachtel[6], Boris Macek[6], George Iliakis[7], Luitpold V Distel[4,5], Daniel Zips[1,2], Mahmoud Toulany[1,2]

[1]Division of Radiobiology and Molecular Environmental Research, Department of Radiation Oncology, University of Tuebingen, Tuebingen Germany, [2]German Cancer Consortium (DKTK), partner site Tuebingen, German Cancer Research Center (DKFZ) Heidelberg, Germany, [3]Quantitative Biology Center (QBiC), University of Tuebingen, Tuebingen, Germany, [4]Department of Radiation Oncology, Universitätsklinikum Erlangen, Friedrich-Alexander-Universität Erlangen-Nürnberg, Erlangen, Germany. [5]Comprehensive Cancer Center Erlangen-EMN (CCC ER-EMN), Universitätsklinikum Erlangen, Friedrich-Alexander-Universität Erlangen-Nürnberg, Erlangen, Germany. [6]Proteome Center Tuebingen, University of Tuebingen, Tuebingen, Germany. [7]Divison of Experimental Radiation Oncology, Department of Radiation Oncology, Institutsgruppe 1, Bauteil A, 4.038, Hufelandstr. 55, 45122 Essen, Germany.

Fig. S1 Khozooei *et al.* 2022

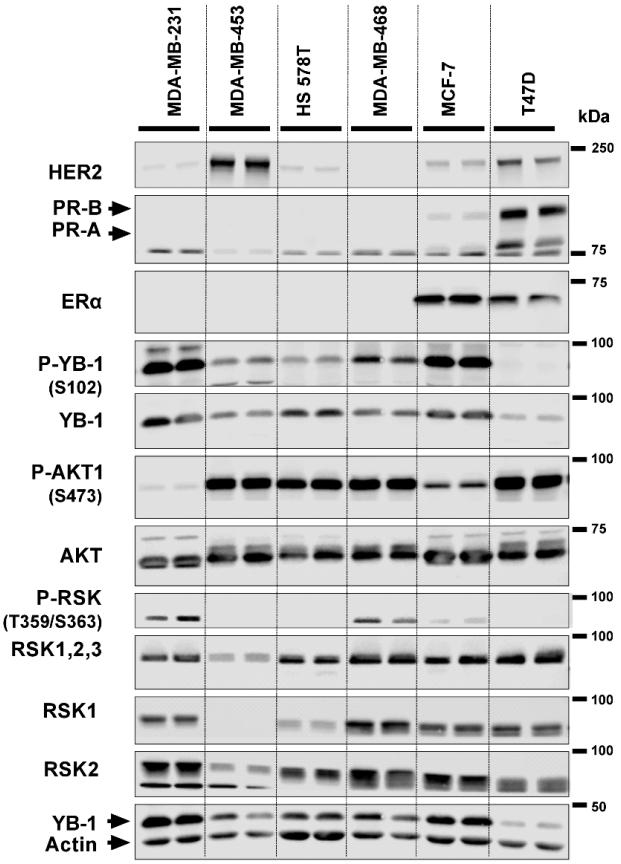

Fig. S1 The pattern of expression of the estrogen-, progesterone- and HER2 receptors, as well as the activation status of YB-1, AKT and RSK in the indicated cell lines under study.

The protein samples were isolated from the indicated cells. The same samples were loaded to two acrylamide gels. Following electrophoresis and blotting, the pattern of expression of HER2, ER and PR, as well as the phosphorylation level of YB-1, RSK, AKT were detected by specific antibodies. P-YB-1, P-RSK, P-AKT blots were stripped and incubated with antibodies against total protein. Actin was detected as the loading control from the YB-1 blot without stripping as loading control for E blot in which the receptors were detected.

Fig. S2 Khozooei *et al.* 2022

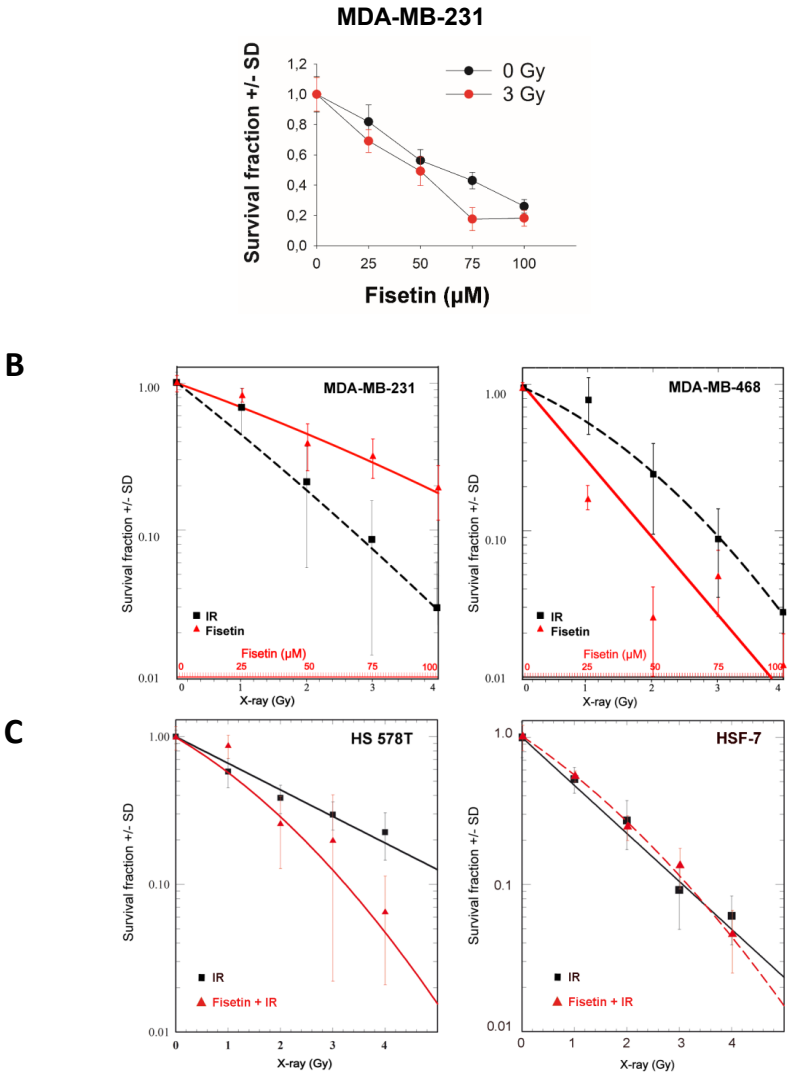

Fig. S2 The radiosensitizing effect of fisetin in combination with single dose irradiation

(A) Indicated cells were treated with different concentrations of fisetin for 72 h and mock irradiation or irradiated with 3 Gy . **(B)** Cells were treated with indicated concentrations of fisetin or DMSO (0.07%) for 72 h and DMSO treated cells were irradiated with a single dose of 0 to 4 Gy IR. **(C)** Cells treated with DMSO (0.07%) or fisetin (75 µM) for 72 h and mock irradiated or irradiated with a single dose of 0 to 4 **(C)**. Immediately after IR or 24 h after fisetin treatment clonogenic assay was performed as described in the *Methods* section. The data points represent the mean surviving fraction ± SD of 6 data from one experiment **(A)**, 12 data from two experiment in MDA-MB-231 and 6 data from 1 experiment in MDA-MB-468 **(B)** and 12 data from 2 experiments **(C)**.

Fig. S3 Khozooei *et al.* 2022

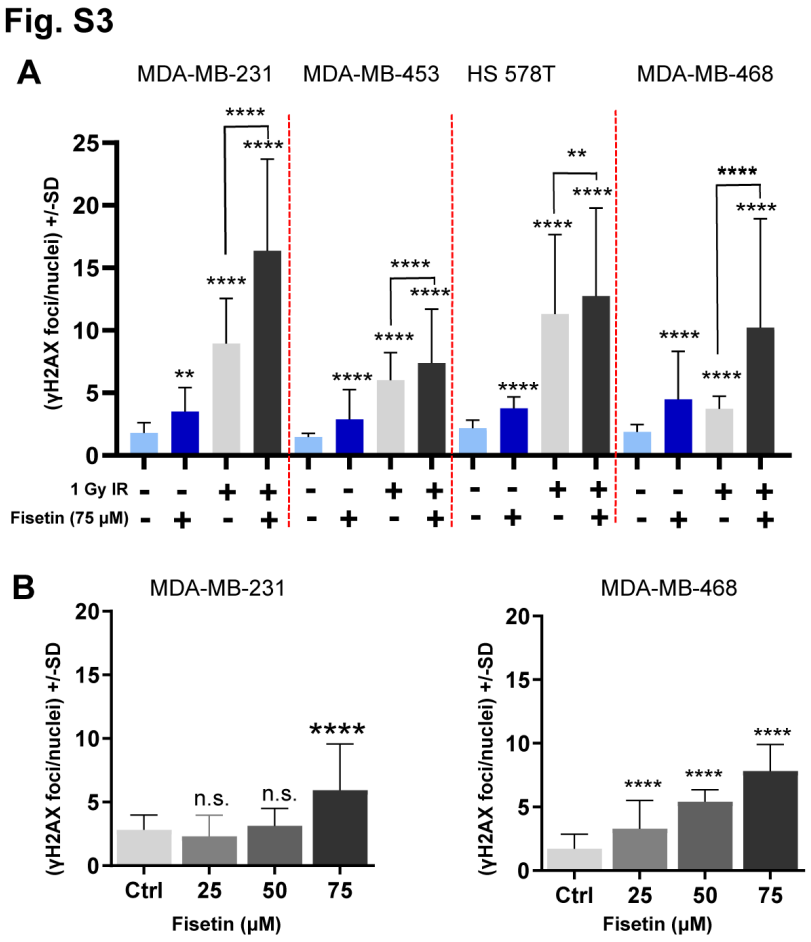

Fig. S3 Frequency of DSB induction after fisetin, IR and the combination of fisetin and ITR.

(A) Indicated cells were treated with fisetin (75 µl) or DMSO (0.07%) for 24 h and mock irradiated or irradiated with 1 Gy. Thirty minutes after irradiation ɣH2AX foci assay was performed as described in the *Methods* section. The bars indicate the mean ɣH2AX ± SD in 170 nuclei (MDA-MB-231) or 200 nuclei (MDA-MB-468, HS 578T, MDA-MB-468) from 2 independent experiments. **(B)** MDA-MB-231 and MDA-MB-468 cells were treated with indicated concentrations of fisetin. The DMSO concentration was adjusted to 0.07%. ɣH2AX foci assay was performed after 24 h. The bars indicate the mean ɣH2AX ± SD in 540 nuclei (MDA-MB-231) and 300 nuclei (MDA-MB-468) from 2 independent experiments. The asterisks indicate a significant difference in mean ɣH2AX ± SD compared to control or hee indicated conditions (*p< 0.05, **p< 0.01, ***p< 0.001), ****p< 0.0001; students t-test). n.s.: not significant.

Fig. S4 Khozooei *et al.* 2022

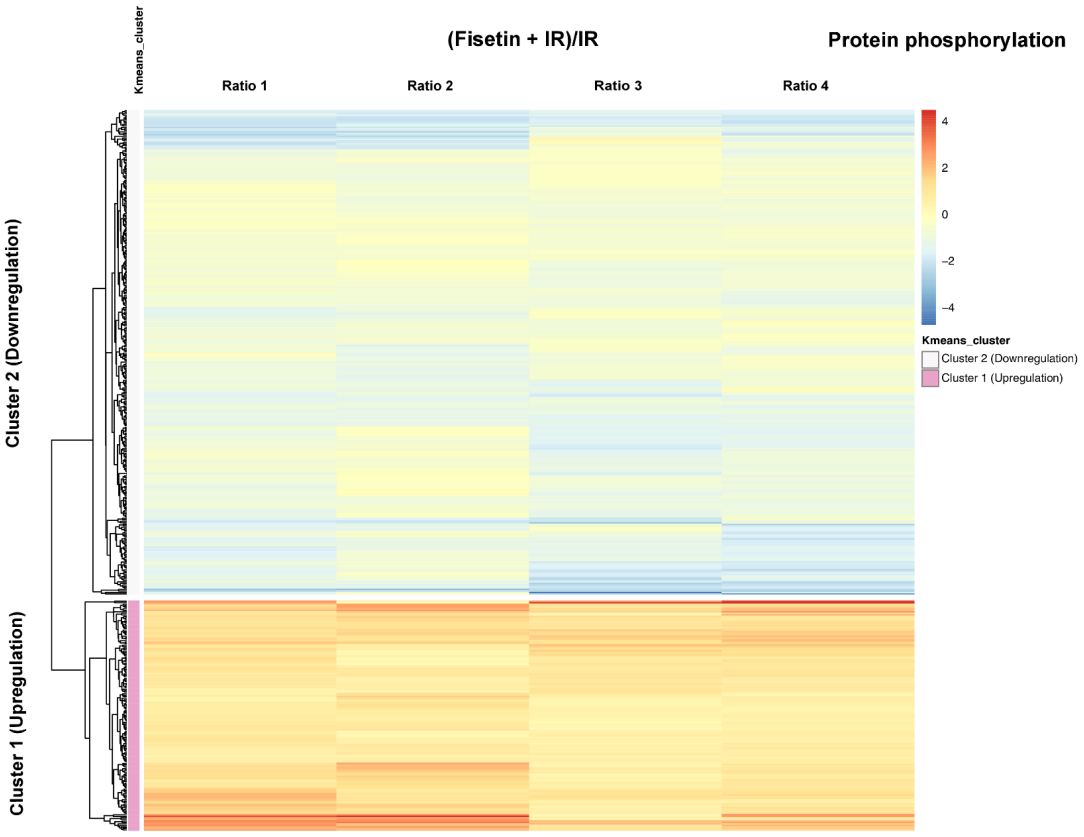

Fig. S4 Heat map, gene ontology and pathway analysis of phosphosites in MDA-MB-468 cells.

MDA-MB-468 cells were treated with 75 µM fisetin or DMSO for 24 hours and were irradiated at 4 Gy. Thirty minutes after IR, the proteins were extracted and the phosphoproteomic study was performed as described in the *Methods* section. **(A)** K means clustering showing in the heat map indicates up-regulated and down-regulated clusters for the analyzed phosphosites. GO analysis for enriched up-regulated **(B)** and down-regulated **(C)** phosphosites are indicated. The X-axis shows the number of genes, which are involved in the indicated pathways. The Y-axis represents pathways, which are ordered based on significance as indicated by the p-adj value

Fig. S5 Khozooei *et al.* 2022

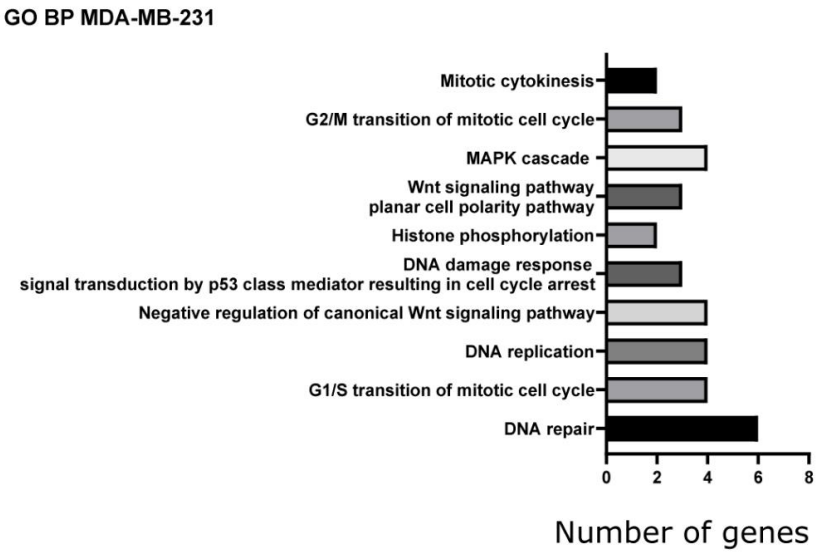

Fig. S5 Gene ontology analysis of MDA-MB-231 after pretreatment with fisetin.

MDA-MB-231 cells were treated with 75 µM fisetin or DMSO for 24 hours. Afterwards, the cells were mock irradiated or irradiated at 4 Gy. Thirty minutes after IR, the proteins were extracted and the phosphoproteomic study was performed as described in the *Methods* section. Gene ontology analysis was performed, and the deregulated genes involved in DNA damage response were categorized in different pathways.

Appendix B

Publication II

Radiotherapy and Oncology 188 (2023) 109867

Contents lists available at ScienceDirect

Radiotherapy and Oncology

journal homepage: www.thegreenjournal.com

Original Article

Fisetin overcomes non-targetability of mutated *KRAS* induced YB-1 signaling in colorectal cancer cells and improves radiosensitivity by blocking repair of radiation-induced DNA double-strand breaks

Shayan Khozooei [a,1], Soundaram Veerappan [a,1], Irina Bonzheim [b], Stephan Singer [b], Cihan Gani [a], Mahmoud Toulany [a,*]

[a] Department of Radiation Oncology, University Hospital Tübingen, Tübingen; and [b] Department of Pathology and Neuropathology, University Hospital Tuebingen, Tuebingen, Germany

ARTICLE INFO

Article history:
Received 24 February 2023
Received in revised form 20 July 2023
Accepted 20 August 2023
Available online 25 August 2023

Keywords:
Y-box binding protein-1
Colorectal cancers
DNA double-strand breaks
Fisetin
RSK/AKT dual targeting
p21-activated kinase

ABSTRACT

Background and purpose: *KRAS* is frequently mutated, and the Y-box binding protein 1 (YB-1) is overexpressed in colorectal cancer (CRC). Mutant *KRAS* (*KRAS*^{mut}) stimulates YB-1 through MAPK/RSK and PI3K/AKT, independent of epidermal growth factor receptor (EGFR). The p21-activated kinase (PAK) family is a switch-site upstream of AKT and RSK. The flavonoid compound fisetin inhibits RSK-mediated YB-1 signaling. We sought the most effective molecular targeting approach that interferes with DNA double strand break (DSB) repair and induces radiosensitivity of CRC cells, independent of *KRAS* mutation status.

Materials and Methods: KRAS activity and *KRAS* mutation were analyzed by Ras-GTP assay and NGS. Effect of dual targeting of RSK and AKT (DT), the effect of fisetin as well as targeting PAK by FRAX486 and EGFR by erlotinib on YB-1 activity was tested by Western blotting after irradiation *in vitro* and *ex vivo*. Additionally, the effect of DT and FRAX486 on DSB repair pathways was tested in cells expressing reporter constructs for the DSB repair pathways by flow cytometry analysis. Residual DSBs and clonogenicity were examined by γH2AX- and clonogenic assays, respectively.

Results: Erlotinib neither blocked DSB repair nor inhibited YB-1 phosphorylation under *KRAS* mutation condition *in vitro* and *ex vivo*. DT and FRAX486 effectively inhibited YB-1 phosphorylation independent of *KRAS* mutation status and diminished homologous recombination (HR) and alternative non-homologous end joining (NHEJ) repair. DT and FRAX486 inhibited DSB repair in CaCo2 but not in isogenic *KRAS*^{G12V} cells. Fisetin inhibited YB-1 phosphorylation, blocked DSB repair and increased radiosensitivity, independent of *KRAS* mutation status.

Conclusion: Combination of fisetin with radiotherapy may improve CRC radiation response, regardless of *KRAS*^{mut} status.

Advanced and metastatic colorectal cancers (CRCs) necessitate the use of adjuvant and/or neoadjuvant chemo- or chemoradiotherapy (CRT) regimens alongside surgical resection [1,2]. The treatment options depend on the stage and location of the cancer, as well as the patient's overall health. Chemotherapy is recommended for those metastatic CRCs that cannot initially be treated by surgery or is given as adjuvant therapy after surgery. Radiotherapy is more often used to treat rectal cancer than colon cancer. For rectal cancer, radiotherapy or CRT may be used as neoadjuvant therapy to shrink the tumor before surgery [3]. The response rate to standard chemotherapies have been assessed to be variable and quite low, at 10–60% [1,4]. Standard neoadjuvant chemoradiotherapies also display a very low pathological complete response of 15–20% [5]. On the other hand, recent advances in the field of targeted therapy have proven to significantly elevate the efficacy of chemotherapy and CRT [6,7]. The effectiveness of molecular targeted therapy largely relies on the genetic composition of the cancer. In this context, the effect of cetuximab-based anti-epidermal growth factor receptor (EGFR) therapy has been observed to be abrogated by the expression of *KRAS* mutation in colorectal cancers [8,9]. Generally, about 44% of colorectal cancers harbor *KRAS* mutations [9], in which targeting EGFR, which lies upstream of KRAS in the kinase cascade, will not be beneficial.

Y-box binding protein-1 (YB-1) is a multifunctional protein [10] that is highly expressed and phosphorylated at residue serine 102 (S102) in CRC tissues compared to normal tissues [11–13]. YB-1 is mainly phosphorylated by the serine/threonine protein kinase AKT

* Corresponding author at: Department of Radiation Oncology, University Hospital Tübingen, Hoppe-Seyler-Str. 3, 72076 Tübingen, Germany.
E-mail address: mahmoud.toulany@uni-tuebingen.de (M. Toulany).
[1] These authors share the first authorship.

https://doi.org/10.1016/j.radonc.2023.109867
0167-8140/

and a p90 ribosomal s6 kinase (RSK). Thus, YB-1 lies at the crossroads of the phosphoinositide-3-kinase (PI3K) and mitogen-activated protein kinase (MAPK) cascades and acts as one of the resultant phosphorylation sinks for receptor tyrosine kinase (RTK)-mediated cell survival and proliferation signals [14–16]. As a consequence, YB-1 has been implicated to play a significant role in pathways that are thought to promote the hallmark characteristics of cancer and therapy resistance [12,17–19].

p21-activated serine/threonine kinase (PAK) proteins are a family of conserved non-receptor serine/threonine kinases that integrate various survival signaling pathways regulated by RAS oncogenes. Among the six PAK isoforms, PAK1, downstream to KRAS, directly interacts with PDK1 and stimulates AKT activity. In the interaction with PDK1, PAK1 is also phosphorylated and activated by PDK1 [20]. Thus, PAK1 can potentially be one of the kinases regulated by oncogenic KRAS that stimulates AKT phosphorylation, independent of PI3K. A functional interaction exists between ERK1/2 and PAK1. Within this interaction, PAK1 activates ERK1/2 through MEK1/2 [21] and ERK1/2 also activates PAK1 [22]. Thus, according to the literature described above, it is rational to propose that PAK family members are the switch-point in the crosstalk between AKT and RSK involved in YB-1 phosphorylation.

The expression and phosphorylation of YB-1 stimulate the repair of ionizing radiation (IR)-induced double-strand breaks (DSBs), which are the most lethal type of DNA damage, and mediate radioresistance in breast cancer cells (BCC) [23,24]. Targeting YB-1 S102 phosphorylation through the dual inhibition of AKT and RSK was found to effectively block repair of IR-induced DSBs in BCC [24]. A recent study reported that the flavonoid compound fisetin effectively inhibits YB-1 phosphorylation and, in parallel with the induction of DSBs, inhibits the repair of IR-induced DSBs [25].

We investigated the effect of dual targeting (DT) of AKT and RSK, targeting PAK, targeting EGFR, and fisetin treatment on YB-1 S102 phosphorylation, repair of IR-induced DSBs and radiation response in CRC cells. The DT approach and targeting PAK strongly reduced YB-1 phosphorylation, independent of *KRAS* mutation status, *in vitro*. In the *ex vivo* study, DT completely inhibited YB-1 phosphorylation, while PAK targeting had a moderate inhibitory effect. Both approaches inhibited DSB repair in CaCo2 parental but not in CaCo2 $KRAS^{G12V}$ cells. However, neither approach affected post-irradiation cell survival independent of *KRAS* mutation status. Erlotinib inhibited YB-1 phosphorylation in *KRAS* wild-type ($KRAS^{wt}$) cells but not in $KRAS^{G12V}$ mutated cells or $KRAS^{G12V}$ mutated tumor tissue, without inhibiting DSB repair in any cell line. Fisetin inhibited YB-1 phosphorylation, interfered with DSB repair, and reduced post-irradiation cell survival independent of *KRAS* mutation status.

Materials and methods

Cell lines

The human CRC cell lines, $KRAS^{wt}$ SW48 (ATCC, CCL-231), and the heterozygous $KRAS^{G13D}$ mutated HCT116 (ATCC, CCL-247) were cultured in Dulbecco's Modified Eagle's Medium (DMEM) routinely supplemented with 10% (v/v) Fetal Calf Serum (FCS) and 1% (v/v) Penicillin-Streptomycin (stock of 10,000 U/mL Penicillin and 10,000 µg/mL Streptomycin) (P/S). Additionally, a $KRAS^{wt}$ CRC cell line, CaCo2 (ATCC, HTB-37), stably transfected with a doxycycline-inducible $KRAS^{G12V}$ expression system [26] was used. The cells were cultured as described previously [27]. U2OS osteosarcoma cells expressing reporter constructs for DSB repair pathways, *i.e.,* homologous recombination (HR), classical non-homologous end joining (C-NHEJ) and alternative NHEJ (Alt-NHEJ) repair pathways, developed in the laboratory of Dr. Jeremy Stark [28] were cultured in DMEM containing 10% FCS, 1% P/S and 2 µg/ml of puromycin.

Antibodies, reagents, inhibitor treatment, hypoxia treatment and irradiation

The antibodies and reagents used are described in the Supplementary Information. The AKT inhibitor MK2206, the RSK inhibitor LJI308, the EGFR inhibitor Erlotinib, the PAK inhibitor FRAX486, and fisetin were reconstituted in dimethyl sulfoxide (DMSO). Doxycycline, Puromycin, and Blasticidine were reconstituted in ultrapure water. For each treatment, the inhibitors were diluted to the required working concentration in culture medium as described in every figure-legend before being applied to the test cultures, while control cultures received an equivalent amount of DMSO. Severe hypoxia treatment (<0.01% O_2) was applied using the BD-GasPak™ EZ Pouch-Systems. Irradiation was performed as described before [25].

KRAS activity assay and Western blotting

The levels of cellular GTP-bound KRAS were measured using a RAS activity assay kit, by following the manufacturer's protocol and as described in detail previously [29]. The variations in cellular phospho-protein and total-protein levels with different treatments were assessed by Western blotting as described previously [30]. The protein bands were visualized using a LI-COR Biosciences chemiluminescence detection system (Bad Homburg, Germany).

Analysis of YB-1 signaling cascade in tumor tissue ex vivo

Patients who had undergone initial surgical treatment were included in the study. Previous neoadjuvant treatment or CRT were the rule-out criteria. The study was approved by the Ethics Committee of the Medical Faculty University Tuebingen (confirmation 525/2020BO) and patients gave signed informed consent. Tumor materials were collected and cultured as describe before [31]. Cultures were treated with the indicated inhibitors for 24 h and protein samples were isolated from the tumor pieces 30 minutes post-irradiation and Western blotting was performed.

γH2AX foci assay, flow cytometric analysis of apoptosis and analyzing DSB repair pathway

γH2AX foci assay, flow cytometric analysis of apoptosis and analyzing DSB repair pathway were performed as described before [25]. Flow cytometric analysis was carried out using BD FACSCanto™ System and the data were analyzed by Floreada.io. To analyze the off-target effect of the inhibitors on GFP intensity, U2OS cells expressing the indicated DSB repair constructs were transfected with a plasmid encoding GFP (800 ng/ml) from transfection kit #VCA-1003 (Lonza, Cologne, Germany) using lipofectamine LTX. Twenty-four hours after transfection, cells were treated with the inhibitors for an additional 24 h. Thereafter, images were captured using a fluorescence microscope and the mean intensity of GFP in GFP positive cells was measured using Image J software (https://imagej.nih.gov) and graphed.

KRAS sequencing

Genomic DNA was extracted from paraffin sections and used for *KRAS* sequencing, as described in Supplementary Information.

Clonogenic assay, statistical analysis and densitometries

The clonogenic assay was performed to test the post-irradiation cell survival in CaCo2 parental, CaCo2-$KRAS^{G12V}$ and SW48 cells, both with and without pretreatment with the indicated inhibitors. The pretreatments consisted of fisetin (75 µM for 24 h), dual inhibition of AKT (5 µM MK2206 for 2 h) and RSK (10 µM LJI308 for 2 h), or inhibition of PAK (10 µM FRAX486 for 2 h). Thereafter, irra-

diation (0, 2 or 4 Gy) was performed and 24 h after irradiation, cells were trypsinized and plated in 6-well plates in medium containing 20% FCS without additional treatment. The survival fraction for each radiation dose was calculated and graphed as previously described [25], using SigmaPlot (Version 7.0, SPSS Inc., Chicago, Illinois, USA). Statistical analysis and densitometries were performed as described before using GraphPad Prism (Version 9.4.1, San Diego, USA) and Image Studio Lite (Version 5.2, LI-COR Biosciences, Bad Homburg, Germany) [25].

Results

The YB-1 phosphorylation status was examined in colorectal cancer (CRC) cells with activating mutations in the KRAS/MAPK pathway. Compared with *KRAS*^{wt} SW48 and CaCo2 cells, HCT116 cells with a heterozygous *KRAS*^{G13D} mutation revealed increased KRAS activity, as shown by the level of KRAS bound to the RAS binding domain of Raf1 (Raf1-RBD). Similarly, inducing the expression of *KRAS*^{G12V} mutation in CaCo2 with doxycycline (2 μg/ml) stimulated KRAS activity 72 h after doxycycline treatment (Fig. 1A). YB-1 showed increased phosphorylation at S102 not only in cell lines with an activating mutation in *KRAS*, but also in *KRAS*^{wt} SW48 cells (Fig. 1A). Phosphorylation of YB-1 in CaCo2 cells after overexpression of *KRAS*^{G12V} was enhanced 3-fold (Fig. 1A). The Western blot (Fig. 1B) and densitometry values (Fig. 1C) indicate a time-dependent increase in phosphorylation of YB-1 along with an increase in the expression of *KRAS*^{mut} and the exogenous *KRAS*^{G12V} gene expression marker GFP within 6 days of doxycycline treatment in CaCo2 cells. This was in association with an increase in phosphorylation of ERK1/2 and AKT (Fig. 1B-C). Since the role of RSK downstream of ERK1/2 as well as AKT on YB-1 phosphorylation has been proposed [14,15], we examined the long-term (72 h) effect of targeting RSK and AKT on YB-1. In CaCo2 parental cells, the effect of AKT inhibitor MK2206 (5 μM) seemed to be stronger than the effect of RSK inhibitor LJI308 (10 μM) on YB-1 phosphorylation (Fig. 1D). In contrast, after *KRAS*^{G12V} induction, stimulated YB-1 phosphorylation became dependent on RSK but not AKT as shown by Western blot (Fig. 1D). Since LJI308 is an ATP competitive inhibitor of RSK N-terminal kinase domain, it did not inhibit RSK phosphorylation at T359/S363, which are not reported to be dependent on RSK kinase activity. Regardless of *KRAS* mutation status, DT of RSK and AKT was the most effective approach to block YB-1 phosphorylation (Fig. 1D).

In CRC cells, inhibition of RSK by LJI308 under non-irradiated conditions leads to the activation of AKT [11]. AKT is a key component in IR-induced DNA damage repair (DDR). Since YB-1 also plays a major role in DDR signaling, we tested pattern of YB-1 phosphorylation after irradiation in CRC cells pretreated with the RSK and AKT inhibitors. A pronounced IR-induced phosphorylation of YB-1 in parental CaCo2 cells was slightly inhibited by MK2206 (5 μM, 72 h) but not by LJI308 (10 μM, 72 h) (Fig. S1, Densitometry). *KRAS*^{G12V} stimulated YB-1 phosphorylation was not further stimulated by IR (Fig. S1). However, it was inhibited by LJI308 but not by MK2206. DT of AKT and RSK efficiently inhibited YB-1 phosphorylation independent of *KRAS* mutation status (Fig. S1).

In further experiments, the signaling pathways underlying YB-1 phosphorylation were investigated *in vitro* and *ex vivo*. The data presented in Fig. 2A indicates that similar to the RSK/AKT dual targeting, the PAK inhibitor FRAX486 inhibits YB-1 phosphorylation independent of *KRAS* mutation status *in vitro*, which was not reactivated with time upon PAK inhibition (Fig. S2). FRAX486 also effectively reduced YB-1 phosphorylation in all tested CRC cell lines, including SW48 and HCT116 (Fig. S3), with a stronger effect in *KRAS*^{wt} cells than in *KRAS*^{mut} cells (Fig. S3). Since functional control of EGFR on the PI3K/AKT and MAPK/ERK pathways is known to be impaired after *KRAS* mutations, the EGFR inhibitor erlotinib (10 μM, 72 h) did not block YB-1 phosphorylation in *KRAS*^{G12V} expressing CaCo2 cells (Fig. 2A). In the *ex vivo* analyses, RSK/AKT DT effectively inhibited YB-1 phosphorylation in the tumor samples of all four patients (Fig. 2B, D-F). The effects of FRAX486 and erlotinib on YB-1 phosphorylation were inconsistent among different patient samples. FRAX486 did not inhibit YB-1 phosphorylation in patient sample #1 and #4 (Fig. 2B, F) but it did in sample #3 (Fig. 2E). Erlotinib did not inhibit YB-1 phosphorylation in patient sample #1 and #4 (Fig. 2B, F) but it inhibited this phosphorylation in #2 and #3 (Fig. 2D-E). Sequencing of the *KRAS* gene revealed a *KRAS*^{G12V} point mutation in patient sample #1 but not in the samples #2, #3, and #4 (Fig. 2C). Surprisingly, the pattern of YB-1 phosphorylation after treatment in some of the two replicates of the same tumor tissue was found to be different. In this regard, one of the examples highlighting the differential response is the level of IR-induced YB-1 phosphorylation in the replicates of control (ctrl) conditions in tissue #2 and tissue #3 (Fig. 2D). Another example is the inhibition of IR-induced YB-1 phosphorylation using the AKT inhibitor MK2206 and PAK inhibitor FRAX486 in one of the replicates in tissue #2 (Fig. 2D). Similarly, a difference could also be observed in terms of YB-1 phosphorylation between the two replicates treated with MK2206 in patient sample #3 (Fig. 2E). In contrast, the pattern of AKT phosphorylation in two replicates was similar in the patient sample #2, *i.e.*, it was induced by irradiation, inhibited by MK2206 and DT and slightly reduced by FRAX486 (Fig. 2D). On the other hand, all the replicates of patient sample #4 showed similar patterns of YB-1 and AKT phosphorylation, except for the replicates treated with erlotinib (Fig. 2F). LJI308 was more effective than MK2206 on YB-1 phosphorylation in all four tumor tissues (Fig. 2B, D-F). Given that a potential hypoxic area in tumor slices can impact the signaling pattern with and without inhibitor treatment, we replicated the experiment depicted in Fig. 2A under normoxic and severe hypoxic conditions. Surprisingly, we observed a suppression in the phosphorylation of RSK, AKT, and YB-1 in response to hypoxia (Fig. S4) in both CaCo2 parental cells as well as cells overexpressing *KRAS*^{G12V}.

We have previously reported that fisetin inhibits YB-1 phosphorylation and impairs the repair of IR-induced DSBs by suppressing the c-NHEJ and HR repair pathways [25]. Here we could show that pretreatment with the combination of the AKT inhibitor MK2206 (5 μM) and the RSK inhibitor LJI308 (10 μM), indicated as DT, or the PAK inhibitor FRAX486 (10 μM) for 24 h inhibit repair of I-SceI-induced DSB by HR and Alt-NHEJ in U2OS cells, as shown by the FACS plots (Fig. 3B) and percentage of GFP-positive cells (Fig. 3C). FRAX486 inhibited C-NHEJ, but the effect of DT on this pathway was not significant (Fig. 3C). To exclude nonspecific effect of the inhibitors used on GFP expression, U2OS cells were transiently transfected with a plasmid encoding enhanced GFP and treated with the inhibitors as described above. DT did not affect GFP expression in any of the cell lines tested. In contrast, FRAX486 markedly reduced GFP expression/fluorescence intensity in all cell lines (Fig. 3D). Effect of DT and FRAX486 on phosphorylation of YB-1 and YB-1 activating cascades in U2OS cells has been shown in Fig. 3E.

Due to the observed effect of the applied approaches on the key DSB repair pathways, in subsequent experiments, we investigated the effect of dual targeting of RSK/AKT, single targeting of PAK, and the effect of fisetin on residual DSBs, apoptosis, and radiosensitivity. Overexpression of *KRAS*^{G12V} enhanced absolute number of γH2AX foci in non-irradiated as well as irradiated conditions (Fig. 4A-B,D, Figs. S6A-C). DT of RSK/AKT as well as targeting PAK by FRAX486 impaired repair of IR-induced DSB in only CaCo2 parental cells (Fig. 4A-B, Figs. S6A-B). However, DT did not affect post-irradiation cell survival of both parental and *KRAS*-mutated CaCo2 cells (Fig. S7). Targeting PAK by FRAX486 slightly induced radiosensitization in *KRAS*-mutated CaCo2 cells but not in parental cells (Fig. S7). EGFR inhibitor erlotinib not only did not abrogate DSB repair in either of the cells (Fig. S5) but it also significantly stimulated repair after irradiation in *KRAS*^{G12V} cells. Such an effect was also observed in *KRAS*^{wt} cells in the presence or absence of

Fisetin overcomes non-targetability of mutated KRAS/YB-1 survival signaling in CRC

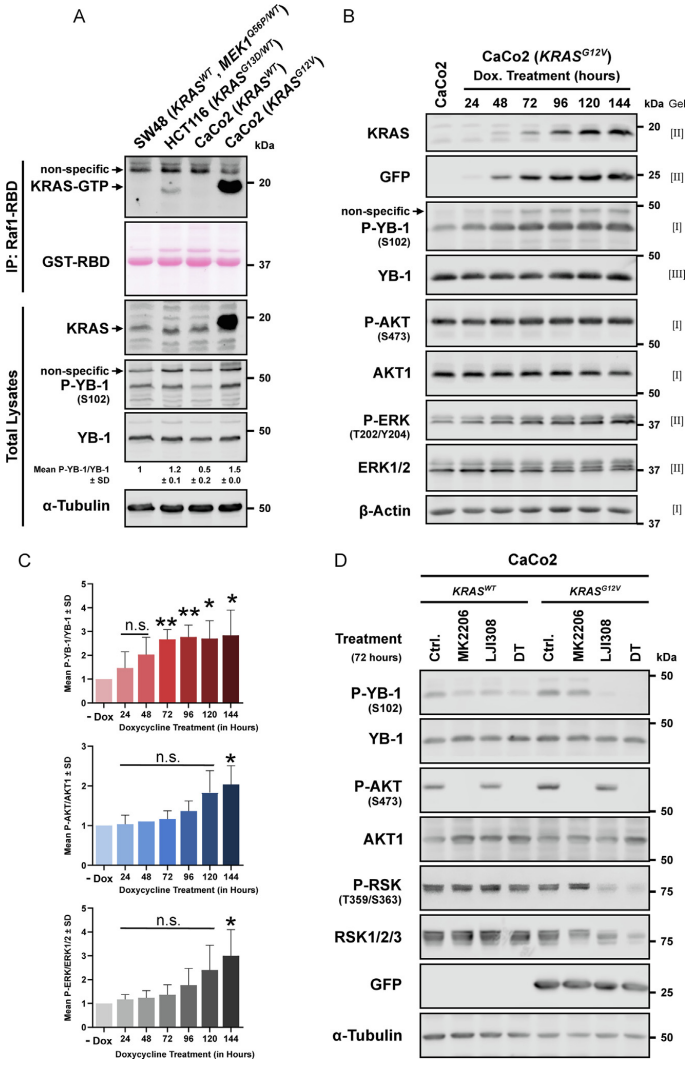

Fig. 1. YB-1 is highly phosphorylated in CRC cells with an activating mutation in MAPK pathways. (A) Protein samples were isolated from the indicated CRC cells without treatment or 72 h after treatment with doxycycline (2 μg/ml) to induce *KRAS*^{G12V} (CaCo2-*KRAS*^{G12V}). Activated KRAS was pulled down after IP of Raf1-RBD as described in the Method section and subjected to SDS-PAGE along with the total lysate. Indicated proteins were detected by Western blotting. GST-RBD was visualized by Ponceau S staining. Densitometry shows the mean ratio of P-YB-1/YB-1 from 2 experiments normalized to 1 in *KRAS*^{wt} SW48 cells. (B) CaCo2 cells were treated with doxycycline (2 μg/ml) for the indicated time points. Protein samples were isolated and used for Western blotting. (C) Mean ratio of P-YB-1/YB-1, P-AKT/AKT1, and P-ERKs (ERK1/2)/ERK1/2 based on the data presented in panel B from 3 biological replicates. In one of the replicates, total YB-1 was detected from a different gel (gel-III), whereas P-YB-1 was detected from gel-I. The asterisks indicate significant difference in phosphorylation of the indicated proteins after expression of KRAS^{G12V} compared to the control condition without doxycycline (- Dox) treatment (*p < 0.05, **p < 0.01, students t-test) (N = 3), n.s. = non-significant. (D) The CaCo2 parental cells and the cells after 72 h pretreatment with doxycycline (CaCo2-*KRAS*^{G12V}) were treated with the AKT inhibitor (MK2206, 5 μM), the RSK inhibitor (LJI308, 10 μM), or a combination of both inhibitors as a DT approach for 72 h, and the protein samples were isolated and used for Western blotting. Similar data was obtained from two additional replicates in which cells were treated with doxycycline for 48 h prior to inhibitor treatment. (A-B, D). Blots were then stripped and incubated with antibodies against total proteins. α-Tubulin or β-actin was detected as loading control.

irradiation (Fig. S5). The flavonoid compound fisetin was recently described as an effective approach to block YB-1 phosphorylation, impair DSB repair, and increase radiosensitivity in triple-negative BCC [32]. We investigated whether fisetin is effective in inhibiting phosphorylation of YB-1 and impairing DSB repair in CRC cells. Pretreatment with fisetin (75 μM for 24 h) inhibited YB-1, RSK and ERK1/2 phosphorylation in CaCo2 parental cells. In *KRAS*^{G12V} cells, fisetin inhibited phosphorylation of YB-1 and RSK but induced ERK1/2 phosphorylation (Fig. 4C). In neither of the cell lines phospho-AKT was inhibited by fisetin (Fig. 4C). Fisetin treatment significantly inhibited DSB repair, (Fig. 4D, Fig. S6C) and induced radiosensitization independent of *KRAS* mutation status (Fig. 4E). The radiosensitizing effect of fisetin was markedly stronger in *KRAS*^{G12V} than in the *KRAS*^{wt} parental cells (Fig. 4E). The com-

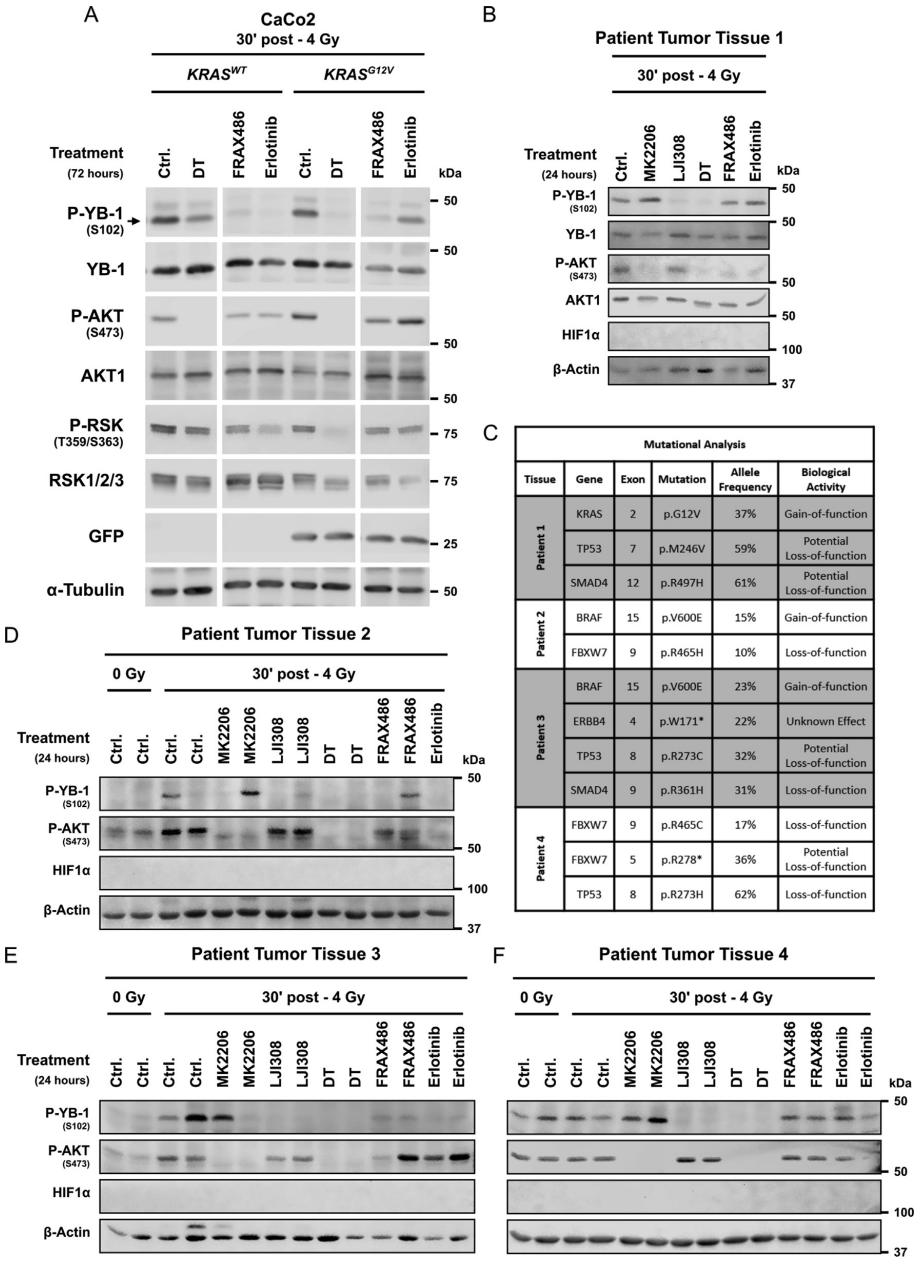

Fig. 2. Underlying signaling pathways in YB-1 phosphorylation *Ex vivo*. (A) CaCo2 cells were treated without or with doxycycline (2 μg/ml) for 72 h and treated with the combination of the AKT inhibitor MK2206 (5 μM) and RSK inhibitor LJI308 (10 μM), indicated as DT, PAK inhibitor FRAX486 (10 μM) or EGFR inhibitor erlotinib (10 μM) for 72 h. Concentration of DMSO was kept identical in all treatment conditions (0.125%). Thereafter, cells were irradiated (4 Gy) and protein samples were isolated 30 min after irradiation. Phospho-proteins were detected by Western blotting using phospho-specific antibodies. Blots were stripped and incubated with the corresponding antibody against total proteins. GFP was detected to verify exogenous $KRAS^{G12V}$ expression. Similar data was obtained from two additional replicates in which cells were treated with doxycycline for 48 h prior to inhibitor treatment. (B, D-F) Cultured tumor tissues were treated with the indicated inhibitors as described in panel A for 24 h. Thereafter, the cultures were mock irradiated (D-F) or irradiated with 4 Gy (B, D-F). Protein samples were isolated 30 min post-IR and subjected to SDS-PAGE. Level of indicated phospho-proteins were detected by Western blotting using phospho-specific antibodies, followed by stripping and incubating with AKT1 and YB-1 (B) antibodies. α-Tubulin (A) and β-actin (B, D-F) were detected as loading control. (C) Gene mutational analysis of patient tissue sample obtained by NGS, indicating protein variants and their allele frequency.

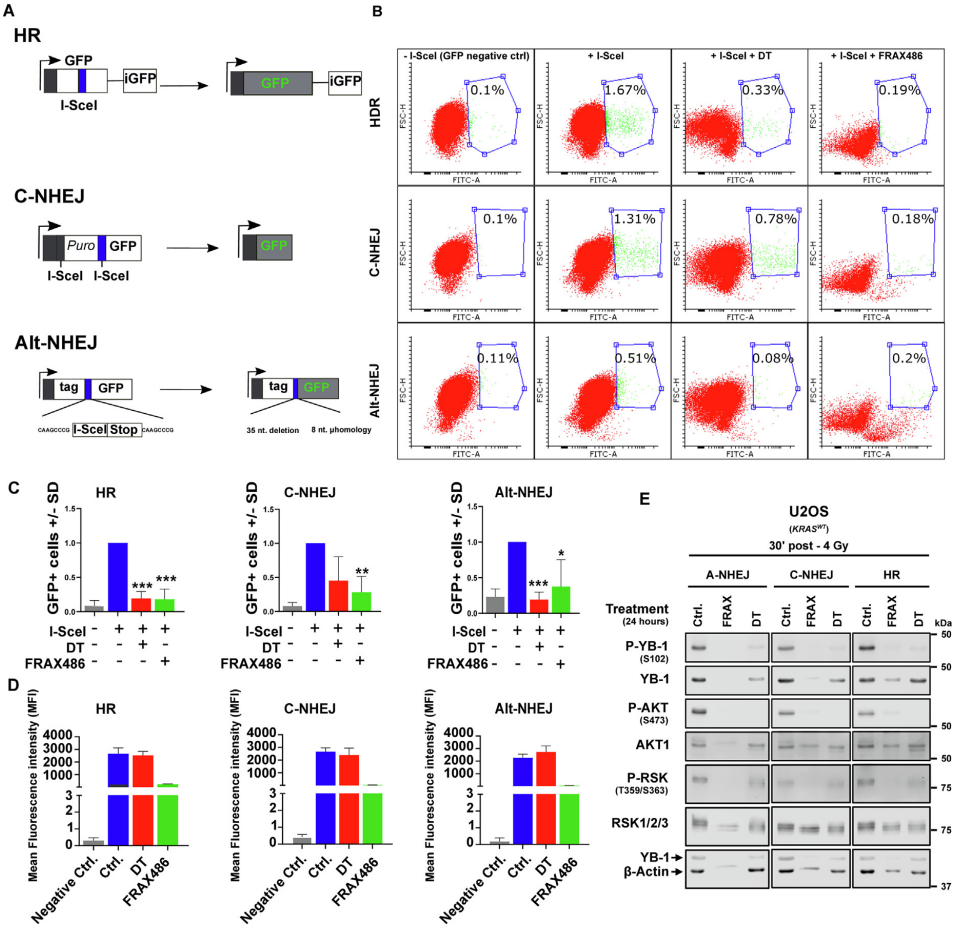

Fig. 3. Impact of targeting PAK and DT of RSK/AKT on NHEJ and HR repair pathways. U2OS cells stably expressing DSB repair constructs (A) were either transiently transfected with an inducible endonuclease I-SceI plasmid (800 ng/ml) or not transfected as a negative control (-I-SceI condition). (B) Cells were treated with the DT (5 μM MK2206, and 10 μM RSK inhibitor LJI308,), or FRAX486 (10 μM). Control cells (+I-SceI condition) received DMSO (0.125%). Twenty-four hours after treatment with the inhibitors, nuclear translocation of I-SceI was induced by triamcinolonacetonid (100 ng/ml) and 24 h later the percentage of GFP positive cells were determined using FACS. (C) Histograms show the mean percentage of GFP-positive cells ± SD from three independent experiments normalized to the positive control condition treated with DMSO. Asterisks indicate a significant inhibition of the indicated repair pathways by the applied treatments (*p < 0.05, **p < 0.01, ***p < 0.001; students t-test). (D) U2OS cells were transfected with a plasmid encoding GFP. Cells were treated with the inhibitors 24 h after transfection for an additional 24 h. The mean intensity of GFP in GFP positive cells in the captured images was measured and graphed. Histograms show mean GFP intensity ± SD in 20 cells from 2 biological replicates. (E) U2OS cells were treated as described in part (B). Twenty-four hours after treatment, cells were irradiated with 4 Gy. Protein samples were isolated 30 min post-IR, subjected to SDS-PAGE and level of indicated phospho-proteins were detected by Western blotting. Blots were stripped and incubated with the corresponding antibodies against total proteins. β-actin was detected as loading control.

bination of fisetin with IR led to enhanced residual DSB, that was beyond an additive effect compared to the irradiation and fisetin treatment conditions in SW48 cells (Fig. S8A). This effect seems to be translated to radiosensitization as shown in Fig. S8B. To further test whether the elevated γH2AX foci is due to enhanced apoptosis rather than impaired repair of radiation-induced DSBs, we tested apoptosis induction in CaCo2 *KRAS*^{G12V} cells after fisetin, irradiation and the combination treatment conditions. Data shown in Fig. S9 indicates that fisetin but not irradiation induces apoptosis and the frequency of apoptotic cells in sub-G1 phase is not enhanced after combining irradiation with fisetin (Fig. S9). Additionally, the stimulation of IR-induced apoptosis was observed only after treatment with FRAX486 but not AKT/RSK DT (Fig. S10).

Discussion

CRC has a high frequency of *KRAS* mutations, which are often associated with resistance to radiotherapy via activation of down-

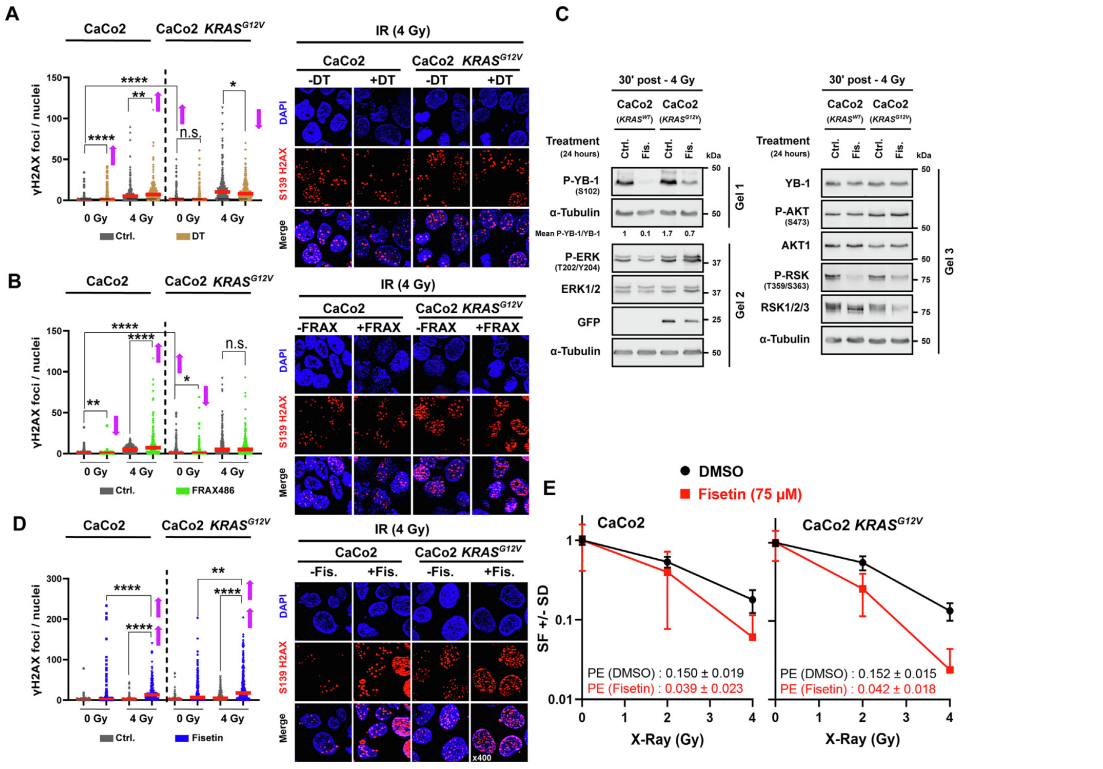

Fig. 4. Effect of DT of RSK/AKT and targeting PAK and treatment with fisetin on DSB repair. (A-E) CaCo2 cells were treated with or without doxycycline (2 μg/ml) for 48 h. (A-B) γH2AX assay was performed 24 h after irradiation without pretreatment or after 2 h pretreatment with the combination of MK2206 (5 μM) and LJI308 (10 μM), indicated as DT (A) or FRAX486 (10 μM) (B). (C) Cells were treated for 24 h with or without fisetin (75 μM). Protein samples were then isolated and loaded in three gels and electrophoresis was performed. Phosphorylated proteins and total proteins were detected with specific antibodies from the respective gel. α-Tubulin was detected separately in each gel as a loading control. (D) Cells were treated with fisetin (75 μM for 24 h) and mock irradiated or irradiated with 4 Gy, and the γH2AX foci assay was performed 24 h after irradiation. (A-B, D) The scatter plots represent the distribution of cells with different number of γH2AX foci. Red lines within the scatter plots represent mean number of foci per nuclei. Asterisks indicate significant difference in the frequency of γH2AX foci between the indicated conditions (*p < 0.05, **p < 0.01, ****p < 0.0001; students t-test) analyzed in 300 cells from 4 independent experiments (A, D) and 260 cells from 3 independent experiments (B). (A-B, D) The representative images after the described treatments in combination with irradiation. (E) Clonogenic survival assay was performed in CaCo2 and CaCo2 *KRAS*^{G12V} cells 24 h after mock irradiation or irradiation with 2 Gy or 4 Gy with or without 24 h of pretreatment with fisetin (75 μM). The data points represent the mean surviving fraction ± SD of 12 data from two experiments. Ctrl.: Control, DT: Dual targeting, n.s.: non-significant, FRAX: FRAX486, Fis.: Fisetin, PE: Plating efficiency, SD: standard deviation, SEM: standard error of mean. (A-B, D) Arrows represent significant increase or decrease in residual DSBs after treatment with the indicated inhibitors before irradiation.

stream survival signals. YB-1 is a multifunctional protein that plays a stimulatory role in a number of DNA repair mechanisms. It is highly expressed in CRC and is constitutively phosphorylated at S102 in *KRAS*-mutated cells. Of the various approaches tested with pharmacological inhibitors, EGFR kinase inhibitor erlotinib did not inhibit YB-1 phosphorylation under the *KRAS*^{mut} condition *in vitro* and *ex vivo* as well as in tumor tissue expressing oncogenic mutation in *KRAS* gene or genes that are known to stimulate KRAS signaling pathways. DT of RSK and AKT as well as the targeting of PAK family members by FRAX486 effectively inhibited YB-1 phosphorylation in both *KRAS*^{wt} and *KRAS*^{mut} cells *in vitro*. An effective inhibition of phospho-YB-1 was achieved by DT approach, *ex vivo*. DSB repair was inhibited by DT and FRAX486 only in *KRAS*^{wt} cells. In contrast, fisetin inhibited RSK/YB-1 signaling, impaired DSB repair and induced radiosensitization, independent of *KRAS* mutational status.

In agreement with previous reports [11,23], *KRAS*^{mut} cells HCT116 (*KRAS*^{G13D}) and CaCo2 (*KRAS*^{G12V}) showed constitutive and increased YB-1 phosphorylation. Unexpectedly, however, increased phosphorylation of YB-1 was also observed in *KRAS*^{wt} SW48 cells (see Fig. 1A). A further literature search revealed that SW48 cells have a heterozygous activating *MEK1*^{Q56P} mutation [32], a protein downstream of KRAS and upstream of RSK, a major YB-1 kinase. This supports the hypothesis that activation of KRAS or downstream KRAS components leads to increased phosphorylation of YB-1. Consistent with this, an increase in the expression of *KRAS* mutation resulted in an increase in PI3K/AKT and MAPK signaling and correlated with an increase in YB-1 phosphorylation (see Fig. 1B). Similar to *KRAS* mutation, exposure to IR can also stimulate KRAS activity [29], and activation of YB-1 as shown in BCC. [23,24,27]. Consistent with this, induction of YB-1 phosphorylation was observed in *KRAS*^{wt} CaCo2 cells but not in *KRAS*^{G12V} cells after irradiation (see Fig. S1).

Discovering the most effective approach to block YB-1 phosphorylation is a prerequisite for developing a strategy to disrupt YB-1-mediated activation of DDR signaling after IR exposure. AKT and RSK are considered the major kinases for the S102 residue of YB-1 [14,15]. However, changes in the activation level of individual kinases due to the mutational status of *KRAS* or other upstream components affect the influence of individual kinases on YB-1 phosphorylation [33]. In support of this, in the isogenic CaCo2 cell system, YB-1 phosphorylation was observed to be AKT-dependent in $KRAS^{wt}$ cells and RSK-dependent in $KRAS^{mut}$ cells (see Fig. 1D, Fig. S1). A previous work had shown that simultaneously targeting AKT and RSK efficiently inhibited basal, and chemotherapy induced YB-1 phosphorylation in $KRAS^{wt}$ SW48 and in $KRAS^{mut}$ HCT116 cells [11]. Consistent with this report, our present study also showed that DT of RSK and AKT efficiently reduced YB-1 phosphorylation independent of *KRAS* mutation status in non-irradiated and irradiated cells (see Fig. 1D, Fig. S1).

Effective inhibition of YB-1 phosphorylation by DT of RSK and AKT indicates a potential crosstalk between the two pathways [34]. In search of the switch-point in the crosstalk, we examined the function of PAK and EGFR and showed the PAK family members as the involved molecules. Not surprisingly, EGFR inhibition did not inhibit YB-1 phosphorylation in $KRAS^{G12V}$ cells (see Fig. 2). In contrast, PAK inhibition strongly reduced YB-1 phosphorylation in both, $KRAS^{wt}$ as well as $KRAS^{mut}$ cells *in vitro* with the lack of reactivation of YB-1 after long-term treatment (see Fig. S2). Nevertheless, data from *ex vivo* studies indicated that DT of RSK/AKT was superior to PAK inhibition (see Fig. 2B, D-E). Consistent with the *in vitro* studies, EGFR inhibition also did not block YB-1 phosphorylation in the tumor tissue with a *KRAS* mutation (see Fig. 2B). However, in one of the tumor tissues with wild-type *KRAS* (tissue sample #4), EGFR inhibition seemingly had no effect on YB-1 phosphorylation (see Fig. 2F). According to our sequencing data, we have observed that some patients exhibit loss of function mutations in the F-Box and WD Repeat Domain Containing 7 (*FBXW7*) gene (see Fig. 2C). Increased activation of ERK1/2 has been observed in esophageal squamous cell carcinoma cells with loss of function mutations in the *FBXW7* gene [35]. Since ERK1/2 lies directly downstream of KRAS and upstream of RSK, this could explain the $KRAS^{\mathbf{mut}}$ characteristics displayed by tissue sample #4 in terms of YB-1 phosphorylation, as seen with the absence of induction of YB-1 phosphorylation post-irradiation, reduced effect of PAK targeting and EGFR targeting, and a preference towards the MAPK/RSK pathway over the PI3K/AKT pathway (see Fig. 2F). Although tissue sample #2 also harbors a loss of function mutation in *FBXW7*, the allele frequency of the mutation seems to be quite low, which may also explain the heterogeneity between the replicates of sample #2 (see Fig. 2D). On the other hand, sample #4 which seems to display a more uniform pattern in terms of YB-1 phosphorylation harbors two loss of function mutations in *FBXW7*, with one mutation potentially leading to the truncation of the functional region of the protein [36]. The allele frequency of both mutations also seems to be higher when compared to sample #2 (see Fig. 2C). This could explain the $KRAS^{mut}$-like phenotype of sample #4 and the heterogenous phenotype of sample #2. Similar to sample #2, the level of YB-1 phosphorylation in sample #3 also varied between two biological replicates taken from the same tumor tissue with the same treatment (see Fig. 2E). This may again be indicative of genomic heterogeneity and variability within tumors of the same origin, necessitating a molecular targeting strategy with different combinations, e.g., DT of RSK/AKT, to overcome the selective effect caused by heterogeneity. Although the number of patient samples is limited, this data may suggest that tumor heterogeneity and the mutational status of the oncogenome can also be governing factors of the efficacy of DT of AKT/RSK or PAK inhibition. The observed variations in YB-1 signaling between similar treatment conditions may also be attributed to the differential levels of oxygenation in different tumor slices. *In vitro* experiments to determine the effect of severe hypoxia on YB-1 signaling revealed that the phosphorylation of AKT, RSK, and YB-1 are drastically reduced under severe hypoxic conditions (see Fig. S4). Although the tumor samples did not display detectable expression of HIF1α (see Fig. 2B, D-F), differential oxygenation and potential hypoxic regions cannot be completely ruled-out. To solidify these conclusions, a greater number of tumor samples should be tested.

The impact of targeting YB-1 on DSB repair has been shown to be the same as that after *KRAS* knockdown in $KRAS^{mut}$ BCC [23]. A study by Yang et al. showed that a number of isogenic CRC SW48 cell lines carrying $KRAS^{G12C}$, $KRAS^{G12D}$, or $KRAS^{G12V}$ allele mutations, as well as HCT116 cells expressing a $KRAS^{G13D}$ mutation, become radioresistant upon $KRAS^{\mathbf{mut}}$ expression [37], which was due to the upregulation of NRF2-53BP1-mediated NHEJ repair of DSBs [37]. Since YB-1 stimulates NRF2 expression [38], stimulating DSB repair by the above-described heterozygous mutations of *KRAS* may be YB-1-dependent. In an obvious conflict with the stimulatory role of mutated *KRAS* on DSB repair, in our study, overexpression of $KRAS^{G12V}$ enhanced residual DSBs (see Fig. 4A-B,D, Fig. S6A-C). This should be a difference caused by the use of different types of $KRAS^{\mathbf{mut}}$ expression systems. In the study by Yang et al. [37] mutated *KRAS* was stably expressed in the cells which would lead to the adaptation to the KRAS-mediated cellular replication stress. However, in the CaCo2 cells used in our study, we transiently overexpressed mutated *KRAS*, which would promote replication stress [39] and result in enhanced residual γH2AX foci in non-irradiated as well as in irradiated conditions.

DT of RSK/AKT was shown to effectively inhibit S102 phosphorylation *in vitro* and *ex vivo*. However, similar to PAK targeting, this approach inhibited DSB repair in the parental CaCo2 cells but not in isogenic $KRAS^{G12V}$ cells (see Fig. 4A-B, Fig. S6A-B). Although the EGFR inhibitor erlotinib inhibited YB-1 S102 phosphorylation in the $KRAS^{wt}$ CaCo2 cells, it did not inhibit AKT phosphorylation and DSB repair in these cells upon irradiation (see Fig. S5). Lack of effect on DSB repair might be because of YB-1-independent function of AKT in C-NHEJ and HR repair of DSBs [40–42], as outlined in Fig. 5. In $KRAS^{G12V}$ cells, since the cells also have endogenous $KRAS^{wt}$, inhibition of EGFR could lead to the abrogation of survival signaling pathways downstream to $KRAS^{wt}$. This can result in a compensatory enhancement of signaling pathways that are initiated from $KRAS^{mut}$, leading to stimulated DSB repair (see Fig. S5). Since S102 phosphorylation is involved in DSB repair [24], this data may indicate that other reported post-translational modification (PTMs) of YB-1 [38,43–45] may also be involved in DSB repair, an issue that remains to be investigated.

The flavonoid compound fisetin impairs YB-1 phosphorylation by inhibiting binding of RSK to YB-1 [46]. Here, we showed that fisetin blocks YB-1 phosphorylation and impairs DSB repair independent of *KRAS* mutation (see Fig. 4C-D, Fig. S6C). One of the potential mechanisms by which fisetin inhibits DSB repair in $KRAS^{mut}$ cells as well might be by inhibiting other PTMs of YB-1 in addition to S102 phosphorylation. Fisetin inhibits few other proteins involved in DDR signaling [25], which might be a second potential mechanism of the function of fisetin in inhibiting DSB repair and inducing radiosensitization, as outlined in Fig. 5. Inhibition of DSB repair by fisetin in the present study, regardless of *KRAS* mutation status, is consistent with the recent publication on the inhibition of DSB repair by this compound in BCC, which was shown to be through suppression of C-NHEJ and HR repair pathways [25]. Based on the upregulation of the C-NHEJ pathway by *KRAS* mutation [37], and the increase in residual DSBs upon inhibition of this pathway in *KRAS*-mutated BCC [25], it seems that C-NHEJ plays the major role in DSB repair and radioresistance in cells harboring *KRAS* mutations. In line with this conclusion, inhibition of C-NHEJ by DT in $KRAS^{wt}$ U2OS cells (Fig. 3B-C) was not significant. Although, the effect of PAK inhibitor FRAX486 on C-NHEJ was significant, on the one side this effect was weaker than the effect of FRAX486 on HR. On the other side, part of this observed effect might be because of FRAX486 inherently suppressing GFP

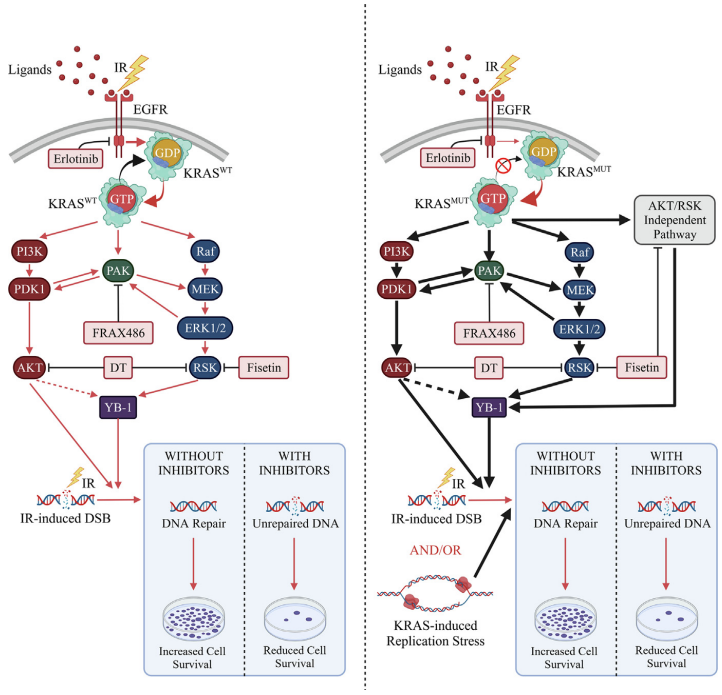

Fig. 5. Schematic comparison of signaling cascades downstream of wild type and mutated *KRAS* that are involved in YB-1 phosphorylation, DNA repair, and cell survival. Mutations in *KRAS* contribute to replication stress and increased downstream signaling, resulting in constitutive activation of DNA repair pathways. Additionally, AKT and RSK independent pathways may be activated in response to *KRAS* mutation. Fisetin inhibits both, AKT and RSK-dependent as well as -independent pathways and contributes to a reduction in post-irradiation cell survival. The schematic figure was created with BioRender.com.

expression or fluorescence intensity (see Fig. 3D). This could be one of the reasons behind the absence of any effect of DT or PAK targeting in $KRAS^{mut}$ cells.

IR inhibits clonogenic activity by inducing different types of cell-death, namely DSB-mediated mitotic catastrophe and apoptosis. In this study we could show that fisetin inhibits DSB repair and induces radiosensitization in CaCo2-$KRAS^{G12V}$ cells without stimulating IR-induced apoptosis (see Fig. 4, Fig. S6 and S9). In contrast, FRAX486 stimulated apoptosis and slightly radiosensitized cells without affecting DSB repair (see Figs. S6, S7 and S10). On the other hand, DT did neither affect DSB repair and radiosensitivity nor stimulated apoptosis (see Fig. S6, S7 and S10). From these data it might be concluded that impaired DSB repair to a certain degree is necessary but not sufficient for IR-induced clonogenic inactivation.

Collectively, to our knowledge this is the first report to introduce fisetin as a strategy that may improve CRT outcome in CRC, independent of *KRAS* mutation status.

Funding

This study was supported by a grant from the Deutsche Forschungsgemeinschaft (DFG, TO 685/2-3 to M.T.).

CRediT authorship contribution statement

Shayan Khozooei: Conceptualization, Validation, Formal analysis, Investigation, Data curation, Writing – original draft, Writing – review & editing. **Soundaram Veerappan:** Conceptualization, Validation, Formal analysis, Investigation, Data curation, Writing – original draft, Writing – review & editing. **Irina Bonzheim:** Validation, Formal analysis, Investigation, Data curation, Writing – original draft. **Stephan Singer:** Validation, Formal analysis, Data curation. **Cihan Gani:** Conceptualization, Resources, Project administration. **Mahmoud Toulany:** Conceptualization, Validation, Formal analysis, Investigation, Data curation, Writing – original draft, Writing – review & editing, Supervision, Project administration, Funding acquisition.

Declaration of Competing Interest

The authors declare that they have no known competing financial interests or personal relationships that could have appeared to influence the work reported in this paper.

Acknowledgements:

We would like to thank Cristine Sers (Laboratory of Molecular Tumor Pathology and Systems Biology, Institute of Pathology,

Charité Universitätsmedizin Berlin, Berlin, Germany) for kindly providing CaCo2 cells. We thank Simone Rebholz for assisting with the clonogenic assay experiments. We thank Sabrina Baumeister, Silke Theden and Sarah Butzer for their administrative support for the *ex vivo* study.

Appendix A. Supplementary material

Supplementary data to this article can be found online at https://doi.org/10.1016/j.radonc.2023.109867.

References

[1] Aparicio J, Esposito F, Serrano S, Falco E, Escudero P, Ruiz-Casado A, et al. Metastatic colorectal cancer. First line therapy for unresectable disease. J Clin Med 2020:9.
[2] Rodriguez-Bigas MA, Lin EH, Crane CH. Surgical management of colorectal cancer. Holland-Frei Cancer Medicine. BC Decker; 2003.
[3] Häfner MF, Debus J. Radiotherapy for colorectal cancer: Current standards and future perspectives. Visc Med 2016;32:172–7.
[4] Botrel TEA, Clark LGO, Paladini L, Clark OAC. Efficacy and safety of bevacizumab plus chemotherapy compared to chemotherapy alone in previously untreated advanced or metastatic colorectal cancer: a systematic review and meta-analysis. BMC Cancer 2016;16:677.
[5] Hoendervangers S, Burbach JPM, Lacle MM, Koopman M, van Grevenstein WMU, Intven MPW, et al. Pathological complete response following different neoadjuvant treatment strategies for locally advanced rectal cancer: A systematic review and meta-analysis. Ann Surg Oncol 2020;27:4319–36.
[6] Rodriguez J, Zarate R, Bandres E, Viudez A, Chopitea A, Garcia-Foncillas J, et al. Combining chemotherapy and targeted therapies in metastatic colorectal cancer. World J Gastroenterol 2007;13:5867–76.
[7] Elbanna M, Chowdhury NN, Rhome R, Fishel ML. Clinical and preclinical outcomes of combining targeted therapy with radiotherapy. Front Oncol 2021;11:749496.
[8] Ridouane Y, Lopes G, Ku G, Masud H, Haaland B. Targeted first-line therapies for advanced colorectal cancer: a Bayesian meta-analysis. Oncotarget 2017;8:66458–66.
[9] Hobbs GA, Der CJ, Rossman KL. RAS isoforms and mutations in cancer at a glance. J Cell Sci 2016;129:1287–92.
[10] Lasham A, Print CG, Woolley AG, Dunn SE, Braithwaite AW. YB-1: oncoprotein, prognostic marker and therapeutic target? Biochem J 2013;449:11–23.
[11] Maier E, Attenberger F, Tiwari A, Lettau K, Rebholz S, Fehrenbacher B, et al. Dual targeting of Y-box binding protein-1 and Akt inhibits proliferation and enhances the chemosensitivity of colorectal cancer cells. Cancers (Basel) 2019:11.
[12] Kim A, Shim S, Kim YH, Kim MJ, Park S, Myung JK. Inhibition of Y box binding protein 1 suppresses cell growth and motility in colorectal cancer. Mol Cancer Ther 2020;19:479–89.
[13] Yan X, Yan L, Zhou J, Liu S, Shan Z, Jiang C, et al. High expression of Y-box-binding protein 1 is associated with local recurrence and predicts poor outcome in patients with colorectal cancer. Int J Clin Exp Path 2014;7:8715–23.
[14] Stratford AL, Fry CJ, Desilets C, Davies AH, Cho YY, Li Y, et al. Y-box binding protein-1 serine 102 is a downstream target of p90 ribosomal S6 kinase in basal-like breast cancer cells. Breast Cancer Res 2008;10:R99.
[15] Sutherland BW, Kucab J, Wu J, Lee C, Cheang MC, Yorida E, et al. Akt phosphorylates the Y-box binding protein 1 at Ser102 located in the cold shock domain and affects the anchorage-independent growth of breast cancer cells. Oncogene 2005;24:4281–92.
[16] Mendoza MC, Er EE, Blenis J. The Ras-ERK and PI3K-mTOR pathways: cross-talk and compensation. Trends Biochem Sci 2011;36:320–8.
[17] Dhillon J, Astanehe A, Lee C, Fotovati A, Hu K, Dunn SE. The expression of activated Y-box binding protein-1 serine 102 mediates trastuzumab resistance in breast cancer cells by increasing CD44+ cells. Oncogene 2010;29:6294–300.
[18] Shiota M, Itsumi M, Yokomizo A, Takeuchi A, Imada K, Kashiwagi E, et al. Targeting ribosomal S6 kinases/Y-box binding protein-1 signaling improves cellular sensitivity to taxane in prostate cancer. Prostate 2014;74:829–38.
[19] D'Costa NM, Lowerison MR, Raven PA, Tan Z, Roberts ME, Shrestha R, et al. Y-box binding protein-1 is crucial in acquired drug resistance development in metastatic clear-cell renal cell carcinoma. J Exp Clin Cancer Res 2020;39:33.
[20] King CC, Gardiner EM, Zenke FT, Bohl BP, Newton AC, Hemmings BA, et al. p21-activated kinase (PAK1) is phosphorylated and activated by 3-phosphoinositide-dependent kinase-1 (PDK1). J Biol Chem 2000;275:41201–9.
[21] Wang Z, Fu M, Wang L, Liu J, Li Y, Brakebusch C, et al. p21-activated kinase 1 (PAK1) can promote ERK activation in a kinase-independent manner. J Biol Chem 2013;288:20093–9.
[22] Yuan L, Santi M, Rushing EJ, Cornelison R, MacDonald TJ. ERK activation of p21 activated kinase-1 (Pak1) is critical for medulloblastoma cell migration. Clin Exp Metastasis 2010;27:481–91.
[23] Toulany M, Schickfluss TA, Eicheler W, Kehlbach R, Schittek B, Rodemann HP. Impact of oncogenic K-RAS on YB-1 phosphorylation induced by ionizing radiation. Breast Cancer Res 2011;13:R28.
[24] Lettau K, Zips D, Toulany M. Simultaneous targeting of RSK and AKT efficiently inhibits YB-1-mediated repair of ionizing radiation-induced DNA double-strand breaks in breast cancer cells. Int J Radiat Oncol Biol Phys 2021;109:567–80.
[25] Khozooei S, Lettau K, Barletta F, Jost T, Rebholz S, Veerappan S, et al. Fisetin induces DNA double-strand break and interferes with the repair of radiation-induced damage to radiosensitize triple negative breast cancer cells. J Exp Clin Cancer Res 2022;41:256.
[26] Rossner F, Gieseler C, Morkel M, Royer HD, Rivera M, Blaker H, et al. Uncoupling of EGFR-RAS signaling and nuclear localization of YBX1 in colorectal cancer. Oncogenesis 2016;5:e187.
[27] Tiwari A, Rebholz S, Maier E, Dehghan Harati M, Zips D, Sers C, et al. Stress-induced phosphorylation of nuclear YB-1 depends on nuclear trafficking of p90 ribosomal S6 kinase. Int J Mol Sci 2018;19.
[28] Gunn A, Stark JM. I-Scel-based assays to examine distinct repair outcomes of mammalian chromosomal double strand breaks. Methods Mol Biol 2012;920:379–91.
[29] Toulany M, Baumann M, Rodemann HP. Stimulated PI3K-AKT signaling mediated through ligand or radiation-induced EGFR depends indirectly, but not directly, on constitutive K-Ras activity. Mol Cancer Res 2007;5:863–72.
[30] Toulany M, Dittmann K, Baumann M, Rodemann HP. Radiosensitization of Ras-mutated human tumor cells in vitro by the specific EGF receptor antagonist BIBX1382BS. Radiother Oncol 2005;74:117–29.
[31] Menegakis A, von Neubeck C, Yaromina A, Thames H, Hering S, Hennenlotter J, et al. γH2AX assay in ex vivo irradiated tumour specimens: A novel method to determine tumour radiation sensitivity in patient-derived material. Radiother Oncol 2015;116:473–9.
[32] Jing C, Li H, Du Y, Cao H, Liu S, Wang Z, et al. MEK inhibitor enhanced the antitumor effect of oxaliplatin and 5fluorouracil in MEK1 Q56Pmutant colorectal cancer cells. Mol Med Rep 2019;19:1092–100.
[33] Tiwari A, Iida M, Kosnopfel C, Abbariki M, Menegakis A, Fehrenbacher B, et al. Blocking Y-box binding protein-1 through simultaneous targeting of PI3K and MAPK in triple negative breast cancers. Cancers (Basel) 2020;12.
[34] Misale S, Fatherree JP, Cortez E, Li C, Bilton S, Timonina D, et al. KRAS G12C NSCLC models are sensitive to direct targeting of KRAS in combination with PI3K inhibition. Clin Cancer Res 2019;25:796–807.
[35] Pan Y, Liu J, Gao Y, Guo Y, Wang C, Liang Z, et al. FBXW7 loss of function promotes esophageal squamous cell carcinoma progression via elevating MAP4 and ERK phosphorylation. J Exp Clin Cancer Res 2023;42:75.
[36] Liu Y, Chen H, Bao H, Zhang J, Wu R, Zhu L. Comprehensive characterization of FBXW7 mutational and clinicopathological profiles in human colorectal cancers. Front Oncol 2023;13:1154432.
[37] Yang L, Shen C, Estrada-Bernal A, Robb R, Chatterjee M, Sebastian N, et al. Oncogenic KRAS drives radioresistance through upregulation of NRF2-53BP1-mediated non-homologous end-joining repair. Nucleic Acids Res 2021;49:11067–82.
[38] El-Naggar AM, Somasekharan SP, Wang Y, Cheng H, Negri GL, Pan M, et al. Class I HDAC inhibitors enhance YB-1 acetylation and oxidative stress to block sarcoma metastasis. EMBO Rep 2019;20:e48375.
[39] Di Micco R, Fumagalli M, Cicalese A, Piccinin S, Gasparini P, Luise C, et al. Oncogene-induced senescence is a DNA damage response triggered by DNA hyper-replication. Nature 2006;444:638–42.
[40] Mueck K, Rebholz S, Harati MD, Rodemann HP, Toulany M. Akt1 stimulates homologous recombination repair of DNA double-strand breaks in a Rad51-dependent manner. Int J Mol Sci 2017;18.
[41] Toulany M, Lee KJ, Fattah KR, Lin YF, Fehrenbacher B, Schaller M, et al. Akt promotes post-irradiation survival of human tumor cells through initiation, progression, and termination of DNA-PKcs-dependent DNA double-strand break repair. Mol Cancer Res 2012;10:945–57.
[42] Bozulic L, Surucu B, Hynx D, Hemmings BA. PKBalpha/Akt1 acts downstream of DNA-PK in the DNA double-strand break response and promotes survival. Mol Cell 2008;30:203–13.
[43] Hartley AV, Wang B, Mundade R, Jiang G, Sun M, Wei H, et al. PRMT5-mediated methylation of YBX1 regulates NF-kappaB activity in colorectal cancer. Sci Rep 2020;10:15934.
[44] Martin M, Hua L, Wang B, Wei H, Prabhu L, Hartley AV, et al. Novel Serine 176 phosphorylation of YBX1 activates NF-kappaB in colon cancer. J Biol Chem 2017;292:3433–44.
[45] Prabhu L, Mundade R, Wang B, Wei H, Hartley AV, Martin M, et al. Critical role of phosphorylation of serine 165 of YBX1 on the activation of NF-kappaB in colon cancer. Oncotarget 2015;6:29396–412.
[46] Sechi M, Lall RK, Afolabi SO, Singh A, Joshi DC, Chiu SY, et al. Fisetin targets YB-1/RSK axis independent of its effect on ERK signaling: insights from in vitro and in vivo melanoma models. Sci Rep 2018;8:15726.

Supplementary Material and Methods

Fisetin overcomes non-targetability of mutated *KRAS* in colorectal cancer cells and improves radiosensitivity by blocking repair of radiation-induced DNA double-strand breaks

Antibodies and reagents

The antibodies used for Western blotting – P-YB-1 (S102) (#2900), YB-1 (#9744), P-AKT (S473) (#4060), AKT1 (#2967), P-p90RSK (T359/S363) (#9344), RSK1/RSK2/RSK3 (#9355), P-p42/44 MAPK (ERK1/2) (T202/Y204) (#4377), p42/44 MAPK (ERK1/2) (#4695) – were purchased from Cell Signaling Technology (Frankfurt, Germany). Another AKT1 antibody (#610877) and HIF1α antibody (#610959) were purchased from BD Biosciences (Heidelberg, Germany). The KRAS antibody (#OP24) and the α-Tubulin antibody (#CP06) were purchased from Calbiochem (Schwalbach, Germany). Another KRAS antibody (#NBP2-45536) was purchased from Novus Biologicals (Wiesbaden Nordenstadt, Germany). The GFP antibody (#3H9) was purchased from ChromoTek GmbH (Planegg-Martinsried, Germany). The β-Actin antibody (#A2066) was purchased from Sigma-Aldrich (Taufkirchen, Germany). The anti-phospho-Histone H2AX (S139) antibody (#9718) used for immunofluorescence assays was purchased from Cell Signaling Technology (Frankfurt, Germany). The Cy3-conjugated donkey anti-rabbit secondary antibody (#711-166-152) used for immunofluorescence assays was purchased from Dianova GmbH (Hamburg, Germany). The RSK inhibitor LJI308 (#S7871), the AKT inhibitor MK2206 (#S1078), and the PAK inhibitor FRAX486 (#S7807) were purchased from Selleckchem (Munich, Germany). The EGFR inhibitor erlotinib was from Hoffmann-La Roche (Basel, Switzerland). Fisetin (#S2298) was purchased from Selleckchem (Munich, Germany). Doxycycline (#A2951) was purchased from AppliChem (Darmstadt, Germany). Puromycin (#P8833) and blasticidin (#15205) were purchased from Sigma-Aldrich (Taufkirchen, Germany). 20X LumiGLO Reagent and 20X Peroxide (#7003) were purchased from Cell Signaling Technology and used to visualize proteins on nitrocellulose membranes using horse-radish peroxidase tagged secondary antibodies. DAPI-containing mounting medium (#50011) was purchased from ibidi GmbH, (Gräfelfing, Germany) and was used for immunofluorescence assays. RAS activity assay reagent (Raf-1 RBD, agarose) (#14-278) was purchased from Sigma-Aldrich (Taufkirchen,

Germany). Lipofectamine LTX reagent was purchased from Invitrogen (Darmstadt, Germany). BD-GasPak™ EZ Pouch-Systems (B260683) was purchased from Fisher Scientific (Schwerte, Germany)

***KRAS* sequencing**

Genomic DNA was extracted from macrodissected 5 µm paraffin sections using the Maxwell® RSC DNA FFPE Kit and the Maxwell® RSC Instrument (Promega, Madison, WI, USA) according to the manufacturer's instructions. Targeted mutation analysis of *KRAS* hotspot codon 12 was performed by Next Generation Sequencing (Ion GeneStudio S5 prime, Thermo Fisher Scientific, Waltham, MA, USA) using an AmpliSeq Custom Panel covering *KRAS* exon 2. Amplicon library preparation and semiconductor sequencing was done according to the manufacturers' manuals using the Ion AmpliSeq Library Kit v2.0, the Ion Library TaqMan Quantitation Kit on the LightCycler 480 (Roche), the Ion 510 & Ion 520 & Ion 530 Kit – Chef on the Ion Chef and the Ion 530 Chip Kit (Thermo Fisher Scientific). Variant calling of non-synonymous somatic variants compared to the human reference sequence was performed using Ion Reporter Software (Thermo Fisher Scientific).

Fig. S1

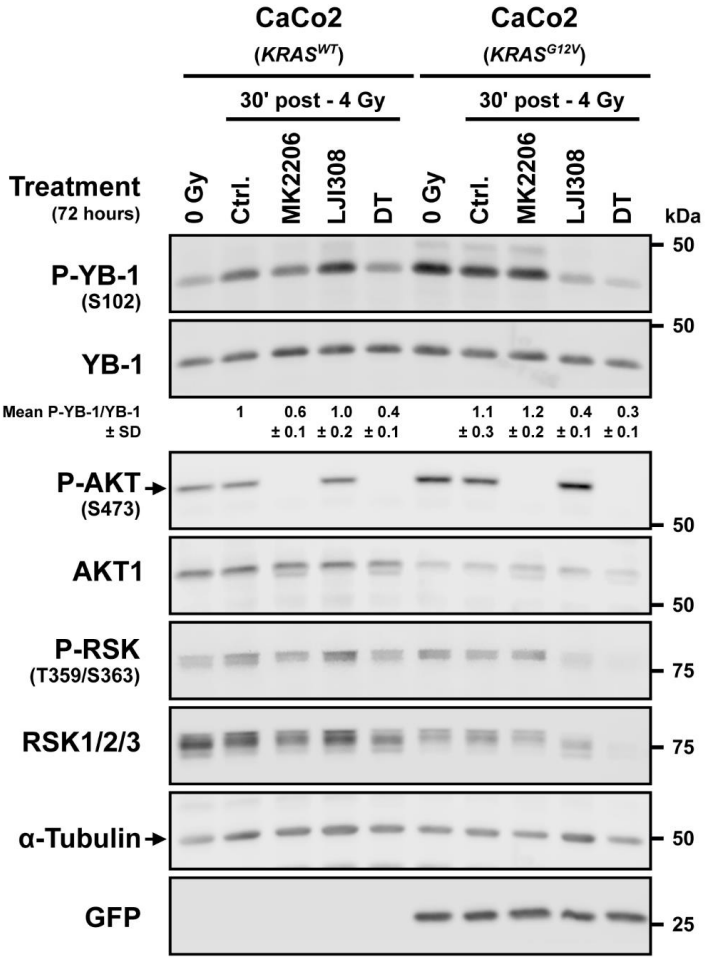

Fig. S1. DT of RSK and AKT is an effective approach to block YB-1 signaling in irradiated CRC cells independent of *KRAS* mutation status. CaCo2 cells were treated with and without doxycycline (2 µg/ml) for 48 h and treated with AKT inhibitor MK2206 (5 µM), RSK inhibitor LJI308 (10 µM) or the combination of both inhibitors as the DT. Concentration of DMSO was kept identical in different treated conditions (0.125%). Seventy-two hours after treatment cells were mock irradiated or irradiated with 4 Gy. Thirty minutes after irradiation protein samples were isolated and subjected to SDS-PAGE and level of indicated phospho-proteins were detected by Western blotting using phospho-specific antibodies. Blots were stripped and incubated with the corresponding antibody against total proteins. Densitometry values represent ratio of mean phospho-YB-1 to total-YB-1 from 3 independent experiments normalized to 1 in irradiated CaCo2 parental cells. GFP was detected to verify exogenous $KRAS^{G12V}$ expression. α-Tubulin was detected as loading control.

Fig. S2

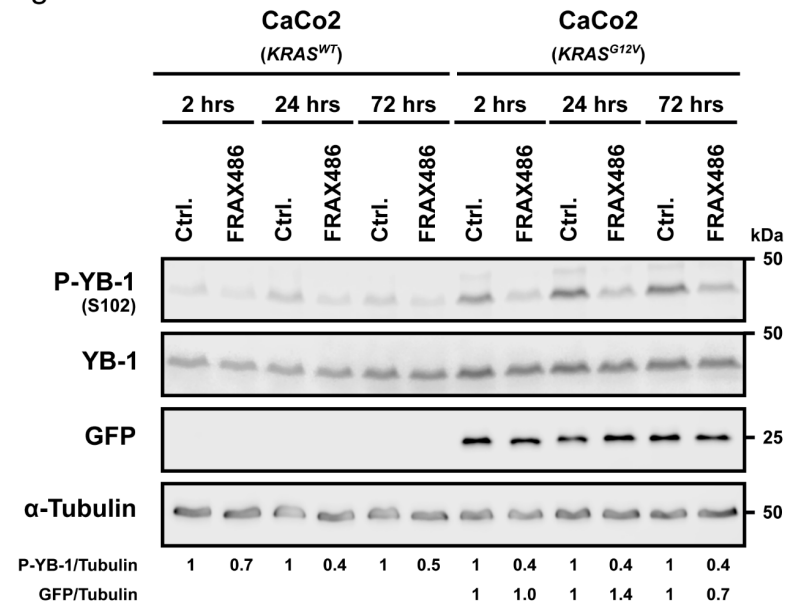

Fig. S2. Long-term inhibition of PAK does not result in reactivation of YB-1. CaCo2 cells were treated with and without doxycycline (2 µg/ml) for 48 h and treated with the PAK inhibitor FRAX486 (10 µM). At the indicated timepoints after treatment, protein samples were isolated and subjected to SDS-PAGE and level of phospho-YB-1 was detected by Western blotting using phospho-specific antibody. The blot was stripped and incubated with the corresponding antibody against total YB-1. GFP was detected as an indication for the expression of *KRAS*^{G12V}. Densitometry values represent ratio of phospho-YB-1 to α-Tubulin and GFP to α-Tubulin normalized to 1 in the corresponding control. Ctrl.: Control.

Fig. S3

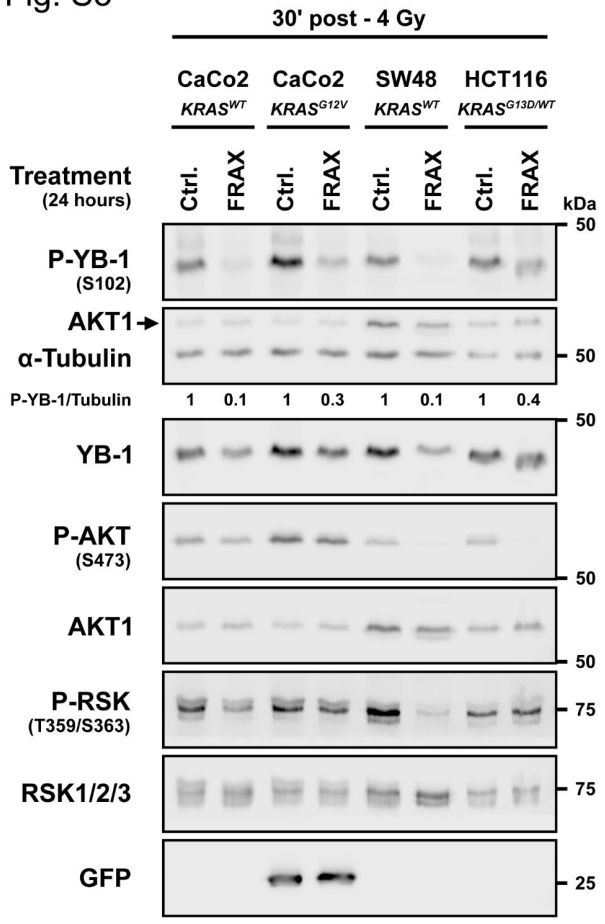

Fig. S3. PAK targeting inhibits YB-1 S102 phosphorylation, independent of *KRAS* mutation status. Indicated cells were treated with FRAX486 (10 μM). After 24 h, the cells were mock irradiated or irradiated with 4 Gy. Thirty minutes after irradiation protein samples were isolated and subjected to SDS-PAGE. Indicated phospho-proteins were detected by Western blotting using phospho-specific antibodies. Blots were stripped and incubated with the corresponding antibody against total proteins. Densitometry values represent the ratio of phospho-YB-1 to α-Tubulin normalized to the control in each cell line. GFP was detected as an indication for the expression of $KRAS^{G12V}$. CaCo2 cells were pretreated with doxycycline (2 μg/ml) for 48 h to induce $KRAS^{G12V}$ expression, Similar results were obtained in the repeated experiment. Ctrl.: Control, FRAX: FRAX486.

Fig. S4

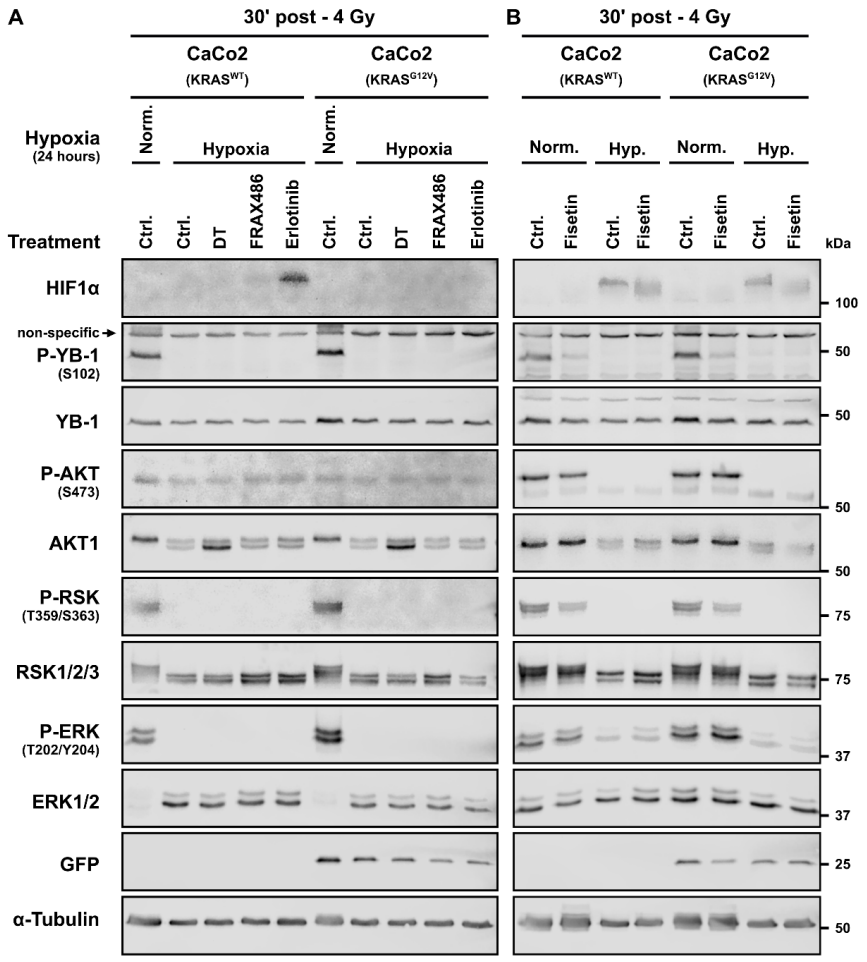

Fig. S4. The effect of hypoxia on DT of RSK/AKT, targeting PAK, targeting EGFR, and treatment with fisetin in *KRAS* mutant and *KRAS* wild type CaCo2 cells. (A) CaCo2 cells were treated with or without doxycycline (2 µg/ml) for 72 hours. Following doxycycline treatment, the cells were exposed to the combination of the AKT inhibitor MK2206 (5 µM) and RSK inhibitor LJI308 (10 µM), referred to as DT, the PAK inhibitor FRAX486 (10 µM), or the EGFR inhibitor Erlotinib (10 µM) for 48 hours. This was followed by 24 hours of incubation under normoxia or severe hypoxia (<0.01% O2). The concentration of DMSO was maintained at 0.125% in all treated conditions. **(B)** CaCo2 cells were treated with or without doxycycline (2 µg/ml) for 48 hours, and then treated with fisetin (75 µM) for 24 hours, under normoxia or hypoxia. The concentration of DMSO was maintained at 0.125% in all treated conditions. **(A-B)** Twenty-four hours after exposure to normoxia or hypoxia, the cells were either mock irradiated or irradiated with 4 Gy. Thirty minutes after irradiation, protein samples were isolated and subjected to SDS-PAGE. The indicated phospho-proteins were detected by Western blotting using phospho-specific antibodies. The blots were stripped and incubated with the corresponding antibody against total proteins. GFP was detected as an indication of $KRAS^{G12V}$ expression. Ctrl.: Control, DT: Dual targeting, Norm.: Normoxia, Hyp.: Hypoxia.

Fig. S5

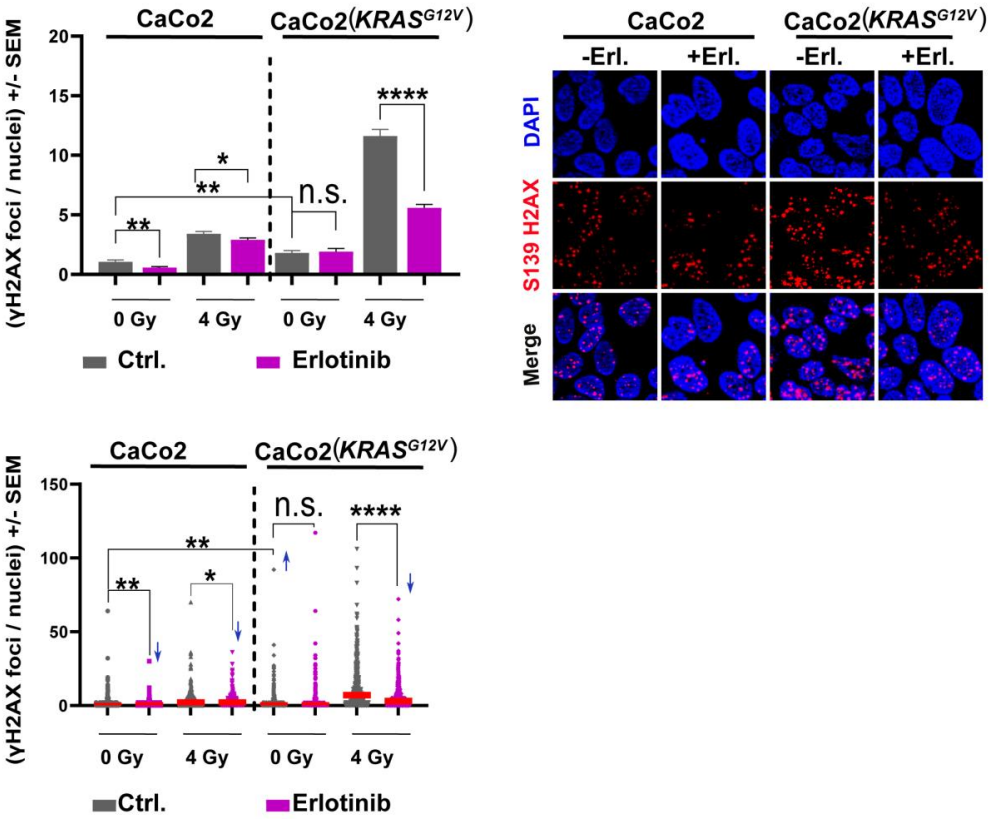

Fig. S5. The EGFR kinase inhibitor erlotinib does not impair DSB repair in CaCo2 cells after IR exposure. CaCo2 cells were treated with or without doxycycline (2 µg/ml) for 48 h and treated without or with erlotinib (10 µM) for 72 h. Thereafter, cells were mock irradiated or irradiated with 4 Gy. γH2AX assay was performed 24 h after irradiation. The asterisks indicate significant difference in mean γH2AX ± SEM between the indicated conditions (*$p < 0.05$, **$p < 0.01$, ****$p < 0.0001$; students t-test) analyzed in 660 cells from 3 independent experiments shown as bar graph as well as scatter plot. The representative images after the described treatment in combination with irradiation. SEM: standard error of mean, Erl.: Erlotinib, n.s.: non-significant, Ctrl.: Control.

Fig. S6

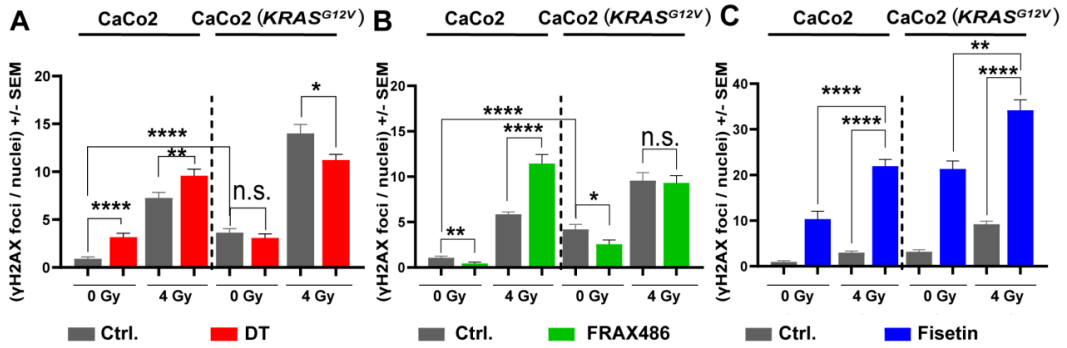

Fig. S6. The effect of KRAS, DT of RSK/AKT, targeting PAK and treatment with fisetin on DSB repair. (A-B) CaCo2 cells were either treated with doxycycline (2 µg/ml) for 48 hours or left untreated. The γH2AX assay was performed 24 hours after irradiation without pretreatment or after a 2-hour pretreatment with the combination of the AKT inhibitor MK2206 (5 µM) and RSK inhibitor LJI308 (10 µM), referred to as DT **(A)**, or the PAK inhibitor FRAX486 (10 µM) **(B)**. **(C)** Cells treated with or without doxycycline (for 48 hours) and fisetin (75 µM for 24 hours) were mock irradiated or irradiated with 4 Gy, and the γH2AX foci assay was performed 24 hours after irradiation. **(A-C)** The histograms represent the mean number of γH2AX foci per nucleus under the indicated treatment conditions. Asterisks indicate a significant difference in the mean γH2AX ± SEM between the indicated conditions (*$p < 0.05$, **$p < 0.01$, ****$p < 0.0001$; Student's t-test). The analysis was conducted on 300 cells from 4 independent experiments **(A, C)** and 260 cells from 3 independent experiments **(B)**. Ctrl.: Control, SEM: standard error of the mean, DT: Dual targeting, n.s.: non-significant.

Fig. S7

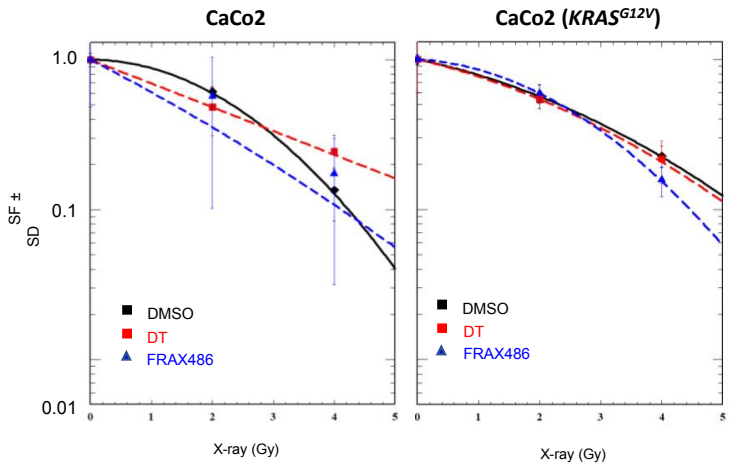

Fig. S7: The Effect of dual targeting of AKT and RSK and inhibition of PAK by FRAX486 on the post-irradiation survival of CaCo2 Parental Cells and CaCo2 *(KRASG12V)* cells. The cells were either untreated or treated with doxycycline (2 µg/ml) for 48 hours. The clonogenicity assay was conducted immediately after irradiation (0, 2, and 4 Gy) without any pretreatment or after a 2-hour pretreatment with either the combination of the AKT inhibitor MK2206 (5 µM) and the RSK inhibitor LJI308 (10 µM), referred to as dual targeting (DT), or the PAK inhibitor FRAX486 (10 µM). Survival fraction ± SD from 12 data points obtained from 2 independent experiments has been graphed. SF: Survival fraction, SD: standard deviation.

Fig. S8

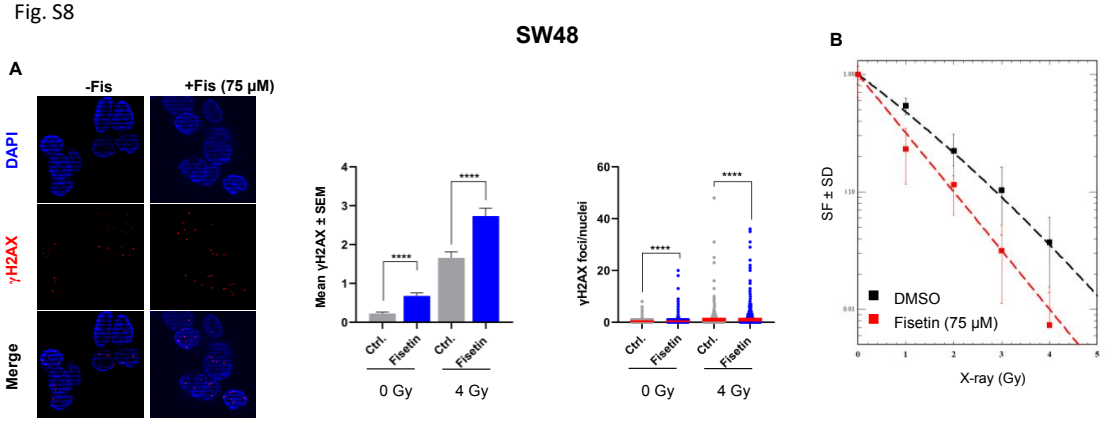

Fig. S8. The effect of fisetin on DSB repair and post-irradiation cell survival. SW48 cells were treated with or without fisetin (75 µM) for 24 hours. **(A)** Thereafter, cells were mock irradiated or irradiated with 4 Gy. The γH2AX assay was performed 24 hours after irradiation. The histograms represent the mean number of γH2AX foci per nucleus under the indicated treatment conditions. The asterisks indicate a significant difference in the mean γH2AX ± SEM between the indicated conditions (****$p < 0.0001$; Student's t-test). The analysis was conducted on 500 cells from 3 independent experiments, and the results are shown as a bar graph and scatter plot. Representative images are provided after the described treatment in combination with 4 Gy irradiation. **(B)** A clonogenic survival assay was performed 24 h after mock irradiation or irradiation with single doses of 0 to 4 Gy. Survival fraction ± SD from 18 data points obtained from 3 independent experiments has been graphed. SEM: standard error of the mean, SD: standard deviation, Fis.: Fisetin, Ctrl.: Control., SF: Survival fraction

Fig. S9

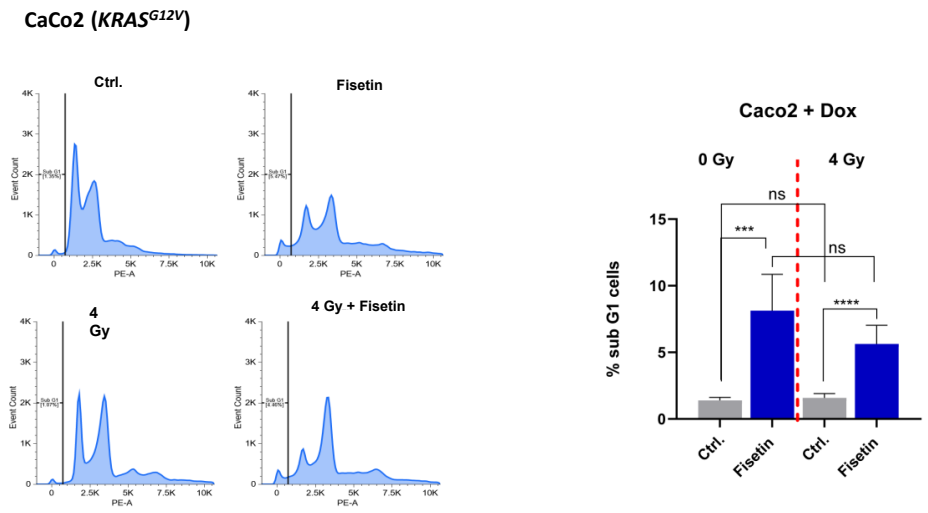

Fig. S9. The effect of fisetin on apoptosis. CaCo2 cells were treated with doxycycline (2 µg/ml) for 48 hours. Subsequently, the cells were treated with fisetin (75 µM) for 24 hours and subjected to mock irradiation or irradiated with 4 Gy. After 24 hours of irradiation, the cells were collected, and fluorescence-activated cell sorting (FACS) analysis was performed. The percentage of cells in the sub G1 cell cycle phase was calculated as the mean ± SD from 6 data points obtained from 2 independent experiments and presented in a graph. Ctrl.: Control.

Fig. S10

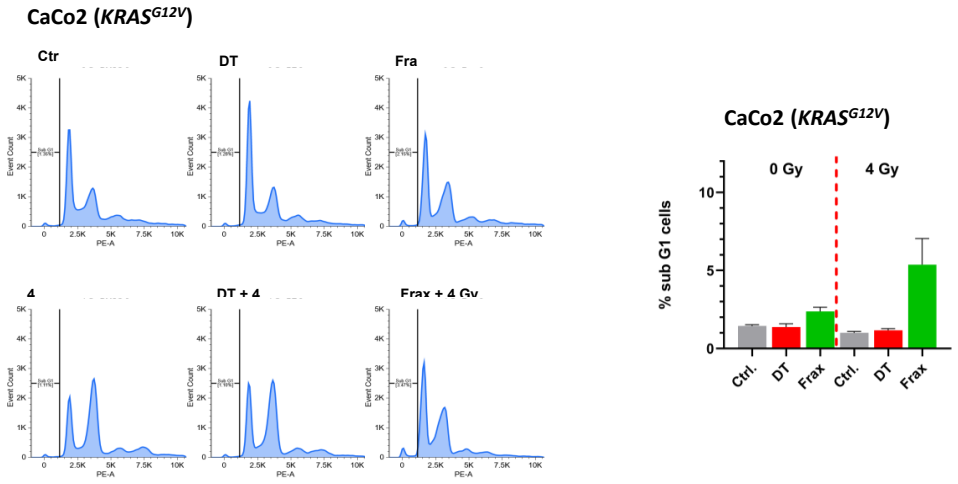

Fig. S10. The effect of DT of RSK/AKT and targeting PAK on apoptosis. The effect of dual targeting (DT) of RSK/AKT and targeting PAK on apoptosis was investigated. CaCo2 cells were treated with doxycycline (2 µg/ml) for 48 hours, followed by treatment with the AKT inhibitor MK2206 (5 µM) and RSK inhibitor LJI308 (10 µM) for 2 hours, referred to as DT, or the PAK inhibitor FRAX486 (10 µM). After treatment, the cells were either mock irradiated or irradiated with 4 Gy. After 24 hours of irradiation, the cells were collected and subjected to fluorescence-activated cell sorting (FACS) analysis. The percentage of cells in the sub G1 cell cycle was calculated as the mean ± SD from 3 data points obtained from 1 experiment and graphed. Ctrl.: Control, DT: Dual targeting, n.s.: non-significant.

Table S1. Mutation status of genes involved in stimulation of YB-1 signaling cascades in the indicated CRC cell lines. WT: Wild-type

Cell Lines	EGFR	ERBB3	KRAS	HRAS	MAP2K1	PIK3CA	AKT2	AKT3
HCT116	WT	p.Q261*/WT p.Q202*/WT	p.G13D/WT	WT	WT	p.H1047R/WT	WT	WT
SW48	p.G719S/WT p.G674S/WT	WT	WT	p.G161R/WT	p.Q56P/WT p.H119Y/WT p.D351G/WT p.D175G/WT	p.G914R/WT	p.R251W/WT p.R189W/WT	p.R465Q/WT
CaCo2	WT	p.D857N/WT p.D798N/WT p.D98N/WT	WT	WT	WT	WT	WT	WT
CaCo2+ doxycycline (2 µg/ml)	WT	p.D857N/WT p.D798N/WT p.D98N/WT	WT p.G12V (dox-inducible expression)	WT	WT	WT	WT	WT

Databases:

Cancer Dependency Map Database: https://depmap.org/

COSMIC Database: https://cancer.sanger.ac.uk/cosmic

Appendix C

Publication III

Strahlentherapie und Onkologie (2023) 199:1110–1127
https://doi.org/10.1007/s00066-023-02092-8

REVIEW ARTICLE

YB-1 activating cascades as potential targets in *KRAS*-mutated tumors

Shayan Khozooei[1] · Soundaram Veerappan[1] · Mahmoud Toulany[1]

Received: 2 March 2023 / Accepted: 23 April 2023 / Published online: 2 June 2023

Abstract
Y-box binding protein-1 (YB-1) is a multifunctional protein that is highly expressed in human solid tumors of various entities. Several cellular processes, *e.g.* cell cycle progression, cancer stemness and DNA damage signaling that are involved in the response to chemoradiotherapy (CRT) are tightly governed by YB-1. *KRAS* gene with about 30% mutations in all cancers, is considered the most commonly mutated oncogene in human cancers. Accumulating evidence indicates that oncogenic KRAS mediates CRT resistance. AKT and p90 ribosomal S6 kinase are downstream of KRAS and are the major kinases that stimulate YB-1 phosphorylation. Thus, there is a close link between the *KRAS* mutation status and YB-1 activity. In this review paper, we highlight the importance of the KRAS/YB-1 cascade in the response of *KRAS*-mutated solid tumors to CRT. Likewise, the opportunities to interfere with this pathway to improve CRT outcome are discussed in light of the current literature.

Keywords Y-box binding protein-1 · Oncogenic KRAS · Chemoradiotherapy · Molecular targeting · DNA damage response signaling

Y-box binding protein-1 (YB-1)

The Y-box binding family of proteins are multifunctional RNA/DNA binding proteins that bind to the Y-box, an inverted CCAAT sequence [1]. These proteins belong to the cold shock domain (CSD) protein family, which has been shown to play an important role in regulating cell proliferation and development [2]. This family of proteins consists of 3 members that share similar structures: YB-1/DNA-binding protein B (DBPB), YB-2/DNA-binding protein C (DBPC), and YB-3/DNA-binding protein A (DBPA). YB-1 is highly expressed in solid tumors of various entities [3–14] and regulates all cancer hallmarks, *e.g.*, it stimulates DNA damage response (DDR), which results in chemoradiotherapy (CRT) resistance [15–20]. YB-2 is a germ cell specific Y-box binding protein that is also overexpressed in some human malignancies such as seminoma and ovarian dysgerminomas [21]. YB-3 is more functional during embryo development [22]. It has been shown to bind to similar mRNAs as YB-1 [22, 23]. However, the binding of YB-3 to mRNAs is more commonly observed in the absence of YB-1, and it is therefore proposed that YB-3 is transcriptionally regulated by YB-1 [22]. The oncogenic impacts of YB-3 have also been described previously [24–29]. In support of the oncogenic effect of YB-3, silencing YB-3 was shown to induce chemosensitization to 5-fluorouracil in gastric cancer and colorectal cancer (CRC) [23, 30]. Silencing YB-3 was also shown to induce E-cadherin expression and inhibit β-catenin and cyclin D1 expression and thereby inhibited gastric cancer proliferation [23].

Structurally, the Y-box binding family of proteins contain an N-terminal Alanine/Proline-rich domain (A/P) (amino acid (aa) residues 1–50), a highly conserved CSD (aa 51–129), and a C-terminal domain (CTD) (aa 129–324) ([31]; Fig. 1). The CSD of YB-1 is crucial for specific RNA/DNA binding characteristics [32]. The structure of CSD consists of a five stranded β-barrel containing two RNA binding motifs ribonucleoprotein (RNP) particle domain-1 (RNP1) and RNP2 [33]. YB-1, as a transcription factor, binds via the CSD to gene promoters to regulate the transcription of various genes [34]. As a main player in RNP complexes, YB-1 is also involved in translational regulation [35–37]. The CTD contains positively and negatively charged aa, but overall the CTD is positively charged

S. Khozooei and S. Veerappan share first authorship.

✉ Prof. Dr. Mahmoud Toulany
mahmoud.toulany@uni-tuebingen.de

[1] Division of Radiobiology and Molecular Environmental Research, Department of Radiation Oncology, University of Tuebingen, Tuebingen, Germany

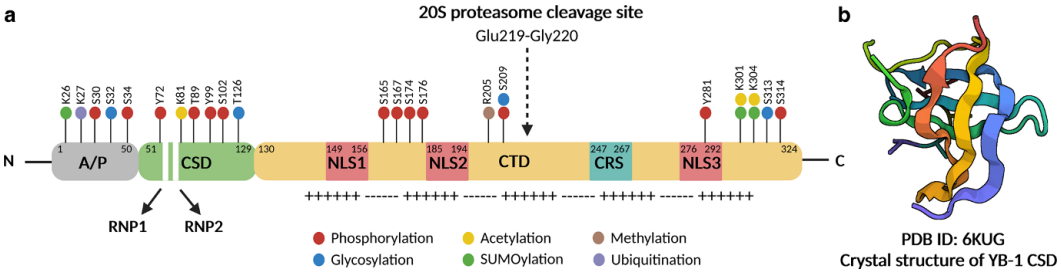

Fig. 1 Schematic representation and crystal structure of YB-1. **a** YB-1 consists of three domains: N-terminal *A/P*, *CSD*, and *CTD* comprising 324 *aa*. The CSD contains two RNA binding motifs (*RNP1* and *RNP2*). The CTD contains three *NLS* and one *CRS*. There is also a 20S proteasome cleavage site between aa Glu219-Gly220. The CTD of YB-1 contains clusters of positive and negative charges represented as '+' and '–' respectively. Various post-translational modification sites are shown. **b** The CSD of YB-1, from aa 51 to aa 129, is involved in nucleic acid binding and structurally contains a five-stranded β-barrel with two RNA-binding motifs with consensus sequences-RNP1 and RNP2. *aa* amino acid, *A/P* domain alanine/proline-rich domain, *CRS* cytoplasmic retention signal, *CSD* cold shock domain, *CTD* C-terminal domain, *Glu219* Glutamic acid 219, *Gly220* Glycin 220, *NLS* nuclear localization signals, *PTM* Post translational modification, *RNP1* ribonucleoprotein particle domain-1, *RNP2* ribonucleoprotein particle domain-2, *YB-1* Y-box binding protein 1. Created with BioRender.com

([38]; Fig. 1). The CTD of YB-1 also contains a cytoplasmic retention signal (CRS) (aa 247–267) and three nuclear localization signals (NLS); NLS1 (aa 149–156), NLS2 (aa 185–194) and NLS3 (aa 276–292) [39]. Besides, a specific site for the 20S proteasome cleavage exists between Glutamic actid 219 (Glu219) and Glycine 220 (Gly220) [39]. YB-1 is majorly observed in the cytoplasm and the function of YB-1 in translational regulation could be attributed to its cytoplasmic localization. The basic charges of CTD enhance the binding of YB-1 to mRNA through multimerization with other YB-1 proteins on the mRNAs [38]. This phenomenon leads to compaction of the mRNAs and thus translation repression [40]. In contrast to the function of YB-1 in translational repression, YB-1 induces the translation of subsets of mRNAs through recruiting mRNAs to the polysomal chains to promote translation [41]. This has been shown to occur via a cap-independent manner and through internal ribosomal entry sites (IRES) [42, 43]. It is interesting to note that free messenger RNPs (mRNPs) have high ratio of YB-1/mRNA in the mRNP (∼4 mol YB-1/mol mRNA) indicating translation repression, whereas low ratio of YB-1/mRNA in the mRNP (∼2 mol YB-1/mol mRNA) results in translation activation [42, 44–46]. This is due to the ability of YB-1 to displace eIF4G from mRNAs [47]. Therefore, YB-1 has both effects on the translation of mRNAs; either activation or suppression of translation. There are a number of studies showing the oncogenic role of cytoplasmic YB-1 [43, 48–50]. For instance, it has been shown that YB-1 promotes translation of HIF1α in an IRES-dependent manner [42]. Mechanistically, YB-1 directly binds to HIF1α mRNA and melts the secondary structures formed in the IRES at the 5′-untranslated region (5′-UTR) by its helicase activity to induce more efficient translation of HIF1α and consequently promotes sarcoma metastasis [42]. Similarly, YB-1 also induces the translation of Snail1, Twist, and other mRNAs regulating Epithelial-Mesenchymal Transition (EMT) in breast cancer cells [43]. In breast cancer brain metastasis, YB-1 translationally regulates ErbB2 mRNA by disrupting its secondary structures as well and promotes ErbB2 translation [48]. In CRC, YB-1 translationally activates insulin-like growth factor-I receptor (IGF-IR) and promotes liver metastasis [51]. Additionally, another study showed that cytoplasmic YB-1 induces tumorigenicity, enhances migratory properties and invasiveness of melanoma cells [49]. Besides, YB-1 also regulates stress granule (SG) formation by activating G3BP1 at the translational level in sarcoma cells [50]. The SGs are formed in response to hypoxia and metabolic stress to block overall protein synthesis. Interestingly, it has been shown that SGs play an important role in tumor progression [50]. The mechanism of translation activation of G3BP1 by YB-1 is similar to HIF1α, Snail1 and Twist [50]. An overview of the role of YB-1 in translation regulation is shown in Fig. 2. YB-1 can also translocate to the nucleus under certain conditions such as UV irradiation [52] and hypoxia [53] or after cisplatin treatment [54]. Nuclear YB-1 in addition to regulation of gene expression implicated in cell proliferation, stress response, and drug resistance, directly interacts with different proteins involved in DNA repair [19].

Regulation of YB-1 expression

The regulation of YB-1 expression has not been extensively studied and remains poorly understood. At the genetic level, the *YBX1* gene promoter has thus far been reported to consist of three identified regulatory sequences—GATA response elements, E-Box motifs, and GC-rich sequences. Although the *YBX1* promoter contains GATA binding elements, both GATA1 and GATA2 were identified to acti-

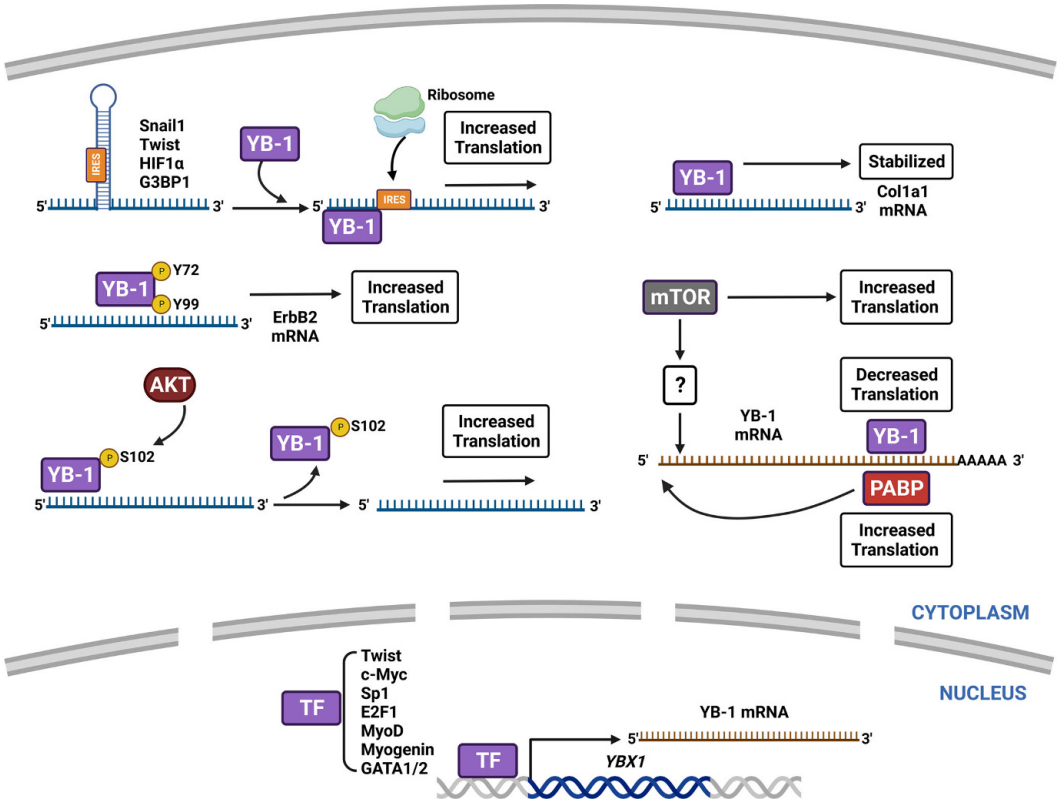

Fig. 2 The role of YB-1 in translation regulation. YB-1 regulates translation of Snail1, Twist, HIF1α, and G3BP1 mRNAs in a cap-independent and IRES-dependent manner by resolving secondary RNA structures. In addition, YB-1 also stabilizes Col1a1 mRNA in the cytoplasm. PTMs on YB-1 regulate the role of YB-1 in translational regulation. Phosphorylation of Y72 and Y99 on YB-1 increases binding to ErbB2 mRNA and enhances translational elongation by removing secondary structures on ErbB2 mRNA, thus promoting ErbB2 translation. On the other hand, AKT-mediated S102 phosphorylation of YB-1 prevents its binding to the 5′-UTR cap of mRNAs, thereby preventing YB-1 mediated RNA silencing and activating mRNA translation. YB-1 translationally regulates its own mRNA by interacting with the 3′-UTR of its mRNA and preventing binding of the translation initiation factors eIF4A and eIF4B. PABP has been shown to promote translation of YB-1 in a poly-A-tail-independent manner. The YB-1 promoter has been shown to have three identified regulatory sequences-GATA response elements, E-box motifs, and GC-rich sequences that can be regulated by different TFs. *AKT/PKB* Protein kinase B, *Col1A1* collagen α1(I), *G3BP1* Ras GTPase-activating protein-binding protein 1, *HIF1α* Hypoxia-inducible factor 1-alpha, *PABP* Poly(A)-binding protein, *PTMs* Post-translational modifications, *S102* Serine 102, *Snail1* Snail family zinc finger 1, *Y72* Tyrosine 72, *Y99* Tyrosine 99, *YB-1* Y-box binding protein-1, *TF* Transcription factor, *Twist 1* Twist-related protein 1, *IRES* internal ribosomal entry sites, *mTOR* mammalian target of rapamycin, *c-Myc* cellular myelocytomatosis oncogene, *Sp1* specificity protein 1, *E2F1* E2F transcription factor 1, *MyoD* Myoblast determination protein 1, *GATA1/2* GATA-binding factor 1/2. Created with BioRender.com

vate the *YBX1* promoter through an unconventional GATA sequence in the 5′-UTR of the *YBX1* gene in erythroid cells [55]. In response to cisplatin-exposure, the c-Myc-Max complex has also been shown to transactivate the *YBX1* gene promoter by binding to the upstream E-box motifs via interaction with p73, in turn inducing a 6-fold increase in cellular YB-1 mRNA level [56]. While c-Myc drives the transcription of YB-1 mRNA, YB-1 has also been shown to regulate c-Myc expression at the translational level, stimulating a feed-forward loop [57]. Twist is another transcription factor that binds to E-box sequences, and has been shown to induce the expression of the *YBX1* gene in cisplatin-resistant cells [58]. As in the case of c-Myc, YB-1 can also induce the translation of Twist mRNA [43]. The GC-rich sequences in the *YBX1* promoter have also been determined to be important for transcription. These regions can interact with Sp1 and E2F1 proteins, and mutations in these regions have been shown to downregulate YB-1 transcription [59]. Sp1 and E2F1 have been shown to regulate the transcription of YB-1 during early stages of differenti-

ation in myocytes [59]. Subsequently, during the formation of myotubes, MyoD and myogenin replace Sp1 and E2F1 and regulate the transcription of YB-1 by binding to the proximal E-box sequence in the *YBX1* promoter [59]. At the translational level, YB-1 can regulate its own expression by interacting with the 3′-UTR of its mRNA and preventing the binding of eukaryotic translation initiation factors eIF4A and eIF4B [60]. Alternatively, Poly(A)-binding protein (PABP) has also been shown to induce the translation of the YB-1 mRNA in a poly-A-tail-independent manner [61]. The mTOR pathway has also been implicated to regulate the translation of YB-1 mRNA and the 5′-UTR has been shown to be vital for this regulation [62]. On the other hand, the stability of the YB-1 mRNA can be regulated by various micro-RNAs (miRNA) such as miR-216a [63], miR-382 [64], and miR-375 [65], which have been shown to mediate degradation of the YB-1 mRNA.

Post-translational modifications of YB-1

The functions and subcellular localization of YB-1 can be regulated by post-translational modifications (PTMs) that occur under different conditions. Phosphorylation, a well-studied PTM of YB-1, occurs at multiple sites, including serine 102 (S102), which is located on the CSD. The S102 phosphorylation is shown to promote binding of YB-1 to the epidermal growth factor receptor (EGFR) and ErbB2 promoters, which in turn induces gene transcription [66, 67]. In contrast, structural analysis of the CSD of YB-1 has demonstrated that S102 phosphorylation decreases CSD stability and therefore reduces binding affinity to single-stranded DNA (ssDNA) [32]. This inconsistency might be explained by the fact that the binding affinity could be sequence specific. Furthermore, other additional PTMs on YB-1 can also affect its binding affinity to DNA. It is also important to note that the structural analysis was performed on an isolated CSD with a C-terminal extension, and not the whole YB-1 protein [32]. In addition, the interaction between the CSD and ssDNA was tested. This could also explain the discrepancy between the results from the cellular and test-tube experiments. Additionally, AKT-dependent S102 phosphorylation of YB-1 prevents its binding to the 5′-UTR cap of mRNAs and thus activates mRNA translation [44, 68]. Therefore, DNA and RNA binding capacity of YB-1 is modulated by this phosphorylation. Additionally, this phosphorylation can promote the translocation of YB-1 to the nucleus [69, 70]. However, a previous study could show that YB-1 phosphorylation at S102 induced by ionizing radiation (IR), treatment with epidermal growth factor (EGF), and the conditional expression of $KRAS^{G12V}$ does not induce nuclear translocation of YB-1 [71]. This inconsistency could be due to the difference in stimuli and patterns of PTMs required for YB-1 nuclear translocation. In this regard, it was reported that phosphorylation of YB-1 at S209, which is located on the NLS, impairs YB-1 translocation to the nucleus even when S102 is phosphorylated [72]. Similarly, phosphorylation at S165 and S176 decreases NLS accessibility and therefore inhibits YB-1 translocation to the nucleus [73]. Phosphorylation of tyrosine 281 (Y281) residue within the NLS is also shown to correlate with nuclear shuttling of YB-1 [39]. Interestingly, it has been shown that phosphorylation on S30 and S34 are required for nuclear translocation of YB-1, which in turn controls the *MKNK1* gene splicing in *JAK2* mutated cells [74]. Recently, Threonine 89 (T89) has also been shown to be phosphorylated by DNA-PKcs after IR or cisplatin treatment and this leads to nuclear shuttling of YB-1 [75]. Subcellular localization of YB-1 may also be regulated by cellular RNA content and the RNA binding ability of YB-1 can be modulated by PTMs such as phosphorylation of Y72 and Y99 [48, 76]. In turn, decreased cytoplasmic RNA levels have been shown to increase the nuclear localization of YB-1 [77]. In addition, translocation of YB-1 to the nucleus can be mediated by 20S proteasome cleavage, which removes the CRS [73].

Studies on other YB-1 PTMs have shown that phosphorylation at S165 and S176 lead to the activation of NF-κB by enhancing NF-κB binding to DNA [78, 79]. YB-1 phosphorylation at these residues as well as at S167, S174 and S314 promotes cytokinesis [80]. The acetylation of YB-1 can also regulate its function. Acetylation of lysine 81 (K81) has been shown to suppress the binding of YB-1 to 5′-UTRs of mRNAs and consequently blocks translation [81]. In addition, YB-1 secretion relies on K301 and K304 acetylation in the CTD [82]. YB-1 ubiquitination [83] is another PTM that regulates YB-1 through proteasomal degradation. It is also reported that Homologous to E6AP C-Terminus (HECT) domain and Ankyrin repeat containing E3 ubiquitin ligase 1 (HACE1) assembles the linkage of ubiquitin to YB-1 at K27 and subsequently promotes YB-1 secretion [84]. Another PTM that can occur on YB-1 is methylation. It has been reported that arginine methyltransferase PRMT5 mediates NF-κB activation in CRC by adding a methyl group to arginine 205 (R205) of YB-1 [85]. Small ubiquitin-related modifiers (SUMO proteins) are 15 kDa in size and are covalently bound to lysine residues in target proteins, resulting in changes in protein function, interaction, and localization [86]. K26, K301 and K304 are critical for YB-1 SUMOylation. It is interesting to note that SUMOylation on these residues promotes the interaction of YB-1 with proliferating cell nuclear antigen (PCNA), but has no effect on the protein stability, subcellular localization, or transcription activity [87]. It has been reported that interaction of YB-1 with PCNA inhibits mismatch binding activity of MutSα and therefore increases frequency of spontaneous mutations [88]. Twenty-four hours day-night rhythms are

controlled by the circadian clock [89]. The circadian clock has been shown to regulate YB-1 SUMOylation in a zebrafish model, which in turn modulates its subcellular localization [90]. It has been reported that in the beginning of light phase, YB-1 is present in the nucleus and downregulates cyclin A2 expression [90]. On the other hand, a study by Mai et al. [87] has shown that YB-1 has $GV^{131}PV^{133}QG$, a SUMO-interacting motif (SIM), that facilitates non-covalent binding to SUMO proteins [87]. In hepatocellular carcinoma cells, glycosylation of YB-1 at S32, T126, S209, and S313 has been shown to promote cell proliferation [91]. Furthermore, YB-1 glycosylation at T126 promotes S102 phosphorylation in hepatocellular carcinomas [91].

Role of YB-1 in cell cycle progression

Alterations in the cell cycle are associated with increased cell proliferation, leading to tumor development [92]. Inhibition of YB-1 by small interfering RNA (siRNA) is reported to delay the G1/S transition by regulating the G1 phase of the cell cycle. Among cell cycle regulators, cyclin A, cyclin D, and transcription factor E2F are transcriptionally regulated by YB-1 [92, 93]. Cyclin D has Y-box sequences to which YB-1 directly binds and regulates its transcription. In osteosarcoma cells, knockdown of YB-1 decreases the mRNA level and protein expression of cyclin D1 and the protein expression of cyclin A [92]. In addition to regulating the G1/S transition, YB-1 also regulates the expression of cyclin B1 in the G2/M transition, which also has Y-box sequences in its promoter [94]. Consistent with this, *YBX1* knockout murine models of triple-negative breast cancer (TNBC) and lung cancer showed a significant reduction in tumor growth [93, 95].

Role of YB-1 in DNA repair

CRT induces DNA damage in cells, leading to the activation of DNA repair mechanisms in the nucleus. YB-1 is activated in the nucleus immediately after the induction of DNA damage for example after exposure to IR [71]. Consistent with its function in DNA repair, YB-1 has been shown to interact directly with several DNA repair proteins, including Ku80, MSH2, DNA polymerase δ, and WRN. Interestingly, YB-1 exhibits endonucleolytic and exonucleolytic activities on DNA [96]. Indeed, a study by Toulany et al. [97] was the first, which showed that knocking down YB-1 in breast cancer cells impairs double-strand break (DSB) repair and sensitizes them to IR *in vitro* [97]. Similarly, it was demonstrated that pharmacological inhibition of p90 ribosomal S6 kinase (RSK), an upstream regulator of YB-1, inhibited ATM phosphorylation after IR [98]. In line with these studies, a recent study by Khozooei et al. demonstrated that inhibiting RSK mediated YB-1 phosphorylation using the flavonoid compound fisetin impairs repair of IR-induced DSBs by suppressing key DSB repair pathways and causes radiosensitization in TNBC cells [99]. In addition to the role of YB-1 in the repair of IR-induced DNA damages, YB-1 was also shown to recognize cisplatin-induced damage by binding to cisplatin-altered DNA [100]. This was also confirmed by another study showing that YB-1 binds preferentially to apurinic DNA rather than to unmodified DNA [101]. YB-1 also regulates poly (ADP-Ribose) polymerase 1 (PARP1) activity [102] and decreases the efficiency of PARP1 inhibitors [103]. In addition, C-terminal truncated YB-1 formed by proteolysis accumulates in the nucleus and interacts with DNA repair proteins such as Mre11 and Rad50 [19]. Therefore, it can be concluded that YB-1 plays a critical role in regulating DNA repair which might affect CRT response.

Prognostic value of YB-1 in *KRAS* mutated cancers

The prognostic value of YB-1 in cancer patients with different tumors has been previously reviewed [104, 105]. The *KRAS* gene is frequently mutated in pancreatic cancer, CRC and lung cancer ([106]; Table 1). Point-mutations in *KRAS* have been shown to result in the constitutive phosphorylation of YB-1 at S102 [97]. Thus, YB-1 may have prognostic value in oncology in general and in *KRAS*-mutated tumors in particular.

In pancreatic cancers, which have the highest frequency of *KRAS* mutation, only a few studies have been performed on the prognostic value of YB-1. Shinkai et al. [107] showed that the intensity of YB-1 expression and positivity of nuclear YB-1 expression were higher in pancreatic ductal adenocarcinoma than in pancreatic intraepithelial neoplasia and normal pancreatic tissues [107]. Nuclear YB-1 expression was significantly associated with dedifferentiation, lymphatic/venous invasion and unfavorable prognosis [107]. Additionally Lu et al. [63] showed that YB-1 is overexpressed in pancreatic cancer cell lines and patient tissue samples. In patient tissues, high levels of YB-1 correlated with perineural invasion [63]. In CRC, Shiraiwa et al. [108] showed that patients with stage III CRC, who have high expression of YB-1 in the nucleus, have a lower 5-year- and recurrence-free survival (RFS) than patients with low nuclear YB-1 expression [108]. It was also found that YB-1 mRNA levels were increased in CRC tumor tissues [108]. In addition, YB-1 expression and lymph node metastasis were shown to be correlated in CRC patients [14]. Importantly, it was also demonstrated that increased expression of YB-1 predicts liver recurrence following resection in the case of colorectal metastases [109]. In another study by Zhang et al. [110], a substantial increase in cytoplasmic YB-1 was detected in rectal cancer tissue when compared to noncancerous tissue, although,

Table 1 Percentage of *KRAS* mutations and most common *KRAS* mutational variants in different cancer subtypes. Percentage of *KRAS* mutations were curated from the somatic mutations data of the publicly available AACR GENIE v13.0 dataset [205] using the cBioPortal for Cancer Genomics (https://www.cbioportal.org/) [206, 207]. All data were collected exclusively for cancer types with a minimum of 100 studied and sequenced cases with at least 5% of cases containing an oncogenic mutation in *KRAS*. Most commonly occurring mutational variants were determined from the same representative dataset. The database was accessed on the 7th of February, 2023

Cancer Type	Percentage (%) of *KRAS* mutations	No. of Samples Screened	No. of Samples with *KRAS* mutations	Most commonly occurring mutational variants
Pancreatic Cancer	78.27	6880	5385	G12D, G12V, G12R
Ampullary Cancer	50.71	353	179	G12D, G12V, G12C
Appendiceal Cancer	50.07	739	370	G12D, G12V, G13D
Small Bowel Cancer	49.03	465	228	G12D, G12V, G13D
Colorectal Cancer	43.12	15,487	6678	G12D, G12V, G13D
NSCLC	27.38	24,117	6604	G12C, G12V, G12D
Endometrial Cancer	19.10	5090	972	G12D, G12V, G13D
Hepatobiliary Cancer	12.93	3456	447	G12D, G12V, Q61H
Germ Cell Tumor	9.45	1069	101	G12V, G12A, G12D
Cervical Cancer	9.35	866	81	G12D, G12V
Ovarian Cancer	8.66	6097	528	G12V, G12D
B-Lymphoblastic Leukemia/ Lymphoma	8.63	997	86	G12D, G13D
Myelodysplastic/ Myeloproliferative Neoplasms	7.97	602	48	G12D
Gastrointestinal Neuroendocrine Tumor	7.48	682	51	G12D
Mastocytosis	6.86	102	7	–
Esophagogastric Cancer	6.82	4750	324	G12D, G13D, G12V
Bladder Cancer	6.48	4675	303	G12D, G12V
Histiocytosis	6.08	526	32	K117N

interestingly, nuclear YB-1 was not detected [110]. Depending on the tumor type, the subcellular localization of YB-1 may vary [105]. High expression of cytoplasmic and nuclear YB-1 predicts poor prognosis, which may influence therapeutic response [3–5, 7–14], as reviewed in [104, 105]. Consistent with the function of YB-1 as a transcription factor [111], nuclear YB-1 expression has been positively correlated with EGFR expression in CRC [108] as well as in non-small cell lung cancer (NSCLC) [112]. In one of the first studies by Shibahara et al. [9], nuclear expression of YB-1 was detected in 44.9% of the 196 NSCLC tumor tissues analyzed in association with poor prognosis [9]. Nuclear YB-1 expression as a negative prognostic marker in NSCLC was confirmed in further studies [113, 114].

Despite the solid data on the association between nuclear YB-1 expression and prognosis in pancreatic cancer, CRC, and NSCLC, there is no study on the predictive value of S102 phosphorylation of YB-1, especially in *KRAS*-mutated tumors.

KRAS

Kirsten Rat Sarcoma Viral Oncogene Homologue (KRAS) is a frequently mutated oncogenic protein, belonging to the RAS family of plasma membrane associated small guanosine triphosphatases (GTPases). The RAS GTPases, encoded by three genes (*HRAS, NRAS*, and *KRAS*), have been observed to be mutated in approximately 30% of all human cancers, with the *KRAS* isoform accounting for about 75% of *RAS* mutations [115]. Under normal physiological conditions and in its wild-type form, KRAS can switch between a guanosine triphosphate (GTP)-bound active state and a guanosine diphosphate (GDP)-bound inactive state in response to ligand-induced stimulation of receptor tyrosine kinases (RTKs). KRAS positively regulates signaling pathways associated with promoting cell survival, proliferation, and cell cycle progression.

Structural biology, function, and regulation of KRAS

The *KRAS* gene encodes two splice variants—KRAS4A and KRAS4B, which share N-terminal sequence similarity and are only different in the aa sequence of their C-terminal regions [116]. Of the two isoforms, KRAS4B has been studied primarily due to its abundance in terms of expres-

sion in comparison to KRAS4A in cancers [117]. However, increasing evidence suggests that KRAS4A may play a vital role in oncogenesis and cancer progression [117]. Structurally, both KRAS protein isoforms consist of two major domains—the N-terminal G-domain and the C-terminal Hyper Variable Region (HVR). The G-domain, ranging from aa residues 1–166, forms the core of the KRAS proteins and consists of the GDP/GTP-binding catalytic region. This catalytic region contains three functional components called Switch-I (S-I), Switch-II (S-II), and phosphate-binding loop (P-loop). S-I and S-II are the regions of the G-domain that flexibly change conformation to interact with GTP [118, 119], and this change in conformation is thought to drive the activation of KRAS [120]. S-I and S-II also form important interactions with RAS effectors, guanine nucleotide exchange factors (GEFs), and GTPase-activating proteins (GAPs), and are imperative to the regulation and functionality of the KRAS protein [121]. The P-loop augments the GTPase function of KRAS by interacting with the phosphate groups of GDP/GTP [119, 122], and complexing with Mg^{2+}, a cofactor essential for the hydrolysis of GTP [118, 120].

The C-terminal domain of KRAS plays an important role in the membrane anchorage, localization, and hence the biological activity of the KRAS protein [123]. Membrane localization is important for the interaction of KRAS with the proteins that regulate its activation. The stimulation of plasma membrane associated RTKs by their ligands initiates an intracellular signaling cascade. The activation of KRAS occurs via intermediary proteins, which include adapters and GEFs. Adapters bind to activated RTKs and promote the activation and recruitment of GEFs to the plasma membrane. Activated GEFs catalyze the exchange of GDP, which is bound to inactive KRAS, with GTP, and thus activate KRAS in the process. The binding of different GEFs to KRAS is generally mediated from various angles and acts by modifying the conformation of the nucleotide-binding pocket formed by S-I, S-II, and the P-loop [121].

The natural deactivation of KRAS occurs upon the hydrolysis of GTP to GDP. However, since the intrinsic GTPase activity of KRAS is very minimal, it requires the assistance of GAPs to undergo deactivation. GAPs accelerate the GTP hydrolysis process by several magnitudes [124], and are important for the negative regulation of KRAS-induced signaling cascades [121].

The impact of *KRAS* mutations in cancer biology and therapy

Oncogenic mutations of *KRAS* are typically reported to be within the S-I, S-II, and the P-loop, where the biological properties and sequence of aa are integral to the binary state of KRAS. The most common *KRAS* mutations occur at codons G12 (83%) and G13 (14%) of exon 2 and at codon Q61 (2%) of exon 3 [125], within regions encoding the P-loop and S-II respectively. The most common *KRAS* mutational variants in different cancer subtypes have been summarized in Table 1.

Oncogenic point mutations at these hotspots affect the ability of GAPs to bind to KRAS and mediate GTP hydrolysis, in turn locking KRAS in an active conformation [126]. Active KRAS stimulates downstream signaling via various pathways, many responsible for transformative hallmarks such as cell cycle progression, cell proliferation, survival, and migration [127]. Signals originating from active KRAS are primarily transduced via the RAF/MEK/ERK, PI3K/AKT, and RalGDS signaling axes, which are predominantly upregulated in the event of oncogenic *KRAS* mutations [128–131]. These pathways overlap at various levels and interact with each other through a complex network of proteins. This extensive network of interactions confers cancer cells with the ability to induce feedback signaling in the presence of anomalies in alternative pathways [132].

As a result of its supremacy over cell survival signaling, activating mutations in *KRAS* are often associated with poor prognosis [133–136] and radiotherapy resistance [137]. The effect of *KRAS* mutations on the outcome of various conventional therapeutic regimes has been widely investigated in different cancers, and mutations in *KRAS* have often been associated with a negative influence on CRT [138–140] and certain targeted therapies [141–144]. In fact, a meta-analysis study in CRC patients also showed that combining EGFR/VEGF targeted antibodies with FOLFOX/FOLFIRI (Folinic acid, fluorouracil and oxaliplatin/Folinic acid, fluorouracil and irinotecan) chemotherapeutic regimens could have a beneficial effect on patients with *KRAS*-wild-type tumors whereas not an insignificant effect, but a detrimental effect on patients with *KRAS*-mutant tumors [144].

Although all the oncogenic mutational variants of *KRAS* exhibit constitutive activity, there exist differences in the functionality between the allelic variants, of which the differences between the G12, G13, and Q61 codons are the most studied [145–149]. Similarly, the different substitutional variants (*e.g.*, G12D, G12V, G12C) of *KRAS* also display differences in functionality and GTPase activity [149–152]. The difference in functionality also contributes to a divergence in the preference of downstream signaling pathways [145, 149, 150, 153]. For example, in a study using NSCLC cell lines, $KRAS^{G12D}$ was shown to be associated with increased PI3K/AKT and MEK/ERK signaling while $KRAS^{G12C}$ and $KRAS^{G12V}$ were associated with RalGDS signaling [153]. Another study in isogenic CRC cells showed that differences in signaling networks exist between G12 substitutional variants [154]. These differences were also

discernable between G12 and G13 substitution mutations [154].

The differences in the biochemical properties of the allelic variants of KRAS also give rise to diverse clinical outcomes [152, 155] and these outcomes have been assessed to be tissue-specific [156]. For instance, in a study conducted in Chinese patients with NSCLC, G12V mutations correlated with a poor progression-free survival (PFS) compared to non-G12V mutations [157]. Similarly, another clinical study showed that G12C mutations presented with a dismal disease-free survival (DFS) compared to non-G12C mutations in resected lung adenocarcinoma [158]. In patients of pancreatic ductal adenocarcinoma, the G12D mutation was associated with worse overall survival (OS) when compared to G12V and G12R mutants [159]. A study in stage III CRC patients treated with adjuvant FOLFOX chemotherapy also showed that the G12D/G12V mutations were associated with shorter RFS when compared to other G12 mutations [160]. Another study investigating the prognostic impact of G12C mutations in metastatic CRC showed that G12C mutations were associated with a shorter PFS and OS [161]. Different mutations of *KRAS* also have been shown to have varying effects on the outcome of EGFR targeted therapy. An *in vitro* study has shown that G13 mutations are relatively susceptible to targeting EGFR when compared to G12 mutations [162]. Therefore, mutations in *KRAS* majorly affect disease outcome and treatment sensitivity, and the specific influence of different allelic and substitutional variants of *KRAS* on disease outcome ranges across a wide spectrum.

YB-1 activating components in *KRAS*-mutated tumors cells

YB-1 undergoes various PTMs at residues within all three structural domains (Fig. 1). However, the phosphorylation of the S102 residue within the CSD has been extensively studied and is thought to be extremely crucial in terms of functionality. The phosphorylation at this residue is majorly orchestrated by the serine/threonine protein kinases AKT and RSK [70, 163, 164]. Therefore, YB-1 lies at the crossroads of the phosphoinositide-3-kinase (PI3K) and mitogen-activated protein kinase (MAPK) cascades, downstream of KRAS.

The MAPK cascade represents one of the primarily activated pathways downstream to KRAS. The cascade begins when activated KRAS activates rapidly activated fibrosarcoma (RAF) kinase. RAF phosphorylates and activates MAPK kinase (MEK), which further transfers phosphorylation to extracellular signal-regulated kinase (ERK), activating it in the process. Active ERK phosphorylates downstream substrates, which include the 4 isoforms of RSK. The activation of RSK is regulated by a subsequent series of phosphorylation. When RSK is fully active, it can further phosphorylate its substrates, which include the S102 residue of YB-1 [163]. *KRAS*-mutant cells have been reported to display an addiction towards the MAPK pathway [165]. This has also been shown to be true in the context of YB-1 S102 phosphorylation, in which *KRAS*-mutant cells seem to prefer the RSK pathway [95]. RSK was also determined to be the major kinase of YB-1 S102 in *KRAS* wild-type cells without oncogenic mutations in the PI3K pathway [95, 98]. Although RSK displays a very high YB-1 S102 kinase function when compared to AKT under *in vitro* conditions [163], targeting RSK leads to the compensatory activation of YB-1 through AKT [98].

The p21-activated kinases (PAK1-6) are a family of six conserved serine/threonine kinases, which play a role in the PI3K and MAPK cascades. These cascades interact with each other at various levels [133]. The RAS proteins can also regulate PAK through the TIAM1/RAC/PAK axis [166]. On the other hand, the PAK proteins have been described to play a role in both, AKT [167] as well as RAF kinase [168–170], MEK [168, 169, 171–173], and ERK [168, 169, 171, 173] activation. PAKs have also been shown to be reciprocally phosphorylated by AKT [174, 175], phosphoinositide-dependent kinase-1 (PDK1) [176], PI3K [177, 178], and RAF [179] kinases. Hence, the PAK proteins could also be a switch-point and a point of crosstalk between the kinase cascades implicated in YB-1 S102 phosphorylation.

Strategies to target the KRAS/YB-1 cascade

KRAS mutations play a major role in resistance to CRT, which justifies the direct targeting of KRAS or KRAS signaling pathways in combination with conventional therapeutic strategies. *KRAS* mutation is also a limiting factor for the application of well-established EGFR-targeting approaches [141, 144, 180–183]. Historically, it has been challenging to target KRAS directly, and efforts have been made to identify other targetable proteins in the KRAS pathway. The discovery of methods to inhibit farnesylation of RAS, which is important for membrane localization, marked the beginning of a series of tools to target malignant *KRAS* mutations [184, 185].

Targeting PTMs of KRAS

Although farnesyltransferase inhibitors (FTIs) have shown promise in preclinical studies [185–188], they have not achieved effective clinical outcomes [189–192], mainly due to the compensatory activity of cellular geranylgeranyltransferase 1 [193, 194]. Subsequently, inhibitors that si-

multaneously target farnesyltransferase and geranylgeranyltransferase 1 (FGTIs) reached clinical trials and showed promising results [195, 196]. However, various studies suggest that FTIs and FGTIs also suppress the prenylation of other proteins, and that their effect on cancer cells may also be KRAS independent [197–200]. To date, FGTIs have been tested in Phase I clinical trials and require further investigation.

Antisense oligonucleotides and siRNA approaches against *KRAS*

Alternative approaches developed to target *KRAS*-mutated malignancies include antisense oligonucleotides (ASOs) and siRNA against *KRAS*, GEF inhibitors, and downstream pathway inhibitors. ASOs and siRNA can be tailored to target either *KRAS* in general or the *KRAS* mutation in particular, and show promising preclinical results [201–205]. However, a major challenge in the clinical development of ASOs and siRNA therapeutics is the lack of an efficient and long-term delivery platform. A long-term release system for siRNA against $KRAS^{G12D}$, termed as siG12D LODER (Local Drug EluteR), is currently being investigated as a delivery system in Phase II clinical trials [206] (NCT01676259).

Targeting KRAS nucleotide exchange factors

The second approach to target mutant *KRAS* includes inhibiting the nucleotide exchange cycle of KRAS. Son of sevenless 1 (SOS1) is a key GEF for KRAS and one of the first inhibitors against the SOS1 protein proved to be successful in preclinical studies and is currently being tested in Phase I clinical trials (NCT04111458) [207]. Apart from SOS1 inhibitors, various Src homology-2 domain-containing protein tyrosine phosphatase-2 (SHP2) inhibitors are also in clinical trials for *KRAS*-mutant tumors (NCT04528836, NCT05163028, NCT03114319). SHP2 is a protein tyrosine phosphatase and plays an integral role in activating SOS1.

Targeting KRAS downstream pathways

Inhibition of downstream KRAS signaling is another approach to target mutant *KRAS* tumors by inhibiting the MAPK and PI3K cascade to overcome KRAS-mediated survival signaling. Targeting components of either MAPK or PI3K pathway alone proved unsuccessful in *KRAS*-mutated tumors due to compensatory activation of the alternative pathway [208–210]. On the other hand, simultaneously targeting upstream proteins of both signaling pathways, such as MEK and PI3K, has been shown to be poorly tolerated and ineffective in clinical practice [211].

Mutant KRAS specific inhibitors

Recent advances in the development of highly specific drugs directly targeting mutant KRAS are groundbreaking discoveries in the field of targeted therapy. The first inhibitor against mutant KRAS, sotorasib, was developed against $KRAS^{G12C}$ [212] and approved by the Food and Drug Administration (FDA). $KRAS^{G12C}$, although predominant in lung cancer, is present in a very small proportion of cases of pancreatic cancer and CRC, where the G12D and G12V mutations predominate (Table 1). Further studies and clinical data also show that resistance to $KRAS^{G12C}$-targeted inhibitors is frequently acquired [213–215]. In addition, targeting $KRAS^{G12C}$ in real-life situations where tumors are genetically heterogeneous could promote the selective spread of tumors with other *KRAS* substitution mutations. To overcome these shortcomings, $KRAS^{G12D}$ and $KRAS^{G12V}$ inhibitors are currently being developed and show promise in the preclinical setting [216–218].

Targeting YB-1

Given the critical role that KRAS cascades play in YB-1 phospho-S102-mediated activity and the key role of YB-1 in cancer hallmarks, targeting YB-1 is another alternative strategy to combat mutant *KRAS*. YB-1 has effects on cancer cells due to its extensive interaction with key cancer-related proteins and signaling pathways [219]. In consequence, approaches aimed at blocking the functions of YB-1, which occur mainly through S102 phosphorylation, could significantly improve the efficacy of cancer therapies [220]. The main approaches that have been studied to block YB-1 function in tumor cells have been discussed below.

Dual targeting strategies to block YB-1 S102 phosphorylation

Dual targeting of PI3K and RSK has been shown to be highly effective in treating breast cancer cells both *in vitro* and *in vivo* [221]. Consistent with this, previous studies have shown that AKT and RSK phosphorylate YB-1 at S102. However, different cellular contexts and mutational statuses could influence the dependence of YB-1 phosphorylation on either signaling pathway [11, 95, 98, 222, 223]. In *KRAS*-mutant cells, the MAPK pathway has been shown to be primarily involved in phosphorylation of YB-1 S102. Therefore, targeting RSK may be beneficial, and several RSK inhibitors are currently in clinical trials, as reviewed elsewhere [104]. Recently, Ushijima et al. [224] have demonstrated that PMD-026, an oral RSK1-4 inhibitor, decreased YB-1 S102 phosphorylation as well as androgen receptor variant 7 (AR-V7) mRNA levels in prostate cancer cells [224]. A single treatment with PMD-

026 or in combination with enzalutamide and darolutamide resulted in inhibition of cell proliferation and induction of apoptosis [224]. In an *in vivo* mouse xenograft model, PMD-026 suppressed tumor progression [224]. PMD-026 is currently being investigated in Phase I clinical trials for TNBC patients (NCT04115306).

Although RSK targeting is highly effective, there are some reports that targeting RSK to block YB-1 S102 phosphorylation activates AKT. This compensatory activation has been shown to impair treatment success and, conversely, results in phosphorylation of YB-1 at S102 [98, 222]. Moreover, in the clinical setting, targeting only RSK-mediated YB-1 phosphorylation may not be useful due to the highly heterogeneous nature of tumors, in which *KRAS*-mutated and *KRAS*-wild-type cells may coexist. In tumor cells without *KRAS* mutation but with mutations in the PI3K pathway, phosphorylation of YB-1 at S102 depends mainly on AKT [95]. In this context, dual targeting of RSK and AKT may be beneficial to achieve therapeutically significant results, as preclinical studies in colorectal and breast cancer have shown [98, 222]. Dual inhibition of PI3K and MEK proved to be toxic in the clinical setting [211]. This is because many downstream components of the two signaling pathways responsible for regulating various cellular processes are blocked. Therefore, simultaneous targeting of AKT and RSK, which are downstream effectors and known YB-1 S102 kinases, may be well tolerated and a better approach to block YB-1 S102-mediated function.

The application of multikinase inhibitors is a complementary approach to the dual targeting strategy. The multikinase inhibitor TAS0612, which inhibits AKT, p70S6K, and RSK, is currently being tested in clinical trials as an oral therapeutic for patients with advanced or metastatic solid tumor cancers (NCT04586270). TAS0612 decreases phosphorylation of YB-1 at S102, inhibits cell division, and increases sensitivity to estrogen-blocking drugs such as tamoxifen and fulvestrant in TNBC cells [225]. Remarkably, tumor development was also significantly suppressed by TAS0612 *in vivo* [225].

Targeting switch-points in the crosstalk between the PI3K/AKT and MAPK/RSK pathways

An alternative to blocking YB-1 activity by dual targeting is to target the proteins involved in the crosstalk between AKT and RSK. Focal adhesion kinase (FAK) and PAK are two proteins that can act as mediators of the crosstalk between AKT and RSK. FAK inhibition has been shown to increase the radiosensitivity of *KRAS*-mutated NSCLC [226]. According to another report by Dong et al. [227], anaplastic lymphoma kinase (ALK) inhibitor ceritinib and enzalutamide together had potent inhibitory effects on androgen receptor (AR) positive TNBC cell proliferation both *in vitro* and in mouse models [227]. In addition to ALK, ceritinib also targets CDC42 kinase 1 (ACK1) and its downstream effector FAK [227]. Consistent with FAK's role as a crosstalk mediator, ceritinib inhibited FAK/YB-1 signaling by reducing YB-1 phosphorylation at S102 in AR-positive TNBC cells [227]. It has also been observed that the FAK/YB-1 axis leads to paclitaxel resistance in TNBCs. In this context, the combination of ceritinib with paclitaxel strongly inhibited cell proliferation and tumor growth in TNBC cells [227].

Targeting YB-1 mRNA binding through an alternative pathway

Abelson (ABL) family of tyrosine kinases may be effective targets for blocking YB-1 mRNA binding activity. In this regard, it has also been proposed that ABL inhibition results in sensitization of *KRAS*-mutated lung adenocarcinoma tumors to docetaxel *in vivo* [228]. Another study showed that a combination of nilotinib (DDR1-ABL inhibitor) and lapatinib (EGFR/ErbB2 inhibitor), sensitized *KRAS*-mutant tumoroid models of CRC and recurrent glioblastoma to radiation [229]. Interestingly, ABL inhibition also prevents YB-1 phosphorylation at Y72 and Y99, which disrupts YB-1 binding to the ErbB2 mRNA and blocks ErbB2 expression, and consequently ablates metastatic outgrowth in breast cancer brain metastasis [48].

Indirectly targeting YB-1 using natural compounds

Fisetin is a natural flavonoid compound with anti-cancer activity as demonstrated in various tumor models [230, 231]. Fisetin impairs binding of RSK1 and RSK2 to YB-1 and inhibits melanoma growth *in vivo* [232]. A recent study by Khozooei et al. [99] showed that fisetin inhibits phosphorylation of YB-1 at S102, similar to the RSK inhibitors LJI308 and BI-D1870 [99]. Similarly, it interferes with DSB repair after irradiation, mainly by inhibiting homologous recombination (HR) and classical non-homologous end joining (C-NHEJ) [99]. Fisetin induces radiosensitization in TNBC cells independent of *KRAS* mutation status [99]. Fisetin has also been reported to bind to the CSD of YB-1, resulting in inhibition of AKT-mediated S102 phosphorylation [233]. Additionally, a study by Huang et al. [234] demonstrated that fisetin impairs ZC3H13-mediated N6-methyladenosine modification of PHF10 mRNA and therefore reduces PHF10 translation in pancreatic cancer and inhibits HR repair of DNA DSBs [234]. It remains to be investigated whether the function of fisetin on PHF10 expression is dependent on RSK/YB-1 signaling. Similar to fisetin, luteolin is a natural flavonoid compound known as an RSK1/2 inhibitor that blocks phosphorylation of YB-1 at S102 in TNBC cells [235]. The combination of luteolin and

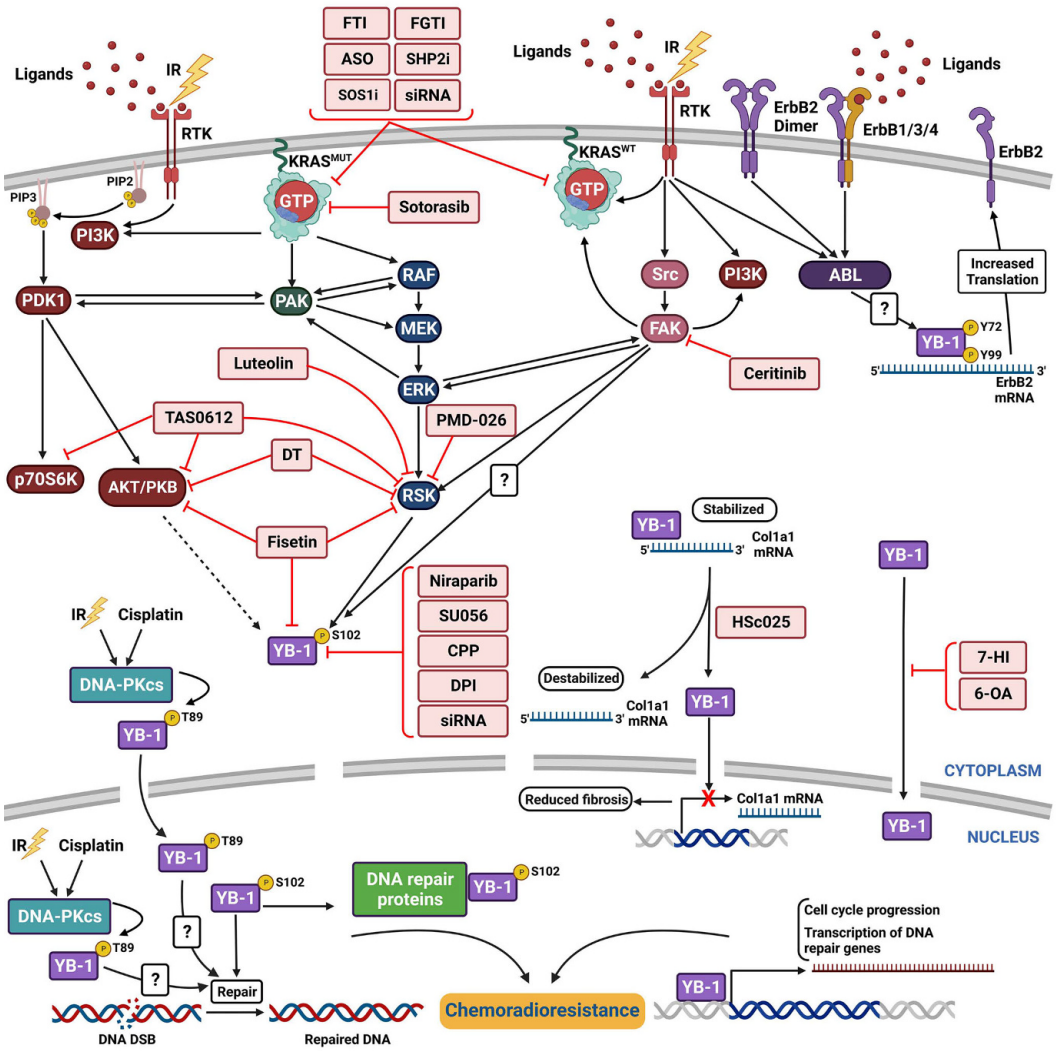

paclitaxel was found to significantly increase apoptosis in TNBC cells [236]. 7-hydroxyindirubin (7-HI) is one of the derivatives of plant-based dye, indirubin [237]. 7-HI blocks actinomycin D-triggered translocation of YB-1 to the nucleus and enhances the anticancer effect of actinomycin D in drug-resistant liver cancer cells [237]. Aloe-emodin (AE) is a bioactive anthraquinone compound that blocks YB-1 expression in ErbB2-overexpressed breast cancer cells and inhibits cell migration and invasion [238]. Interestingly, AE blocked the proliferation of cancer stem cells and inhibited tumor growth in mice [238]. 6-O-Angeloylplenolin is a bioactive compound extracted from *Centipeda minima* [239], and exhibits anti-cancer properties in lung cancer both *in vitro* and *in vivo* [240, 241]. 6-O-Angeloylplenolin reduced vincristine-induced YB-1 nuclear translocation, and additionally, combination therapy with vincristine reduced colorectal tumor growth *in vivo* [241].

Direct targeting of YB-1

Besides inhibitors of upstream YB-1 signaling, research is also underway to develop approaches that directly target YB-1. A recent study by El Hage et al. [242] identified several candidate molecules that bind to YB-1 and are poten-

Fig. 3 The central role of KRAS in the activation of YB-1 upstream pathways. S102 phosphorylation of YB-1 can be mediated by MAPK/RSK, PI3K/AKT, and Src/FAK cascades. $KRAS^{mut}$-induced YB-1 phosphorylation at S102 is mainly orchestrated by the MAPK/RSK pathway. S102 phosphorylation is thought to play a role in DNA repair and, consequently, may contribute to KRAS-mediated chemoradiotherapy (*CRT*) resistance either by directly participating in DNA repair or by interacting with other DNA repair proteins. Alternatively, DNA-PKcs may phosphorylate YB-1 at T89 in response to ionizng radiation (*IR*) or DNA-damaging agents, resulting in nuclear translocation of YB-1. In addition, YB-1 may also mediate CRT resistance by regulating the expression of various DNA repair and cell cycle genes. Alternatively, the ErbB protein family may induce phosphorylation of YB-1 at Y72 and Y99 via ABL kinases. These tyrosine phosphorylations of YB-1 contribute to the enhancement of ErbB2 mRNA translation and result in increased expression of ErbB2. A summary of the different approaches to affect KRAS/YB-1 signaling at different levels is shown in *red boxes*. The question mark (?) denotes unknown mechanisms. *6-OA* 6-O-Angeloylplenolin, *7-HI* 7-hydroxyindirubin, *ABL* Abelson family of tyrosine kinases, *AKT/PKB* Protein kinase B, *ASO* Antisense oligonucleotide, *Col1A1* collagen α1(I), *CPP* 9-mer cell permeable peptide, *DPI* 2,4-Dihydroxy-5-pyrimidinyl imidothiocarbamate, *DNA-PKcs* DNA-dependent protein kinase catalytic subunit, *DSB* Double strand break, *DT* Dual targeting, *ERK* Extracellular signal-regulated kinase, *FAK* Focal adhesion kinase, *FGTI* Farnesyltransferase and geranylgeranyltransferase 1 inhibitor, *FTI* Farnesyltransferase inhibitor, *GTP* Guanosine triphosphate, *IR* Ionizing radiation, *KRAS* Kirsten Rat Sarcoma Viral Oncogene Homologue, *MEK* MAPK kinase, *mRNA* Messenger RNA, *MUT* Mutant, *P* Phosphate group, *p70S6K* p70 ribosomal S6 kinase, *PAK* p21-activated family of protein kinases, *PDK1* Phosphoinositide-dependent kinase-1, *PI3K* Phosphoinositide 3-kinase, *PIP2* Phosphatidylinositol 4,5-bisphosphate, *PIP3* Phosphatidylinositol (3,4,5)-trisphosphate, *RAF* Rapidly activated fibrosarcoma kinase, *RSK* p90 ribosomal S6 kinase, *RTK* Receptor tyrosine kinase, *S102* Serine 102, *SHP2i* Src homology-2 domain-containing protein tyrosine phosphatase-2 inhibitor, *Src* SRC Proto-Oncogene, *siRNA* small interfering RNA, *SOS1i* Son of sevenless 1 inhibitor, *WT* Wild-type, *Y72* Tyrosine 72, *Y99* Tyrosine 99, *YB-1* Y-box binding protein 1, *?* Unknown effector. *Black arrows* indicate the direction of signal transduction and *red inhibitory arrows* display targets of the indicated inhibitors. Created with BioRender.com

tially capable of disrupting YB-1-RNA interactions [242]. In this study, niraparib, a PARP-1 inhibitor currently being investigated in Phase II clinical trials for ovarian cancer and TNBC (NCT02657889), is one of the top candidates that specifically binds to the quercetin pocket of the CSD of YB-1 and consequently hinders its interaction with RNA [242]. A recent study investigated the direct inhibition of YB-1 expression by a fluorine-based small molecule, SU056, in the treatment of ovarian cancer cells *in vitro* and *in vivo* [243]. In addition, they have shown that SU056 reduces ovarian cancer cell proliferation *in vitro* and *in vivo* and the combination of SU056 with paclitaxel shows a synergistic effect [243].

2,4-Dihydroxy-5-pyrimidinyl imidothiocarbamate (DPI) is another direct inhibitor of YB-1 which induces apoptosis and has a potential inhibitory effect on breast cancer cell proliferation [244]. The combination of DPI with doxorubicin inhibited accumulation of YB-1 in the nucleus and sensitized cells to doxorubicin without causing toxicity in mouse models [244].

HSc025, a direct inhibitor of YB-1 mRNA binding activity, binds to the CTD of YB-1 [245], and in turn induces nuclear shuttling. The forced nuclear translocation of YB-1 induced by HSc025 [76, 245] has been shown to reduce renal damage and fibrosis by inhibiting the Col1a1 mRNA stabilizing cytoplasmic function of YB-1 and promoting its activity as a transcriptional repressor of the Col1a1 promoter in the nucleus [76]. Although HSc025 has not been tested in cancer models, it could have potential therapeutic abilities through the prevention of YB-1-mRNA binding. For instance, a study in acute myeloid leukemia showed that preventing the binding of YB-1 to oncogenic mRNAs such as the Myc mRNA, reduces proliferation of leukemia cells, while normal cells remain unaffected [41]. Similarly, in myeloproliferative neoplasms, YB-1 was shown to mediate MKNK1 mRNA splicing in $JAK2^{V617F}$ mutant cells, wherein, the disruption of YB-1 resulted in RNA mis-splicing and interruption of the transcriptional control of ERK signaling [74].

YB-1 blocking peptide is another approach to target YB-1. A 9-mer cell permeable peptide was generated by Law et al. [246] to interfere with YB-1 phosphorylation at S102 [246]. This peptide could block cell proliferation and sensitize breast and prostate cancer cells to trastuzumab [246]. A peptide with similar function was shown to inhibit IR-induced YB-1 S102 phosphorylation and to interfere with DSB repair in breast cancer cells [98]. As with KRAS, targeting YB-1 by siRNA seems to be an effective approach to overcome YB-1 function in oncology [97, 99, 247]. However, the application of both, peptides and siRNA, in *in vivo* models and clinical settings remain to be challenging. A summary of the potential targets for interfering with KRAS/YB-1 signaling is shown in Fig. 3.

Conclusion

KRAS is a commonly mutated *RAS* isoform that leads to constitutive activation of the gene product and multiple RAS-dependent signal transduction cascades. Expression of mutant *KRAS* stimulates DDR signaling, which is associated with a limited response to conventional CRT and increases cell survival after irradiation. Approximately 70% of *RAS* mutations occur in *KRAS*. Therefore, molecular targeting strategies against KRAS and key downstream signaling pathways such as PI3K/AKT and MAPK/ERK were initially proposed as potential strategies in combination with CRT. Unfortunately, after extensive preclinical studies, the results of few early clinical trials have shown limited benefit from such therapies. The discovery of mutation-specific $KRAS^{G12C}$ inhibitors was groundbreaking in the field of KRAS targeting and a light at the end of the

tunnel. However, the initial clinical data on the inhibitors as monotherapy are not satisfactory, and the main reason for this is the presence of both intrinsic and acquired resistance. One of the most important resistance mechanisms may depend in part on the high redundancy of KRAS signaling, which controls the activation of multiple feedback pathways. Thus, molecular targeting strategies against KRAS cascades should dive deeper and target those activated effector molecules that sit at the bottom of the pool and are preferably regulated by multiple mutant KRAS signaling cascades. In this context, effector molecules such as the multifunctional protein YB-1, which is phosphorylated/activated by the major mutant KRAS downstream survival pathways, may be better candidates. Based on the efficacy of different strategies to target YB-1 in preclinical models, as reviewed here, further studies are needed to clarify the effect of these strategies in clinical settings in patients with *KRAS*-mutated tumors.

Funding This study was supported by a grant from the Deutsche Forschungsgemeinschaft (DFG, TO 685/2-3).

Conflict of interest S. Khozooei, S. Veerappan and M. Toulany declare that they have no known competing financial interests or personal relationships that could have appeared to influence the work reported in this paper.

References

1. Dolfini D, Mantovani R (2013) Targeting the Y/CCAAT box in cancer: YB-1 (YBX1) or NF-Y? Cell Death Differ 20(5):676–685
2. Lindquist JA, Mertens PR (2018) Cold shock proteins: from cellular mechanisms to pathophysiology and disease. Cell Commun Signal 16(1):63
3. Zhan Y et al (2022) YB1 associates with oncogenetic roles and poor prognosis in nasopharyngeal carcinoma. Sci Rep 12(1):3699
4. Yahata H et al (2002) Increased nuclear localization of transcription factor YB-1 in acquired cisplatin-resistant ovarian cancer. J Cancer Res Clin Oncol 128(11):621–626
5. Nishio S et al (2014) Nuclear Y-box-binding protein-1 is a poor prognostic marker and related to epidermal growth factor receptor in uterine cervical cancer. Gynecol Oncol 132(3):703–708
6. Dahl E et al (2009) Nuclear detection of Y-boxprotein-1 (YB-1) closely associates with progesterone receptor negativity and is a strong adverse survival factor in human breast cancer. BMC Cancer 9(1):410
7. Fushimi F et al (2013) Peroxiredoxins, thioredoxin, and Y-box-binding protein-1 are involved in the pathogenesis and progression of dialysis-associated renal cell carcinoma. Virchows Arch 463(4):553–562
8. Sheridan CM et al (2015) YB-1 and MTA1 protein levels and not DNA or mRNA alterations predict for prostate cancer recurrence. Oncotarget 6(10):7470–7480
9. Shibahara K et al (2001) Nuclear expression of the Y-box binding protein, YB-1, as a novel marker of disease progression in non-small cell lung cancer1. Clin Cancer Res 7(10):3151–3155
10. Guo T et al (2017) YB-1 regulates tumor growth by promoting MACC1/c-Met pathway in human lung adenocarcinoma. Oncotarget 8(29):48110–48125
11. Sinnberg T et al (2012) MAPK and PI3K/AKT mediated YB-1 activation promotes melanoma cell proliferation which is counteracted by an autoregulatory loop. Exp Dermatol 21(4):265–270
12. Song YH et al (2014) Twist1 and Y-box-binding protein-1 are potential prognostic factors in bladder cancer. Urol Oncol 32(1):31.e1–31.e7
13. Chao H-M et al (2016) Y-box binding protein-1 promotes hepatocellular carcinoma-initiating cell progression and tumorigenesis via Wnt/β-catenin pathway. Oncotarget 8(2):2604–2616
14. Yan X et al (2014) High expression of Y-box-binding protein 1 is associated with local recurrence and predicts poor outcome in patients with colorectal cancer. Int J Clin Exp Pathol 7(12):8715–8723
15. Zhang Y et al (2012) Overexpression of Y-box binding protein-1 in cervical cancer and its association with the pathological response rate to chemoradiotherapy. Med Oncol 29(3):1992–1997
16. Mylona E et al (2014) Y-box-binding protein 1 (YB1) in breast carcinomas: relation to aggressive tumor phenotype and identification of patients at high risk for relapse. Eur J Surg Oncol 40(3):289–296
17. Shibahara K et al (2004) Targeted disruption of one allele of the Y-box binding protein-1 (YB-1) gene in mouse embryonic stem cells and increased sensitivity to cisplatin and mitomycin C. Cancer Sci 95(4):348–353
18. Chatterjee M et al (2008) The Y-box binding protein YB-1 is associated with progressive disease and mediates survival and drug resistance in multiple myeloma. Blood 111(7):3714–3722
19. Kim ER et al (2013) The proteolytic YB-1 fragment interacts with DNA repair machinery and enhances survival during DNA damaging stress. Cell Cycle 12(24):3791–3803
20. Johnson TG et al (2019) Why be one protein when you can affect many? The multiple roles of YB-1 in lung cancer and mesothelioma. Front Cell Dev Biol 7:221
21. Kohno Y et al (2006) Expression of Y-box-binding protein dbpC/contrin, a potentially new cancer/testis antigen. Br J Cancer 94(5):710–716
22. Lyabin DN et al (2020) YB-3 substitutes YB-1 in global mRNA binding. RNA Biol 17(4):487–499
23. Wang GR et al (2009) Upregulation of human DNA binding protein A (dbpA) in gastric cancer cells. Acta Pharmacol Sin 30(10):1436–1442
24. Liu RT et al (2016) RNAi-mediated downregulation of DNA binding protein A inhibits tumorigenesis in colorectal cancer. Int J Mol Med 38(3):703–712
25. Yasen M et al (2005) The up-regulation of Y-box binding proteins (DNA binding protein A and Y-box binding protein-1) as prognostic markers of hepatocellular carcinoma. Clin Cancer Res 11(20):7354–7361
26. Hayashi J et al (2002) Somatic mutation and SNP in the promoter of dbpA and human hepatocarcinogenesis. Int J Oncol 21(4):847–850
27. Nakatsura T et al (2001) Gene cloning of immunogenic antigens overexpressed in pancreatic cancer. Biochem Biophys Res Commun 281(4):936–944
28. Hohlfeld R et al (2018) Crosstalk between Akt signaling and cold shock proteins in mediating invasive cell phenotypes. Oncotarget 9(27):19039–19049
29. Wang W et al (2016) Antimicrobial peptide LL-37 promotes the proliferation and invasion of skin squamous cell carcinoma by upregulating DNA-binding protein A. Oncol Lett 12(3):1745–1752
30. Tong C et al (2020) Knockdown of DNA-binding protein A enhances the chemotherapy sensitivity of colorectal cancer via suppressing the Wnt/β-catenin/Chk1 pathway. Cell Biol Int 44(10):2075–2085
31. Yang X-J et al (2019) Crystal structure of a Y-box binding protein 1 (YB-1)–RNA complex reveals key features and residues interacting with RNA. J Biol Chem 294(28):10998–11010

32. Zhang J et al (2020) Structural basis of DNA binding to human YB-1 cold shock domain regulated by phosphorylation. Nucleic Acids Res 48(16):9361–9371
33. Matsumoto K, Wolffe AP (1998) Gene regulation by Y-box proteins: coupling control of transcription and translation. Trends Cell Biol 8(8):318–323
34. Lyabin DN, Eliseeva IA, Ovchinnikov LP (2014) YB-1 protein: functions and regulation. Wiley Interdiscip Rev RNA 5(1):95–110
35. Evdokimova VM et al (1998) The major core protein of messenger ribonucleoprotein particles (p50) promotes initiation of protein biosynthesis in vitro. J Biol Chem 273(6):3574–3581
36. Evdokimova VM et al (1995) The major protein of messenger ribonucleoprotein particles in somatic cells is a member of the Y-box binding transcription factor family. J Biol Chem 270(7):3186–3192
37. Minich WB, Maidebura IP, Ovchinnikov LP (1993) Purification and characterization of the major 50-kDa repressor protein from cytoplasmic mRNP of rabbit reticulocytes. Eur J Biochem 212(3):633–638
38. Hamon L, Budkina K, Pastré D (2022) YB-1 structure/function relationship in the packaging of mRNPs and consequences for translation regulation and stress granule assembly in cells. Biochemistry 87(1):S20–S31
39. van Roeyen CRC et al (2013) Cold shock Y-box protein-1 proteolysis autoregulates its transcriptional activities. Cell Commun Signal 11(1):63
40. Hamon L, Budkina K, Pastre D (2022) YB-1 structure/function relationship in the packaging of mRNPs and consequences for translation regulation and stress granule assembly in cells. Biochemistry (Mosc) 87(1):S20–S93
41. Perner F et al (2022) YBX1 mediates translation of oncogenic transcripts to control cell competition in AML. Leukemia 36(2):426–437
42. El-Naggar AM et al (2015) Translational activation of HIF1α by YB-1 promotes sarcoma metastasis. Cancer Cell 27(5):682–697
43. Evdokimova V et al (2009) Translational activation of snail1 and other developmentally regulated transcription factors by YB-1 promotes an epithelial-mesenchymal transition. Cancer Cell 15(5):402–415
44. Evdokimova V et al (2001) The major mRNA-associated protein YB-1 is a potent 5′ cap-dependent mRNA stabilizer. EMBO J 20(19):5491–5502
45. Evdokimova VM, Ovchinnikov LP (1999) Translational regulation by Y-box transcription factor: involvement of the major mRNA-associated protein, p50. Int J Biochem Cell Biol 31(1):139–149
46. Minich WB, Ovchinnikov LP (1992) Role of cytoplasmic mRNP proteins in translation. Biochimie 74(5):477–483
47. Nekrasov MP et al (2003) The mRNA-binding protein YB-1 (p50) prevents association of the eukaryotic initiation factor eIF4G with mRNA and inhibits protein synthesis at the initiation stage. J Biol Chem 278(16):13936–13943
48. McKernan CM et al (2022) ABL kinases regulate translation in HER2+ cells through Y-box-binding protein 1 to facilitate colonization of the brain. Cell Rep 40(9):111268
49. Kosnopfel C et al (2018) YB-1 expression and phosphorylation regulate tumorigenicity and invasiveness in melanoma by influencing EMT. Mol Cancer Res 16(7):1149–1160
50. Somasekharan SP et al (2015) YB-1 regulates stress granule formation and tumor progression by translationally activating G3BP1. J Cell Biol 208(7):913–929
51. Chu P-C et al (2018) Mutant KRAS promotes liver metastasis of colorectal cancer, in part, by upregulating the MEK-Sp1-DNMT1-miR-137-YB-1-IGF-IR signaling pathway. Oncogene 37(25):3440–3455
52. Koike K et al (1997) Nuclear translocation of the Y-box binding protein by ultraviolet irradiation. FEBS Lett 417(3):390–394
53. Rauen T et al (2016) Cold shock protein YB-1 is involved in hypoxia-dependent gene transcription. Biochem Biophys Res Commun 478(2):982–987
54. Woolley AG et al (2011) Prognostic association of YB-1 expression in breast cancers: a matter of antibody. PLoS One 6(6):e20603
55. Yokoyama H et al (2003) Regulation of YB-1 gene expression by GATA transcription factors. Biochem Biophys Res Commun 303(1):140–145
56. Uramoto H et al (2002) p73 Interacts with c-Myc to regulate Y-box-binding protein-1 expression. J Biol Chem 277(35):31694–31702
57. Bommert KS et al (2013) The feed-forward loop between YB-1 and MYC is essential for multiple myeloma cell survival. Leukemia 27(2):441–450
58. Shiota M et al (2008) Twist promotes tumor cell growth through YB-1 expression. Cancer Res 68(1):98–105
59. Kobayashi S et al (2015) YB-1 gene expression is kept constant during myocyte differentiation through replacement of different transcription factors and then falls gradually under the control of neural activity. Int J Biochem Cell Biol 68:1–8
60. Skabkina OV et al (2005) YB-1 autoregulates translation of its own mRNA at or prior to the step of 40S ribosomal subunit joining. Mol Cell Biol 25(8):3317–3323
61. Skabkina OV et al (2003) Poly(A)-binding protein positively affects YB-1 mRNA translation through specific interaction with YB-1 mRNA. J Biol Chem 278(20):18191–18198
62. Lyabin DN, Eliseeva IA, Ovchinnikov LP (2012) YB-1 synthesis is regulated by mTOR signaling pathway. PLoS One 7(12):e52527
63. Lu J et al (2017) YB-1 expression promotes pancreatic cancer metastasis that is inhibited by microRNA-216a. Exp Cell Res 359(2):319–326
64. Zhao X et al (2020) Circ-SAR1A promotes renal cell carcinoma progression through miR-382/YBX1 axis. Cancer Manag Res 12:7353–7361
65. Liu SL, Sui YF, Lin MZ (2016) MiR-375 is epigenetically downregulated due to promoter methylation and modulates multi-drug resistance in breast cancer cells via targeting YBX1. Eur Rev Med Pharmacol Sci 20(15):3223–3229
66. Stratford AL et al (2007) Epidermal growth factor receptor (EGFR) is transcriptionally induced by the Y-box binding protein-1 (YB-1) and can be inhibited with Iressa in basal-like breast cancer, providing a potential target for therapy. Breast Cancer Res 9(5):R61
67. Wu J et al (2006) Disruption of the Y-box binding protein-1 results in suppression of the epidermal growth factor receptor and HER-2. Cancer Res 66(9):4872–4879
68. Bader AG, Vogt PK (2008) Phosphorylation by Akt disables the anti-oncogenic activity of YB-1. Oncogene 27(8):1179–1182
69. Gieseler-Halbach S et al (2017) RSK-mediated nuclear accumulation of the cold-shock Y-box protein-1 controls proliferation of T cells and T-ALL blasts. Cell Death Differ 24(2):371–383
70. Sutherland BW et al (2005) Akt phosphorylates the Y-box binding protein 1 at Ser102 located in the cold shock domain and affects the anchorage-independent growth of breast cancer cells. Oncogene 24(26):4281–4292
71. Tiwari A et al (2018) Stress-induced phosphorylation of nuclear YB-1 depends on nuclear trafficking of p90 ribosomal S6 kinase. Int J Mol Sci 19(8):2441. https://doi.org/10.3390/ijms19082441
72. Sogorina EM et al (2022) YB-1 phosphorylation at serine 209 inhibits its nuclear translocation. Int J Mol Sci 23(1):428
73. Mehta S et al (2020) Dephosphorylation of YB-1 is required for nuclear localisation during G(2) phase of the cell cycle. Cancers (Basel) 12(2):315
74. Jayavelu AK et al (2020) Splicing factor YBX1 mediates persistence of JAK2-mutated neoplasms. Nature 588(7836):157–163
75. Nöthen T et al (2023) DNA-dependent protein kinase mediates YB-1 (Y-box binding protein)-induced double strand break repair. ATVB 43(2):300–311

76. Wang J et al (2016) Therapeutic nuclear shuttling of YB-1 reduces renal damage and fibrosis. Kidney Int 90(6):1226–1237
77. Kretov DA et al (2020) Inhibition of transcription induces phosphorylation of YB-1 at Ser102 and its accumulation in the nucleus. Cells 9(1):104
78. Prabhu L et al (2015) Critical role of phosphorylation of serine 165 of YBX1 on the activation of NF-κB in colon cancer. Oncotarget 6(30):29396–29412
79. Martin M et al (2017) Novel serine 176 phosphorylation of YBX1 activates NF-kappaB in colon cancer. J Biol Chem 292(8):3433–3444
80. Mehta S et al (2020) Critical role for cold shock protein YB-1 in cytokinesis. Cancers (Basel) 12(9):2473. https://doi.org/10.3390/cancers12092473
81. El-Naggar AM et al (2019) Class I HDAC inhibitors enhance YB-1 acetylation and oxidative stress to block sarcoma metastasis. EMBO Rep 20(12):e48375
82. Frye BC et al (2009) Y-box protein-1 is actively secreted through a non-classical pathway and acts as an extracellular mitogen. EMBO Rep 10(7):783–789
83. Kim W et al (2011) Systematic and quantitative assessment of the ubiquitin-modified proteome. Mol Cell 44(2):325–340
84. Palicharla VR, Maddika S (2015) HACE1 mediated K27 ubiquitin linkage leads to YB-1 protein secretion. Cell Signal 27(12):2355–2362
85. Hartley AV et al (2020) PRMT5-mediated methylation of YBX1 regulates NF-κB activity in colorectal cancer. Sci Rep 10(1):15934
86. Geiss-Friedlander R, Melchior F (2007) Concepts in sumoylation: a decade on. Nat Rev Mol Cell Biol 8(12):947–956
87. Mai RT et al (2022) Sumoylation participates in the regulation of YB-1-mediated mismatch repair deficiency and alkylator tolerance. Am J Cancer Res 12(12):5462–5483
88. Chang YW et al (2014) YB-1 disrupts mismatch repair complex formation, interferes with MutSα recruitment on mismatch and inhibits mismatch repair through interacting with PCNA. Oncogene 33(43):5065–5077
89. Reppert SM, Weaver DR (2002) Coordination of circadian timing in mammals. Nature 418(6901):935–941
90. Pagano C et al (2017) The tumor-associated YB-1 protein: new player in the circadian control of cell proliferation. Oncotarget 8(4):6193–6205
91. Liu Q et al (2016) Hyper-O-GlcNAcylation of YB-1 affects Ser102 phosphorylation and promotes cell proliferation in hepatocellular carcinoma. Exp Cell Res 349(2):230–238
92. Fujiwara-Okada Y et al (2013) Y-box binding protein-1 regulates cell proliferation and is associated with clinical outcomes of osteosarcoma. Br J Cancer 108(4):836–847
93. Lasham A et al (2012) YB-1, the E2F pathway, and regulation of tumor cell growth. J Natl Cancer Inst 104(2):133–146
94. Jurchott K et al (2003) YB-1 as a cell cycle-regulated transcription factor facilitating cyclin A and cyclin B1 gene expression. J Biol Chem 278(30):27988–27996
95. Tiwari A et al (2020) Blocking Y-box binding protein-1 through simultaneous targeting of PI3K and MAPK in triple negative breast cancers. Cancers (Basel) 12(10):2795. https://doi.org/10.3390/cancers12102795
96. Gaudreault I, Guay D, Lebel M (2004) YB-1 promotes strand separation in vitro of duplex DNA containing either mispaired bases or cisplatin modifications, exhibits endonucleolytic activities and binds several DNA repair proteins. Nucleic Acids Res 32(1):316–327
97. Toulany M et al (2011) Impact of oncogenic K-RAS on YB-1 phosphorylation induced by ionizing radiation. Breast Cancer Res 13(2):R28
98. Lettau K, Zips D, Toulany M (2021) Simultaneous targeting of RSK and AKT efficiently inhibits YB-1-mediated repair of ionizing radiation-induced DNA double-strand breaks in breast cancer cells. Int J Radiat Oncol Biol Phys 109(2):567–580
99. Khozooei S et al (2022) Fisetin induces DNA double-strand break and interferes with the repair of radiation-induced damage to radiosensitize triple negative breast cancer cells. J Exp Clin Cancer Res 41(1):256
100. Ise T et al (1999) Transcription factor Y-box binding protein 1 binds preferentially to cisplatin-modified DNA and interacts with proliferating cell nuclear antigen. Cancer Res 59(2):342–346
101. Hasegawa SL et al (1991) DNA binding properties of YB-1 and dbpA: binding to double-stranded, single-stranded, and abasic site containing DNAs. Nucleic Acids Res 19(18):4915–4920
102. Naumenko KN et al (2020) Regulation of poly(ADP-ribose) polymerase 1 activity by Y-box-binding protein 1. Biomolecules 10(9):1325
103. Alemasova EE et al (2018) The multifunctional protein YB-1 potentiates PARP1 activity and decreases the efficiency of PARP1 inhibitors. Oncotarget 9(34):23349–23365
104. Lettau K et al (2021) Targeting the Y-box binding protein-1 axis to overcome radiochemotherapy resistance in solid tumors. Int J Radiat Oncol Biol Phys 111(4):1072–1087
105. Kosnopfel C, Sinnberg T, Schittek B (2014) Y-box binding protein 1—a prognostic marker and target in tumour therapy. Eur J Cell Biol 93(1):61–70
106. Toulany M (2023) Targeting K-Ras-mediated DNA damage response in radiation oncology: current status, challenges and future perspectives. Clin Transl Radiat Oncol 38:6–14
107. Shinkai K et al (2016) Nuclear expression of Y-box binding protein-1 is associated with poor prognosis in patients with pancreatic cancer and its knockdown inhibits tumor growth and metastasis in mice tumor models. Int J Cancer 139(2):433–445
108. Shiraiwa S et al (2016) Nuclear Y-box-binding protein-1 expression predicts poor clinical outcome in stage III colorectal cancer. Anticancer Res 36(7):3781–3788
109. Ardito F et al (2014) Strong YB-1 expression predicts liver recurrence following resection for colorectal metastases. J Gastrointest Surg 18(11):1987–1993
110. Zhang Y et al (2015) The expression level and prognostic value of Y-box binding protein-1 in rectal cancer. PLoS One 10(3):e119385
111. Nagasu S et al (2019) Yboxbinding protein 1 inhibits apoptosis and upregulates EGFR in colon cancer. Oncol Rep 41(5):2889–2896
112. Kashihara M et al (2009) Nuclear Y-box binding protein-1, a predictive marker of prognosis, is correlated with expression of HER2/ErbB2 and HER3/ErbB3 in non-small cell lung cancer. J Thorac Oncol 4(9):1066–1074
113. Gessner C et al (2004) Nuclear YB-1 expression as a negative prognostic marker in nonsmall cell lung cancer. Eur Respir J 23(1):14–19
114. Jiang L et al (2017) Positive expression of Y-box binding protein 1 and prognosis in non-small cell lung cancer: a meta-analysis. Oncotarget 8(33):55613–55621
115. Prior IA, Hood FE, Hartley JL (2020) The frequency of Ras mutations in cancer. Cancer Res 80(14):2969–2974
116. Raso E (2020) Splice variants of RAS-translational significance. Cancer Metastasis Rev 39(4):1039–1049
117. Nuevo-Tapioles C, Philips MR (2022) The role of KRAS splice variants in cancer biology. Front Cell Dev Biol 10:1033348
118. Schlichting I et al (1990) Time-resolved X-ray crystallographic study of the conformational change in Ha-Ras p21 protein on GTP hydrolysis. Nature 345(6273):309–315
119. Milburn MV et al (1990) Molecular switch for signal transduction: structural differences between active and inactive forms of protooncogenic ras proteins. Science 247(4945):939–945
120. Vetter IR, Wittinghofer A (2001) The guanine nucleotide-binding switch in three dimensions. Science 294(5545):1299–1304

121. Bos JL, Rehmann H, Wittinghofer A (2007) GEFs and GAPs: critical elements in the control of small G proteins. Cell 129(5):865–877
122. Saraste M, Sibbald PR, Wittinghofer A (1990) The P-loop—a common motif in ATP- and GTP-binding proteins. Trends Biochem Sci 15(11):430–434
123. Willumsen BM et al (1984) The p21 ras C-terminus is required for transformation and membrane association. Nature 310(5978):583–586
124. Gideon P et al (1992) Mutational and kinetic analyses of the GTPase-activating protein (GAP)-p21 interaction: the C-terminal domain of GAP is not sufficient for full activity. Mol Cell Biol 12(5):2050–2056
125. Hobbs GA, Der CJ, Rossman KL (2016) RAS isoforms and mutations in cancer at a glance. J Cell Sci 129(7):1287–1292
126. Cammarata MB et al (2016) Impact of G12 mutations on the structure of K-Ras probed by ultraviolet photodissociation mass spectrometry. J Am Chem Soc 138(40):13187–13196
127. Pylayeva-Gupta Y, Grabocka E, Bar-Sagi D (2011) RAS oncogenes: weaving a tumorigenic web. Nat Rev Cancer 11(11):761–774
128. Zhang XF et al (1993) Normal and oncogenic p21ras proteins bind to the amino-terminal regulatory domain of c-Raf-1. Nature 364(6435):308–313
129. Moodie SA et al (1993) Complexes of Ras.GTP with Raf-1 and mitogen-activated protein kinase kinase. Science 260(5114):1658–1661
130. Rodriguez-Viciana P et al (1997) Role of phosphoinositide 3-OH kinase in cell transformation and control of the actin cytoskeleton by Ras. Cell 89(3):457–467
131. White MA et al (1996) A role for the Ral guanine nucleotide dissociation stimulator in mediating Ras-induced transformation. J Biol Chem 271(28):16439–16442
132. Eser S et al (2014) Oncogenic KRAS signalling in pancreatic cancer. Br J Cancer 111(5):817–822
133. Jones RP et al (2017) Specific mutations in KRAS codon 12 are associated with worse overall survival in patients with advanced and recurrent colorectal cancer. Br J Cancer 116(7):923–929
134. Imamura Y et al (2012) Specific mutations in KRAS codons 12 and 13, and patient prognosis in 1075 BRAF wild-type colorectal cancers. Clin Cancer Res 18(17):4753–4763
135. Buscail L, Bournet B, Cordelier P (2020) Role of oncogenic KRAS in the diagnosis, prognosis and treatment of pancreatic cancer. Nat Rev Gastroenterol Hepatol 17(3):153–168
136. Goulding RE et al (2020) KRAS mutation as a prognostic factor and predictive factor in advanced/metastatic non-small cell lung cancer: a systematic literature review and meta-analysis. Cancer Treat Res Commun 24:100200
137. Gurtner K et al (2020) Radioresistance of KRAS/TP53-mutated lung cancer can be overcome by radiation dose escalation or EGFR tyrosine kinase inhibition in vivo. Int J Cancer 147(2):472–477
138. Duldulao MP et al (2013) Mutations in specific codons of the KRAS oncogene are associated with variable resistance to neoadjuvant chemoradiation therapy in patients with rectal adenocarcinoma. Ann Surg Oncol 20(7):2166–2171
139. Mak RH et al (2015) Outcomes by tumor histology and KRAS mutation status after lung stereotactic body radiation therapy for early-stage non-small-cell lung cancer. Clin Lung Cancer 16(1):24–32
140. Metro G et al (2014) Clinical outcome with platinum-based chemotherapy in patients with advanced nonsquamous EGFR wild-type non-small-cell lung cancer segregated according to KRAS mutation status. Clin Lung Cancer 15(1):86–92
141. Lievre A et al (2006) KRAS mutation status is predictive of response to cetuximab therapy in colorectal cancer. Cancer Res 66(8):3992–3995
142. Benvenuti S et al (2007) Oncogenic activation of the RAS/RAF signaling pathway impairs the response of metastatic colorectal cancers to anti-epidermal growth factor receptor antibody therapies. Cancer Res 67(6):2643–2648
143. Forster T et al (2020) Cetuximab in pancreatic cancer therapy: a systematic review and meta-analysis. Oncology 98(1):53–60
144. Ridouane Y et al (2017) Targeted first-line therapies for advanced colorectal cancer: a Bayesian meta-analysis. Oncotarget 8(39):66458–66466
145. Smith MJ, Neel BG, Ikura M (2013) NMR-based functional profiling of RASopathies and oncogenic RAS mutations. Proc Natl Acad Sci U S A 110(12):4574–4579
146. Lu S et al (2016) The structural basis of oncogenic mutations G12, G13 and Q61 in small GTPase K-Ras4B. Sci Rep 6:21949
147. Khrenova MG et al (2014) Modeling the role of G12V and G13V Ras mutations in the Ras-GAP-catalyzed hydrolysis reaction of guanosine triphosphate. Biochemistry 53(45):7093–7099
148. Chen CC et al (2013) Computational analysis of KRAS mutations: implications for different effects on the KRAS p.G12D and p.G13D mutations. PLoS One 8(2):e55793
149. Hunter JC et al (2015) Biochemical and structural analysis of common cancer-associated KRAS mutations. Mol Cancer Res 13(9):1325–1335
150. Munoz-Maldonado C, Zimmer Y, Medova M (2019) A comparative analysis of individual RAS mutations in cancer biology. Front Oncol 9:1088
151. Buhrman G, Wink G, Mattos C (2007) Transformation efficiency of RasQ61 mutants linked to structural features of the switch regions in the presence of Raf. Structure 15(12):1618–1629
152. Haigis KM (2017) KRAS alleles: the devil is in the detail. Trends Cancer 3(10):686–697
153. Ihle NT et al (2012) Effect of KRAS oncogene substitutions on protein behavior: implications for signaling and clinical outcome. J Natl Cancer Inst 104(3):228–239
154. Hammond DE et al (2015) Differential reprogramming of isogenic colorectal cancer cells by distinct activating KRAS mutations. J Proteome Res 14(3):1535–1546
155. Garassino MC et al (2011) Different types of K-Ras mutations could affect drug sensitivity and tumour behaviour in non-small-cell lung cancer. Ann Oncol 22(1):235–237
156. Cook JH et al (2021) The origins and genetic interactions of KRAS mutations are allele- and tissue-specific. Nat Commun 12(1):1808
157. Jia Y et al (2017) Characterization of distinct types of KRAS mutation and its impact on first-line platinum-based chemotherapy in Chinese patients with advanced non-small cell lung cancer. Oncol Lett 14(6):6525–6532
158. Nadal E et al (2014) KRAS-G12C mutation is associated with poor outcome in surgically resected lung adenocarcinoma. J Thorac Oncol 9(10):1513–1522
159. Dai M et al (2022) Prognostic value of KRAS subtype in patients with PDAC undergoing radical resection. Front Oncol 12:1074538
160. Park HE et al (2021) Tumor microenvironment-adjusted prognostic implications of the KRAS mutation subtype in patients with stage III colorectal cancer treated with adjuvant FOLFOX. Sci Rep 11(1):14609
161. Chida K et al (2021) The prognostic impact of KRAS G12C mutation in patients with metastatic colorectal cancer: a multicenter retrospective observational study. Oncologist 26(10):845–853
162. Rabara D et al (2019) KRAS G13D sensitivity to neurofibromin-mediated GTP hydrolysis. Proc Natl Acad Sci USA 116(44):22122–22131
163. Stratford AL et al (2008) Y-box binding protein-1 serine 102 is a downstream target of p90 ribosomal S6 kinase in basal-like breast cancer cells. Breast Cancer Res 10(6):R99
164. Evdokimova V et al (2006) Akt-mediated YB-1 phosphorylation activates translation of silent mRNA species. Mol Cell Biol 26(1):277–292
165. Lee CS et al (2019) MAP kinase and autophagy pathways cooperate to maintain RAS mutant cancer cell survival. Proc Natl Acad Sci U S A 116(10):4508–4517

166. Takacs T et al (2020) The effects of mutant Ras proteins on the cell signalome. Cancer Metastasis Rev 39(4):1051–1065
167. Higuchi M et al (2008) Scaffolding function of PAK in the PDK1-Akt pathway. Nat Cell Biol 10(11):1356–1364
168. Beeser A et al (2005) Role of group A p21-activated kinases in activation of extracellular-regulated kinase by growth factors. J Biol Chem 280(44):36609–36615
169. Lu H et al (2017) PAK signalling drives acquired drug resistance to MAPK inhibitors in BRAF-mutant melanomas. Nature 550(7674):133–136
170. Zang M, Hayne C, Luo Z (2002) Interaction between active Pak1 and Raf-1 is necessary for phosphorylation and activation of Raf-1. J Biol Chem 277(6):4395–4405
171. Eblen ST et al (2002) Rac-PAK signaling stimulates extracellular signal-regulated kinase (ERK) activation by regulating formation of MEK1-ERK complexes. Mol Cell Biol 22(17):6023–6033
172. Park ER, Eblen ST, Catling AD (2007) MEK1 activation by PAK: a novel mechanism. Cell Signal 19(7):1488–1496
173. Wang Z et al (2013) p21-activated kinase 1 (PAK1) can promote ERK activation in a kinase-independent manner. J Biol Chem 288(27):20093–20099
174. Tang Y et al (2000) The Akt proto-oncogene links Ras to Pak and cell survival signals. J Biol Chem 275(13):9106–9109
175. Zhou GL et al (2003) Akt phosphorylation of serine 21 on Pak1 modulates Nck binding and cell migration. Mol Cell Biol 23(22):8058–8069
176. King CC et al (2000) p21-activated kinase (PAK1) is phosphorylated and activated by 3-phosphoinositide-dependent kinase-1 (PDK1). J Biol Chem 275(52):41201–41209
177. Ebi H et al (2013) PI3K regulates MEK/ERK signaling in breast cancer via the Rac-GEF, P-Rex1. Proc Natl Acad Sci U S A 110(52):21124–21129
178. Thillai K et al (2017) Deciphering the link between PI3K and PAK: an opportunity to target key pathways in pancreatic cancer? Oncotarget 8(8):14173–14191
179. McCarty SK et al (2014) BRAF activates and physically interacts with PAK to regulate cell motility. Endocr Relat Cancer 21(6):865–877
180. Linardou H et al (2008) Assessment of somatic k-RAS mutations as a mechanism associated with resistance to EGFR-targeted agents: a systematic review and meta-analysis of studies in advanced non-small-cell lung cancer and metastatic colorectal cancer. Lancet Oncol 9(10):962–972
181. Normanno N et al (2009) Implications for KRAS status and EGFR-targeted therapies in metastatic CRC. Nat Rev Clin Oncol 6(9):519–527
182. Knickelbein K, Zhang L (2015) Mutant KRAS as a critical determinant of the therapeutic response of colorectal cancer. Genes Dis 2(1):4–12
183. Eberhard DA et al (2005) Mutations in the epidermal growth factor receptor and in KRAS are predictive and prognostic indicators in patients with non-small-cell lung cancer treated with chemotherapy alone and in combination with erlotinib. J Clin Oncol 23(25):5900–5909
184. Sumi S et al (1992) Inhibition of pancreatic adenocarcinoma cell growth by lovastatin. Gastroenterology 103(3):982–989
185. Kohl NE et al (1994) Protein farnesyltransferase inhibitors block the growth of ras-dependent tumors in nude mice. Proc Natl Acad Sci U S A 91(19):9141–9145
186. Sun J et al (1995) Ras CAAX peptidomimetic FTI 276 selectively blocks tumor growth in nude mice of a human lung carcinoma with K-Ras mutation and p53 deletion. Cancer Res 55(19):4243–4247
187. Santillo M et al (1996) Inhibitors of Ras farnesylation revert the increased resistance to oxidative stress in K-Ras transformed NIH 3T3 cells. Biochem Biophys Res Commun 229(3):739–745
188. Hunt JT et al (2000) Discovery of (R)-7-cyano-2,3,4, 5-tetrahydro-1-(1H-imidazol-4-ylmethyl)-3-(phenylmethyl)-4-(2-thienylsulfonyl)-1H-1,4-benzodiazepine (BMS-214662), a farnesyltransferase inhibitor with potent preclinical antitumor activity. J Med Chem 43(20):3587–3595
189. Macdonald JS et al (2005) A phase II study of farnesyl transferase inhibitor R115777 in pancreatic cancer: a Southwest oncology group (SWOG 9924) study. Invest New Drugs 23(5):485–487
190. Rao S et al (2004) Phase III double-blind placebo-controlled study of farnesyl transferase inhibitor R115777 in patients with refractory advanced colorectal cancer. J Clin Oncol 22(19):3950–3957
191. Cohen SJ et al (2003) Phase II and pharmacodynamic study of the farnesyltransferase inhibitor R115777 as initial therapy in patients with metastatic pancreatic adenocarcinoma. J Clin Oncol 21(7):1301–1306
192. Adjei AA et al (2003) Phase II study of the farnesyl transferase inhibitor R115777 in patients with advanced non-small-cell lung cancer. J Clin Oncol 21(9):1760–1766
193. Whyte DB et al (1997) K- and N-Ras are geranylgeranylated in cells treated with farnesyl protein transferase inhibitors. J Biol Chem 272(22):14459–14464
194. Lerner EC et al (1997) Inhibition of the prenylation of K-Ras, but not H- or N-Ras, is highly resistant to CAAX peptidomimetics and requires both a farnesyltransferase and a geranylgeranyltransferase I inhibitor in human tumor cell lines. Oncogene 15(11):1283–1288
195. Martin NE et al (2004) A phase I trial of the dual farnesyltransferase and geranylgeranyltransferase inhibitor L-778,123 and radiotherapy for locally advanced pancreatic cancer. Clin Cancer Res 10(16):5447–5454
196. Hahn SM et al (2002) A Phase I trial of the farnesyltransferase inhibitor L-778,123 and radiotherapy for locally advanced lung and head and neck cancer. Clin Cancer Res 8(5):1065–1072
197. Sepp-Lorenzino L et al (1995) A peptidomimetic inhibitor of farnesyl:protein transferase blocks the anchorage-dependent and -independent growth of human tumor cell lines. Cancer Res 55(22):5302–5309
198. End DW et al (2001) Characterization of the antitumor effects of the selective farnesyl protein transferase inhibitor R115777 in vivo and in vitro. Cancer Res 61(1):131–137
199. Di Paolo A et al (2001) Inhibition of protein farnesylation enhances the chemotherapeutic efficacy of the novel geranylgeranyltransferase inhibitor BAL9611 in human colon cancer cells. Br J Cancer 84(11):1535–1543
200. Song SY et al (2000) K-Ras-independent effects of the farnesyl transferase inhibitor L-744,832 on cyclin B1/Cdc2 kinase activity, G2/M cell cycle progression and apoptosis in human pancreatic ductal adenocarcinoma cell. Neoplasia 2(3):261–272
201. Ross SJ et al (2017) Targeting KRAS-dependent tumors with AZD4785, a high-affinity therapeutic antisense oligonucleotide inhibitor of KRAS. Sci Transl Med 9(394):eaal5253. https://doi.org/10.1126/scitranslmed.aal5253
202. Aoki K et al (1995) Liposome-mediated in vivo gene transfer of antisense K-ras construct inhibits pancreatic tumor dissemination in the murine peritoneal cavity. Cancer Res 55(17):3810–3816
203. Tsuchida T et al (1998) Hammerhead ribozyme specifically inhibits mutant K-ras mRNA of human pancreatic cancer cells. Biochem Biophys Res Commun 253(2):368–373
204. Kita K et al (1999) Growth inhibition of human pancreatic cancer cell lines by anti-sense oligonucleotides specific to mutated K-ras genes. Int J Cancer 80(4):553–558
205. Smakman N et al (2005) Dual effect of Kras(D12) knockdown on tumorigenesis: increased immune-mediated tumor clearance and abrogation of tumor malignancy. Oncogene 24(56):8338–8342
206. Golan T et al (2015) RNAi therapy targeting KRAS in combination with chemotherapy for locally advanced pancreatic cancer patients. Oncotarget 6(27):24560–24570

207. Gort E et al (2020) A phase I, open-label, dose-escalation trial of BI 1701963 as monotherapy and in combination with trametinib in patients with KRAS mutated advanced or metastatic solid tumors. J Clin Oncol 38(15):TPS3651–TPS3651
208. Wee S et al (2009) PI3K pathway activation mediates resistance to MEK inhibitors in KRAS mutant cancers. Cancer Res 69(10):4286–4293
209. Toulany M et al (2016) Dual targeting of PI3K and MEK enhances the radiation response of K-RAS mutated non-small cell lung cancer. Oncotarget 7(28):43746–43761
210. Toulany M et al (2014) ERK2-dependent reactivation of Akt mediates the limited response of tumor cells with constitutive K-RAS activity to PI3K inhibition. Cancer Biol Ther 15(3):317–328
211. Shapiro GI et al (2020) Phase Ib study of the MEK inhibitor cobimetinib (GDC-0973) in combination with the PI3K inhibitor pictilisib (GDC-0941) in patients with advanced solid tumors. Invest New Drugs 38(2):419–432
212. Lanman BA et al (2020) Discovery of a covalent inhibitor of KRAS(G12C) (AMG 510) for the treatment of solid tumors. J Med Chem 63(1):52–65
213. Tanaka N et al (2021) Clinical acquired resistance to KRAS(G12C) inhibition through a novel KRAS switch-II pocket mutation and polyclonal alterations converging on RAS-MAPK reactivation. Cancer Discov 11(8):1913–1922
214. Awad MM et al (2021) Acquired resistance to KRAS(G12C) inhibition in cancer. N Engl J Med 384(25):2382–2393
215. Blaquier JB, Cardona AF, Recondo G (2021) Resistance to KRAS(G12C) inhibitors in non-small cell lung cancer. Front Oncol 11:787585
216. Mao Z et al (2022) KRAS(G12D) can be targeted by potent inhibitors via formation of salt bridge. Cell Discov 8(1):5
217. Hallin J et al (2022) Anti-tumor efficacy of a potent and selective non-covalent KRAS(G12D) inhibitor. Nat Med 28(10):2171–2182
218. Koltun E et al (2021) Abstract 1260: first-in-class, orally bioavailable KRASG12V(ON) tri-complex inhibitors, as single agents and in combinations, drive profound anti-tumor activity in preclinical models of KRASG12V mutant cancers. Cancer Res 81(13):1260–1260
219. Lasham A et al (2012) YB-1: oncoprotein, prognostic marker and therapeutic target? Biochem J 449(1):11–23
220. Sangermano F, Delicato A, Calabrò V (2020) Y box binding protein 1 (YB-1) oncoprotein at the hub of DNA proliferation, damage and cancer progression. Biochimie 179:205–216
221. Serra V et al (2013) RSK3/4 mediate resistance to PI3K pathway inhibitors in breast cancer. J Clin Invest 123(6):2551–2563
222. Maier E et al (2019) Dual targeting of Y-box binding protein-1 and Akt inhibits proliferation and enhances the chemosensitivity of colorectal cancer cells. Cancers (Basel) 11(4):562. https://doi.org/10.3390/cancers11040562
223. Kosnopfel C et al (2017) Human melanoma cells resistant to MAPK inhibitors can be effectively targeted by inhibition of the p90 ribosomal S6 kinase. Oncotarget 8(22):35761–35775
224. Ushijima M et al (2022) An oral first-in-class small molecule RSK inhibitor suppresses AR variants and tumor growth in prostate cancer. Cancer Sci 113(5):1731–1738
225. Shibata T et al (2020) Targeting phosphorylation of Y-box–binding protein YBX1 by TAS0612 and everolimus in overcoming antiestrogen resistance. Mol Cancer Ther 19(3):882–894
226. Tang KJ et al (2016) Focal adhesion kinase regulates the DNA damage response and its inhibition radiosensitizes mutant KRAS lung cancer. Clin Cancer Res 22(23):5851–5863
227. Dong S et al (2022) Ceritinib is a novel triple negative breast cancer therapeutic agent. Mol Cancer 21(1):138
228. Khatri A et al (2019) ABL kinase inhibition sensitizes primary lung adenocarcinomas to chemotherapy by promoting tumor cell differentiation. Oncotarget 10(20):1874–1886
229. Gupta K et al (2022) Identification of synergistic drug combinations to target KRAS-driven chemoradioresistant cancers utilizing tumoroid models of colorectal adenocarcinoma and recurrent glioblastoma. Front Oncol 12:840241
230. Khan N et al (2013) Fisetin: a dietary antioxidant for health promotion. Antioxidants Redox Signal 19(2):151–162
231. Syed DN et al (2008) Dietary agents for chemoprevention of prostate cancer. Cancer Lett 265(2):167–176
232. Sechi M et al (2018) Fisetin targets YB-1/RSK axis independent of its effect on ERK signaling: insights from in vitro and in vivo melanoma models. Sci Rep 8(1):15726
233. Khan MI et al (2014) YB-1 expression promotes epithelial-to-mesenchymal transition in prostate cancer that is inhibited by a small molecule fisetin. Oncotarget 5(9):2462–2474
234. Huang C et al (2022) ZC3H13-mediated N6-methyladenosine modification of PHF10 is impaired by fisetin which inhibits the DNA damage response in pancreatic cancer. Cancer Lett 530:16–28
235. Lin Y et al (2008) Luteolin, a flavonoid with potential for cancer prevention and therapy. Curr Cancer Drug Targets 8(7):634–646
236. Reipas KM et al (2013) Luteolin is a novel p90 ribosomal S6 kinase (RSK) inhibitor that suppresses Notch4 signaling by blocking the activation of Y-box binding protein-1 (YB-1). Oncotarget 4(2):329–345. https://doi.org/10.18632/oncotarget.834
237. Tanaka T et al (2021) 7-Hydorxyindirubin is capable of specifically inhibiting anticancer drug-induced YB-1 nuclear translocation without showing cytotoxicity in HepG2 hepatocellular carcinoma cells. Biochem Biophys Res Commun 544:15–21
238. Ma J-W et al (2016) Aloe-emodin inhibits HER-2 expression through the downregulation of Y-box binding protein-1 in HER-2-overexpressing human breast cancer cells. Oncotarget 7(37):58915–58930
239. Chan C et al (2016) Qualitative and quantitative analysis of chemical constituents of centipeda minima by HPLC-QTOF-MS & HPLC-DAD. J Pharm Biomed Anal 125:400–407
240. Liu YQ et al (2015) Skp1 in lung cancer: clinical significance and therapeutic efficacy of its small molecule inhibitors. Oncotarget 6(33):34953–34967
241. Li C et al (2018) Sesquiterpene lactone 6-O-angeloylplenolin reverses vincristine resistance by inhibiting YB-1 nuclear translocation in colon carcinoma cells. Oncol Lett 15(6):9673–9680
242. El Hage K et al (2023) Targeting RNA:protein interactions with an integrative approach leads to the identification of potent YBX1 inhibitors. Elife 12:e80387
243. Tailor D et al (2021) Y box binding protein 1 inhibition as a targeted therapy for ovarian cancer. Cell Chem Biol 28(8):1206–1220.e6
244. Gunasekaran VP et al (2018) Identification of 2,4-dihydroxy-5-pyrimidinyl imidothiocarbomate as a novel inhibitor to Y box binding protein-1 (YB-1) and its therapeutic actions against breast cancer. Eur J Pharm Sci 116:2–14
245. Higashi K et al (2011) A novel small compound that promotes nuclear translocation of YB-1 ameliorates experimental hepatic fibrosis in mice. J Biol Chem 286(6):4485–4492
246. Law JH et al (2010) Molecular decoy to the Y-box binding protein-1 suppresses the growth of breast and prostate cancer cells whilst sparing normal cell viability. PLoS One 5(9):e12661
247. Izumi H et al (2016) Optimal sequence of antisense DNA to silence YB-1 in lung cancer by use of a novel polysaccharide drug delivery system. Int J Oncol 48(6):2472–2478